AN ABSTRACT OF THE DISSERTATION OF

Katya R. Jay for the degree of Doctor of Philosophy in Integrative Biology presented on September 15, 2021.

Title: Investigating the Role of Dune Grasses, Carbon Storage, and Marine Nutrient Subsidies to the Functions and Services of U.S. Central Atlantic Coastal Dune Ecosystems

Abstract approved:

_____

Sally D. Hacker

Sandy beaches and dunes cover approximately one-third of the world's ice-free coastlines and provide ecosystem services including coastal protection, recreation, wildlife habitat, and carbon sequestration. These dynamic interface habitats are variably shaped by wind, waves, sedimentary processes, and vegetation feedbacks. Positive biophysical feedbacks lead to the formation of vegetated coastal dunes when wind-blown sand is captured by burial-tolerant vegetation such as dune grasses. By promoting sand capture and stabilization over time, dune grasses help shape foredunes and protect coastlines from wave overtopping and inundation. Moreover, foredunes store carbon both in the vegetation and in the foredune sand itself, serving as a potentially important ecosystem in mitigating rising levels of greenhouse gases. Thus, it is integral to understand the contribution of dunes to important coastal ecosystem functions and services.

In this dissertation, I investigate the role of dune grasses in shaping barrier island foredunes and their ecosystem services along the U.S. Atlantic Coast. The

North Carolina Outer Banks is a sandy barrier island system with alongshore variability in its beach and foredune geomorphology, vegetation composition and density, sand supply, and oceanographic conditions. These barrier islands are also particularly vulnerable to coastal erosion due to their low elevation and exposure to sea level rise and extreme storm events. Furthermore, the ranges of two native dune grass species, *Uniola paniculata* and *Ammophila breviligulata*, overlap in this region. Due to differences in their functional morphology, growth density, physiology, and sand accretion properties, these grasses are thought to have species-specific effects on foredune morphology. Although studies have documented the importance of dune grasses to dune building processes in this region, less is known about the factors that control dune grass productivity and the role of dune grasses in shaping foredune morphology and ecosystem services including carbon storage.

Here I use a combination of observational surveys, laboratory analyses, and statistical models to examine the physical and ecological feedbacks in foredunes to better understand the factors important to foredune morphology, carbon storage, and dune grass productivity along the North Carolina Outer Banks. In Chapter 2, I explore the interactive effects of sand supply, beach geomorphology, and vegetation on foredune morphology. Specifically, I ask: 1) What is the relative contribution of shoreline change rate, beach morphology, and dune grass density and species identity in shaping foredune morphology over space and time? and 2) Do the dune grass species *A. breviligulata* and *U. paniculata* affect foredune morphology in species-specific ways, and if so, how? I found that beach morphometrics and sand supply to the beach (i.e., shoreline change rate, beach width, and backshore slope) were the

most important factors (72-90% of explained variance) influencing foredune morphology, particularly height and width, while grass density explained a smaller proportion of the variance (10-28%). However, grass density metrics were more important when changes in foredune morphology were considered (36-50% of explained variance). In particular, I found that an increase in *A. breviligulata* density was associated with an increase in foredune width and a decrease in foredune height, corroborating previous findings that the more lateral growth form of *A. breviligulata*, compared to that of *U. paniculata*, has species-specific effects on foredune morphology.

In Chapter 3, I measure carbon storage in dune grasses and sand in North Carolina Outer Banks foredune ecosystems and examine the role of beach geomorphology and sand deposition in shaping variability in carbon stocks. In doing so, I ask: 1) How much carbon is stored in Outer Banks foredunes and how does carbon storage vary by carbon stock type, island, foredune profile location, and dominant dune grass species? 2) Does carbon storage in these foredunes decrease with depth, and are changes in sand carbon with depth related to changes in dune grass carbon? and 3) If carbon storage varies spatially, what geomorphological and ecological factors best explain this variability across the study region? I found that aboveground grass carbon stocks (0.004-0.19 kg C/m^2) were comparable to those in eelgrass beds and salt marshes (0.03-2.30 kg C/m^2) on a per area basis, while sediment organic carbon values in our study system (0.9 ± 0.6 kg C/m^3) were significantly lower compared to previous measurements in other dunes (2.2 kg C/m^3 in Italian dunes and up to 4.7 kg C/m^3 in U.K. dunes) and other coastal ecosystems

(averaging 10 and 28 kg C/m^3 in salt marshes and mangroves, respectively). Carbon storage in Outer Banks foredunes varied between aboveground grass (0.1 ± 0.1 kg C/m^2), belowground grass (1.1 ± 1.6 kg C/m^3), and sand (0.9 ± 0.6 kg C/m^3) carbon stocks, with the largest proportion contained in the belowground grass. Belowground and aboveground carbon stocks varied at both regional (island) and local (foredune profile locations) scales, with values generally increasing from north to south along the Outer Banks coast and in the landward direction along the foredune profile. I found that variability in sand carbon density was related to patterns in dune sand deposition, beach slope, and grass density, with the relative importance of these factors varying between islands and dune profile locations. Islands with high sand deposition and high grass density tended to have low sand carbon density, while profile locations with lower sand deposition and higher grass density tended to have high sand carbon density, suggesting that self-reinforcing feedbacks between vegetation and sediment determine sand carbon values in these foredunes.

In Chapter 4, I examine whether dune grass production and foliar nitrogen content vary at regional and local scales as a result of marine subsidies, sand nitrate concentrations, and proxies for sand supply to the foredune (i.e., beach and foredune morphology). Specifically, I ask: 1) Do macrophyte wrack biomass and composition, sand nitrate concentration, and dune grass production vary at local and regional scales? Do dune grasses utilize marine derived nitrogen ($\delta^{15}N$) and, if so, how does $\delta^{15}N$ and %N vary across species, foredune profile locations, and islands? and 3) What factors, including macrophyte wrack biomass, sand nitrate, and sand supply metrics, are important to dune grass production and foliar nitrogen metrics? I found

that proxies for sand supply and marine subsidies both influence dune grass production and that dune grasses growing on the seaward portion of foredunes utilize marine nutrients. Specifically, dune grass production and foliar %N were higher in areas with greater sand nitrate concentration, taller foredunes, and eroding beaches. Dune grasses growing at the foredune toe had greater $\delta^{15}N$ in their tissues compared to those growing at the foredune crest and heel, and $\delta^{15}N$ levels increased with foredune height and sand supply. Taken together, these findings suggest that differences in sand nitrate concentrations with latitude, along with beach and foredune sand supply metrics, mediate the delivery of marine subsidies to foredune vegetation and thus dune grass production.

The results of this dissertation provide insights into the complex dynamics that shape coastal barrier island foredunes and their ecosystem services. By quantifying the role of dune grasses, carbon storage, and marine nutrient subsidies to the ecosystem functions and services of U.S. Central Atlantic coastal dunes, we can better manage this vulnerable ecosystem given anticipated shifts in dune grass distributions, sea level rise, and extreme storms as a result of climate change.

Investigating the Role of Dune Grasses, Carbon Storage, and Marine Nutrient Subsidies to the Functions and Services of U.S. Central Atlantic Coastal Dune Ecosystems

by
Katya R. Jay

A DISSERTATION

submitted to

Oregon State University

in partial fulfillment of
the requirements for the
degree of

Doctor of Philosophy

Presented September 15, 2021
Commencement June 2022

Doctor of Philosophy dissertation of Katya R. Jay presented on September 15, 2021

APPROVED:

Major Professor, representing Integrative Biology

Head of the Department of Integrative Biology

Dean of the Graduate School

I understand that my dissertation will become part of the permanent collection of Oregon State University libraries. My signature below authorizes release of my dissertation to any reader upon request.

Katya R. Jay, Author

ACKNOWLEDGEMENTS

I am grateful to the many people who have made this dissertation possible through their support, guidance, and encouragement over the past five years. First and foremost, I would like to acknowledge my advisor, Sally Hacker, for her unwavering support, patience, and mentorship throughout this entire process. I am thankful to her for pushing me to grow as a scientist and writer all while encouraging me and supporting my goals. Sally has always been available as much as needed to plan projects, discuss findings, and provide her insight and feedback on grants and manuscripts, and I could not have done this without her. I am also very grateful to Peter Ruggiero, who taught me all about coastal geomorphology, shared his enthusiasm for quantitative coastal science with me, and provided valuable input in the formulation of my dissertation research. Thanks to Rebecca Terry for her scientific mentorship and advice and Steven Dundas for serving as my Graduate Council Representative. Thanks to Debashis Mondal and Duo Jiang for serving as Statistics minor professors on my committee.

I benefitted greatly from collaborations throughout the course of my dissertation. I would like to thank Laura Moore for all her advice and guidance over the years and for sharing her expertise in coastal geomorphology and barrier island processes. In addition, I am thankful to everyone from OSU and UNC Chapel Hill who participated in our North Carolina field campaigns, including Elsemarie Mullins, Michael Itzkin, Ian Reeves, Hannah Lawrence, Nick Cohn, Evan Goldstein, Katharine Anarde, and others, for all their help with data collection and for all the fun times. I learned so much from all of you. Special thanks to Paige Hovenga for all her

help planning our NC field campaigns and for working together to come up with alternative plans when we had to deal with impending tropical storms and ferry closures. I am also grateful to her for showing me the ropes of processing topographic data and answering all my questions about coastal geomorphology.

I am fortunate to have been part of the Hacker lab with such wonderful friends, mentors, and colleagues over the years, including Vanessa Constant, Caitlin Magel, Reuben Biel, Risa Askerooth, John Stepanek, Rebecca Mostow, and Zech Meunier. I am so glad we got to share many office conversations, field work trips, and snacks over the years. Thank you for all your advice and guidance and for making sure that grad school was as fun as possible. I am also grateful for the help of many undergraduate researchers, especially Lucas Parvin, Judith Quintana, Annaliese Ballowe, and Julia Padilla: all the sample processing and laboratory analyses that they conducted helped make this dissertation research possible.

Many thanks to the Integrative Biology Department office staff, including Tara Bevandich, Traci Durrell-Khalife, Tresa Bowlin, and Trudy Powell, for all their assistance over the years and for always knowing the answers to my questions. I am grateful to the IB department for providing teaching assistantships and funds through the Zoology Research Fund. I have also benefitted greatly from financial assistance from The Garden Club of America, the Geological Society of America, and NOAA. Special thanks to the IB graduate students and BI 21X TAs for creating such a supportive and welcoming grad community.

I am grateful to Sarah Boyer for introducing me to scientific research, showing me the joys of fieldwork, and providing me with countless opportunities

during my undergraduate studies. Sarah's mentorship and my experiences in her lab were invaluable in my journey to graduate school.

I am also grateful to all the wonderful people I met during my time in Corvallis that helped keep me grounded, as well as to friends near and far for all their support through this process. Special thanks to Kaelyn Lemon, Sofia Marcus-Myers, Alisa Kotash, Bryce Penta, Trevor Pereyda, Molly Guiney, and Mia Nguyen for all the laughter and fun adventures over the years.

Lastly, I thank my family, including my parents and my older brother Sebastian, for all their love and support over the years. My parents brought me into the outdoors from a young age and instilled a love for the natural world in me. They have always encouraged me to pursue my interests in science and helped me to achieve my goals along the way.

I would not have been able to complete this dissertation without the constant love and friendship of my partner, Cedric. From helping with field work and coding issues to reminding me what really mattered, he has always been my biggest supporter and my best friend. I am thankful to him for constantly making me laugh and being my number one adventure buddy.

CONTRIBUTION OF AUTHORS

Chapter 2: Drs. Sally D. Hacker, Peter Ruggiero, and Laura J. Moore contributed to the conception and funding of the study, as well as fieldwork, writing, and editing the manuscript. Paige Hovenga assisted with fieldwork, provided guidance for processing topography and shoreline change rate data, and edited the manuscript.

Chapter 3: Drs. Sally D. Hacker and Cedric J. Hagen contributed to the conception of the study, as well as writing and editing the manuscript. Drs. Sally D. Hacker, Peter Ruggiero, and Laura J. Moore contributed to the funding of the study. Dr. Cedric J. Hagen and John Stepanek assisted with fieldwork and conception of the methods. All authors reviewed and edited the manuscript.

Chapter 4: Dr. Sally D. Hacker contributed to the conception and funding of the study, as well as writing and editing the manuscript. Lucas Parvin helped with sand nitrate analyses and Judith Quintana helped with the processing of the plant samples for elemental composition analyses.

TABLE OF CONTENTS

TABLE OF CONTENTS (Continued)

TABLE OF CONTENTS (Continued)

Page

TABLE OF CONTENTS (Continued)

TABLE OF CONTENTS (Continued)

LIST OF FIGURES

LIST OF FIGURES (Continued)

Figure Page

LIST OF TABLES

LIST OF TABLES (Continued)

LIST OF APPENDICES

LIST OF APPENDIX FIGURES

LIST OF APPENDIX FIGURES

LIST OF APPENDIX TABLES

DEDICATION

This dissertation is dedicated to my parents, Clara Steiner-Jay and David Jay.

Investigating the Role of Dune Grasses, Carbon Storage, and Marine Nutrient Subsidies to the Functions and Services of U.S. Central Atlantic Coastal Dune Ecosystems

Chapter 1 – General Introduction

As interface habitats between the land and ocean, coastal ecosystems collectively provide more substantial ecosystem services than those provided by a single ecosystem (Barbier et al. 2011). Coastal ecosystems act as natural barriers to storm overwash and erosion by attenuating wave energy and providing sediment to beaches (Ruggiero et al. 2001, Morton 2002, Barbier et al. 2011). They provide significant value to the public in the form of recreation and tourism (Everard et al. 2010). In addition, coastal ecosystems including salt marshes, mangroves, and seagrass beds have been shown to accumulate carbon rapidly due to their high plant productivity and high sediment accumulation rates, indicating that these ecosystems may be important in regulating climate via the global carbon cycle (Mcleod et al. 2011, Beaumont et al. 2014, Howard et al. 2017, Macreadie et al. 2019). Coastal ecosystems are increasingly at risk from sea level rise, rising temperatures, heightened storm intensity, and land use change, all of which can alter the provisioning of ecosystem services (Feagin et al. 2005, Halpern et al. 2008, Intergovernmental Panel on Climate Change 2014).

One coastal ecosystem that is particularly important is that of sandy beaches and dunes. These ecosystems cover approximately one-third of the world's ice-free coastlines (Luijendijk et al. 2018) and are shaped by a combination of wave conditions, aeolian forces, sedimentary processes, and feedbacks with vegetation (Hesp 1989, Ruggiero et al. 2018). Foredunes, or the seaward-most dune ridge parallel to the shoreline, form as a result of physical and ecological feedbacks that occur when wind-blown sand is transported and captured by burial-tolerant vegetation such as dune grasses (Woodhouse

1978, Hesp 1989, Hacker et al. 2012, Zarnetske et al. 2012, 2015, Duran and Moore 2013, Keijsers et al. 2015, Brown and Zinnert 2018, Mullins et al. 2019, Biel et al. 2019, Charbonneau et al. 2021). These feedbacks lead to the development of a vegetated foredune over time, increasing dune elevation and reducing coastal vulnerability. Given their role in promoting sand capture and dune stabilization over time, dune grasses help shape foredunes and fortify coastlines against wave overtopping and inundation. Moreover, foredunes store carbon both in their vegetation and sand, potentially serving to sequester carbon and mitigate rising carbon dioxide levels (Beaumont et al. 2014, Drius et al. 2016).

While previous research has established the key role of dune grasses in shaping foredunes and their ecosystem functions and services, less is known about the environmental factors controlling dune grass growth and productivity. Foredunes are thought to be stressful, nutrient-limited environments (Willis 1963, Ehrenfeld 1990, Day et al. 2004, Jones et al. 2004), yet dune plant productivity and biomass are often high and comparable to values in other vegetated coastal systems (van der Valk 1974, Ripley and Pammenter 2008). Resource subsidies, or the flow of nutrients and energy from adjacent ecosystems (e.g., Polis et al. 1997, Loreau et al. 2003, Leroux and Loreau 2008), may provide an important source of nutrients to foredune vegetation. Previous studies have established connections between marine subsidies (in the form of macrophyte wrack), beach sand nutrient levels, and food web dynamics (Dugan et al. 2003, 2011, Barreiro et al. 2013, Gómez et al. 2018), but less is known about the role of marine nutrients to dune grass growth (see Cardona and García 2008, Del Vecchio et al. 2013, Constant 2019).

Although coastal dunes provide critical ecosystem services, more research is needed to understand the factors that shape their ecosystem functions and services and forecast how they may change in the future. The goal of this dissertation is to investigate the interactive roles of dune grasses, geomorphological processes, and marine subsides in shaping barrier island foredunes and their ecosystem services along the U.S. Central Atlantic Coast. Specifically, I investigate the relative roles of physical and ecological factors in determining foredune morphology, I quantify dune carbon storage, and I explore the role of marine nutrient subsidies to dune grass production along the North Carolina Outer Banks coastline.

The North Carolina Outer Banks are a group of sandy barrier islands with high spatial variability in beach geomorphology (Dolan and Lins 1985, Hovenga et al. 2019, 2021), vegetation species and density (Woodhouse et al. 1977, Hacker et al. 2019a), shoreline orientation, wave energy, and underlying stratigraphy (Lazarus and Murray 2011). The most widespread native dune grass in this region is *Uniola paniculata* (sea oats), a drought and burial-tolerant C_4 grass that extends from Virginia south to Florida (Seneca 1969). *Ammophila breviligulata* (American beachgrass) is a native mid-Atlantic dune-building C_3 grass that extends from North Carolina north to Canada and is thought to be less heat-tolerant (Goldstein et al. 2018). These two species overlap in the North Carolina Outer Banks, where *U. paniculata* dominates dunes in much of the region, but *A. breviligulata* becomes more abundant in the northern reaches of the Outer Banks. Two other native grasses that are common in the Outer Banks region and may influence dune building are *Spartina patens* (saltmeadow cordgrass) and *Panicum amarum* (bitter

panicgrass). Past research in this region suggests that dune grass species may impact foredune morphology in species-specific ways (Seneca et al. 1976, Woodhouse et al. 1977, Woodhouse 1978, Hacker et al. 2019a). For example, experimental plantings showed that foredunes with *A. breviligulata* monocultures were wider and larger in volume compared to the steeper, narrower dunes created by the *U. paniculata* and *P. amarum* (Woodhouse et al. 1977).

Understanding foredune biophysical feedbacks and ecosystem services is especially critical on the U.S. Atlantic Coast, which is characterized by high population density and is often lined with low-lying barrier islands that are vulnerable to coastal erosion, sea level rise, hurricanes, development, and subsidence (e.g., Paerl et al. 2019). Studies show that the Mid-Atlantic region is a 'hot spot' of sea level rise rates relative to global rates; for example, the area just north of Cape Hatteras, North Carolina is experiencing particularly high rates of sea level rise due to the weakening and offshore shift of the Gulf Stream (Sallenger et al. 2012, Ezer et al. 2013).

While some ecosystem services, such as coastal protection and recreation, have been studied extensively in foredunes, very little is known about their carbon storage capacity despite being productive ecosystems with dense vegetation and high sedimentation rates (Olff et al. 1993, Jones et al. 2008, Drius et al. 2016). Only a handful of studies worldwide have measured carbon storage in coastal dune ecosystems (United Kingdom: Jones et al. 2008, Beaumont et al. 2014; Italy: Drius et al. 2016; Australia: Turner and Laliberté 2015; and North America: Tackett and Craft 2010). Carbon storage in dunes likely varies based on plant productivity, species composition, coastal

geomorphology, and sand supply (Middleton and McKee 2001, Barbier et al. 2011). In addition, as coastal habitat area is lost due to land use change and sea level rise, the ability of foredunes to store carbon may be reduced. Thus, there is an important need to quantify the amount of carbon being stored in U.S. Atlantic Coast foredunes, characterize carbon storage variability according to vegetation and beach and dune geomorphology, and forecast how this potentially valuable coastal ecosystem service may be altered by climate change.

In Chapter 2, I explore the interactive effects of sand supply, beach geomorphology, and vegetation on foredune morphology. Using vegetation community and beach and dune topography surveys, I first explore the patterns in beach and foredune morphology, shoreline change rate, and dune grass density at 90 cross-shore transects along the Outer Banks coastline. I then use regression models and hierarchical partitioning analyses to determine whether metrics of beach geomorphology, shoreline change rate, or dune grass density explain the variation in foredune morphology [foredune height, foredune width, foredune toe elevation, and foredune aspect ratio (height:width)] in space and time. In particular, I ask: 1) What is the relative contribution of shoreline change rate, beach morphology, and dune grass density and species in shaping foredune morphology over space and time? and 2) Do the dune grass species *A. breviligulata* and *U. paniculata* affect foredune morphology in species-specific ways, and if so, how?

In Chapter 3, I quantify carbon storage in Outer Banks foredunes and examine the role of dune grass and sand deposition in shaping alongshore variability in carbon stocks.

I collected sediment cores and dune grasses from a subset of transects across the study region to quantify the magnitude of different foredune carbon stocks (aboveground vegetation, belowground vegetation, and sand) and assess variability in these stocks at local (foredune profile) and regional (island) scales. Specifically, I ask: 1) How much carbon is stored in Outer Banks barrier island foredunes and how does carbon storage vary by carbon stock type, island, foredune profile location, and dominant dune grass species? 2) Does carbon storage in these foredunes decrease with depth, and are changes in sand carbon with depth related to changes in dune grass carbon? and 3) If carbon storage varies spatially, which geomorphological and ecological factors best explain this variability across the study region?

In Chapter 4, I examine whether dune grass production and foliar nitrogen content vary at regional and local scales as a result of marine subsidies and proxies for sand supply to the foredune (i.e., beach and foredune morphology). I first explore the patterns in marine subsidies (macrophyte wrack and sand nitrate concentration), dune grass production (shoot density and biomass), and foliar nitrogen content and source (via plant tissue %N and $\delta^{15}N$) in four common dune grasses across local and regional scales of Outer Banks islands. Finally, I use regression models to relate dune grass production and foliar nitrogen metrics to measurements of marine subsidies and proxies for sand supply to the foredune (i.e., beach and foredune morphology). In particular, I ask: 1) Do macrophyte wrack biomass and composition, sand nitrate concentration, and dune grass production vary at local and regional scales? 2) Do dune grasses utilize marine derived nitrogen (isotopically heavy; ^{15}N) and, if so, how do foliar $\delta^{15}N$ and %N measurements

vary across species, foredune profile locations, and islands? and 3) What factors, including macrophyte wrack biomass, sand nitrate, and sand supply metrics, are important to dune grass production and foliar nitrogen metrics?

Using interdisciplinary approaches, each chapter of my dissertation fills a critical knowledge gap by exploring new and unstudied aspects of dune ecosystems, as well as building on prior research. The results of this dissertation provide insights into the complex dynamics that shape coastal barrier island foredunes and their ecosystem services. By quantifying the role of dune grasses, carbon storage, and marine nutrient subsidies to the ecosystem functions and services of U.S. Central Atlantic coastal dunes, we can better manage this vulnerable ecosystem given anticipated range shifts in dune grass distributions, sea level rise, and extreme storms as a result of current and future climate change.

1.1 References

Barbier, E. B., S. D. Hacker, C. Kennedy, E. W. Koch, A. C. Stier, and B. R. Silliman. 2011. The value of estuarine and coastal ecosystem services. Ecological Monographs 81:169–193.

Barreiro, F., M. Gómez, J. López, M. Lastra, and R. de la Huz. 2013. Coupling between macroalgal inputs and nutrients outcrop in exposed sandy beaches. Hydrobiologia 700:73–84.

Beaumont, N. J., L. Jones, A. Garbutt, J. D. Hansom, and M. Toberman. 2014. The value of carbon sequestration and storage in coastal habitats. Estuarine, Coastal and Shelf Science 137:32–40.

Biel, R. G., S. D. Hacker, and P. Ruggiero. 2019. Elucidating coastal foredune ecomorphodynamics in the U.S. Pacific Northwest via Bayesian Networks. Journal of Geophysical Research: Earth Surface 124:1919–1938.

Brown, J. K., and J. C. Zinnert. 2018. Mechanisms of surviving burial: Dune grass interspecific differences drive resource allocation after sand deposition. Ecosphere 9:e02162.

Cardona, L., and M. García. 2008. Beach-cast seagrass material fertilizes the foredune vegetation of Mediterranean coastal dunes. Acta Oecologica 34:97–103.

Charbonneau, B. R., S. M. Dohner, J. P. Wnek, D. Barber, P. Zarnetske, and B. B. Casper. 2021. Vegetation effects on coastal foredune initiation: Wind tunnel experiments and field validation for three dune-building plants. Geomorphology 378:107594.

Constant, V. 2019. Coastal dunes as meta-ecosystems: Connecting marine subsidies to ecosystem functions on the U.S. Pacific Northwest coast. PhD dissertation, Oregon State University.

Day, F. P., C. Conn, E. Crawford, and M. Stevenson. 2004. Long-term effects of nitrogen fertilization on plant community structure on a coastal barrier island dune chronosequence. Journal of Coastal Research 20:722–730.

Del Vecchio, S., N. Marbà, A. Acosta, C. Vignolo, and A. Traveset. 2013. Effects of *Posidonia oceanica* beach-cast on germination, growth and nutrient uptake of coastal dune plants. PLOS ONE 8:e70607.

Dolan, R., and H. Lins. 1985. The Outer Banks of North Carolina. U.S. Geological Survey, Washington, DC.

Drius, M., M. L. Carranza, A. Stanisci, and L. Jones. 2016. The role of Italian coastal dunes as carbon sinks and diversity sources. A multi-service perspective. Applied Geography 75:127–136.

Dugan, J. E., D. M. Hubbard, M. D. McCrary, and M. O. Pierson. 2003. The response of macrofauna communities and shorebirds to macrophyte wrack subsidies on exposed sandy beaches of southern California. Estuarine, Coastal and Shelf Science 58:25–40.

Dugan, J. E., D. M. Hubbard, H. M. Page, and J. P. Schimel. 2011. Marine macrophyte wrack inputs and dissolved nutrients in beach sands. Estuaries and Coasts 34:839–850.

Duran, O., and L. J. Moore. 2013. Vegetation controls on the maximum size of coastal dunes. Proceedings of the National Academy of Sciences 110:17217–17222.

Ehrenfeld, J. G. 1990. Dynamics and processes of barrier island vegetation. Reviews in Aquatic Sciences 2:437–480.

Everard, M., L. Jones, and B. Watts. 2010. Have we neglected the societal importance of sand dunes? An ecosystem services perspective. Aquatic Conservation: Marine and Freshwater Ecosystems 20:476–487.

Ezer, T., L. P. Atkinson, W. B. Corlett, and J. L. Blanco. 2013. Gulf Stream's induced sea level rise and variability along the U.S. mid-Atlantic coast. Journal of Geophysical Research: Oceans 118:685–697.

Feagin, R. A., D. J. Sherman, and W. E. Grant. 2005. Coastal erosion, global sea-level rise, and the loss of sand dune plant habitats. Frontiers in Ecology and the Environment 3:359–364.

Goldstein, E. B., E. V. Mullins, L. J. Moore, R. G. Biel, J. K. Brown, S. D. Hacker, K. R. Jay, R. S. Mostow, P. Ruggiero, and J. C. Zinnert. 2018. Literature-based latitudinal distribution and possible range shifts of two US east coast dune grass species (*Uniola paniculata* and *Ammophila breviligulata*). PeerJ 6:e4932.

Gómez, M., F. Barreiro, J. López, and M. Lastra. 2018. Effect of upper beach macrofauna on nutrient cycling of sandy beaches: metabolic rates during wrack decay. Marine Biology 165:133.

Hacker, S. D., K. R. Jay, N. Cohn, E. B. Goldstein, P. A. Hovenga, M. Itzkin, L. J. Moore, R. S. Mostow, E. V. Mullins, and P. Ruggiero. 2019. Species-specific functional morphology of four US Atlantic Coast dune grasses: Biogeographic implications for dune shape and coastal protection. Diversity 11:1–16.

Hacker, S. D., P. Zarnetske, E. Seabloom, P. Ruggiero, J. Mull, S. Gerrity, and C. Jones. 2012. Subtle differences in two non-native congeneric beach grasses significantly affect their colonization, spread, and impact. Oikos 121:138–148.

Halpern, B. S., S. Walbridge, K. A. Selkoe, C. V. Kappel, F. Micheli, C. D'Agrosa, J. F. Bruno, K. S. Casey, C. Ebert, H. E. Fox, R. Fujita, D. Heinemann, H. S. Lenihan, E. M. P. Madin, M. T. Perry, E. R. Selig, M. Spalding, R. Steneck, and R. Watson. 2008. A global map of human impact on marine ecosystems. Science 319:948–952.

Hesp, P. A. 1989. A review of biological and geomorphological processes involved in the initiation and development of incipient foredunes. Proceedings of the Royal Society of Edinburgh, Section B: Biological Sciences 96:181–201.

Hovenga, P. A., P. Ruggiero, N. Cohn, K. R. Jay, S. D. Hacker, M. Itzkin, and L. Moore. 2019. Drivers of dune evolution in Cape Lookout National Seashore, NC. Pages 1283–1296 Coastal Sediments 2019. World Scientific, Tampa/St. Petersburg, Florida, USA.

Hovenga, P. A., P. Ruggiero, E. B. Goldstein, S. D. Hacker, and L. J. Moore. 2021. The relative role of constructive and destructive processes in dune evolution on Cape Lookout National Seashore, North Carolina, USA. Earth Surface Processes and Landforms:esp.5210.

Howard, J., A. Sutton-Grier, D. Herr, J. Kleypas, E. Landis, E. Mcleod, E. Pidgeon, and S. Simpson. 2017. Clarifying the role of coastal and marine systems in climate mitigation. Frontiers in Ecology and the Environment 15:42–50.

Intergovernmental Panel on Climate Change. 2014. Climate change 2014: impacts, adaptation, and vulnerability: Working Group II contribution to the fifth assessment report of the Intergovernmental Panel on Climate Change. Page (C. B. Field and V. R. Barros, Eds.). Cambridge University Press, New York, NY.

Jones, M. L. M., A. Sowerby, D. L. Williams, and R. E. Jones. 2008. Factors controlling soil development in sand dunes: evidence from a coastal dune soil chronosequence. Plant and Soil 307:219–234.

Jones, M. L. M., H. L. Wallace, D. Norris, S. A. Brittain, S. Haria, R. E. Jones, P. M. Rhind, B. R. Reynolds, and B. A. Emmett. 2004. Changes in Vegetation and Soil Characteristics in Coastal Sand Dunes along a Gradient of Atmospheric Nitrogen Deposition. Plant Biology 6:598–605.

Keijsers, J. G. S., A. V. De Groot, and M. J. P. M. Riksen. 2015. Vegetation and sedimentation on coastal foredunes. Geomorphology 228:723–734.

Lazarus, E. D., and A. B. Murray. 2011. An integrated hypothesis for regional patterns of shoreline change along the Northern North Carolina Outer Banks, USA. Marine Geology 281:85–90.

Leroux, S. J., and M. Loreau. 2008. Subsidy hypothesis and strength of trophic cascades across ecosystems. Ecology Letters 11:1147–1156.

Loreau, M., N. Mouquet, and R. D. Holt. 2003. Meta-ecosystems: a theoretical framework for a spatial ecosystem ecology. Ecology Letters 6:673–679.

Luijendijk, A., G. Hagenaars, R. Ranasinghe, F. Baart, G. Donchyts, and S. Aarninkhof. 2018. The state of the world's beaches. Scientific Reports 8:6641.

Macreadie, P. I., A. Anton, J. A. Raven, N. Beaumont, R. M. Connolly, D. A. Friess, J. J. Kelleway, H. Kennedy, T. Kuwae, P. S. Lavery, C. E. Lovelock, D. A. Smale, E. T. Apostolaki, T. B. Atwood, J. Baldock, T. S. Bianchi, G. L. Chmura, B. D. Eyre, J. W. Fourqurean, J. M. Hall-Spencer, M. Huxham, I. E. Hendriks, D. Krause-Jensen, D. Laffoley, T. Luisetti, N. Marbà, P. Masque, K. J. McGlathery, J. P. Megonigal, D. Murdiyarso, B. D. Russell, R. Santos, O. Serrano, B. R. Silliman, K. Watanabe, and C. M. Duarte. 2019. The future of blue carbon science. Nature Communications 10:3998.

Mcleod, E., G. L. Chmura, S. Bouillon, R. Salm, M. Björk, C. M. Duarte, C. E. Lovelock, W. H. Schlesinger, and B. R. Silliman. 2011. A blueprint for blue carbon: toward an improved understanding of the role of vegetated coastal habitats in sequestering CO_2. Frontiers in Ecology and the Environment 9:552–560.

Middleton, B. A., and K. L. McKee. 2001. Degradation of mangrove tissues and implications for peat formation in Belizean island forests. Journal of Ecology 89:818–828.

Morton, R. A. 2002. Factors Controlling Storm Impacts on Coastal Barriers and Beaches: A Preliminary Basis for near Real-Time Forecasting. Journal of Coastal Research 18:486–501.

Mullins, E., L. J. Moore, E. B. Goldstein, T. Jass, J. Bruno, and O. D. Vinent. 2019. Investigating dune-building feedback at the plant level: Insights from a multispecies field experiment. Earth Surface Processes and Landforms 44:1734–1747.

Olff, H., J. Huisman, and B. F. V. Tooren. 1993. Species dynamics and nutrient accumulation during early primary succession in coastal sand dunes. The Journal of Ecology 81:693–706.

Paerl, H. W., N. S. Hall, A. G. Hounshell, R. A. Luettich, K. L. Rossignol, C. L. Osburn, and J. Bales. 2019. Recent increase in catastrophic tropical cyclone flooding in coastal North Carolina, USA: Long-term observations suggest a regime shift. Scientific Reports 9:10620.

Polis, G. A., W. B. Anderson, and R. D. Holt. 1997. Toward in integration of landscape and food web ecology: The dynamics of spatially subsidized food webs. Annual Review of Ecology and Systematics 28:289.

Ripley, B. S., and N. W. Pammenter. 2008. Physiological characteristics of coastal dune pioneer species from the Eastern Cape, South Africa, in relation to stress and disturbance. Pages 137–154 *in* M. L. Martínez and N. P. Psuty, editors. Coastal Dunes. Springer Berlin Heidelberg, Berlin, Heidelberg.

Ruggiero, P., S. Hacker, E. Seabloom, and P. Zarnetske. 2018. The role of vegetation in determining dune morphology, exposure to sea-level rise, and storm-induced coastal hazards: A U.S. Pacific Northwest perspective. Pages 337–361 *in* L. J. Moore and A. B. Murray, editors. Barrier Dynamics and Response to Changing Climate. Springer International Publishing, Cham.

Ruggiero, P., P. D. Komar, W. G. McDougal, J. J. Marra, and R. A. Beach. 2001. Wave runup, extreme water levels and the erosion of properties backing beaches. Journal of Coastal Research 17:13.

Sallenger, A. H., K. S. Doran, and P. A. Howd. 2012. Hotspot of accelerated sea-level rise on the Atlantic coast of North America. Nature Climate Change 2:884–888.

Seneca, E. D. 1969. Germination response to temperature and salinity of four dune grasses from the Outer Banks of North Carolina. Ecology 50:45–53.

Seneca, E. D., W. W. Woodhouse, and S. W. Broome. 1976. Dune stabilization with *Panicum amarum* along the North Carolina coast. U.S. Army Corps of Engineers, Coastal Research Center, Fort Belvoir, VA, USA.

Tackett, N. W., and C. B. Craft. 2010. Ecosystem development on a coastal barrier island dune chronosequence. Journal of Coastal Research 264:736–742.

Turner, B. L., and E. Laliberté. 2015. Soil development and nutrient availability along a 2 million-year coastal dune chronosequence under species-rich Mediterranean shrubland in southwestern Australia. Ecosystems 18:287–309.

van der Valk, A. G. 1974. Mineral cycling in coastal foredune plant communities in Cape Hatteras National Seashore. Ecology 55:1349–1358.

Willis, A. J. 1963. Braunton Burrows: The effects on the vegetation of the addition of mineral nutrients to the dune soils. Journal of Ecology 51:353–374.

Woodhouse, W. W. 1978. Dune building and stabilization with vegetation. Coastal Engineering Research Center (U.S.).

Woodhouse, W. W., E. D. Seneca, and S. W. Broome. 1977. Effect of species on dune grass growth. International Journal of Biometeorology 21:256–266.

Zarnetske, P. L., S. D. Hacker, E. W. Seabloom, P. Ruggiero, J. R. Killian, T. B. Maddux, and D. Cox. 2012. Biophysical feedback mediates effects of invasive grasses on coastal dune shape. Ecology 93:1439–1450.

Zarnetske, P. L., P. Ruggiero, E. W. Seabloom, and S. D. Hacker. 2015. Coastal foredune evolution: the relative influence of vegetation and sand supply in the US Pacific Northwest. Journal of The Royal Society Interface 12:20150017.

Chapter 2 – Sand supply and dune grass species affect foredune shape along the U.S. Central Atlantic Coast

Katya R. Jay[1], Sally D. Hacker[1], Paige A. Hovenga[2], Laura J. Moore[3], Peter Ruggiero[4]

Affiliations:

1. Department of Integrative Biology, Oregon State University, 3029 Cordley Hall, Corvallis, OR 97331, USA.
2. College of Engineering, Oregon State University, 101 Kearney Hall, Corvallis, OR 97330, USA.
3. Department of Geological Sciences, University of North Carolina at Chapel Hill, 104 South Road, Mitchell Hall, Chapel Hill, NC 27559, USA.
4. College of Earth, Ocean, and Atmospheric Sciences, Oregon State University, 104 CEOAS Administration Building, Corvallis, OR 97330, USA.

In Review

2.1 Abstract

Coastal foredunes form via biophysical feedbacks between sand accretion and burial-tolerant vegetation and protect coastlines from hazards such as sea level rise and extreme storms. Accelerated coastal erosion and climate-driven shifts in dune grass species ranges will likely alter foredune shape and protective services but the mechanisms are understudied, especially at large spatial scales. Here we assess the relative roles of sand supply, beach morphology, and vegetation in determining foredune morphology and its change along a 300-km stretch of the US Central Atlantic coast. We surveyed coastal topography and vegetation to determine beach and dune morphometrics [i.e., beach width, foredune height, foredune width, and foredune aspect ratio (height:width)], shoreline change rate (SCR; a proxy for sand supply to the beach), and grass density for four widespread dune grasses (*Uniola paniculata*, *Ammophila breviligulata*, *Panicum amarum*, *Spartina patens*) along North Carolina barrier islands. Regression models provided evidence that foredune morphology and change metrics are correlated with three main factors: multidecadal SCR (1997-2016), beach morphology, and change in dune grass density. Multidecadal SCR and beach width explained the most variation in, and were positively correlated with, foredune height and width, and were negatively correlated with foredune aspect ratio (height divided by width). In addition, grass density and changes in grass density contributed significantly to foredune morphology change. We found a positive relationship between change in *A. breviligulata* density and foredune width, which aligns with previous studies on the US Atlantic and Pacific Northwest coasts. Our results demonstrate the interactive roles of dune grass

functional morphology, beach morphology, and beach sand supply in dune building processes on highly vulnerable coastlines.

2.2 Introduction

Coastal dunes serve as the first line of defense against erosion and overtopping by ocean waves (Sallenger 2000, Ruggiero et al. 2001, Seabloom et al. 2013) and provide other substantial ecosystem services including recreation, wildlife habitat, and carbon sequestration (Barbier et al. 2011, Drius et al. 2016, Biel et al. 2017). This coastal ecosystem is increasingly at risk as a result of sea level rise and heightened storm intensity (Intergovernmental Panel on Climate Change 2014), as well as pressures from coastal development, which can alter the provisioning of critical ecosystem services (Halpern et al. 2008, Biel et al. 2017). Predicting how coastal dunes, and the services they provide, will change in the future requires an understanding of the relative roles of the physical and ecological processes that shape their structure and function.

Coastal foredunes, or the most seaward dune ridge parallel to the shoreline, are shaped by the interplay between climatic, oceanographic, geomorphic, and ecological processes (e.g., Hesp 1989, Ruggiero et al. 2018). Climate and oceanographic processes affect sea level and wind and wave conditions, which can determine shoreline change rate (SCR), or the rate at which sand is deposited or eroded from the beach. Beach morphology ranges from dissipative (shallow with a wide surf zone) to reflective (steep with a narrower surf zone) depending on beach slope, sediment grain size, and wave conditions (Short and Hesp 1982, Wright and Short 1984). Observational and modeling

studies suggest that foredune morphology is largely shaped by SCR and beach morphology, and can vary depending on the relative importance of beach and dune sediment budgets (e.g., Hesp 1989, 2002, Hacker et al. 2012, Zarnetske et al. 2012, 2015, Duran and Moore 2013, Keijsers et al. 2015, 2016, Moore et al. 2016, Biel et al. 2019). For example, short and narrow foredunes are characteristic of highly eroding, reflective beaches whereas tall and narrow foredunes can form on neutral or slightly retreating shorelines (Hesp and Walker 2013, Duran and Moore 2013, Davidson-Arnott et al. 2018). In contrast, tall, wide foredunes and short, wide foredunes are characteristic of wide and dissipative beaches, where SCRs are high and/or progradational (e.g., Hesp 1984, Psuty 1986).

Once sediment reaches the back-beach via aeolian and wave-driven sediment transport (Cohn et al. 2019b), vegetation can play a key role in shaping foredunes. Burial-tolerant vegetation, such as dune grasses and forbs, slows sand-laden wind causing deposition, which stimulates plant growth and, in turn, leads to further sand deposition (Woodhouse 1978, Hesp 1989, 2002, Hacker et al. 2012, Zarnetske et al. 2012, 2015, Duran and Moore 2013, Keijsers et al. 2015, Harris et al. 2017, Brown and Zinnert 2018, Charbonneau and Casper 2018, Mullins et al. 2019, Biel et al. 2019, Charbonneau et al. 2021). Early studies noted relationships between grass species and dune shape (e.g., Godfrey and Godfrey 1973, Van der Valk 1975, Godfrey 1977, Woodhouse et al. 1977), and more recent empirical and modeling studies suggest that plant density, plant morphology, and differences in lateral versus vertical belowground growth patterns can contribute to the development of a wide range of foredune shapes from short and wide to

tall and narrow and from discontinuous (hummocky or nebkha dunes) to continuous (linear foredunes) (Hesp 2002, Hacker et al. 2012, Zarnetske et al. 2012, Goldstein et al. 2017, Biel et al. 2019, Hesp et al. 2021). Previous research has shown that in addition to sand supply to the beach, dune grass density and growth form are significant moderating factors to dune morphology (Olson 1958, Esler 1970, Arens 1996, Hacker et al. 2012, Zarnetske et al. 2012, 2015, Biel et al. 2019, Hesp et al. 2019). In one study on the US Pacific Northwest coast, Zarnetske et al. (2015) found that timescale determined the relative importance of geomorphic and ecological factors; at annual scale, sand supply to the beach explained a greater proportion of the variation in foredune morphology, but at decadal scale, beachgrass density was more important. In another study over a greater spatial extent, Biel et al. (2019) found that ~50% of the variability in foredune height was attributed to measures of sand supply to the beach, while invasive *Ammophila* beachgrass density comprised another 10% of the variability. Interestingly, as a result of its thinner and denser shoots, the presence of *A. arenaria* (European beachgrass) led to more vertical sand deposition and taller, steeper foredunes compared to *A. breviligulata* (American beachgrass) dominated dunes, which tended to be shorter and wider.

Here, we build on these previous studies by assessing the relative roles of beach sand supply, beach morphology, and vegetation in determining foredune morphology, and its change, along a 300-km stretch of the U.S. Central Atlantic coast. These dunes are highly vulnerable to sea level rise, coastal erosion, and extreme storms. Despite their vulnerability, we know surprisingly little about the processes determining dune morphology, which plays a key role in wave attenuation and flooding risk on barrier

islands (Sallenger 2000), particularly at regional spatial scales. The most widespread species of dune grass in this region is *Uniola paniculata* L. (sea oats), a drought-tolerant C_4 grass that extends from Virginia (VA) to Florida (Seneca 1969, Goldstein et al. 2018). Secondary in abundance is *Ammophila breviligulata* Fernald (American beachgrass), a mid-Atlantic C_3 grass that extends from North Carolina (NC) to Canada and is thought to be heat-intolerant (Goldstein et al. 2018). A transition zone between these species occurs in the NC Outer Banks, where *U. paniculata* dominates dunes in the southern Outer Banks and *A. breviligulata* dominates farther north (Goldstein et al. 2018, Hacker et al. 2019a). Two other dune grass species that are prevalent in the Outer Banks and have similar distributions to *U. paniculata* are *Spartina patens* (Aiton) Muhlenberg (saltmeadow cordgrass) and *Panicum amarum* Elliott (bitter panicgrass).

Past research in this system shows evidence that dune grasses may be important in determining foredune morphology. Previous studies in North Carolina starting in the 1960s used experimental plantings to compare the dune building properties of *U. paniculata*, *A. breviligulata*, and *P. amarum* (Seneca et al. 1976, Woodhouse et al. 1977, Woodhouse 1978). Results showed that foredunes with monocultures of each species achieved similar crest elevations after eight years, but foredunes with *A. breviligulata* monocultures were wider and larger in volume compared to the steeper, narrower dunes created by the other two species (Woodhouse et al. 1977). A recent study by Hacker et al. (2019) described the functional morphology and sand accretion properties of four dune building grass species (the three mentioned above and *Spartina patens*), providing mechanisms for the observed differences in dune building capabilities of these plants, as

previously observed by Esler (1970). They found that *U. paniculata* had fewer, taller shoots compared to *A. breviligulata*, which had dense, clumped shoots and was correlated with the highest rate of sand accretion. In addition, their findings suggested that shoot density and growth form was a stronger factor in determining sand accretion than shoot morphology *per se*.

In this study, our goal was to consider the relative role of ecological and geological factors in explaining the variability in foredune morphology across the Outer Banks of North Carolina, one of the most vulnerable shorelines in North America. We asked the following questions:

1) What is the relative contribution of beach sand supply (hereafter shortened to sand supply), beach morphology, and dune grass density and species in shaping foredune morphology over space and time?
2) Do the dune grass species *A. breviligulata* and *U. paniculata* affect foredune morphology in species-specific ways, and if so, how?

We hypothesized that beach sand supply, beach morphology, and dune grass density and species will shape foredune morphology, with beach sand supply metrics explaining the greatest amount of variability in foredune morphology and its change over time. Based on previous studies (Hacker et al. 2019a, Biel et al. 2019), we also expected a positive relationship between dune grass density and foredune morphology, with increases in foredune height associated with the more vertical growth of *U. paniculata* and increases in foredune width associated with the more horizontal growth of *A. breviligulata*.

To explore these questions and hypotheses, we collected two years of vegetation and beach and dune morphometric data at 90 cross-shore transects over a 300 km stretch of the Outer Banks coastline. We used the spatial variability in the dataset to conduct multivariate regression analyses, model selection (Akaike's information criteria), and hierarchical partitioning to first explore the possible correlations between foredune morphology metrics (i.e., height, width, toe elevation, and aspect ratio) and the explanatory variables of dune grass density (including *U. paniculata*, *A. breviligulata*, and both combined), beach morphometrics (i.e., width, backshore slope, and foreshore slope), and sand supply metrics (i.e., annual and multidecadal shoreline change rate) at a regional scale. In this analysis, we harnessed the large variability in explanatory metrics across space to explore whether differences in vegetation density and species identity, as well as measures of sand supply across space, are related to foredune morphology. The second analysis that we conducted considered whether a change in foredune morphology over a year-long period was related to the same explanatory variables across the coast and thus included a change in foredune morphology over time component.

2.3 Materials and methods

2.3.1 Study region

The study region encompasses foredunes along the NC coastline from Shackleford Banks, NC to False Cape, VA (Figure 2.1, Appendix A, Table A1), a 300-km stretch of sandy barrier islands exhibiting spatial variability in beach geomorphology (Hovenga et al. 2019), vegetation species and density (Hacker et al. 2019a), wave energy, shoreline orientation, and underlying stratigraphy (Lazarus and Murray 2011). The region

is characterized by varying levels of development and management, from undeveloped protected areas (e.g., Cape Lookout National Seashore [CALO] and Cape Hatteras National Seashore) to heavily developed, populated coastlines. The NC coastline, including the study region, is eroding at ~0.7 m yr^{-1} on average, but there is significant spatial variability in shoreline erosion and accretion (Miller et al. 2005, Hovenga et al. 2019). With the exception of tropical hurricanes and nor'easters in the fall and winter, the NC coastline is characterized by a moderately energetic seasonal wind and wave climate, including wind speeds of ~6.8 m s^{-1} and average annual significant wave heights of ~1.2 m (Bryant et al. 2016).

2.3.2 Vegetation and topography field surveys

To characterize a suite of ecological and geomorphic variables, we conducted plant community surveys and collected beach and foredune topography at 90 transects in October 2016 (CALO transects) and June 2017 (northern Outer Banks transects) following the methods of Hacker et al. (2012) (Figure 2.1, Appendix A, Table A1). Most of the transects were placed 2–5 km apart but the distance ranged from 0.4–20.4 km depending on island size and beach access, particularly in developed areas where beaches were not accessible by vehicle. Transects were placed perpendicular to the shoreline at each site, starting at approximately mean lower low water (MLLW) and extending through the dune toe (the seaward-most dune extent), the dune crest (the highest point of foredune elevation), and the dune heel (the lowest point on the landward side of the foredune; Figure 2.2). Quadrats (0.25 m^2) were established every 5 m along the transect within which we counted tiller density of each grass species. We used a Network Real

Time Kinematic Differential Global Positioning System (R7 unit, Trimble, Sunnyvale, CA, USA) to measure the elevation along the beach and dune profile and at each quadrat along the foredune. We resampled all 90 cross-shore transects one year after they were originally surveyed (October 2017 for CALO transects and June 2018 for northern Outer Banks transects).

2.3.3 Beach and foredune morphometrics

We extracted beach and foredune morphometrics at each transect from field topography data following the methods of Mull and Ruggiero (2014) (see Figure 2.2 for details of the morphometric measures). Shoreline position, defined as the approximate location of mean high water (MHW), was extracted using the 0.4 m contour referenced to the North American Vertical Datum 1988 (NAVD88) (Hovenga et al. 2019). Foredune morphometric response variables included foredune toe and foredune crest elevation (m; relative to MHW), foredune width (m; horizontal distance between the foredune toe and crest), and foredune aspect ratio (foredune height divided by width). Beach morphometric parameters included beach width (distance between MHW and foredune toe), backshore slope (slope between MHW and foredune toe), and foreshore slope (slope in the vicinity of the shoreline position). Change in foredune and beach morphometrics were calculated as the annual difference between these values.

2.3.4 Shoreline change rate data

We calculated two SCR metrics (i.e., the rate at which the shoreline position at a given location moves seaward or landward and a proxy for sand supply to the beach; Farris and List 2007): annual and multidecadal. Both SCR metrics were annual measures,

or meters of change per year. Annual SCR was calculated for each survey transect using the topographic data to measure the change in shoreline position from one year to the next. Multidecadal SCR was calculated in two ways given the availability of airborne lidar data for different locations within the study region. For the CALO transects, multidecadal SCR was calculated as the average annual change from 1997 to 2016 using airborne lidar data from NOAA's Digital Coast website as described in Hovenga et al. (2019). For the northern Outer Banks from Ocracoke Island to False Cape, VA, multidecadal SCR was calculated as the average annual change from 1997 to 2010 using USGS shoreline position data from Kratzmann et al. (2017). For both multidecadal SCR calculations, cross-shore profiles were extracted at survey transect locations and shoreline positions were defined with a spatially varying MHW contour ranging from 0.33-0.46 meters (referenced to NAVD88).

2.3.5 Statistical analyses

We used R v.3.6.1 (R Development Core Team 2019) for all statistical analyses. Additive and multiplicative linear regression models (glm in R) were used to explore correlations between individual foredune morphology variables and multiple explanatory variables. We used Akaike's information criterion (AIC; multiple top models were considered within 4 ΔAIC; Burnham et al. 2002) to select the top models that best describe the relationships. AIC uses an estimator to predict model error and thus the relative quality of different models for a given set of data. We then used hierarchical partitioning analyses (hier.part in R) with R^2 as the goodness-of-fit metric to quantify the proportion of variance explained by each explanatory variable. Before models were run,

Shapiro-Wilk tests and residual and normal quantile plots were used to assess whether variables conformed to the assumptions of linear regression, and transformations were used if necessary. Two-sided one sample *t*-tests were used to quantify whether changes in beach and foredune morphology and vegetation density metrics (the change from one year to the next) differed from the null value of zero (i.e., no change).

For the models, the response variables included foredune morphology metrics (height, width, toe elevation, and aspect ratio, and the annual change in these parameters) and the explanatory variables included beach sand supply (annual and multidecadal SCR), beach morphology (beach width, annual change in beach width, backshore slope, and foreshore slope), and dune grass density. Dune grass density in the quadrats (per 0.25 m^2) were averaged within transects and included: mean combined tiller density of the four dominant grass species, mean *A. breviligulata* tiller density, mean *U. paniculata* tiller density, mean combined tiller density of *A. breviligulata* and *U. paniculata*, annual change in *A. breviligulata* tiller density, and annual change in *U. paniculata* tiller density. Fifteen transects adjacent to inlets and capes (Figure 2.3a, b, Appendix A, Table A1) with high erosional or progradational multidecadal SCRs were excluded, resulting in 75 transects total used in the statistical analyses.

2.4 Results

2.4.1 Temporal and spatial patterns in beach and foredune morphology and vegetation

Sand supply and beach morphology metrics varied greatly throughout the study region. Of the 75 transects used in our analyses, we found that annual SCR values were more extreme (range: -31.8 to 32.4 m yr^{-1}, mean ± S.E.: 2.9 ± 1.5 m yr^{-1}) than

multidecadal values (-3.8 m to 4.2 m yr^{-1}, -0.5 ± 0.2 m yr^{-1}) and there was no clear pattern with latitude (Figure 2.3a, b). In contrast, multidecadal SCRs show that, over a time period of roughly two decades, beaches in CALO have been primarily eroding (89% have negative values), while many beaches from Ocracoke Island northward have been accreting (59% have positive values) (Figure 2.3b). Beach width ranged from 4.4 m to 99.6 m (38.0 ± 2.2 m), with generally wider beaches in the north (Figure 2.3c). Overall, beach width declined on average by -0.7 ± 1.3 m over the year, but this decrease was not statistically significant (p=0.619; Figure 2.3d). Moreover, multidecadal SCR and beach width were positively correlated, with wider beaches associated with positive and higher multidecadal SCR values. Backshore and foreshore slopes averaged 0.05 ± 0.003 and 0.08 ± 0.004, respectively, with typically more steeply sloped beaches in the north compared to CALO in the south (Figure 2.3f).

Foredune morphology also varied greatly across the study region, with some metrics displaying latitudinal trends. In particular, foredune height (mean ± S.E.: 5.3 ± 0.2 m), width (42.4 ± 3.5 m), and toe elevation (2.1 ± 0.01 m) increased northward (Figure 2.4a-c), while foredune aspect ratio showed no latitudinal trend (Figure 2.4d). Changes in foredune morphology also occurred at the annual timescale, with an average increase in crest elevation of 0.11 ± 0.03 m (Figure 2.4e; t=3.165, df=71, p=0.002) and an average increase in toe elevation of 0.15 ± 0.06 m (Figure 2.4g; t=2.317, df=71, p=0.023). Foredune aspect ratio did not change at the annual timescale (Figure 2.4h; p=0.914).

Our results also show differences in dune grass species tiller density across the study region and over the year. *Uniola paniculata* was most abundant, *A. breviligulata* and *P.amarum* had intermediate abundance, and *S. patens* was least abundant, but this depended on the island (Figure 2.1b) (also see Hacker et al. 2019 for vegetation patterns). The northern islands generally had more *A. breviligulata* and *P. amarum* compared to the southern islands, which had more *U. paniculata*. Average tiller densities did not change over the course of one year for any of the dune grass species (Figure 2.3g, h; *U. paniculata* p=0.935, *P. amarum* p=0.124, *A. breviligulata* p=0.255, and *S. patens* p=0.325).

2.4.2 Regression models, hierarchical partitioning, and controls on foredune morphology

Regression models and hierarchical partitioning analyses showed correlations between foredune morphology and several explanatory variables (beach sand supply, beach morphology, and changes in dune grass density, particularly *A. breviligulata* density), but the relative importance of these factors and the strength of the correlations depended on the foredune morphology metric considered (Figure 2.5, Appendix B, Table B1). For the foredune morphology variables as a group, SCR (range: 20.4–45.3%) and beach morphology (31.2–69.9%) variables made up the greatest proportion of overall variance explained compared to that of the dune grass variables (9.7–28.2%) (Figure 2.5, Appendix B, Table B2).

The top model for foredune height showed positive correlations with multidecadal SCR and an interaction between beach width and backshore slope, but negative correlations with backshore slope and beach width (Figure 2.5, Appendix B, Table B1).

In the next best model (but not a top model due to its ΔAIC > 4), foredune height was positively correlated with multidecadal SCR and beach width, and negatively correlated with change in *A. breviligulata* tiller density. Hierarchical partitioning showed that multidecadal SCR, beach width, combined dune grass density, and change in *A. breviligulata* tiller density comprised 40.6%, 20.3%, 11.1%, and 9.2% of explained variance in foredune height, respectively (Figure 2.5, Appendix B, Table B2).

Top models for foredune width showed positive correlations with both SCR metrics, beach width, and foreshore slope, and a negative correlation with change in *A. breviligulata* density (Figure 2.5, Appendix B, Table B1). Hierarchical partitional showed that beach width, multidecadal SCR, and foreshore slope comprised the greatest proportion of explained variance in foredune width (34.7%, 32.2%, and 10.1%, respectively) (Figure 2.5, Appendix B, Table B2).

Top models for foredune toe elevation showed positive correlations with backshore slope (33.0% explained variance) and multidecadal SCR (20.8% explained variance), and negative correlations with a change in *A. breviligulata* tiller density (21.3 % explained variance) (Figure 2.5, Appendix B, Table B1, Table B2). Finally, models for foredune aspect ratio were less strong overall, but showed negative correlations with multidecadal SCR (13.7% explained variance) and beach width (37.4% explained variance), and positive correlations with backshore slope (24.6% explained variance) (Figure 2.5, Appendix B, Table B1,). In one of our models (but not a top model due to its ΔAIC > 4), foredune aspect ratio was negatively correlated with mean *A. breviligulata* density.

In contrast, for the group of foredune morphology change variables, dune grass variables (range: 34.9–49.5%) and beach morphology (14.6–63.0%) metrics comprised the greatest proportion of explained variance compared to that of the SCR variables (1.2–45.9%) (Figure 2.5, Appendix B, Table B1, Table B2). The proportion of unexplained variance in our hierarchical partitioning models was also higher for the foredune morphology change metrics (Figure 2.5a). Regression models showed that foredune height change was positively correlated with a change in *A. breviligulata* tiller density and negatively correlated with backshore slope (Figure 2.5, Appendix B, Table B1). In addition, backshore slope, change in *A. breviligulata* tiller density, and beach width comprised 46.7%, 31.3%, and 9.6% of variation in foredune height change (Figure 2.5, Appendix B, Table B2). For foredune width change, both top models showed a positive relationship with annual SCR and change in *A. breviligulata* tiller density, and one model showed a positive correlation with beach width while the other showed a positive correlation with backshore slope (Figure 2.5, Appendix B, Table B1). However, the only significant term in these models was change in *A. breviligulata* tiller density. Hierarchical partitioning showed that change in *A. breviligulata* tiller density, beach width, and annual SCR comprised 43.9%, 23.8%, and 15% of explained variance, respectively (Figure 2.5, Appendix B, Table B2). Top models for foredune toe elevation change showed negative correlations with a change in *A. breviligulata* tiller density (34.3% explained variance), multidecadal SCR (19.3% explained variance), and backshore slope (not a significant term in the model), and a positive correlation with beach width (25.0% explained variance) (Figure 2.5, Appendix B, Table B1, Table B2). Foredune aspect ratio change

was negatively correlated with annual SCR (39.8% explained variance) and a change in *A. breviligulata* tiller density (29.8% explained variance) and positively related to a change *U. paniculata* density (16.8% explained variance, although not significant in regression models) (Figure 2.5, Appendix B, Table B1, Table B2).

2.5 Discussion

Our analyses support the role of beach sand supply, beach morphology, and vegetation density as significant factors shaping foredune morphology in US Central Atlantic coast dunes, but the relative importance of these variables varied depending on the foredune morphology metric considered. Overall, we found that taller and wider foredunes were positively associated with increasing beach sand supply (measured as multidecadal SCR) and beach width (Figure 2.5, Appendix B, Table B1, Table B2), as has been found in previous studies (e.g., Short and Hesp 1982, Sherman and Bauer 1993, Hesp and Smyth 2016, Biel et al. 2019). But vegetation density also played a role; combined dune grass density was associated with taller and wider foredunes and explained a similar amount of variability (~10%; Figure 2.5b, Appendix B, Table B2) in these metrics compared to those in Pacific Northwest dunes (Biel et al. 2019). Moreover, as with Biel et al. (2019), an annual change in dune grass density explained a greater proportion of variance in changes in foredune morphology than beach sand supply and beach metrics. There were also strong species-specific differences: *A. breviligulata* density was more important in shaping foredune morphology than *U. paniculata*, particularly with respect to increases in foredune width. Even though beach sand supply had the largest effect on foredune morphology, our results reinforce those of other studies

that detail the importance of vegetation and the biophysical feedbacks it serves to generate (Zarnetske et al. 2012, 2015, Keijsers et al. 2016, Cheng et al. 2019, Biel et al. 2019).

Our statistical models best predicted foredune height and foredune width compared to foredune toe elevation, foredune aspect ratio, or any of the foredune change metrics. For example, most of the foredune change models had lower R^2 values, which may in part be a consequence of the dynamic nature of the NC Outer Banks and the fact that foredune morphology changes were measured over only a one-year period. On the Pacific Northwest coast, Zarnetske et al. (2015) found stronger support for their foredune morphology change models than we did here, possibly because of the longer timescales used in their study and the high sand delivery to those beaches and dunes. In contrast, the NC Outer Banks are characterized by frequent storm events and prevalent destructive forces, leading to pervasive overwash and erosion at our study sites (Hovenga et al. in press); these factors, in comparison to sand supply and dune grass density, could have played a role in some of the foredune morphology changes that we observed.

2.5.1 Relationships between beach sand supply, beach morphology, and foredune morphology

Our regression models and hierarchical partitioning results suggest that foredune morphology is strongly related to SCR and beach width, both factors that drive sand supply to foredunes (Farris and List 2007, Biel et al. 2019), and vary regionally in our study region. Foredunes along Cape Hatteras and northward tended to be taller and wider, where multidecadal SCR values were more positive and beaches were typically wider, and shorter and narrower to the south where SCRs were often negative (Figures 2.3b,

2.4a, b). Besides differences in absolute height and width, we also observed a continuum in foredune shape from high aspect ratio dunes (height more equivalent to width) to low aspect ratio dunes (height much shorter than width) (Figure 2.4d). Foredune aspect ratio was negatively related to both multidecadal SCR and beach width (Appendix B, Table B1, Table B2), indicating that dunes in areas with higher positive SCRs and therefore wider beaches had lower aspect ratios; at our field sites these were relatively high volume dunes that were much wider than tall and gently sloping. Likewise, in areas where SCRs were neutral or negative, and beaches were narrow, foredunes tended to have high aspect ratios and steeper slopes. The factors important to the differences in the absolute height and width of foredunes, as well as their aspect ratio, have been considered in a handful of other empirical studies in different regions of the world (Short and Hesp 1982, Bauer and Davidson-Arnott 2002, Biel et al. 2019). These studies show that taller and wider dunes are typically found on wider beaches. Field and modeling studies have demonstrated that this finding may be explained by longer duration aeolian transport and wind steering (Short and Hesp 1982, Duran and Moore 2013, Hesp and Smyth 2016). Wider beaches allow for sand transport to the dune to occur for a longer period of time before dune topography, associated with taller dunes, steers the wind above the beach, reducing sand transport.

Most beaches along the NC coastline are 20-60 m wide with a handful of exceptions near island inlets and capes, where beach width can exceed 150 m (and dune growth is complicated by high shoreline curvature and associated changes in local wind forcing conditions) or where beaches are more severely eroded (Figure 2.3c). For this

reason, unlike research on the Pacific Northwest coast (Hacker et al. 2012, Zarnetske et al. 2015, Ruggiero et al. 2016, 2018, Biel et al. 2019), beaches in this study area are not wide enough to test the Psuty (1986) conceptual model. The model hypothesizes that on rapidly prograding beaches at the extreme end of positive SCR and beach width, multiple short and wide foredunes will develop over time. Psuty (1986) also posited that foredune development is enhanced (increased height) under slightly negative beach sand supply but high dune sand supply; our data on the NC coast does not fully support this hypothesis, as we observed taller dunes in areas with relatively higher multidecadal SCR and thus greater sand supply to the beach and dune.

2.5.2 Relationships between vegetation density and foredune morphology

Our findings that an increase in *A. breviligulata* density had the greatest effect on foredune height and width, and the annual changes in these values, of all the dune grass species supports previous experimental research showing that *A. breviligulata* builds dunes of similar height, but greater width, compared to *U. paniculata* or a combination of *U. paniculata* and *P. amarum* (Woodhouse et al. 1977). Moreover, our results are similar to findings in the Pacific Northwest where *A. breviligulata* tends to widen foredunes and *A. arenaria* tends to build taller foredunes (Hacker et al. 2012, Zarnetske et al. 2012, 2015, Biel et al. 2019). This widening of foredunes is likely the result of the growth form of *A. breviligulata*, which includes dense, clumped shoots coupled with horizontally-growing rhizomes that spread seaward at the foredune toe (Hacker et al. 2012, 2019a, Biel et al. 2019). *Ammophila arenaria*, in contrast, grows more vertically and more densely, resulting in taller and more steeply sloped dunes. Interestingly, we also found

that an increase in *A. breviligulata* density was negatively correlated with the elevation of the foredune toe (Appendix B, Table B2). The rapid lateral spread of *A. breviligulata* (~2-3 m yr^{-1}; Woodhouse et al. 1977) coupled with high sand supply to dunes would likely result in sand accretion in the seaward direction (downslope), ultimately producing shorter dune toe elevations and wider dunes overall. Furthermore, an increase in *A. breviligulata* density was negatively correlated with a change in foredune aspect ratio, supporting the hypothesis that this beachgrass builds wider, shallower, low aspect ratio dunes. In contrast, an increase in *U. paniculata* density was positively correlated with narrowing and steepening of foredunes, a possible result of slower lateral spread of *U. paniculata* compared to *A. breviligulata* (Woodhouse et al. 1977, Hacker et al. 2019a).

The species-specific differences in foredune morphology that we document here also support the functional morphological characteristics we have documented previously. In the same study region, Hacker et al. (2019) found that, for a given area, *A. breviligulata*, *U. paniculata* and *P. amarum* had similar plant densities but varied in shoot density, with *A. breviligulata* having almost double the number of shoots. As a result, when *A. breviligulata* grows in a monoculture, it accretes ~42% more sand (measured over a one-year period) compared to the other two species. Our results also confirm the finding in Hacker et al. (2019) that, in field settings, other morphological differences in these grasses, including the height and weight of the shoots (e.g., *U. paniculata* had taller and heavier shoots than *A. breviligulata*, *P. amaru*m, or *S. patens*), are unlikely to be as important to sand accretion as shoot density and growth form, a finding that is also

supported by flow studies with vegetation (Zarnetske et al. 2012, ChenChen et al. 2018, Cheng et al. 2019, Hesp et al. 2019, Charbonneau et al. 2021).

Our finding that the change in foredune morphometrics over a year-long period was correlated to vegetation density, particularly *A. breviligulata* density, was an unexpected result. Given that the Outer Banks and Shackleford Banks experience highly variable annual SCRs (Figure 2.3a, b) and frequent disturbances from hurricanes (Hovenga et al. 2019, in press), we expected that physical factors would mostly dominate as controlling factors and that there would be a lag between erosion or deposition events and the growth response of vegetation. For example, (Zarnetske et al. 2015) found that invasive *A. breviligulata* on dunes in northern Oregon and southern Washington, which experience mostly positive SCRs, explained more of the variation in increases in dune height and width at decadal timescales (~50%–75% depending on the metric) compared to interannual timescales (~20–40%). However, despite these differences, it is interesting to note that the variance explained by vegetation at annual timescales is similar between our study and Zarnetske et al. (2015) and suggests that *A. breviligulata* is able to spread and accrete sand relatively quickly especially under positive beach sand supply conditions.

2.5.3 Implications of changes in vegetation and shoreline change rate on foredune morphology

Understanding the relative influence of beach sand supply, beach morphology, and vegetation on coastal dune evolution is especially critical as climate change will mediate these factors, influencing foredune morphology, and in turn, dune ecosystem services. One aspect of climate change to dune morphology that is underappreciated is

possible range shifts in dune grass species. A literature survey conducted by Goldstein et al. (2018) showed that the southern range limit of *A. breviligulata* is Cape Fear, NC, while the northern range limit of *U. paniculata* is Assateague Island in VA and Maryland (a likely result of their differing physiological tolerance). Based on comparisons in the literature, they also found a slight northward range expansion in *U. paniculata*, possibly associated with recent warming trends (range shifts for *A. breviligulata* were inconclusive). However, a glasshouse study by Harris et al. (2017) found that both physiological (electron transport rate) and morphological (relative growth rate, biomass) vigor of *A. breviligulata* diminished when planted in mixture with *U. paniculata*, while *U. paniculata* performance was unaffected by the presence of *A. breviligulata*. These findings suggest that *U. paniculata* could outcompete and displace *A. breviligulata* in parts of its current range as a result of climate change induced warming, with implications for foredune morphology and coastal vulnerability along the US Atlantic coast. A northward shift in *U. paniculata* abundance could alter foredune morphology, with wider, low aspect ratio *A. breviligulata* dominated dunes being replaced by narrower, higher aspect ratio *U. paniculata* dominated dunes. At our field sites, *A. breviligulata* was also associated with taller foredunes, but this result was confounded by latitudinal trends in beach sand supply and our finding that *A. breviligulata* density was negatively correlated with foredune height. While foredune height may be affected by shifts in dune grass dominance, previous experimental work in NC dunes showed that *U. paniculata* and *A. breviligulata* built dunes of similar height (Woodhouse et al. 1977), suggesting that foredune width and aspect ratio are more likely to be affected. These

changes in morphology could alter the protective services that foredunes provide against storm wave runup and inundation. For example, model simulations by Itzkin et al. (in press) suggest that low aspect ratio dunes are more resistant to volumetric erosion during long duration but low intensity storms, while high aspect ratio dunes are more protective during short-duration, high intensity storms. Thus, morphological differences in foredune shape, reinforced over time by dune grass species-specific feedbacks, could have important implications for coastal vulnerability.

Our findings demonstrate the interactive roles of dune grass functional morphology, beach morphology, and beach sand supply in dune building processes on vulnerable Atlantic Coast barrier islands. Understanding how dunes are modified by geologic and climate processes, as well as human-induced changes, will allow us to predict how their ecosystem services are likely to change in the future. Further observations, experimental manipulations, and modeling efforts are needed to fully understand how dune vegetation will respond to climate change and what the consequences will be for foredune evolution.

2.6 Acknowledgements

Funding was provided by the US National Oceanic and Atmospheric Administration (NOAA) via the NOS/NCCOS/CRP Ecological Effects of Sea Level Rise Program (grant no. NA15NOS4780172) to P.R., S.D.H., and L.J.M. and the Garden Club of America Fellowship in Ecological Restoration to K.R.J. Special thanks to R. Mostow, C. Hagen, M. Itzkin, J. Stepanek, E. Mullins, I. Reeves, J. Wood, N. Cohn, E. Goldstein, C. Magel, and R. Biel for assistance with field data collection. We thank two anonymous reviewers for suggestions that improved the manuscript.

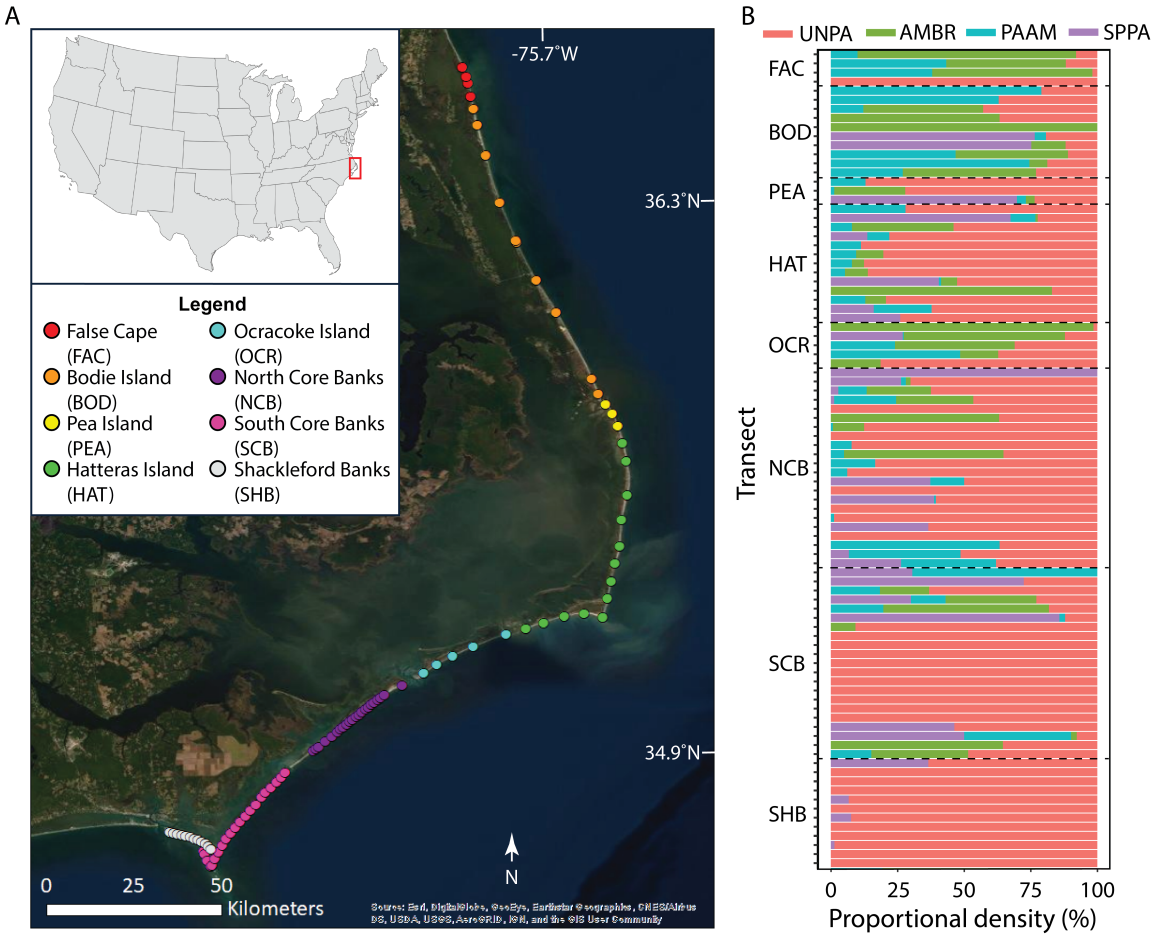

Figure 2.1. Transect locations and dune grass abundance within the study area from north to south. (A) Map of study sites and transect locations along the 300-km stretch of the Atlantic coast from Shackleford Banks, NC to False Cape, VA, USA (see Appendix A, Table A1 for transect locations). (B) Proportional density (tillers $0.25m^{-2}$) of four dominant NC dune grasses [*Uniola paniculata* (UNPA), *Ammophila breviligulata* (AMBR), *Panicum amarum* (PAAM), and *Spartina patens* (SPPA)]. Island abbreviations are givein in the legend and dashed lines represent borders between islands.

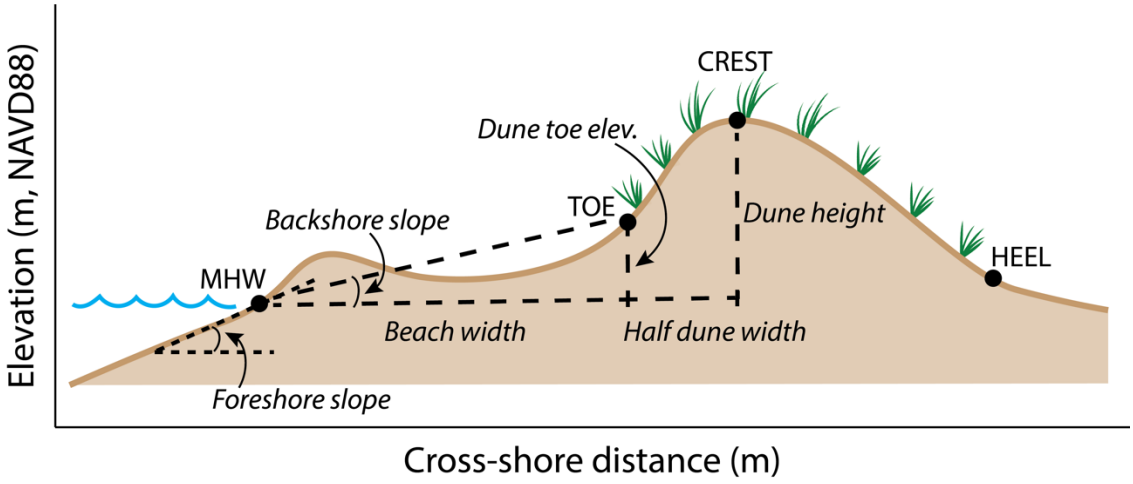

Figure 2.2. Diagram of beach and foredune morphometric parameters measured and calculated using data from real-time kinematic GPS surveys following the methods of Mull and Ruggiero (2014). MHW refers to mean high water, extracted using the 0.3 m MHW contour (NAVD88). Foredune morphometrics measured included the position and elevation of the foredune toe (the seaward extent of the foredune), the foredune crest (the highest point of the foredune), and the foredune heel (the landward extent of the foredune ridge, determined by an elevation minimum). Foredune height and toe elevation were calculated as the difference between MHW and foredune crest and foredune toe elevation, respectively. Foredune width was calculated as one-half dune width, or the horizontal distance between the foredune toe and crest, in order to capture changes in the width of the foredune face. Beach width was calculated as the horizontal distance between MHW and the foredune toe. Change in morphology metrics was calculated as the difference between these parameters from 2016-17. We determined backshore slope as the slope between MHW and the dune toe, and foreshore slope was calculated as the slope in the vicinity of MHW.

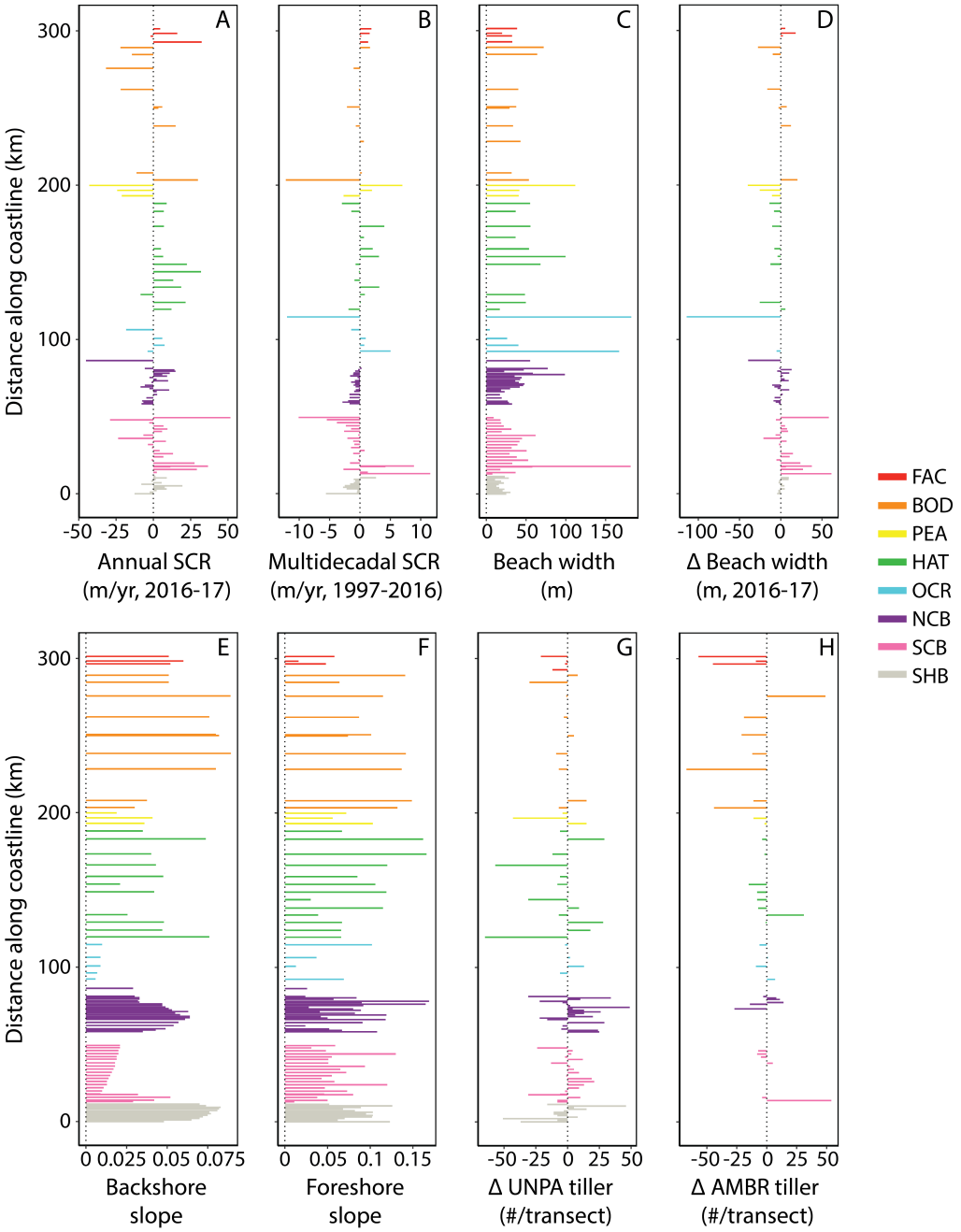

Figure 2.3. Beach sand supply, beach geomorphology, and vegetation density explanatory variables from 2016-2017 (unless otherwise indicated), with distance (km) along coast from the southwestern-most transect. Beach geomorphology variables were calculated as shown in Figure 2.2. (A) Annual shoreline change rate (SCR; m yr^{-1}). (B) Multidecadal SCR (m yr^{-1}). See text for calculation details. (C) Beach width (m). (D) Change in beach width (m). (E) Backshore slope. (F) Foreshore slope. (G) Change in *Uniola paniculata* (UNPA) tiller number. (H) Change in *Ammophila breviligulata* (AMBR) tiller number. Island abbreviations are as described in Figure 2.1.

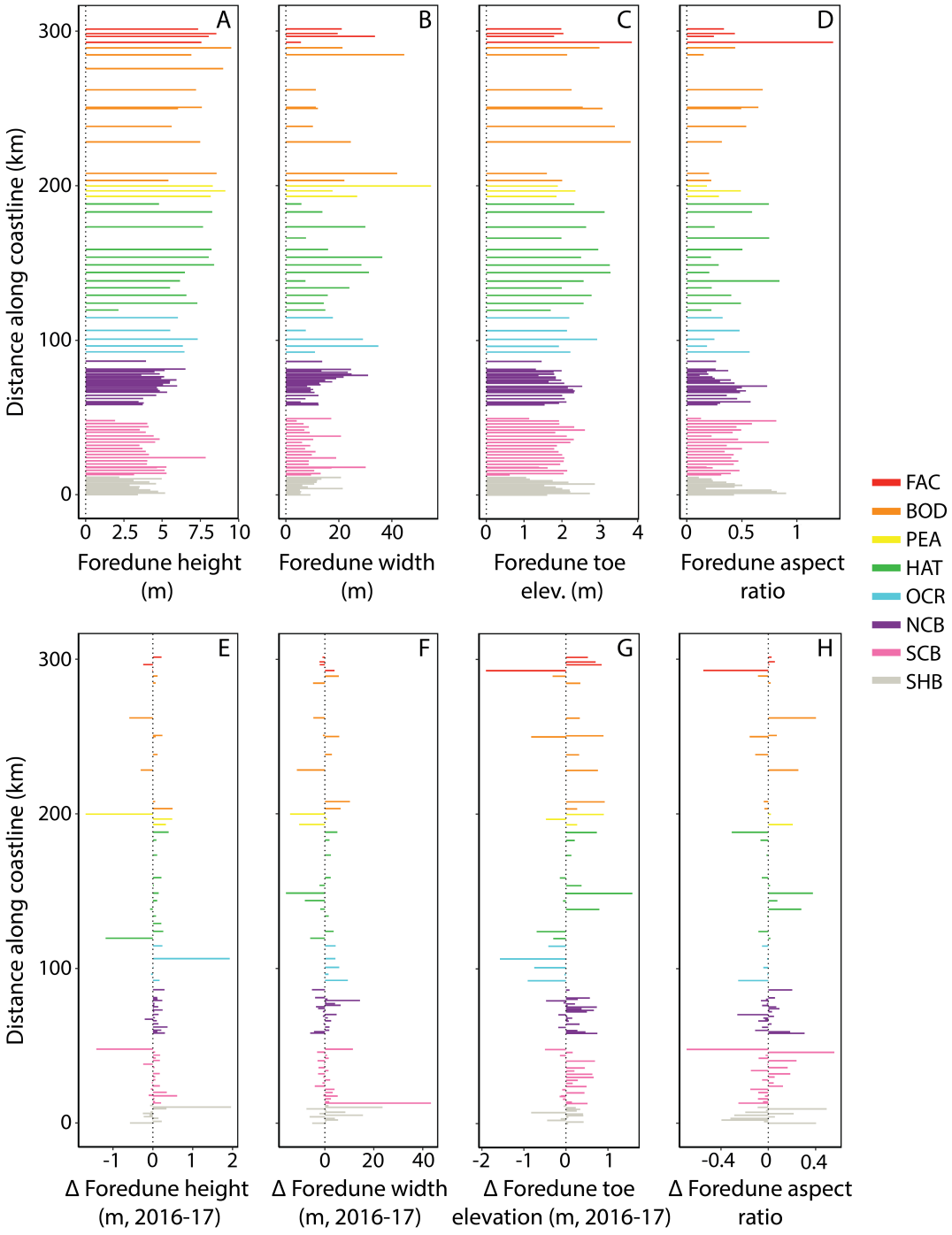

Figure 2.4. Foredune morphology response variables (see Figure 2.2) from 2016-2017, with distance (km) along coast from the southwestern-most transect. Island abbreviations are as described in Figure 2.1.

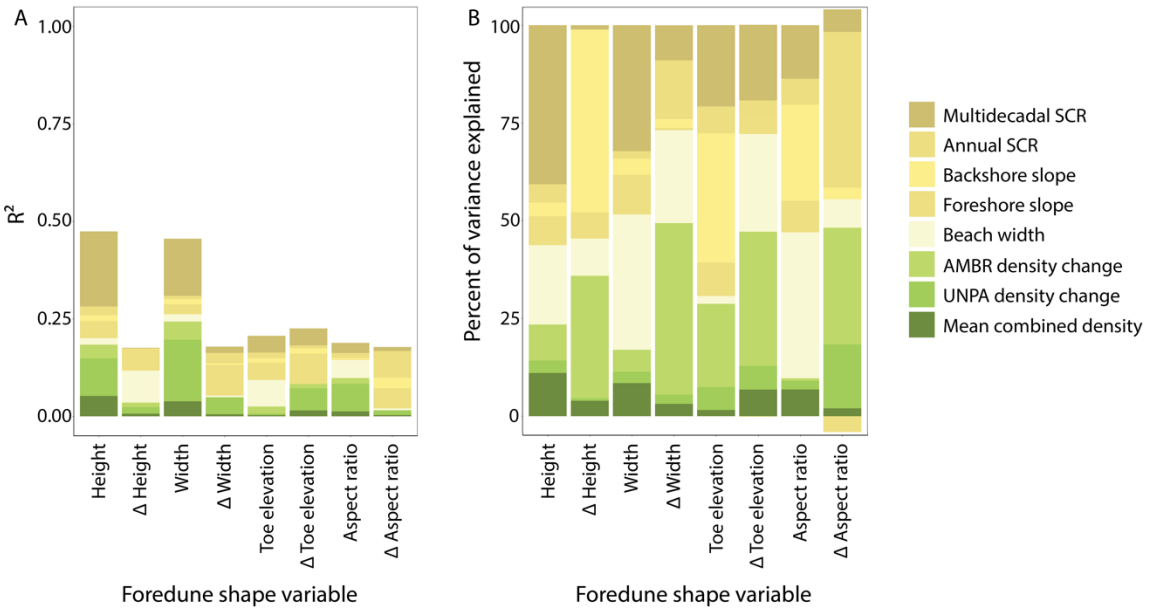

Figure 2.5. Results of hierarchical partitioning analyses. (A) Independent contribution (R^2) of each explanatory variable [shoreline change rate (SCR) and beach morphology (light brown) and dune grass (green)] for each foredune morphology response variable. (B) Variation (%) explained by the same explanatory variables for each foredune morphology response variable. Abbreviations are as described in Figure. 2.1.

2.7 References

Arens, S. M. 1996. Patterns of sand transport on vegetated foredunes. Geomorphology 17:339–350.

Barbier, E. B., S. D. Hacker, C. Kennedy, E. W. Koch, A. C. Stier, and B. R. Silliman. 2011. The value of estuarine and coastal ecosystem services. Ecological Monographs 81:169–193.

Bauer, B. O., and R. G. D. Davidson-Arnott. 2002. A general framework for modeling sediment supply to coastal dunes including wind angle, beach geometry, and fetch effects. Geomorphology 49:89–108.

Biel, R. G., S. D. Hacker, P. Ruggiero, N. Cohn, and E. W. Seabloom. 2017. Coastal protection and conservation on sandy beaches and dunes: context-dependent tradeoffs in ecosystem service supply. Ecosphere 8:e01791.

Biel, R. G., S. D. Hacker, and P. Ruggiero. 2019. Elucidating coastal foredune ecomorphodynamics in the U.S. Pacific Northwest via bayesian networks. Journal of Geophysical Research: Earth Surface 124:1919–1938.

Brown, J. K., and J. C. Zinnert. 2018. Mechanisms of surviving burial: Dune grass interspecific differences drive resource allocation after sand deposition. Ecosphere 9:e02162.

Bryant, M. A., T. J. Hesser, and R. E. Jensen. 2016. Evaluation statistics computed for the Wave Information Studies (WIS). U.S. Army Engineer Research and Development Center, Vicksburg, MS, USA.

Burnham, K. P., D. R. Anderson, and K. P. Burnham. 2002. Model selection and multimodel inference: a practical information-theoretic approach. 2nd ed. Springer, New York.

Charbonneau, B., and B. B. Casper. 2018. Wind tunnel tests inform *Ammophila* planting spacing for dune management. Shore & Beach 86:37–46.

Charbonneau, B. R., S. M. Dohner, J. P. Wnek, D. Barber, P. Zarnetske, and B. B. Casper. 2021. Vegetation effects on coastal foredune initiation: Wind tunnel experiments and field validation for three dune-building plants. Geomorphology:107594.

ChenChen, L., Z. Zhongquan, C. Hong, and Z. Xueyong. 2018. Airflow around single and multiple plants. Agricultural and Forest Meteorology 252:27–38.

Cheng, H., W. He, C. Liu, X. Zou, L. Kang, T. Chen, and K. Zhang. 2019. Transition model for airflow fields from single plants to multiple plants. Agricultural and Forest Meteorology 266–267:29–42.

Cohn, N., P. Ruggiero, G. García-Medina, D. Anderson, K. A. Serafin, and R. G. Biel. 2019. Environmental and morphologic controls on wave-induced dune response. Geomorphology 329:108–128.

Davidson-Arnott, R., P. Hesp, J. Ollerhead, I. Walker, B. Bauer, I. Delgado-Fernandez, and T. Smyth. 2018. Sediment budget controls on foredune height: Comparing simulation model results with field data. Earth Surface Processes and Landforms 43:1798–1810.

Drius, M., M. L. Carranza, A. Stanisci, and L. Jones. 2016. The role of Italian coastal dunes as carbon sinks and diversity sources. A multi-service perspective. Applied Geography 75:127–136.

Duran, O., and L. J. Moore. 2013. Vegetation controls on the maximum size of coastal dunes. Proceedings of the National Academy of Sciences 110:17217–17222.

Esler, A. E. 1970. Manawatu sand dune vegetation. Botam' Division, D.S.l.R.. Auckland 17:6.

Farris, A. S., and J. H. List. 2007. Shoreline change as a proxy for subaerial beach volume change. Journal of Coastal Research 23:740–748.

Godfrey, P. J. 1977. Climate, plant response and development of dunes on barrier beaches along the U.S. East Coast. International Journal of Biometeorology 21:203–215.

Godfrey, P. J., and M. M. Godfrey. 1973. Godfrey 1973 Comparison of geological and geomorphic interactions between altered and unaltered barrier island systems in North Carolina. Pages 239–258 *in* D. R. Coates, editor. Coastal Geomorphology. State Univeristy of New York, Binghamton.

Goldstein, E. B., L. J. Moore, and O. Durán Vinent. 2017. Lateral vegetation growth rates exert control on coastal foredune hummockiness and coalescing time. Earth Surface Dynamics 5:417–427.

Goldstein, E. B., E. V. Mullins, L. J. Moore, R. G. Biel, J. K. Brown, S. D. Hacker, K. R. Jay, R. S. Mostow, P. Ruggiero, and J. C. Zinnert. 2018. Literature-based latitudinal distribution and possible range shifts of two US east coast dune grass species (*Uniola paniculata* and *Ammophila breviligulata*). PeerJ 6:e4932.

Hacker, S. D., P. Zarnetske, E. Seabloom, P. Ruggiero, J. Mull, S. Gerrity, and C. Jones. 2012. Subtle differences in two non-native congeneric beach grasses significantly affect their colonization, spread, and impact. Oikos 121:138–148.

Hacker, S. D., K. R. Jay, N. Cohn, E. B. Goldstein, P. A. Hovenga, M. Itzkin, L. J. Moore, R. S. Mostow, E. V. Mullins, and P. Ruggiero. 2019. Species-specific functional morphology of four US Atlantic Coast dune grasses: Biogeographic implications for dune shape and coastal protection. Diversity 11:82.

Halpern, B. S., S. Walbridge, K. A. Selkoe, C. V. Kappel, F. Micheli, C. D'Agrosa, J. F. Bruno, K. S. Casey, C. Ebert, H. E. Fox, R. Fujita, D. Heinemann, H. S. Lenihan, E. M. P. Madin, M. T. Perry, E. R. Selig, M. Spalding, R. Steneck, and R. Watson. 2008. A global map of human impact on marine ecosystems. Science 319:948–952.

Harris, A. L., J. C. Zinnert, and D. R. Young. 2017. Differential response of barrier island dune grasses to species interactions and burial. Plant Ecology 218:609–619.

Hesp, P. A. 1984. Foredune formation in southeast Australia. Pages 69–97 *in* B. G. Thom, editor. Coastal Geomorphology in Australia. Academic Press, Sydney.

Hesp, P. A. 1989. A review of biological and geomorphological processes involved in the initiation and development of incipient foredunes. Proceedings of the Royal Society of Edinburgh, Section B: Biological Sciences 96:181–201.

Hesp, P. 2002. Foredunes and blowouts: initiation, geomorphology and dynamics. Geomorphology 48:245–268.

Hesp, P. A., and I. J. Walker. 2013. Aeolian environments: coastal dunes. Pages 109–133 *in* J. Shroder, N. Lancaster, D. J. Sherman, and A. C. W. Baas, editors. Treatise on Geomorphology. Academic Press, San Diego, CA.

Hesp, P. A., and T. A. Smyth. 2016. Surfzone-beach-dune interactions: Review and the role of the intertidal beach. Journal of Coastal Research S.I. 75:8–12.

Hesp, P. A., Y. Dong, H. Cheng, and J. L. Booth. 2019. Wind flow and sedimentation in artificial vegetation: Field and wind tunnel experiments. Geomorphology 337:165–182.

Hesp, P. A., A. I. Hernández-Calvento, J. B. Gallego Fernández, G. L. Miot da Silva, M. H. Hernández-Cordero Ruz, and L. García Romero. 2021. Nebkha or not? Climate control on foredune mode. Journal of Arid Environments.

Hovenga, P. A., P. Ruggiero, N. Cohn, K. R. Jay, S. D. Hacker, M. Itzkin, and L. Moore. 2019. Drivers of dune evolution in Cape Lookout National Seashore, NC. Pages 1283–1296 Coastal Sediments 2019. World Scientific, Tampa/St. Petersburg, Florida, USA.

Hovenga, P. A., P. Ruggiero, E. B. Goldstein, S. D. Hacker, and L. J. Moore. in press. The relative role of constructive and destructive processes in dune evolution on Cape Lookout National Seashore, North Carolina, USA. Earth Surface Processes and Landforms.

Intergovernmental Panel on Climate Change. 2014. Climate change 2014: impacts, adaptation, and vulnerability: Working Group II contribution to the fifth assessment report of the Intergovernmental Panel on Climate Change. Page (C. B. Field and V. R. Barros, Eds.). Cambridge University Press, New York, NY.

Itzkin, M., L. J. Moore, P. Ruggiero, and R. G. Biel. in press. The relative influence of dune aspect ratio and beach width on dune erosion as a function of storm duration and surge level. Earth Surface Dynamics.

Keijsers, J. G. S., A. V. De Groot, and M. J. P. M. Riksen. 2015. Vegetation and sedimentation on coastal foredunes. Geomorphology 228:723–734.

Keijsers, J. G. S., A. V. De Groot, and M. J. P. M. Riksen. 2016. Modeling the biogeomorphic evolution of coastal dunes in response to climate change. Journal of Geophysical Research: Earth Surface 121:1161–1181.

Kratzmann, M. G., E. A. Himmelstoss, and E. R. Thieler. 2017. National assessment of shoreline change – A GIS compilation of updated vector shorelines and associated shoreline change data for the Southeast Atlantic Coast. U.S. Geological Survey, Reston, VA, USA.

Lazarus, E. D., and A. B. Murray. 2011. An integrated hypothesis for regional patterns of shoreline change along the Northern North Carolina Outer Banks, USA. Marine Geology 281:85–90.

Miller, T. L., R. A. Morton, and A. H. Sallenger. 2005. National assessment of shoreline change – A GIS compilation of vector shorelines and associated shoreline change data for the U.S. Southeast Atlantic Coast. U.S. Geological Survey, Reston, VA, USA.

Moore, L. J., O. D. Vinent, and P. Ruggiero. 2016. Vegetation control allows autocyclic formation of multiple dunes on prograding coasts. Geology 44:559–562.

Mull, J., and P. Ruggiero. 2014. Estimating storm-induced dune erosion and overtopping along U.S. West Coast beaches. Journal of Coastal Research 298:1173–1187.

Mullins, E., L. J. Moore, E. B. Goldstein, T. Jass, J. Bruno, and O. D. Vinent. 2019. Investigating dune-building feedback at the plant level: Insights from a multispecies field experiment. Earth Surface Processes and Landforms 44:1734–1747.

Olson, J. S. 1958. Rates of succession and soil changes on southern Lake Michigan sand dunes. Botanical Gazette 119:125–170.

Psuty, N. P. 1986. A dune/beach interaction model and dune management. Thalassas 4:11–15.

R Development Core Team. 2019. R: a language and environment for statistical computing. R Foundation for Statistical Computing, Vienna, Austria. www.r-project.org.

Ruggiero, P., P. D. Komar, W. G. McDougal, J. J. Marra, and R. A. Beach. 2001. Wave runup, extreme water levels and the erosion of properties backing beaches. Journal of Coastal Research 17:13.

Ruggiero, P., G. M. Kaminsky, G. Gelfenbaum, and N. Cohn. 2016. Morphodynamics of prograding beaches: A synthesis of seasonal- to century-scale observations of the Columbia River littoral cell. Marine Geology 376:51–68.

Ruggiero, P., S. Hacker, E. Seabloom, and P. Zarnetske. 2018. The role of vegetation in determining dune morphology, exposure to sea-level rise, and storm-induced coastal hazards: A U.S. Pacific Northwest perspective. Pages 337–361 *in* L. J. Moore and A. B. Murray, editors. Barrier Dynamics and Response to Changing Climate. Springer International Publishing, Cham.

Sallenger, A. H. 2000. Storm impact scale for barrier islands. Journal of Coastal Research 16:7.

Seabloom, E. W., P. Ruggiero, S. D. Hacker, J. Mull, and P. Zarnetske. 2013. Invasive grasses, climate change, and exposure to storm-wave overtopping in coastal dune ecosystems. Global Change Biology 19:824–832.

Seneca, E. D. 1969. Germination response to temperature and salinity of four dune grasses from the Outer Banks of North Carolina. Ecology 50:45–53.

Seneca, E. D., W. W. Woodhouse, and S. W. Broome. 1976. Dune stabilization with *Panicum amarum* along the North Carolina coast. U.S. Army Corps of Engineers, Coastal Research Center, Fort Belvoir, VA, USA.

Sherman, D. J., and B. O. Bauer. 1993. Dynamics of beach-dune systems. Progress in Physical Geography: Earth and Environment 17:413–447.

Short, A. D., and P. A. Hesp. 1982. Wave, beach and dune interactions in southeastern Australia. Marine Geology 48:259–284.

Van der Valk, A. G. 1975. The floristic composition and structure of foredune plant communities of Cape Hatteras National Seashore. Chesapeake Science 16:115–126.

Woodhouse, W. W. 1978. Dune building and stabilization with vegetation. Coastal Engineering Research Center (U.S.).

Woodhouse, W. W., E. D. Seneca, and S. W. Broome. 1977. Effect of species on dune grass growth. International Journal of Biometeorology 21:256–266.

Wright, L. D., and A. D. Short. 1984. Morphodynamic variability of surf zones and beaches: a synthesis 56:93–118.

Zarnetske, P. L., S. D. Hacker, E. W. Seabloom, P. Ruggiero, J. R. Killian, T. B. Maddux, and D. Cox. 2012. Biophysical feedback mediates effects of invasive grasses on coastal dune shape. Ecology 93:1439–1450.

Zarnetske, P. L., P. Ruggiero, E. W. Seabloom, and S. D. Hacker. 2015. Coastal foredune evolution: the relative influence of vegetation and sand supply in the US Pacific Northwest. Journal of The Royal Society Interface 12:20150017.

Chapter 3 – Quantifying carbon storage in a U.S. Central Atlantic Coast dune ecosystem: the relative importance of sand deposition and dune grasses

Katya R. Jay[1], Sally D. Hacker[1], Cedric J. Hagen[2], John Stepanek[1], Peter Ruggiero[2], Laura J. Moore[3]

Affiliations:

1. Department of Integrative Biology, Oregon State University, 3029 Cordley Hall, Corvallis, OR 97331, USA.
2. College of Earth, Ocean, and Atmospheric Sciences, Oregon State University, 104 CEOAS Administration Building, Corvallis, OR 97330, USA.
3. Department of Geological Sciences, University of North Carolina at Chapel Hill, 104 South Road, Mitchell Hall, Chapel Hill, NC 27559, USA.

In preparation for publication

3.1 Abstract

Ecosystems can act as natural carbon sinks by removing carbon dioxide from the atmosphere and storing it in water, soil, and vegetation, providing a valuable service in the face of climate change. Coastal ecosystems such as mangroves, salt marshes, and seagrasses sequester large amounts of carbon on a per unit area basis as a result of high productivity and high sediment accumulation rates. However, much less is known about carbon storage in coastal dunes, which are shaped by positive feedbacks between aeolian sediment transport and burial-tolerant vegetation. Only a few previous studies have measured carbon storage in dunes and found that, while stocks per unit area were lower than in other coastal ecosystems, because dunes typically cover larger geographic areas and have deep reserves of sand and belowground vegetation biomass, their carbon stocks were substantial and varied along dune successional gradients. In this study, we measured carbon storage in dune vegetation and sediment along the U.S. Outer Banks coastline and asked: 1) How much carbon is stored in Outer Banks foredunes and does it vary spatially among islands, dune profile locations, and dominant dune grass species? 2) Does sand carbon density vary with depth in dunes, and if so, is this variability related to belowground grass biomass? and 3) Is there a relationship between dune carbon stocks (aboveground grass, belowground grass, sand, and total carbon) and geomorphic and ecological factors including measures of sand deposition, beach and dune geomorphology, and vegetation abundance? We found that aboveground grass carbon stocks (0.004-0.19 kg C/m^2) were comparable to those in eelgrass beds and salt marshes (0.03-2.30 kg C/m^2) on a per area basis, while sediment organic carbon values in our

study system (0.9 ± 0.6 kg C/m^3) were significantly lower compared to previous measurements in other dunes (2.2 kg C/m^3 in Italian dunes and up to 4.7 kg C/m^3 in U.K. dunes) and other coastal ecosystems (averaging 10 and 28 kg C/m^3 in salt marshes and mangroves, respectively). Carbon storage varied between aboveground grass (0.1 ± 0.1 kg C/m^2), belowground grass (1.1 ± 1.6 kg C/m^3), and sand (0.9 ± 0.6 kg C/m^3), with the largest proportion contained in belowground grass. These three carbon stocks varied spatially among islands and dune profile locations, with values generally increasing in the landward direction. We found that variability in sand carbon density was related to patterns in dune sand deposition, beach slope, and grass density, with the relative importance of these factors varying between islands and dune profile locations. Islands with high sand deposition and high grass density tended to have low sand carbon density, while profile locations with lower sand deposition and higher grass density tended to have high sand carbon density, suggesting that self-reinforcing feedbacks between vegetation and sediment may occur at both high and low sand deposition rates. Understanding carbon storage dynamics in dunes is particularly important given the potential for sea level rise, extreme storm events, land-use change, and other climate-driven changes in coastal processes to impact dune ecosystem services.

3.2 Introduction

As global atmospheric carbon dioxide concentrations increase due to human activities including fossil fuel burning and land use change, the role of ecosystems as natural carbon sinks has become an increasingly valuable ecosystem service and a means for climate change mitigation (e.g., Sarmiento and Gruber 2002, Chmura et al. 2003,

Potter 2003, Millenium Ecosystem Asseessment 2005, Reay et al. 2008, Luyssaert et al. 2008, Intergovernmental Panel on Climate Change 2014, Howard et al. 2017). Ecosystem carbon can be measured as a stock, which refers to the amount of carbon stored in a given ecosystem, or as a rate, which refers to the amount of carbon sequestered over time (Beaumont et al. 2014, Palm et al. 2014). Ecosystems sequester carbon by removing it from the atmosphere and storing it in water, soil, and vegetation. Oceans have the largest global carbon stock, followed by fossil fuels buried in rock and sediments, and then vegetation, soils, and detritus (Sarmiento and Gruber 2002, Intergovernmental Panel on Climate Change 2007). In terrestrial systems globally, carbon storage is greater in vegetation (1358 Gt C) compared to soils (640 Gt C). Much of the vegetation carbon stock (roughly 50%) is stored in tropical forests, while high latitude forests contribute much less; on the other hand, low-latitude ecosystems such as tropical forests and savannahs contribute less to soil carbon stocks, with higher-latitude ecosystems containing 53% of global soil carbon (Cao and Woodward 1998). Ocean systems store much more carbon than terrestrial ecosystems: the largest pool is in intermediate/deep waters (37,000 Gt C), followed by surface sediments (1,750 Gt C) and surface waters (900 Gt C; Intergovernmental Panel on Climate Change 2014).

Most research on carbon storage and carbon sequestration has focused on the open ocean and terrestrial ecosystems, while fewer studies have documented carbon in coastal ecosystems (Howard et al. 2017). Recently, though, coastal ecosystems have been recognized for their capacity to store carbon and their role in global carbon cycling, carbon budgets, and climate regulation (Nellemann et al. 2009, Donato et al. 2011,

Mcleod et al. 2011, Beaumont et al. 2014, Howard et al. 2017, Macreadie et al. 2019). To date, most coastal carbon measurements have been made in mangroves, seagrass beds, and salt marshes (e.g., Chmura et al. 2003, Bouillon et al. 2008, Duarte et al. 2010, Kennedy et al. 2010, Breithaupt et al. 2012, Hopkinson et al. 2012, Greiner et al. 2013), where rates of carbon burial are relatively high (averaging 1380-2260 kg C ha^{-1} yr^{-1} compared to 40-51 kg C ha^{-1} yr^{-1} in temperate, tropical, and boreal forests and 540 kg C ha^{-1} yr^{-1} in grasslands; Conant et al. 2001, Jones and Donnelly 2004, Lal 2005, Mcleod et al. 2011, Duarte 2017, Lal et al. 2018). Although the global amount of carbon sequestered by coastal habitats is substantial, it is lower in comparison to more widespread terrestrial and ocean ecosystems (Cao and Woodward 1998, Mcleod et al. 2011, Howard et al. 2017).

Higher carbon sequestration rates on a per area basis in coastal systems are largely a product of high vegetation productivity (both aboveground and belowground) and high sedimentation rates relative to terrestrial ecosystems, allowing for the continued burial of organic matter. Because coastal systems can accumulate sediment vertically, often keeping pace with sea level rise, their sediment carbon stocks can increase over time as compared to terrestrial stocks, which have much lower sedimentation rates (Chmura et al. 2003). In addition, carbon is imported into coastal ecosystems from marine sources and subsequently buried, meaning that they store carbon from both internal and external sources (Mcleod et al. 2011). Previous studies in salt marshes and mangroves show that the origin of carbon stocks can vary widely between systems, where carbon is primarily imported from external sources in some systems and primarily locally

produced in other others, depending on environmental factors (Middelburg et al. 1997, Bouillon et al. 2003, Kristensen et al. 2008).

One coastal ecosystem that has received little attention for its ability to sequester and store carbon is coastal dunes. Coastal dune habitat is a widespread ecosystem that occurs at the interface between the land and the sea and is shaped by both terrestrial and marine processes. While ecosystem services such as coastal protection have been studied extensively in dunes (Sallenger 2000), much less is known about their ability to store carbon, despite being early successional ecosystems with dense vegetation and high sedimentation rates that may accumulate sand rapidly (Olff et al. 1993, Jones et al. 2008, Drius et al. 2016). Carbon storage has been quantified in only a handful of coastal dune systems worldwide (UK: Jones et al. 2008, Beaumont et al. 2014; Italy: Drius et al. 2016; Australia: Turner and Laliberté 2015; and North America: Tackett and Craft 2010; see Table 3.1 for a summary of their findings). Several other studies, focused on nutrient dynamics and soil chronosequences, have measured soil organic carbon (SOC) density or soil organic matter (SOM) content in dune systems without calculating dune carbon storage or sequestration rates (e.g., Berendse et al. 1998, Schaub et al. 2019; see Table 3.1 for values). In the studies that measured rates of carbon sequestration in dunes, values ranged from 56-730 kg C ha^{-1} yr^{-1} (rates are based on SOC stocks, not including vegetation; Jones et al. 2008, Beaumont et al. 2014, Drius et al. 2016). Among all these studies, average SOC content in dunes ranged between 0.03-2.8% depending on region and dune habitat (Table 3.1). Although these values are lower than those reported in mangroves, salt marshes, and eelgrass meadows (averaging 1380-2260 kg C ha^{-1} yr^{-1}),

sandy beaches and dunes have a greater geographic extent than any other coastal system, covering approximately one third of Earth's ice-free coastlines (Luijendijk et al. 2018). They also have deeper reserves of sediment and belowground vegetation compared to other coastal systems. Given this difference in geographic area and volume, coastal dunes have the potential to store considerably more carbon globally.

While previous research provides some insight into the carbon storage potential of coastal dunes, most do not measure carbon over the full range of variability across dune profile locations, dune depths, sediment supply, and plant productivity and species composition (Table 3.1; Middleton and McKee 2001, Kristensen et al. 2008, Barbier et al. 2011). Previous research in marshes and wetlands suggests that many studies have underestimated SOC stocks in these systems as a result of shallow soil sampling (Van de Broek et al. 2016, Kauffman et al. 2020). Thus, because this ecosystem is so widespread, the values vary by 1-2 orders of magnitude between locations and dune habitat types, and measurements may be incomplete or underestimated for a variety of reasons, it is critical to systematically quantify the magnitude and variability of carbon storage in coastal dunes and the potential for future sequestration. In addition, because dune ecosystems face increasing pressure from threats such as sea level rise, heightened storm intensity, and coastal development (Intergovernmental Panel on Climate Change 2014, Ranasinghe 2016, de Winter and Ruessink 2017, Masselink et al. 2020), there is potential to alter carbon sequestration in these systems via erosion and habitat destruction in the future.

Coastal dunes are dynamic systems with high spatial heterogeneity, and they form via physical and ecological processes that may modulate carbon storage. Foredunes, or

the seaward-most dune ridge parallel to the ocean, are shaped by a combination of sea level, wind and wave conditions, sediment supply, beach morphology, and vegetation (Short and Hesp 1982, Hesp 1989, 2002, Sherman and Bauer 1993, Bauer and Davidson-Arnott 2002, Hacker et al. 2012, Hesp and Walker 2013, Duran and Moore 2013, Zarnetske et al. 2015, Keijsers et al. 2016, Ruggiero et al. 2016, Moore et al. 2016, Cohn et al. 2019). Dunes are built via biophysical interactions, where burial-tolerant vegetation such as dune grasses slows sand-laden wind, leading to feedbacks between vegetation growth and sand deposition, where plant growth is stimulated by further sand deposition (Hacker et al. 2012, Zarnetske et al. 2012, Keijsers et al. 2015, Brown and Zinnert 2018, Mullins et al. 2019, Biel et al. 2019, Charbonneau et al. 2021). Early research demonstrated relationships between dune shape and dune grass species (Godfrey and Godfrey 1973, Van der Valk 1975, Woodhouse et al. 1977), while more recent studies provide evidence that plant density, morphology, and belowground growth patterns all contribute to the development of a spectrum of different dune morphologies (Hesp 2002, Hacker et al. 2012, 2019, Zarnetske et al. 2012, Goldstein et al. 2017, Biel et al. 2019).

The combination of physical and ecological factors that shape beach and dune morphology likely play an important role in determining dune carbon storage. For example, vegetation density and biomass determine standing carbon stocks and influence the amount of organic matter available for burial. In turn, the amount of sand deposited on, or removed from the dune, can dictate how much organic matter from vegetation is buried each year. The amount of carbon contained in the sand transported to the dunes (determined by marine inputs) could also be an important contributor to dune carbon

storage. At a larger scale, the geomorphic processes that shape beaches and dunes, including storm overwash, aeolian sand transport, and inlet dynamics (for barrier systems), may influence carbon storage as they can rapidly bury or expose organic matter following depositional or erosional events (Rossi and Rabenhorst 2019). Extreme storm events and sea level rise have the potential to increase or decrease carbon stocks both in the accumulated sediments and vegetation, depending on the net effect of erosional and depositional processes, which are often spatially heterogeneous (Macreadie et al. 2019).

Here we explore the carbon storage capacity of foredunes along the Outer Banks of the U.S. Central Atlantic coast, a 320-km string of vegetated barrier islands that are highly vulnerable to coastal erosion from sea level rise and extreme storms (Sallenger et al. 2012, Hovenga et al. 2019, 2021, Paerl et al. 2019). This region has widespread dunes that exhibit dramatic variation in beach and dune geomorphology, sand supply, and vegetation density and composition, making it an ideal system to study dune carbon storage (Van der Valk 1975, Stockdon et al. 2007, Kratzmann et al. 2017, Goldstein et al. 2018, Hacker et al. 2019, Hovenga et al. 2019, 2021). Two native grass species dominate Central Atlantic barrier islands: the most widespread is *Uniola paniculata*, a drought-tolerant C_4 grass extending from Virginia to Florida (Seneca 1969), followed by *Ammophila breviligulata*, a temperate C_3 grass extending from North Carolina (NC) to Canada (Goldstein et al. 2018, Hacker et al. 2019). Their ranges overlap in the NC Outer Banks, where previous research shows that *A. breviligulata* tends to create continuous, linear dunes while *U. paniculata* typically builds steeper, more hummocky dunes (Woodhouse et al. 1977). Two other less abundant grasses, *Panicum amarum* and

Spartina patens, are found in the NC Outer Banks and are similar to *U. paniculata* in distribution (Hacker et al. 2019). A recent study examining the functional morphology and sand accretion properties of all four species found that *A. breviligulata* was correlated with higher sand accretion due to its dense, clumped growth form, while *U. paniculata* had lower sand accretion as a result of fewer, larger shoots that were more evenly spaced (Hacker et al. 2019). Thus, these dune grasses may vary in their ability to sequester carbon due to differences in their growth form, growth density, and sand capture ability.

In addition to vegetation density and composition, carbon storage in dunes should also depend on rates of sand supply to the beach and dune and the amount of carbon imported from marine sources, which includes nutrients in seawater as well as larger deposits of wrack delivered by tides and waves. There are latitudinal gradients in marine dissolved organic carbon (DOC) offshore of the NC coastline (Mannino et al. 2016) that may influence the amount of carbon being imported to the dunes. The NC Outer Banks are situated near a dynamic offshore boundary in ocean circulation, where cold shelf/slope currents including the Labrador Current flow south along the Mid-Atlantic Bight (the region extending from Cape Cod, Massachusetts to Cape Hatteras, NC) and collide with the warm, northward Gulf Stream, which turns eastward offshore of Cape Hatteras (Savidge 2004, Mannino et al. 2016). These differences in currents affect the delivery of marine nutrients to the coastline, making Cape Hatteras a biogeophysical transition zone for macroalgae and phytoplankton in addition to dune grasses (Mallin et al. 2000). The region north of Cape Hatteras is characterized by higher DOC levels

compared with the region south of this boundary. In addition, macroalgal diversity is high in this transition zone, where both warm- and cold-adapted species can survive.

In this paper, we measured carbon storage and the possible causes of carbon variation at multiple barrier island foredune locations along a 225-km stretch of the Outer Banks barrier islands (Figure 3.1). We asked the following research questions:

1) How much carbon (in the sand and the dune grasses) is stored in Outer Banks barrier island foredune ecosystems? How does carbon storage vary by carbon stock type, island, foredune profile location, and dominant dune grass species?
2) Does carbon storage in these foredunes vary with depth? Is there a relationship between sand carbon and dune grass carbon with depth in these dunes?
3) If carbon storage varies spatially, what geomorphological and ecological factors explain this variability across our study region?

We expect that carbon storage will vary depending on the stock type, with most carbon, on a per volume basis, stored in belowground plant material and sediments, as has been shown in other coastal systems. We also expect that carbon storage will vary along the Outer Banks islands, in large part because of the geomorphological and ecological differences among the foredunes. We hypothesize that carbon storage will increase along the seaward to landward foredune profile, with back dune locations having greater carbon stocks as a result of denser grasses and later plant successional stages. There could be differences between the carbon stored in the two dominant dune grass species, with *U. paniculata* stands having more carbon than *A. breviligulata* stands due to

its greater biomass per unit area (Hacker et al. 2019). We hypothesize that sand and belowground grass carbon will decrease with depth in the core because grasses and plant litter should contribute most to sand carbon at the top of the core and decrease with depth as belowground plant material decomposes over time. Finally, we hypothesize that grass abundance and sand deposition to the dune, which together determine the amount of organic material available and the rate at which it is buried, will be the most important factors explaining variability in dune carbon storage.

3.3 Methods

3.3.1 Study area

This study was conducted on foredunes along the Outer Banks barrier islands, North Carolina, USA from Bodie Island in the north to South Core Banks in the south (Figure 3.1; Appendix C, Table C1). This 225-km stretch of sandy barrier islands varies spatially in vegetation species and density (Figure 3.2; Hacker et al. 2019, Jay et al. Chapter 2), beach geomorphology and shoreline orientation (Figure 3.2; Hovenga et al. 2019, 2021, Jay et al. Chapter 2), and wave energy and underlying stratigraphy (Lazarus and Murray 2011). The region experiences a moderately energetic seasonal wind and wave climate, apart from hurricanes and nor'easters in fall and winter (Bryant et al. 2016). There is significant variability in shoreline erosion and accretion patterns along the Outer Banks coastline (Hovenga et al. 2021).

3.3.2 Field sample and data collection

From 2016–2019, we surveyed vegetation communities and topography on an annual basis at 112 transects in the study region (see Hacker et al. 2019, Hovenga et al.

2021, Jay et al. Chapter 2). Transects were perpendicular to the shoreline, extending from mean lower low water (MLLW) through the dune toe (the seaward-most dune extent), dune crest (the highest point of foredune elevation), and dune heel (the lowest point on the landward side of the foredune) (see Appendix C, Figure C1). In June 2019, we chose a subset of these established transects (n=11) across the five islands to conduct vegetation and topographic resurveys and collect sediment cores and dune grasses for carbon measurements (see Appendix C, Table C1 and Appendix C, Figure C2 for transect and core collection locations). Sites were chosen to capture variability across the five islands and across the profile locations, as well as gradients in beach and dune sand supply and dominant grass species. Field data collection occurred nine months after Hurricane Florence, which resulted in significant beach and dune erosion in some regions, particularly North Core Banks and South Core Banks in Cape Lookout National Seashore. Two of the three transects on South Core Banks (i.e., SCB_6 and SCB_9) were in areas where the original 2017 foredune had eroded, resulting in a new foredune located landward of that prior foredune (Appendix C, Figure C2). Thus, the profiles for these transects were located on what was the secondary dune behind the 2017 foredune. As described below, the positioning of these transects relative to the 2017 profile was considered in our analyses.

At the 11 transects, we collected plant community and beach and foredune topographic data following the methods of Hacker et al. (2012) and Jay et al. (Chapter 2). Shoot density of each grass species was counted within 0.25 m^2 quadrats every five meters at the toe, crest, and heel of the transects. A Network Real Time Kinematic (RTK)

Differential Global Positioning System (R7 unit, Trimble, Sunnyvale, CA, USA) was used to measure the elevation along the beach and dune profile and at each quadrat (Appendix C, Figure C2).

Sediment cores (to one meter depth) were collected at the toe, crest, and heel (totaling three cores/transect) of the foredune roughly one meter away, but at the same elevation, from the transect to avoid disturbing the permanent transect (Appendix C, Table C1, Appendix C, Figure C2). At each core site, the location and elevation of the core was recorded using an RTK GPS, the stem density of all grasses present in a 0.25 m^2 quadrat was counted, and grass samples of each species present were collected.

Core collection involved driving a 10 cm diameter PVC pipe into the dune using a sledgehammer (see Appendix D, Figure D1 for detailed dune coring methods). Due to the difficulty of extruding a 1-m long core in the field, two core tubes were used for each collection; one was pounded in 0.5 m and carefully extracted, and then a second tube was carefully inserted in the same location without disturbing the sediment to collect the remaining 0.5 m core. A test plug was inserted into each core above the sediment column to prevent sediment loss, and cores were extracted using a truck jack attached to a pipe clamp or dug out using a shovel. Sediment was sampled from the cores at alternating 2-cm depth intervals using a custom-built extruder (i.e., the 0-2 cm layer was sampled, the 2-4 cm layer was discarded, the 4-6 cm layer was sampled, and so on; see Appendix D, Figure D2 for drawings of the extruder and Appendix D, Figure D3 for photos of extruder use). We then collected several tablespoons of sample from within each of these depth intervals, scooping haphazardly to ensure a representative sample.

3.3.3 Core sample processing and sand carbon measurements

The wet weight of the core samples was measured in the field for a subset of samples that were subsequently oven dried at 60˚C for 24 hours and reweighed to obtain bulk density (weight of sample per given volume of sample) and percent moisture (the proportional difference between wet and dry weight) measurements. We estimated bulk density for each sample by calculating a weighted average between dry density measurements and freshwater density based on the average percent moisture in our samples (determined from a subset of samples). The remaining core samples were directly dried at 60˚C for 24 hours. Roots, plant matter, and shells were removed using a 2 mm sieve, and shells were separated from plant material. Sand, plant material, and shells were then weighed separately.

We used a subset of the samples to determine percent organic matter and percent organic carbon content of the sand at different depths of the core. Subsamples were used because of the time and expense involved in directly determining the organic carbon content for all the samples. The first subset, used for organic matter measurements, included all the samples in the top 40 cm of the core, and every third sample from the remainder of the core (see Appendix E, Table E1 for a list of sample depths and measurements from each core). The second subset, used for the percent organic carbon measurements, included three samples per core, totaling nine samples per transect, divided evenly between foredune toe, crest, and heel (96 samples total; see Appendix E, Table E1 for a list of organic matter and organic carbon samples from each core). Samples were chosen based on percent organic matter (see below), where samples with

the highest, median, and lowest percent organic matter were included. We then estimated percent organic carbon for the first subset of samples by determining the relationship between percent organic matter and percent organic carbon for the second subset of samples.

Organic matter content was measured using standard percentage loss on ignition (LOI) techniques (see Heiri et al. 2001). LOI measurements involved burning 2.000 ± 0.002 g of dried sample at 550˚C for 4 h and reweighing once cooled. Burning the samples at 550˚C allowed organic matter to combust without dissociating CO_2 from carbonates in the sand (Dean 1974). The proportion of mass lost relative to the starting mass was calculated and then converted to percent LOI. Organic carbon content was measured via elemental analysis using an ECS 4010 CHNSO Analyzer at the Oregon State University Elemental Analysis Facility. Before measurements were taken, dried sand samples were first homogenized using a Spex Sigma Prep 8000D Mixer/Mill followed by acidification with 1 M HCl to remove carbonates in the sand. Percent organic carbon was calculated from the mass of organic carbon out of the total sample mass.

Two regression relationships were established between percent organic matter (% LOI) and percent organic carbon (% TOC) in order to best estimate % TOC in all the sand samples (note that five samples had % TOC values equal to or greater than % LOI values and were not included in the analyses). The first relationship included all the samples except those from SCB_9, which had a higher ratio of % LOI to % TOC than the other samples (% TOC = 0.310 * % LOI – 0.015, R^2=0.66, $p < 2.2E-16$; see Appendix E,

Table E1). The second relationship was established for SCB_9 (% TOC = 0.509 * % LOI – 0.016, R^2=0.45, p = 0.049; see Appendix E, Table E2).

To calculate sand carbon density (expressed as kg C/m^3) for each sampled depth (see Appendix E, Table E1), we multiplied the bulk density estimates for each sample by their % TOC estimates (converted to a proportion) at that location and then converted to a volumetric kg C/m^3 value (see Equation 1).

*Bulk density (g/cm^3) * proportion TOC = Sand carbon density (g C/cm^3)* (Equation 1)

3.3.4 Dune grass sample processing and carbon measurements

We estimated the aboveground and belowground dune grass carbon density for the three grass species (*U. paniculata*, *A. breviligulata*, and *P. amarum*) at different transect and profile locations. Carbon density was measured as the product of the grass percent carbon multiplied by the average biomass of the grass samples. Note below that aboveground grass carbon density is expressed in area units (kg C in 1 m x 1 m or m^2 area) and the belowground grass and sand carbon density values are expressed in volumetric units (kg C in 1 m x 1 m x 1 m depth or m^3). The two units are interchangeable, and thus can be directly compared, given that they are considering the same amount of area.

The organic carbon content of the grasses was obtained using the following methods. For the aboveground grass samples, we measured carbon content in the tissues of each grass species collected near each core and transect. The organic carbon content in the belowground grass samples was measured in the root and rhizome tissues obtained from the cores. For both sets of samples, grass tissues were first homogenized using a

Spex Sigma Prep 8000D Mixer/Mill and organic carbon content was measured via elemental analysis using an Elementar Vario Macro Cube at the Oregon State University Soil Health Laboratory, Corvallis, Oregon.

To estimate aboveground grass biomass, we first dried and weighed each individual aboveground dune grass shoot collected at the coring sites. We then calculated the aboveground grass biomass (g/m^2) for each species as the product of the mean dune grass shoot weight and the mean shoot density (average shoots/0.25 m^2 measured in the field over the period of 2017-2019 and converted to m^2) for each species at each transect and profile location. Aboveground grass carbon density (kg C/m^2) was then calculated for each quadrat as the product of the species-specific aboveground biomass and the average species-specific percent organic carbon content.

To estimate belowground grass biomass, we used two different methods. The first method involved extrapolating the proportion of the belowground biomass sifted out of each individual core sample (i.e., belowground biomass per given weight of sand) to the entire volume of the core and then a volume of m^3. Belowground grass carbon density (expressed in kg/m^3) for each core was then calculated as the product of the belowground biomass values and organic carbon content measured directly in belowground grass samples (averaged across all sites). The second method involved estimating the spatial variability in belowground grass carbon density for each transect. To do this, we calculated the ratio between aboveground carbon stocks (in quadrats directly above each core) and belowground grass carbon density for each core (based on grass biomass sifted out of core samples) and applied that ratio to the remaining quadrats at each transect and

profile location and converted to kg C/m^3. Finally, to estimate belowground grass carbon density with depth, the proportion of belowground grass biomass was determined for each volume of sand sample and multiplied by organic carbon content measured in belowground plant samples and converted to kg C/m^3.

3.3.5 Beach and foredune morphometrics, shoreline change rate, and sand supply metrics

To determine the potential factors important to dune carbon density, we obtained beach and foredune morphometrics, shoreline change rate, and sand deposition (or erosion) at each of our foredune transects. First, we extracted beach and foredune morphometrics at each transect from field topography data from 2017 following the methods of Mull and Ruggiero (2014) (see Appendix C, Figure C1 for details of the morphometric measures). We also extracted the mean high water (MHW) shoreline position using a 0.4 m contour referenced to the North American Vertical Datum 1988 (NAVD88) (Hovenga et al. 2021). Beach morphometric measures included beach width (distance between MHW and the foredune toe) and backshore slope (slope between MHW and the foredune toe). Foredune morphometric variables included foredune toe, crest, and heel elevation (m; relative to MHW), foredune height (vertical distance between the dune crest elevation and MHW), foredune width (m; horizontal distance between the foredune toe and crest), and foredune aspect ratio (foredune height divided by width). To estimate sand deposition or erosion along the foredune transects, we determined the change in the elevation of the foredune toe, crest, and heel for each year (at the same cross-shore location from 2017-2019) and calculated the total and annual sand deposition (or erosion) at those locations between years.

Finally, we calculated multidecadal shoreline change rate (SCR) (i.e., the mean annual rate at which the shoreline position moves seaward or landward over a multidecadal period; Farris and List 2007). Multidecadal SCR was calculated in two ways given the availability of airborne lidar data for different locations within the study region. For the Cape Lookout National Seashore transects, multidecadal SCR was calculated as the average annual change in shoreline position from 1997 to 2016 using airborne lidar data from NOAA's Digital Coast website as described in (Hovenga et al. 2019, 2021). For the northern Outer Banks from Ocracoke Island to Bodie Island, multidecadal SCR was calculated as the average annual change in shoreline position from 1997 to 2010 using USGS shoreline position data from Kratzmann et al. (2017). For both multidecadal SCR calculations, cross-shore profiles were extracted at survey transect locations and shoreline positions were defined with a spatially varying MHW contour ranging from 0.33-0.46 meters (referenced to NAVD88).

3.3.6 Statistical analyses

We used R v.3.6.1 (R Development Core Team 2019) for all statistical analyses. Residual and normal quantile plots were used to assess whether response variables conformed to the assumptions of the statistical analyses, and transformations were used when necessary.

To assess the patterns of carbon density on foredunes of the Outer Banks barrier islands, we used two-way ANOVA (two explanatory variables and their interactions) and Tukey HSD post-hoc tests, when significant factors were found. If significant interactions were found, we used one-way ANOVAs and Tukey HSD post-hoc tests to compare

between levels of each factor (Underwood 1997). The following ANOVA tests were performed. First, we tested whether there were differences in total carbon stocks among islands and carbon stock type (aboveground and belowground dune grass and sand). Next, we tested whether the response variables of aboveground grass carbon stocks, belowground grass carbon density, and sand carbon density differed among islands and dune profile locations. We also tested whether these same response variables differed among islands and dominant dune grass species. Finally, we conducted separate two-way ANOVAs at the toe, crest, and heel profile locations to determine whether there were differences in sand carbon density among islands and depths of the cores. All three cores from each of the two heavily eroded South Core Banks transects (Appendix C, Figure C2i-k) were categorized as dune heel sites in all statistical analyses.

To determine the possible factors important to dune carbon density in this system, we used multivariate linear regression analyses to evaluate the relative importance of geomorphic and ecological factors associated with the response variables of aboveground grass carbon density, belowground grass carbon density, sand carbon density, total grass carbon density (aboveground and belowground combined), and total carbon density (aboveground grass, belowground grass, and sand combined). For the grass carbon density response variables, we tested the explanatory variables of annual sand deposition to the dune from 2017-2019, multidecadal SCR, beach width, backshore slope, foredune height, foredune width, and foredune aspect ratio). For sand carbon density, explanatory variables tested were annual sand deposition rate to the dune from 2017-2019, multidecadal SCR, grass biomass, grass tiller density, beach width, backshore slope,

foredune height, foredune width, and foredune aspect ratio. To calculate the dune grass density explanatory variable, tiller density of all three species in quadrats (per 0.25 m^2, converted to m^2) from the 2019 surveys was summed and then averaged by transect and dune profile location. For the two eroded South Core Banks sites, tiller density values from 2017 were used to represent the pre-hurricane vegetation community. To calculate the dune grass biomass explanatory variable, the densities of each species from 2019 were then multiplied by their average tiller weights and summed and then averaged by transect and profile location. From the linear regression analyses, top models were selected using sample size corrected Akaike's Information Criterion (AIC_c). To determine the relative contribution of individual predictors in top models we used the R package 'heplots' and the function 'etasq' to calculate multivariate eta-squared (or R^2) (Fox et al. 2018).

3.4 Results

3.4.1 Patterns in geomorphology, sand supply, and dune grasses

Beach and foredune morphology, sand supply, and dune grass metrics varied greatly across our study region (Figure 3.2; Jay et al. Chapter 2). Multidecadal SCR values were largely neutral or slightly negative throughout the study region, indicating either little change or mild erosion of the beaches at these transects (Figure 3.2a). The Bodie Island transect was an exception with greater than 10 m/yr of beach erosion. These beaches tended to be shorter and have steeper backshore slopes (Figure 3.2b, c). The three transects with positive multidecadal SCR values had wider beaches and shallower

backshore slopes (Figure 3.2a, b, c). This was especially the case at SCB_4, which was located at the end of Cape Lookout National Seashore (Figure 3.1).

Foredune height generally increased with latitude along the Outer Banks coastline, with the shortest dunes (~4 m) found on South Core Banks and the tallest dunes (>8 m) found on Hatteras Island (Figure 3.2d). Foredune width varied from ~10-30 m and did not follow the same pattern as foredune height (Figure 3.2e). Instead, foredunes had a spectrum of morphologies from low aspect ratio (shorter, wider dunes; e.g., NCB_16, BOD_1) to higher aspect ratio (height more similar to width; e.g., HAT_7, HAT_12) (Figure 3.2e).

Sand supply to the foredune, measured as the annual change in elevation at the foredune toe, crest, and heel from 2017-2019, tended to be unrelated to SCR (measured from 1997-2016), beach width, or backshore slope (Figure 3.2f). For example, the Bodie Island transect, which is located on a highly eroding beach, had the greatest sand deposition across all profile locations (~0.75-1.0 m/yr) followed by two Hatteras Island transects (HAT_12 and HAT_7), which had only slightly negative SCRs. Moreover, the transects with the most positive SCRs and widest beaches had sand deposition (or erosion) patterns similar to beaches with more neutral or slightly negative SCRs.

Finally, dune grass species abundance (density and biomass) and distribution also varied across the study region and across profile locations (Figure 3.2g-i, Appendix F, Table F1, Figure F1; see Hacker et al. 2019 for more detailed vegetation patterns). *Uniola paniculata* was more widespread and had greater abundance than *A. breviligulata*, but this pattern depended on the island and profile location considered. The northern islands

and the foredune toe locations generally had more *A. breviligulata* compared to the southern islands and foredune heel locations, which tended to have more *U. paniculata*.

3.4.2 Patterns in carbon stocks in dune grass and sand

Total carbon stocks (including dune grasses and sand) on the foredunes of the Outer Banks averaged 2.1 ± 1.8 kg C/m^3 across all islands. Belowground grass carbon density was the largest and most variable component of the total carbon stocks (mean ± SD: 1.1 ± 1.6 kg C/m^3), followed by sand carbon density (0.9 ± 0.6 kg C/m^3) and then aboveground grass carbon stocks (0.1 ± 0.1 kg C/m^2), but there was an island by carbon stock type interaction (Figure 3.3, Table 3.2). ANOVAs and post hoc tests revealed that aboveground grass carbon stocks were significantly lower than belowground grass or sand carbon density at Hatteras Island, North Core Banks, and South Core Banks but there were no differences in the carbon stock types on Bodie Island or Ocracoke Island (Table 3.2). Total carbon stocks also varied by island, ranging from 0.8 (Bodie Island) to 3.8 kg C/m^2 (Ocracoke Island), with Ocracoke Island and South Core Banks having the highest total carbon stocks (Figure 3.3) but the differences depended on the carbon stock considered (Table 3.2). ANOVAs and post hoc tests revealed that both aboveground and belowground grass carbon stocks did not differ across islands, but sand carbon stocks were lowest and highest at Bodie Island and South Core Banks, respectively, and the three other islands did not differ.

3.4.3 Patterns in carbon stocks across islands and foredune profile locations

There were differences in aboveground grass, belowground grass, and sand carbon stocks density and percent carbon among islands and profile locations throughout

the study region (Figure 3.4, Table 3.3, Appendix F, Table F1, Table F2). ANOVAs and post hoc tests for aboveground grass carbon density showed that the dune toe had significantly lower values compared to the dune crest and heel, which did not differ, on all islands except Bodie Island (toe = crest = heel) and Hatteras Island (crest > heel and toe) (Figure 3.3a, Table 3.3). At each profile location, aboveground grass carbon generally did not vary among islands, except at Hatteras Island and Bodie Island where dune crest carbon was higher than at North Core Banks (Hatteras only) and South Core Banks (both islands).

Belowground grass carbon density showed similar patterns to aboveground grass carbon stocks; lower values occurred at the dune toe compared to the dune crest and heel, which did not differ (Figure 3.3b, Table 3.3). In addition, there were no differences in belowground grass carbon density among islands at the dune toe and heel, but values at the dune crest were significantly higher at Ocracoke Island compared to all other islands.

Finally, ANOVAs and post hoc tests showed that sand carbon density varied latitudinally across islands, with southern Outer Banks islands (i.e., South Core Banks and North Core Banks) generally having higher sand carbon than northern Outer Banks islands (i.e., Bodie Island, Hatteras Island, and Ocracoke Island) but this depended on dune profile location (island x profile interaction; Figure 3.4c, Table 3.3). There was also a landward gradient in sand carbon density, in which the dune heel had higher carbon than the dune toe or crest on all islands except at Bodie Island (no differences with profile location) and North Core Banks (no difference between dune heel and toe). Additionally,

on most islands, there were no differences in sand carbon density between the dune toe and crest profile location.

3.4.4 Patterns in carbon stocks in dominant dune grass species

We considered whether there were differences in the dune grass and sand carbon stocks among the dominant dune grass species on the Outer Banks islands. Although there were no differences in tissue carbon content among the dominant dune grass species (i.e., mean ± SD; *U. paniculata* 46.88 ± 0.69 % C, *A. breviligulata* 46.87 ± 0.74 % C, and *P. amarum* 45.94 ± 0.89 % C), carbon stocks did vary depending on the carbon stock type, dune grass species biomass, and island (Figure 3.5, Table 3.4). Except for the aboveground carbon stocks on Bodie Island, which showed equal carbon stocks for both species, dunes dominated by *U. paniculata* had higher aboveground and belowground carbon stocks compared to dunes dominated by *A. breviligulata* (Figure 3.5a, b, Table 3.4). Note that Bodie and Hatteras islands had the highest proportion of *A. breviligulata* and there was no *A. breviligulata* on South Core Banks (Figure 3.2 , Appendix F, Table F1). In addition, of the four islands where both grass species were found, areas dominated by *U. paniculata* had the same or higher sand carbon density than areas dominated by *A. breviligulata*, but these differences were small (Figure 3.5c, Table 3.4). This pattern coincides with differences in where the two grass species occurred across the dune profile (Appendix F, Table F1). When both species were present along the transect, *U. paniculata* tended to be most abundant at the dune crest and heel where sand carbon densities were also high, whereas *A. breviligulata* mostly occurred at the dune toe and crest where carbon densities were lower (Figure 3.4).

3.4.5 Patterns of sand and belowground grass carbon density with core depth

Across islands and profile locations, we found that there were no clear patterns in sand carbon density with core depth, but variability was high (Figure 3.6, Table 3.5, Appendix Table F3). There were also no clear patterns in belowground grass carbon density with core depth, but the values tended to be highest near the top (10-20 cm) and in the middle (30-60 cm) of the core. Belowground grass carbon values were even more variable than sand carbon density likely because of the dispersed nature of plant matter within the cores (Appendix F, Table F3).

Using regression analysis to test whether sand carbon density and belowground grass carbon density (averaged across sample depths) were correlated, we found that there was no detectable relationship between the two. However, for some transects and dune profile locations, sand carbon density and belowground plant carbon density showed similar patterns with depth in the core. These patterns occurred primarily in the dune heel (for example, Bodie Island, Ocracoke Island, and South Core Banks; Appendix F, Figure F2).

3.4.6 Factors important to carbon stocks in Outer Banks foredune ecosystems

Our analyses showed that the patterns in sand carbon, aboveground grass carbon, and total carbon response variables were correlated with several metrics of sand supply, foredune morphology, and vegetation abundance. First, we found that mean sand carbon density was negatively correlated with sand deposition rate (annual from 2017-19) and backshore slope and positively correlated with grass biomass and density (Figure 3.7, Table 3.7). In the top model for sand carbon density, sand deposition rate explained the

most variability (50%) followed by backshore slope (26%) and grass density (4%; Table 3.7). Second, the best supported models for aboveground grass carbon stocks showed a positive correlation with foredune height and sand deposition rate and negative correlation with SCR and beach width, although only foredune height was bordering on statistically significant (9% of variance explained, Table 3.7). Third, we found that patterns for total carbon density (aboveground grass, belowground grass, and sand combined) were similar to those for sand carbon density. Total carbon was positively correlated with SCR and foredune aspect ratio and negatively correlated with sand deposition rate and backshore slope. In the top model for total carbon density, SCR was the only explanatory variable (19% variance explained), while in the next best model, sand deposition rate, backshore slope, and foredune aspect ratio explained 14%, 11%, and 6% of the variance, respectively (Table 3.7). Finally, we found that there were no significant explanatory factors with belowground grass carbon density and total grass carbon density (belowground grass and aboveground grass combined) as response variables.

3.5 Discussion

In this study, we surveyed foredune ecosystems and collected sediment cores along the U.S. Outer Banks barrier islands to quantify the amount of carbon stored in vegetation and dune sands. We asked how much carbon is contained in aboveground grass, belowground grass, and sand stocks in these foredunes and how it compares to other coastal ecosystems. In addition, we explored whether the carbon stocks vary spatially between islands, dune profile locations, and dune grass species within our study

system. We also cored to one meter depth to investigate whether sand and belowground grass carbon vary with depth in the dune. Finally, we assessed the relative importance of sand supply, beach and foredune morphology, and grass abundance metrics in explaining the variability in dune carbon stocks across our study region.

We found that total dune carbon stocks averaged 2.1 ± 1.8 kg C/m^3 and belowground grass carbon typically comprised the largest proportion of total dune carbon stocks (mean ± SD: 1.1 ± 1.6 kg C/m^3), followed by sand carbon (0.9 ± 0.6 kg C/m^3), and aboveground grass carbon (0.1 ± 0.1 kg C/m^2) (Figure 3.3). Sediment organic carbon stocks in our study system were lower than those in other dune ecosystems (e.g., European dunes had 3-8 times greater sand carbon density than in Outer Banks dunes; Table 3.1) and substantially lower than those in other coastal ecosystems including mangroves, marshes, and seagrasses (soil organic carbon density was 10-30 times higher in salt marshes and mangroves; Van de Broek et al. 2016, Atwood et al. 2017, Dontis et al. 2020, Kauffman et al. 2020, Novak et al. 2020). In addition, we found variation in carbon stocks across islands, with higher sand carbon density in the southern Outer Banks and higher aboveground grass carbon stocks in the northern Outer Banks (Figure 3.4). All carbon stocks (aboveground grass, belowground grass, and sand) increased in the landward direction with shifts toward more stable sand and denser plant communities, and areas dominated by *U. paniculata* were associated with greater carbon stocks of all types (research question 1; Figures 3.4, 3.5). Finally, contrary to our expectations, sand carbon density did not vary with depth, and we did not find a relationship between sand

carbon density and that of belowground vegetation (research question 2; Figure 3.6, Table 3.5).

In our regression analyses, sand carbon density was negatively correlated with measures of sand supply to the dune suggesting that high sand deposition sites and profile locations have 'diluted' sand carbon densities. Moreover, across profile locations, those with lower sand deposition and denser and high biomass vegetation had more carbon in their dune sands. We also found similar relationships for total carbon (aboveground grass, belowground grass, and sand carbon combined), including negative correlations with measures of dune sand supply and a positive correlation with SCR (research question 3; Figures 3.7, Table 3.6). Overall, our findings show that carbon storage varies as a result of differences in physical and ecological factors across the dune profile and throughout the study region, with metrics of dune sand deposition being the most important drivers of sand carbon density and total (combined) carbon stocks.

Below we discuss in greater detail the patterns and potential drivers of dune carbon storage, as well as the potential consequences of climate change and extreme storm events on dune ecosystem services along the U.S. Atlantic coastline.

3.5.1 Contextualizing dune carbon storage in Outer Banks foredune ecosystems

While the coring depth varied among studies, sediment organic carbon values on a per area basis from foredunes on the U.S. Outer Banks barrier islands were generally much lower than those reported in other dune systems worldwide (see Table 3.1 for comparisons). For example, percent carbon and sand carbon density measurements on the Italian coast were approximately 3-5 times higher, depending on island and foredune

profile location, with the exception of the foredune heel at South Core Banks, which had similar values (Figure 3.4, Tables 3.1, 3.4; Drius et al. 2016). Likewise, measurements reported for a UK Atlantic dune system were approximately 6-8 times higher than those in our system (Table 3.1; Beaumont et al. 2014). However, when compared to dunes on other US east coast barrier islands (Sapelo Island, Georgia; Tackett and Craft 2010), our system had similar sand percent carbon values, suggesting that dune sand carbon content may be fairly consistent along the U.S. Atlantic coastline (Tables 3.1, 3.4).

These differences in carbon storage among dunes worldwide are likely a result of differences in physical and ecological factors including plant productivity and sand supply. In particular, U.K. coastal dunes have much higher aboveground vegetation biomass, averaging 1375 and 1221 g/m^2 in mobile dunes and fixed dunes, respectively (Beaumont et al. 2014), compared with averages of 100-350 g/m^2 in Outer Banks foredunes. In Italian dunes, landward gradients along the dune profile include shifts toward shrubs and woody vegetation, indicating greater aboveground productivity in these systems as well. In addition, U.S. Atlantic barrier islands are very dynamic systems subjected to frequent disturbance from storms, which can erode dunes and limit soil development and vegetation growth and thus carbon stocks.

How do carbon stocks in dunes compare to other coastal ecosystems? On a per area basis, dune aboveground carbon stocks in our system (0.004 to 0.19 kg C/m^2; Figure 3.4, Appendix F, Table F1) were comparable to those in eelgrass meadows and salt marshes; for example, aboveground carbon stocks ranged from 0.03-2.30 kg C/m^2 in New England eelgrass meadows (Novak et al. 2020) and averaged 0.10 kg C/m^2 in

Florida salt marshes (Dontis et al. 2020). But dune studies, including ours, also show that sediment organic carbon values are substantially lower than those in other coastal ecosystems. For example, soil carbon stocks in New England (2-6 kg C/m^2 Novak et al. 2020) and Pacific Northwest (7-9 kg C/m^3; Kauffman et al. 2020) eelgrass meadows were approximately 10 times greater than sand carbon in NC Outer Banks dunes (Figure 3.4). Soil carbon stocks were even greater in marsh and mangrove systems, with averages of 10, 46, and 28 kg C/m^2 in salt marshes, freshwater marshes, and mangroves, respectively (Van de Broek et al. 2016, Atwood et al. 2017).

When compared to terrestrial grasslands, NC Outer Banks dunes have similar aboveground carbon stocks but much lower soil stocks. For example, estimates for aboveground vegetation carbon stocks in terrestrial grasslands range from 0.05-0.60 kg C/m^2 worldwide (e.g., Cao and Woodward 1998, Bradley et al. 2006, Tanentzap and Coomes 2012, Xia et al. 2014) compared to 0.004 to 0.19 kg C/m^2 in our system (Figure 3.4, Appendix F, Table F1). Soil carbon in grasslands worldwide is roughly ten times greater (i.e., 2.5-17.5 kg C/m^2; 0.5-8 %C; Cao and Woodward 1998, Conant et al. 2001), compared to NC Outer Banks dunes, depending on island and profile location (i.e., 0.25-1.9 kg C/m^2; Figure 3.4, Appendix F, Table F1).

Although dune sand carbon stocks were relatively low when compared with similar coastal or grassland ecosystems, coastal dunes typically cover larger geographic areas and have deep reserves of sand and total carbon in vegetation (Cao and Woodward 1998, Conant et al. 2001, Bradley et al. 2006, Beaumont et al. 2014, Kauffman et al. 2020, Novak et al. 2020). We found that belowground dune grass carbon stocks

comprised a larger proportion of total carbon stocks than sand or aboveground dune grass carbon stocks (Figure 3.3). Dune grasses create extensive underground rhizome networks via vertical and lateral expansion as they form new tillers, increasing their sand capture potential (Hacker et al. 2012, Zarnetske et al. 2012, Charbonneau et al. 2016, Hacker et al. 2019a) and ultimately leading to the burial of additional plant material. Because foredunes can be very tall (up to approximately eight meters in our study system), contain extensive belowground rhizome networks, and contain a high proportion of their carbon in belowground grass stocks, total carbon storage in this system may be significant when scaled to the volume of the dunes.

3.5.2 Local and regional spatial variability in carbon stocks on the Outer Banks barrier islands

We observed substantial variability in beach and foredune geomorphology across our study region (Figure 3.2a-e). At most sites, the beach was either stable or mildly eroding (neutral or slightly negative multidecadal SCR values). Exceptions included Bodie Island, where the beach was eroding at >10 m/yr, and OCR_1 and SCB_4, where beaches were accreting at ~5-10 m/yr (Figure 3.2a). The larger negative multidecadal SCR at Bodie Island is likely related to its proximity to nearby Oregon Inlet (Figure 3.1). Sites with negative multidecadal SCRs tended to have narrower beaches with steeper backshore slopes, while those with strongly positive multidecadal SCRs had wider beaches and shallower backshore slopes (Figure 3.2a-c). Foredune height tends to be greater in areas with slightly negative SCR values (Psuty 1986), which was the case at Hatteras Island and North Core Banks but not at the other islands. Previous research has also shown that foredune morphology is strongly related to beach width and SCR (e.g.,

Short and Hesp 1982, Sherman and Bauer 1993, Biel et al. 2019), but patterns in foredune height and width varied greatly throughout our study region (Figure 3.2d, e). Foredunes were tallest at Hatteras Island and shortest at South Core Banks but had a spectrum of morphologies ranging from low to high aspect ratios. Previous research in the Outer Banks showed that low aspect ratio dunes were found in areas with more positive SCRs and wider beaches (and vice versa; Jay et al. Chapter 2). This pattern held at some of our sites (e.g., SCB_4, OCR_1, HAT_7, HAT_12) but was contradicted at others (e.g., NCB_16, BOD_1).

The variability in carbon stocks we observed between islands and profile locations may be largely attributed to the differences in beach and foredune geomorphology and ecology. Aboveground grass, belowground grass, and sand carbon stocks all varied by island and profile location, but patterns differed between sand and grass carbon stocks (Figure 3.4, Table 3.3). Aboveground grass stocks were higher overall at Bodie and Hatteras Islands and lowest at the dune toe in most cases (except Bodie Island), with no significant differences between the crest and heel (except at Hatteras Island; Figure 3.4a, Table 3.3). Belowground grass carbon was also lowest at the dune toe and did not differ between the crest and heel, with the highest values occurring at Ocracoke Island (Figure 3.4b). On the other hand, sand carbon density was lowest at Bodie Island and highest at South Core Banks, with more similar moderate values at North Core Banks, Ocracoke Island, and Hatteras Island. Sand carbon densities tended to increase in the landward direction along the dune profile due to the combination of higher grass biomass and lower sand deposition that typically occurs at the dune crest and heel

(Figure 3.2f, g). Unsurprisingly, belowground grass carbon followed similar patterns to those of aboveground grass carbon along the dune profile; however, the significantly higher belowground carbon values observed at Ocracoke Island were an unexpected finding (Figure 3.4). These high belowground carbon values may be related to foredune morphology, which was particularly tall and narrow at this site (Appendix C, Figure C2e); this higher surface to volume ratio may lead to a greater concentration of belowground biomass within the dune.

Extreme storm events can also play an important role in shaping the aboveground and belowground carbon stocks in dunes. Two of the South Core Banks transects (SCB_6 and SCB_9) experienced significant erosion in September 2018 as a result of Hurricane Florence, during which a large portion of the foredunes were removed (see Appendix C, Figure C2i, j). All cores at these two transects were collected from the later successional plant communities at the heel of the former foredune, where, prior to the hurricane, dune grass had higher biomass compared to the toe profile location. This dune profile location transition may explain the unexpected high sand carbon values (a remnant of the previous dune profile location) across the entire foredune profile (Figure 3.4c, Appendix C, Figure C2i, j).

The variability we observed in sand carbon density may also be related to other factors we did not measure, including offshore gradients in marine nutrient levels along the Outer Banks coastline, resulting in differences in marine carbon contributions to dune sediments. Marine carbon contributions to foredunes could include nutrients in seawater as well as the decomposition of wrack delivered to beaches; previous studies have

documented connections between wrack biomass, beach sand nutrient levels, and dune vegetation (Dugan et al. 2011, Constant 2019). The offshore boundary in ocean currents near Cape Hatteras may influence the delivery of marine nutrients to the coast; for example, the region north of Cape Hatteras has greater offshore marine DOC levels compared with the southern Outer Banks (Mannino et al. 2016). However, we observed lower sand carbon density in the northern Outer Banks sites compared to South Core Banks, suggesting that the interactive effects of sand deposition and vegetation biomass are more important than marine nutrient inputs.

3.5.3 Patterns in sand and belowground grass carbon density with depth

Surprisingly, we found no apparent patterns or significant differences in sand or belowground grass carbon density with core depth (Figure 3.6, Table 3.5; Appendix F, Figure F2). We expected that sand carbon density would be highest at the top of the core where grasses and plant litter could most contribute to sand carbon, and then decrease with depth as roots and rhizomes decline and/or decompose over time. Instead, we found that there was little relationship between sand carbon density and belowground plant carbon density, and both rarely varied with depth, or if they did, peaked in the middle or near the bottom of the core (Figure 3.6, Appendix F, Figure F2, Table F3). As this is the first study to our knowledge to collect relatively deep cores and quantify the magnitude and variability of dune carbon stocks with depth in foredune ecosystems, no patterns in sand or belowground grass carbon density have been previously reported with core depth. Previous work in Pacific Northwest low and high salt marshes, both of which had much higher magnitude carbon values than Outer Banks dunes, found that soil carbon density

decreased consistently with depth (Kauffman et al. 2020). On the other hand, soil carbon density and soil carbon concentration values were smaller in magnitude and variable with depth in Pacific Northwest seagrass beds, with the highest values occurring deeper than 100 cm (Kauffman et al. 2020). The lack of variability in carbon concentration with depth that we document here underscores the need to collect more replicate cores at each site, as well as core deeper (≥ 1 m), to better understand dune carbon dynamics. At greater depths, carbon concentrations could decrease due to reduced root/rhizome biomass and the presence of more advanced stages of decomposition, or concentrations could potentially increase due to limited oxidation and the presence of water containing carbon. If carbon density does not decrease significantly at greater depths, these dune ecosystems may contain large carbon stocks that vary according to dune volume.

3.5.4 Factors important to foredune carbon stocks

Finally, we wanted to know whether carbon stocks were correlated with various geomorphic and ecological factors including beach and foredune morphometrics, foredune sand supply, and grass abundance metrics on Outer Banks dunes. Overall, we found that dune sand supply, or foredune morphometrics that influence dune sand supply (i.e., backshore slope, foredune height; Figure 3.2c, e) were the most important factors contributing to variability in dune carbon stocks (Figure 3.7, Table 3.6). For example, total foredune carbon stocks and sand carbon stocks were both negatively correlated with dune sand deposition rate and backshore slope (a proxy for sand supply). This finding was somewhat unexpected, as high burial rates have often been associated with high carbon stocks in other coastal ecosystems (e.g., Callaway et al. 2012, Lovelock et al.

2014, Breithaupt et al. 2019). In this system, though, high dune sand supply appears to both 'dilute' dune carbon with low carbon-content beach sand, and reduce the carbon contribution from dune grasses, effectively lowering sand carbon density. Some of our sites received >25 cm of sand annually over a two-year period, with the greatest deposition occurring at Bodie Island where sand carbon density values were very low (Figures 3.2f, h, 3.4c, 3.7).

Our analyses allowed us to explore the interactive effects of sand deposition rate and grass density and biomass on sand carbon density across our study region. Grass density (all species combined) was included in the top model (selected using ΔAIC) for sand carbon density, but it explained a small proportion of the variance compared to dune sand deposition and backshore slope (4% compared to 50% for sand deposition rate and 26% for backshore slope). This finding contradicted our expectation that aboveground vegetation would be one of the most important factors determining sand carbon storage, as has been shown in some other coastal systems (e.g., Greiner et al. 2013, Rossi and Rabenhorst 2019, Kaviarasan et al. 2019). The lack of a strong relationship between dune grasses and sand carbon stocks could be a consequence of how sand deposition interacts with dune grass biomass across islands and profile locations. For example, comparing islands or transects, when sand deposition is high at these locations (for example, at Bodie Island and Ocracoke Island), dune grass biomass is also high likely because of the well-known positive feedbacks between sand accretion and vegetative growth documented in dune systems (e.g., Hacker et al. 2012, Zarnetske et al. 2012, Keijsers et al. 2015, Brown and Zinnert 2018, Mullins et al. 2019, Biel et al. 2019, Charbonneau et

al. 2021). This positive feedback could then be indirectly responsible for ‘diluting’ sand carbon through increased sand accretion. However, across profile locations, gradients in sand deposition and grass density are negatively correlated, where the toe and crest of the dune is characterized by high sand deposition (or erosion) but overall lower dune grass abundance and the heel of the dune shows the opposite pattern, i.e., sand deposition (or erosion) is low and grass abundance is high (Figure 3.7). Under these conditions, we found that sand carbon varies from low at the dune toe and crest to high at the dune heel, where presumably the direct effect of belowground roots and rhizomes, decomposition, and soil formation is greatest. Thus, because the feedbacks between dune sand deposition, grass density, and sand carbon density are self-reinforcing at both high and low sand deposition sites, the importance of vegetation to sand carbon stocks is more complicated and likely depends on its indirect effects on sand deposition and its direct effects on belowground carbon cycling.

Periodic declines in aboveground vegetation following storm disturbance are also an important consideration in these dynamic foredune ecosystems, as has been previously shown in mangrove ecosystems (Breithaupt et al. 2019). Hurricane Florence occurred approximately nine months prior to our coring campaign and eroded and overwashed some of our sites along South Core Banks (e.g., Appendix C, Figure C2i, j), leading to decreased vegetation density at some sites. Therefore, storm events can either wash away dune carbon stocks altogether or interrupt dune vegetation productivity and carbon sequestration as a result.

Our study suggests that carbon stocks in coastal foredunes are linked to the relative importance of geomorphic and vegetation processes on different islands and profile locations along the Outer Banks coastline. While other studies have made such linkages in coastal ecosystems including mangroves, marshes, and barrier islands (e.g., Callaway et al. 2012, Lovelock et al. 2014, Twilley et al. 2018, Rossi and Rabenhorst 2019, Novak et al. 2020), our study is the first that we are aware of to make such connections in foredune ecosystems. For example, Novak et al. (2020) investigated the relative importance of environmental variables to eelgrass carbon stocks and found that sediment grain size, tidal range, shoot density, and wave energy were important factors. In marshes and mangroves, previous studies showed that carbon sequestration varied according to plant community type, sediment characteristics, and sediment accretion rates (Callaway et al. 2012, Lovelock et al. 2014).

Similar to standing carbon stocks, which we documented in our study, carbon accumulation rates can also be impacted by dynamic coastal processes. A study using a cross-shore gradient of barrier island sites in U.S. Atlantic Coast barrier islands, including inland dunes, found evidence that organic carbon was in a rapid accumulation phase and suggested that these barrier island sediments may not reach steady state conditions because carbon accumulation processes are frequently reset due to overwash and burial events (Rossi and Rabenhorst 2019). In this contribution, we quantified standing carbon stocks in dune sand, aboveground vegetation, and belowground vegetation, but we did not establish geochronologic age constraints from which to estimate carbon sequestration or accumulation rates. Although we report differences in

dune carbon stocks across the Outer Banks, carbon accumulation rates may not follow the same patterns; therefore, future work to characterize the temporal dynamics of this ecosystem may provide key insight into the processes controlling dune carbon storage. For example, Lovelock et al. (2014) reported large differences in sediment carbon density across an environmental gradient in mangrove forests, but carbon sequestration rates were similar across the same region due to the differences in vertical sediment accumulation rates. These studies suggest that overall carbon stocks of dune sites with low sand carbon density but higher sand deposition (e.g., Bodie Island and Ocracoke Island) may have similar carbon sequestration rates to dune sites with higher sand carbon density but lower sand deposition (e.g., South Core Banks; Figures 3.2, 3.4). These carbon sequestration rates may also vary temporally as a result of variability in sand deposition rates.

3.5.5 Climate change implications for dune ecosystem services

Understanding how dune carbon storage varies worldwide is especially critical as climate change alters the physical and ecological processes that interact to shape dunes and their ecosystem services such as carbon storage and coastal protection. Coastal dune ecosystems are vulnerable to anthropogenic disturbance, land-use change, sea level rise, increased temperatures, and increased frequency of extreme storm events (Sallenger et al. 2012, Seabloom et al. 2013, Intergovernmental Panel on Climate Change 2014, Ranasinghe 2016, de Winter and Ruessink 2017, Masselink et al. 2020). Human activities and land-use change may lead to increased destruction of dunes, shifts in plant communities, and changes in nutrient cycling (Macreadie et al. 2019), while sea level rise

and extreme storms can lead to dune inundation and erosion (Stockdon et al. 2007, Seabloom et al. 2013, Enríquez et al. 2019, Fernández-Montblanc et al. 2020), all of which have the potential to impact coastal carbon storage in interactive ways (Mcleod et al. 2011). Carbon sequestration rates may increase if sediment accumulation keeps pace with sea level rise, as has been documented in salt marshes, until a critical threshold is reached and the vegetation is drowned (Morris et al. 2002, Mudd et al. 2009). Dunes may be able to migrate landward, but decreases in dune habitat area following erosion and storms could lead to losses of both the stored carbon deposits and the future carbon sequestration capacity of the ecosystem. For example, mangroves, seagrasses, and salt marshes are losing approximately 0.7-7% of their area annually, with significant implications for their carbon stocks (Alongi 2002, Duarte et al. 2005, Bridgham et al. 2006, Waycott et al. 2009, Mcleod et al. 2011). In dunes, modeling and field-based efforts have shown that rates of sea level rise and vegetation growth can determine whether or not foredunes are able to maintain their volume, migrate landward, or revegetate and recover their previous height following disturbance (e.g., Keijsers et al. 2016, van IJzendoorn et al. 2021). In addition, sea level rise-driven beach erosion may constrain dune plant communities to a narrower area, leading to the breakdown of plant successional trajectories (Feagin et al. 2005). Thus, changes in dune morphology and vegetation as a result of climate change could lead to significant losses in dune carbon stocks. In contrast, some studies suggest that global ‘greening’ of ecosystems is occurring as a result of climate change (Zhu et al. 2016). In coastal dunes, Jackson et al. (2019) found global increases in vegetation cover over the past three decades as a result of the

interactive effects of increased temperatures, precipitation, and nutrients. Such changes in vegetation growth and cover could increase belowground dune carbon storage in addition to aboveground vegetation stocks.

Range shifts in the dominant dune grasses across our study region are also likely to occur as a result of climate change, which may have implications for foredune ecosystem services including carbon storage. For example, Goldstein et al. (2018) documented the ranges of *U. paniculata* and *A. breviligulata* on the U.S. Atlantic coast using literature surveys and found a northward increase in the range of *U. paniculata* over the past 60 years. Combined with the results of a glasshouse study where *A. breviligulata* growth declined when growing in mixture with *U. paniculata* (Harris et al. 2017), there is evidence that *U. paniculata* may outcompete *A. breviligulata* within areas of its range as a result of future warming. Based on our measurements of grass morphology and field densities of each species in monoculture, we would predict an increase of approximately 35% in aboveground grass carbon stocks if a dune shifted from an *A. breviligulata* monoculture to a *U. paniculata* monoculture. We do not have direct measurements of belowground biomass for the two species in monoculture, but these differences in aboveground grass carbon could also impact belowground grass and sand carbon stocks. Therefore, *U. paniculata* range shifts may have implications for dune ecosystem services including possible increases in carbon stocks along the U.S. Atlantic coast.

In this study, we present the first comprehensive inventory of coastal foredune carbon storage in North America. Our findings enhance our understanding of the carbon

storage ecosystem service in understudied coastal dune ecosystems and provide insights into physical and ecological factors that may influence carbon storage in these dynamic coastal settings. We found that Outer Banks dune carbon stocks were lower in magnitude compared to values from other dune systems (e.g., Atlantic U.K. dunes, Italian dunes) and that they varied significantly among islands and foredune profile locations as a result of the relative importance of sand supply and dune grass biomass. Belowground vegetation carbon stocks were especially important in Outer Banks dunes, underscoring the need to investigate whether dune carbon densities vary within deeper depths of the foredune. Future research using stable isotopic carbon measurements ($\delta^{13}C$) and linear mixing models to quantify the proportion of dune sand carbon derived from marine versus terrestrial sources (with a focus on transects dominated by *U. paniculata*, which is a C_4 grass with a different $\delta^{13}C$ signature) (e.g., Middelburg et al. 1997) would be valuable to better understand carbon cycling in foredune ecosystems. Quantifying dune carbon sequestration rates along the U.S. Atlantic Coast would elucidate how the carbon stocks reported here may change as a result of altered physical and ecological processes. Additional measurements from other globally distributed foredune ecosystems are also necessary, as carbon stocks and densities vary substantially between regions. Lastly, our improved understanding of dune carbon dynamics can be used to inform predictive models that forecast future changes in dune carbon stocks as a consequence of heightened storm events and sea level rise, providing valuable insight into the future role of coastal dunes in mitigating climate change.

3.6 Acknowledgements

Funding was provided by the National Oceanic and Atmospheric Administration (NOAA) via the NOS/NCCOS/CRP Ecological Effects of Sea Level Rise Program (grant no. NA15NOS4780172) to P.R., S.D.H., and L.J.M., the Geological Society of America to K.R.J, and the Garden Club of America to K.R.J. We thank P. Hovenga, R. Mostow, M. Itzkin, E. Mullins, I. Reeves, J. Wood, H. Lawrence, N. Cohn, E. Goldstein, C. Magel, and R. Biel for assistance with field data collection and P. Hovenga for assistance with topography data processing. We are grateful to M. Goni and K. Welch for assistance with obtaining and interpreting sand percent carbon data, A. Fund for grass percent carbon analyses, A. Thurber for allowing us to use his laboratory facilities for LOI analyses, and E. Peck for advice on core collection and lab methodology. We thank B. Russell for designing and creating our custom-built core extruder.

Table 3.1. Summary of previous studies measuring percent soil organic carbon (SOC), organic carbon stocks (tonnes/ha), and carbon sequestration rates (kg/ha/yr) in coastal dunes. Values are based on sand measurements and do not include dune vegetation.

Reference	Location	Sampling depth (cm)	SOC content (%)	Org. carbon stocks (t/ha)	Carbon sequestration rate (kg/ha/yr)
Tackett & Craft 2010	Sapelo Island, Georgia, US	0-30	0.08 ± 0.01 (top 10 cm); 0.06 ± 0.01 (10-30 cm)	2.5	
Drius et al. 2016	North & Central Adriatic, Italy	0-15	0.13 ± 0.05 (embryo dunes); 0.15 ± 0.12 (mobile dunes); 0.18 ± 0.07 (fixed dunes); 2.84 ± 2.56 (wooded dunes)	3.1 ± 1.3 (embryo dunes); 3.1 ± 1.7 (mobile dunes); 4.1 ± 1.4 (fixed dunes); 31 ± 19.7 (wooded dunes)	57.2 ± 22.8 (embryo dunes); 55.7 ± 31 (mobile dunes); 74.9 ± 25.6 (fixed dunes); 563.5 ± 358.3 (wooded dunes)
Jones et al. 2008	Atlantic UK dunes, North Wales	0-15			582 ± 262 (dry dunes); 730 ± 221 (wet dunes)
Beaumont et al. 2014	Atlantic UK dunes (Wales, Scotland, England, North Ireland)	0-15	0.33 ± 0.22 (mobile dunes); 1.84 ± 1.71 (fixed dunes); 4.38 ± 3.32 (dune slacks);		
Turner & Laliberté 2015	Jurien Bay chronosequence, SW Australia	0-100		Ranges from 29.2-177.2 depending on age	
Schaub et al. 2019	SW Baltic Sea, NE Germany	0-1.5	0.03		
Chen et al. 2015	Cooloola dunes, South Queensland, Australia	0-30	Ranges from 0.03 (bare sand) to 1.44 (vine forest scrub) **(Total C, not org. C)*	Ranges from 0-60 depending on age **(Total C, not org. C)*	

Table 3.2. Two-way ANOVA and Tukey HSD post-hoc test results for total carbon stocks [kg C/m^2 for aboveground (AG) grass and kg C/m^3 for belowground (BG) grass and sand carbon] across islands (see Figure 3.1; Appendix C, Table C1 for island abbreviations) and carbon stock type [AG grass, BG grass, and sand].

Variable	df	SS	F	Prob > F	Tukey HSD post-hoc test	
Total carbon stock						
Island	4	7.2	2.8	2.72E-02		
C stock	2	146.2	113.3	< 2E-16		
Island* C stock	8	14.8	2.9	4.35E-03	**BOD:** AG = BG = Sand **HAT, NCB:** AG < BG = Sand **OCR:** AG = BG = Sand **SCB:** AG < BG < Sand	**AG, BG:** HAT = BOD = OCR = NCB = SCB **Sand:** BOD < HAT = OCR = NCB < SCB
Residuals	291	187.7				

Table 3.3. Two-way ANOVA and Tukey HSD post-hoc test results for aboveground (AG) grass stocks (kg C/m^2) and belowground (BG) grass and sand carbon density (kg C/m^3) across islands (see Figure 3.1; Appendix C, Table C1 for island abbreviations) and dune profile locations (toe, crest, and heel).

Variable	df	SS	F	Prob > F	Tukey HSD post-hoc test	
Aboveground grass carbon (kg C/m^2)						
Island	4	0.10	6.2	7.87E-05		
Profile location	2	0.49	62.9	< 2E-16		
Island* Profile location	8	0.08	2.5	1.14E-02	**BOD:** Toe = Crest = Heel **HAT:** Toe < Crest > Heel, Toe < Heel **OCR, NCB:** Toe < Crest = Heel **SCB:** Toe = Crest = Heel, Toe < Heel	**Toe:** BOD = HAT = OCR = NCB = SCB **Crest:** BOD = HAT = OCR = NCB = SCB, HAT > NCB = SCB, BOD > SCB **Heel:** BOD = HAT = OCR = NCB = SCB
Residuals	300	1.2				
Belowground grass carbon (kg C/m^3)						
Island	4	6.2	8.3	2.36E-06		
Profile location	2	29.0	77.8	< 2E-16		
Island* Profile location	8	12.6	8.4	2.36E-10	**BOD:** Toe = Crest = Heel, Toe < Heel **HAT:** Toe < Crest = Heel **OCR, NCB:** Toe < Crest = Heel **SCB:** Toe < Crest = Heel	**Toe:** BOD = HAT = OCR = NCB = SCB **Crest:** OCR > BOD = HAT = NCB = SCB, NCB > BOD **Heel:** BOD = HAT = OCR = NCB = SCB
Residuals	300	55.8				
Sand carbon (kg C/m^3)						
Island	4	129.5	131.1	< 2E-16		

Table 3.3. (Continued)

Profile location	2	15.1	30.7	3.09E-13		
Island* Profile location	8	9.8	4.9	6.44E-06	**BOD:** Toe = Crest = Heel **HAT, SCB:** Toe = Crest < Heel **OCR:** Toe = Crest = Heel, Toe < Heel **NCB:** Toe > Crest < Heel, Toe = Heel	**Toe:** SCB = NCB > OCR = HAT > BOD, OCR = BOD **Crest:** SCB > HAT = NCB = OCR > BOD **Heel:** SCB > HAT = OCR = NCB > BOD
Residuals	457	112.9				

Table 3.4. Two-way ANOVA and Tukey HSD post-hoc test results for aboveground (AG) grass carbon stocks (kg C/m^2) and belowground (BG) grass carbon and sand carbon density (kg C/m^3) across islands (see Figure 3.1; Appendix C, Table C1 for island abbreviations) and dominant grass species [*Uniola paniculata* (UNPA) and *Ammophila breviligulata* (AMBR)]. South Core Banks sites were excluded from the analyses because AMBR did not occur at those sites.

Variable	df	SS	F	Prob > F	Tukey HSD post-hoc test	
Aboveground grass carbon (kg C/m^2)						
Island	3	0.04	2.9	0.0016		
Species	1	0.23	46.9	6.28E-11		
Island* Species	3	0.06	3.9	0.0098	**BOD:** UNPA = AMBR **HAT:** UNPA > AMBR **OCR:** UNPA > AMBR **NCB:** UNPA > AMBR	**UNPA:** HAT = NCB = OCR = BOD **AMBR:** BOD > HAT= OCR = NCB
Residuals	237	34.81				
Belowground grass carbon (kg C/m^3)						
Island	3	5.6	12.2	1.83E-07		
Species	1	24.9	162.4	< 2E-16		
Island* Species	3	11.2	24.4	8.13E-14	**BOD:** UNPA > AMBR **HAT:** UNPA > AMBR **OCR:** UNPA > AMBR **NCB:** UNPA >AMBR	**UNPA:** OCR > HAT = NCB = BOD **AMBR:** BOD = HAT= OCR= NCB
Residuals	237	36.38				
Sand carbon (kg C/m^3)						
Island	3	21.1	24.8	1.66E-14		
Species	1	1.8	6.5	1.11E-02		

Table 3.4. (Continued)

Island* Species	3	3.9	4.6	3.22E-03	**BOD:** UNPA > AMBR **HAT:** UNPA = AMBR **OCR:** UNPA > AMBR **NCB:** UNPA =AMBR	**UNPA:** HAT = NCB = OCR > BOD **AMBR:** HAT = NCB > OCR = BOD
Residuals	323	91.2				

Table 3.5. Two-way ANOVA and Tukey HSD post-hoc test results for sand carbon density (kg C/m^3) across islands (see Figure 3.1; Appendix C, Table C1 for island abbreviations) and core depths (0-10, 10-20, 20-30, 30-60, and 60-100 cm). Tests were run separately at the dune profile locations of toe, crest, and heel.

	df	SS	F	Prob > F	Tukey HSD post-hoc test
Toe sand carbon density (kg C/m^3)					
Island	4	27.3	24.5	2.94E-14	SCB = NCB > HAT = OCR = BOD, HAT > BOD
Core depth	5	4.0	2.9	0.02	0-10 = 10-20 = 20-30 = 30-60 = 60-100
Island*Core depth	17	6.5	1.9	0.16	
Residuals	103	28.7			
Crest sand carbon density (kg C/m^3)					
Island	4	10.9	15.7	3.90E-10	SCB > NCB = HAT = OCR > BOD
Core depth	5	0.58	0.67	0.65	
Island* Core depth	16	1.7	0.61	0.87	
Residuals	105	18.2			
Heel sand carbon density (kg C/m^3)					
Island	4	68.9	37.6	< 2E-16	SCB > NCB = HAT = OCR = BOD, HAT > BOD
Core depth	5	5.0	2.2	0.06	
Island* Core depth	16	10.7	1.4	0.12	
Residuals	185	84.6			

Table 3.6. Top model results (ΔAIC<2) from multiple regression analyses of the response variables sand carbon density (kg C/m^3), aboveground (AG) grass carbon (kg C/m^2), and total carbon (AG grass, belowground grass, and sand combined) as a function of the explanatory variables of sand supply, beach and foredune morphometrics, and dune grass biomass and density (see Figure 3.2) at the core level. Explanatory variables included together in models were uncorrelated with Pearson correlation coefficient < |0.6|. Significance codes for explanatory variables are: ***p<0.001, **p<0.01, *p<0.05, .p<0.1. Explanatory variables with significant p values are in bold. Response variable transformations were applied following Shapiro–Wilk tests for normality and residual investigations.

Response variable	Model	Model results
Sand carbon density	[ln(Sand C)] = -1.91[**Sand dep rate**]*** – 15.82[**Backshore slope**]*** + 0.005[Grass density]. + 0.27*	AIC_c=30.21 ΔAIC=0 df=29 Adj. R^2=0.70 **Variance explained:** Sand dep rate=0.50, Backshore slope=0.26, Grass density=0.04
	[ln(Sand C)] = -1.79[**Sand dep rate**]*** – 15.85[**Backshore slope**]*** + 0.001[Grass biomass]. + 0.26.	AIC_c=30.70 ΔAIC=0.49 df=29 Adj. R^2=0.70 **Variance explained:** Sand dep rate=0.46, Backshore slope=0.25, Grass biomass=0.03
	[ln(Sand C)] = -1.81[**Sand dep rate**]*** – 14.76[**Backshore slope**]*** + 0.37**	AIC_c=31.56 ΔAIC=1.35 df=30 Adj. R^2=0.67 **Variance explained:** Sand dep rate=0.47, Backshore slope=0.23
AG grass carbon	[AG grass C] = 0.01[Foredune height]. + 0.02	AIC_c=-91.97 ΔAIC=0 df=31 Adj. R^2=0.06 **Variance explained:** Foredune height=0.09

Table 3.6. (Continued)

	[AG grass C] = 0.01[Foredune height]. – 0.003[SCR] + 0.02	AIC_c=-91.36 ΔAIC=0.61 df=30 Adj. R^2=0.09 **Variance explained:** Foredune height=0.10, SCR=0.05
	[AG grass C] = 0.01[Foredune height]. + 0.04[Sand dep rate] + 0.02	AIC_c=-90.45 ΔAIC=1.52 df=30 Adj. R^2=0.06 **Variance explained:** Foredune height=0.07, Sand dep rate=0.03
	[AG grass C] = 0.01[Foredune height]. – 0.0002[Beach width] + 0.03	AIC_c=-90.26 ΔAIC=1.71 df=30 Adj. R^2=0.05 **Variance explained:** Foredune height=0.09, Beach width=0.02
Total carbon (AG+BG+ sand)	[ln(Total C)] = 0.07[**SCR**]* + 0.55***	AIC_c=74.59 ΔAIC=0 df=31 Adj. R^2=0.17 **Variance explained:** SCR=0.19
	[ln(Total C)] = -1.20[**Sand dep rate**]* – 12.90[**Backshore slope**]* + 1.34[Foredune aspect ratio] + 0.63.	AIC_c=75.65 ΔAIC=1.06 df=30 Adj. R^2=0.22 **Variance explained:** Sand dep rate=0.14, Backshore slope=0.11, Foredune aspect ratio=0.06

Table 3.6.

(Continued)

[ln(Total C)] = -1.18[**Sand dep rate**]* – 11.92[**Backshore slope**]. + 1.06***	AIC_c=75.69 ΔAIC=1.10 df=30 Adj. R^2=0.18 **Variance explained:** Sand dep rate=0.13, Backshore slope=0.10
[ln(Total C)] = 0.06[**SCR**]* + 6.10[Foredune aspect ratio] + 0.23	AIC_c=75.97 ΔAIC=1.38 df=30 Adj. R^2=0.17 **Variance explained:** SCR=0.18, Foredune aspect ratio =0.03
[ln(Total C)] = 0.05[SCR]. – 0.61[Sand dep rate] + 0.63***	AIC_c=76.10 ΔAIC=1.51 df=30 Adj. R^2=0.17 **Variance explained:** SCR=0.09, Sand dep rate =0.03
[ln(Total C)] = 0.06[**SCR**]* – 6.10[Backshore slope] + 0.74***	AIC_c=76.30 ΔAIC=1.71 df=30 Adj. R^2=0.16 **Variance explained:** SCR=0.12, Backshore slope=0.02

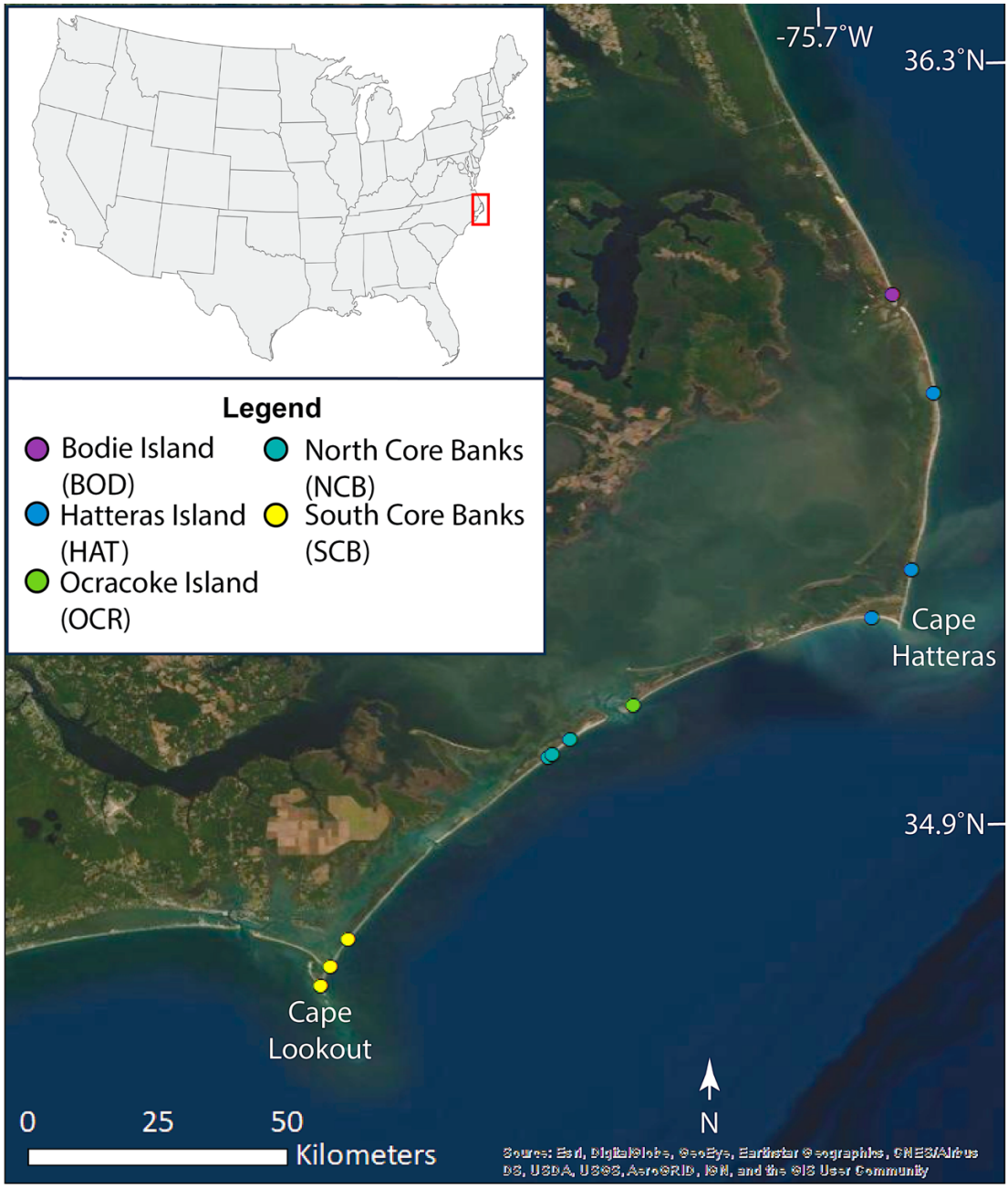

Figure 3.1. Map of transect and sediment core sampling locations (see Appendix C, Table C1 for latitude and longitude) for the foredunes of the Outer Banks barrier islands, from Bodie Island to South Core Banks, North Carolina, USA.

Figure 3.2. Sand supply, beach morphology, and dune grass metrics in the foredunes of the Outer Banks islands, North Carolina, USA, by transect from north to south (see Figure 3.1; Appendix C, Table C1 for island and transect abbreviations and locations). (A) Multidecadal shoreline change rate (SCR) from 1997-2016 (southern Outer Banks transects) and 1997-2010 (northern Outer Banks transects) (m/yr). (B) Beach width (m). (C) Backshore slope. (D) Foredune height (m). (E) Foredune width (m). (F) Annual sand deposition rate at the dune toe, crest, and heel from 2017-19 (m/yr). Note that values at SCB_6 and SCB_9 for 'toe', 'crest', and 'heel' were all designated as heel sites in our analyses. (G) Mean combined grass biomass at the toe, crest, and heel of the dune in 2019 (g/m^2). (H) Mean combined grass density at the toe, crest, and heel of the dune in 2019 ($tillers/m^2$). (I) Mean combined grass biomass (2019, g/m^2) of the dominant grasses averaged across the dune profile and divided into grass species [*Uniola paniculata* (UNPA), *Ammophila breviligulata* (AMBR), and *Panicum amarum* (PAAM)].

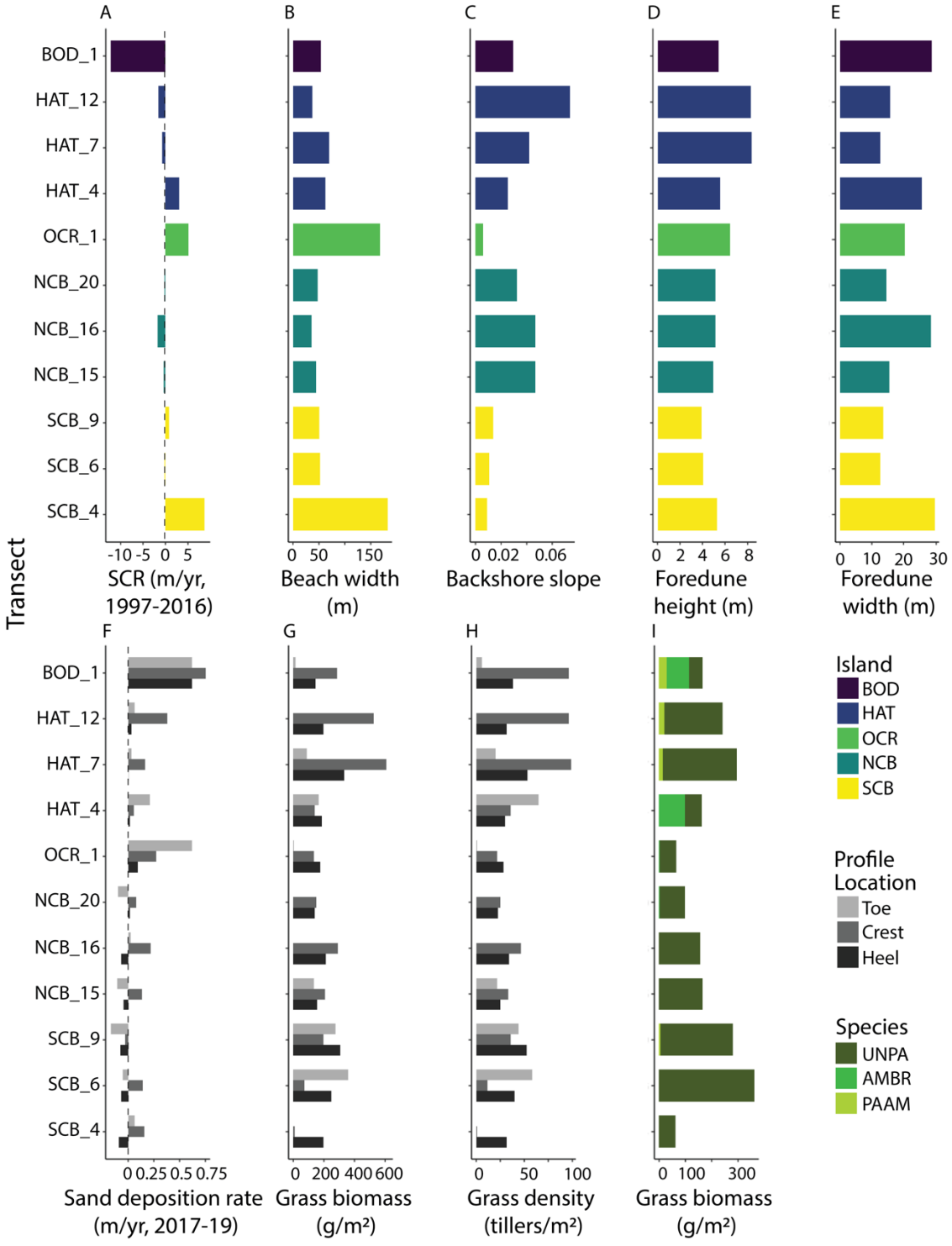
A
B
C
D
E
BOD_1
HAT_12
HAT_7
HAT_4
OCR_1
NCB_20
NCB_16
NCB_15
SCB_9
SCB_6
SCB_4
Transect
-10 -5 0 5
SCR (m/yr, 1997-2016)
0 50 150
Beach width (m)
0 0.02 0.06
Backshore slope
0 2 4 6 8
Foredune height (m)
0 10 20 30
Foredune width (m)
F
G
H
I
0 0.25 0.5 0.75
Sand deposition rate (m/yr, 2017-19)
0 200 400 600
Grass biomass (g/m²)
0 50 100
Grass density (tillers/m²)
0 100 300
Grass biomass (g/m²)
Island
BOD
HAT
OCR
NCB
SCB
Profile Location
Toe
Crest
Heel
Species
UNPA
AMBR
PAAM

Figure 3.2.

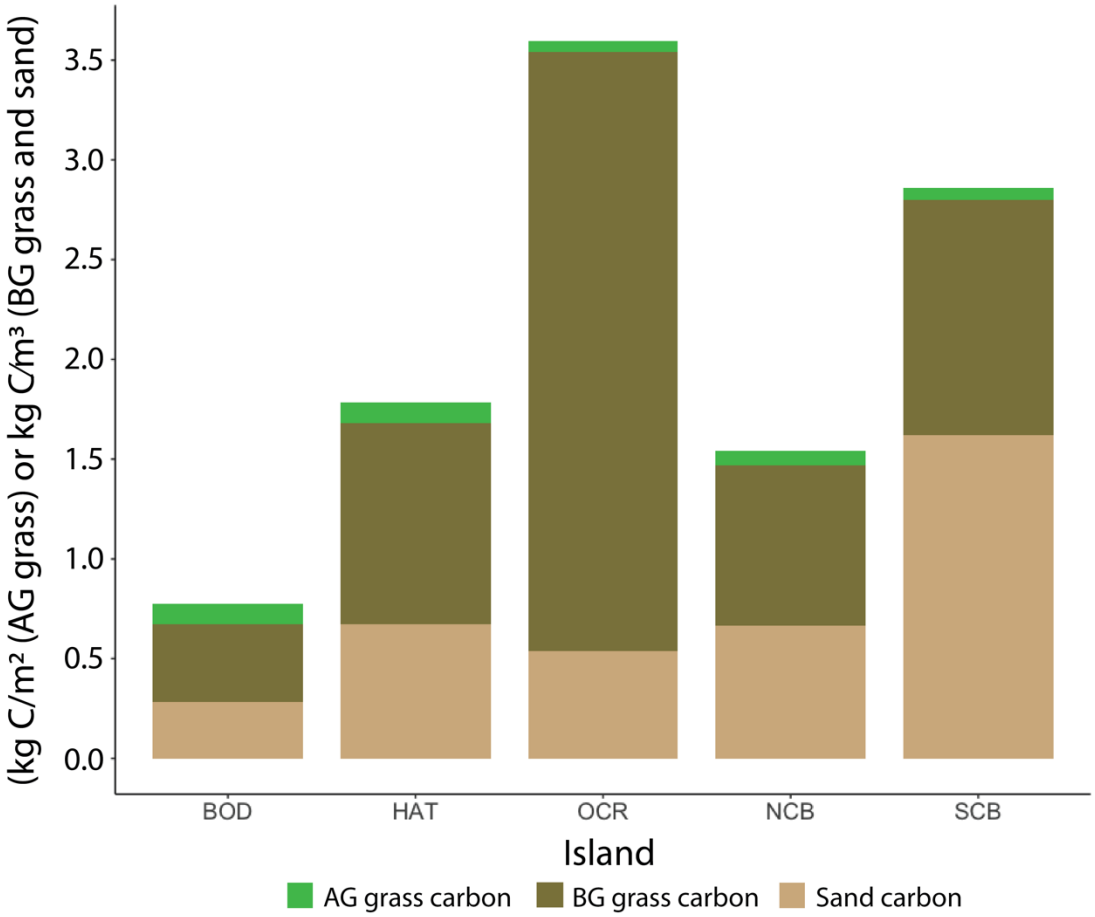

Figure 3.3. Mean total carbon in aboveground (AG) grass (kg C/m^2), belowground (BG) grass (kg C/m^3), and sand (kg C/m^3) on the foredunes of the Outer Banks barrier islands, North Carolina, USA (see Figure 3.1 and Appendix C, Table C1 for island abbreviations and locations). Note that AG carbon density is expressed in area units (kg C in 1 m x 1 m or m^2 area) and BG and sand carbon density values are expressed in volumetric units (kg C in 1 m x 1 m x 1 m depth or m^3). The two units are interchangeable, and thus can be directly compared, given that they are considering the same amount of area. See Table 3.2 for statistics.

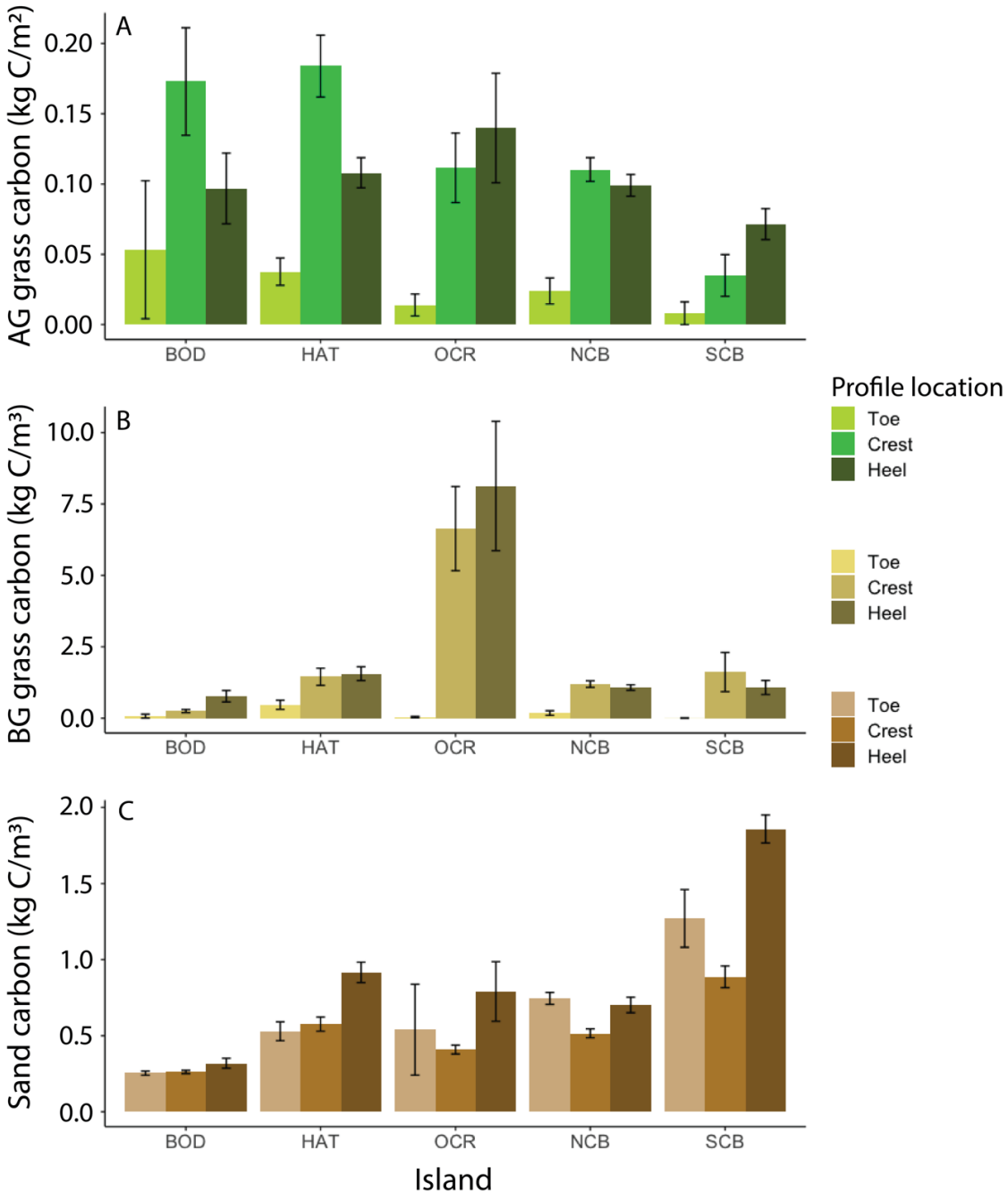

Figure 3.4. Mean ± (SE) for (A) aboveground (AG) dune grass carbon stocks (kg C/m^2), (B) belowground (BG) dune grass carbon density (kg C/m^3), and (C) dune sand carbon (kg C/m^3) at three foredune profile locations (toe, crest, and heel) on the Outer Banks barrier islands, North Carolina, USA (see Figure 3.1 and Appendix C, Table C1 for island abbreviations and locations). See Table 3.3 for statistics.

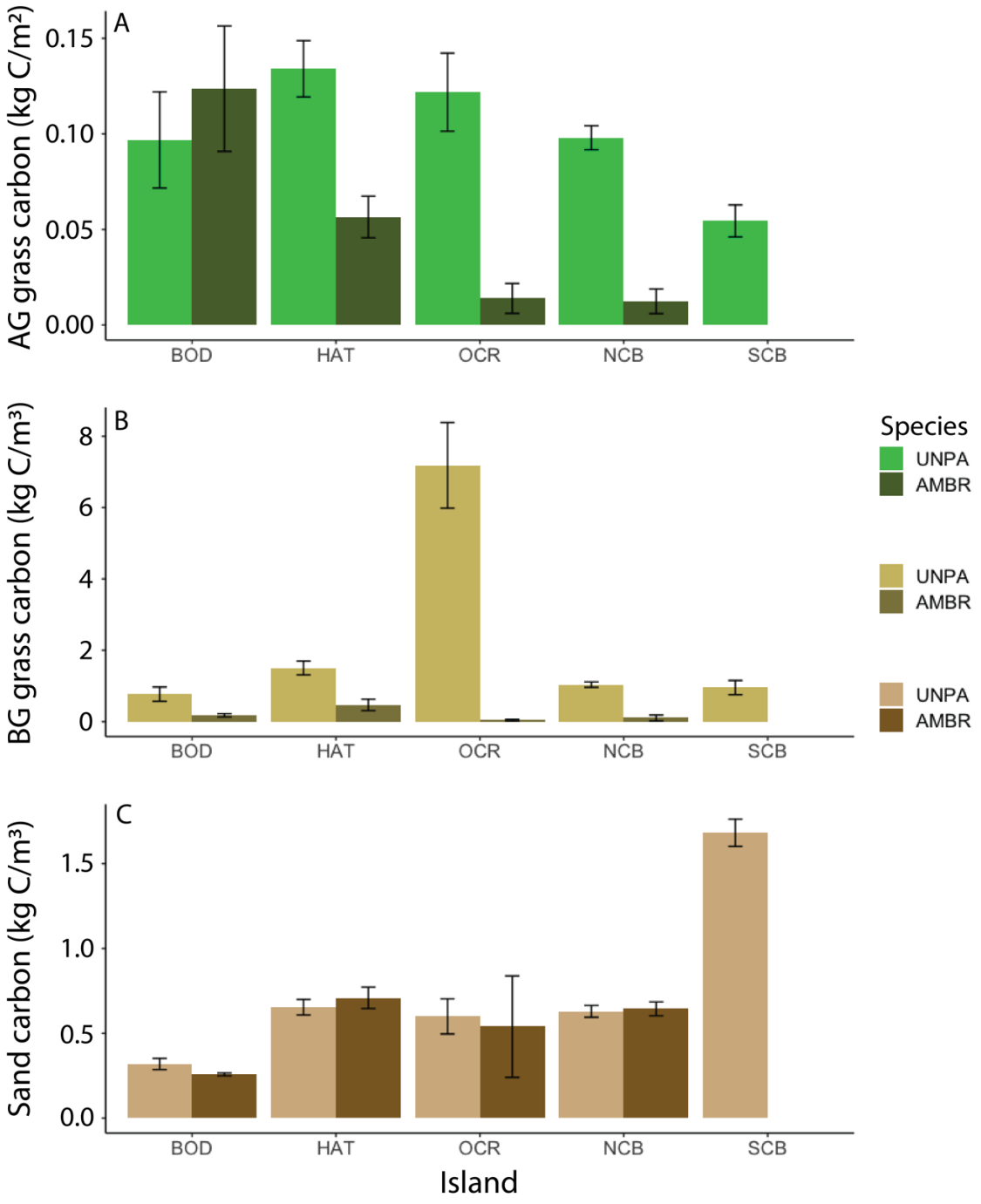

Figure 3.5. Mean ± (SE) for (A) aboveground (AG) dune grass carbon stocks (kg C/m^2), (B) belowground (BG) dune grass carbon density (kg C/m^3), and (C) dune sand carbon (kg C/m^3) for dunes dominated by the two dominant dune grass species [*Uniola paniculata* (UNPA) and *Ammophila breviligulata* (AMBR)] on the Outer Banks barrier islands, North Carolina, USA (see Figure 3.1 and Appendix C, Table C1 for island abbreviations and locations). See Table 3.4 for statistics.

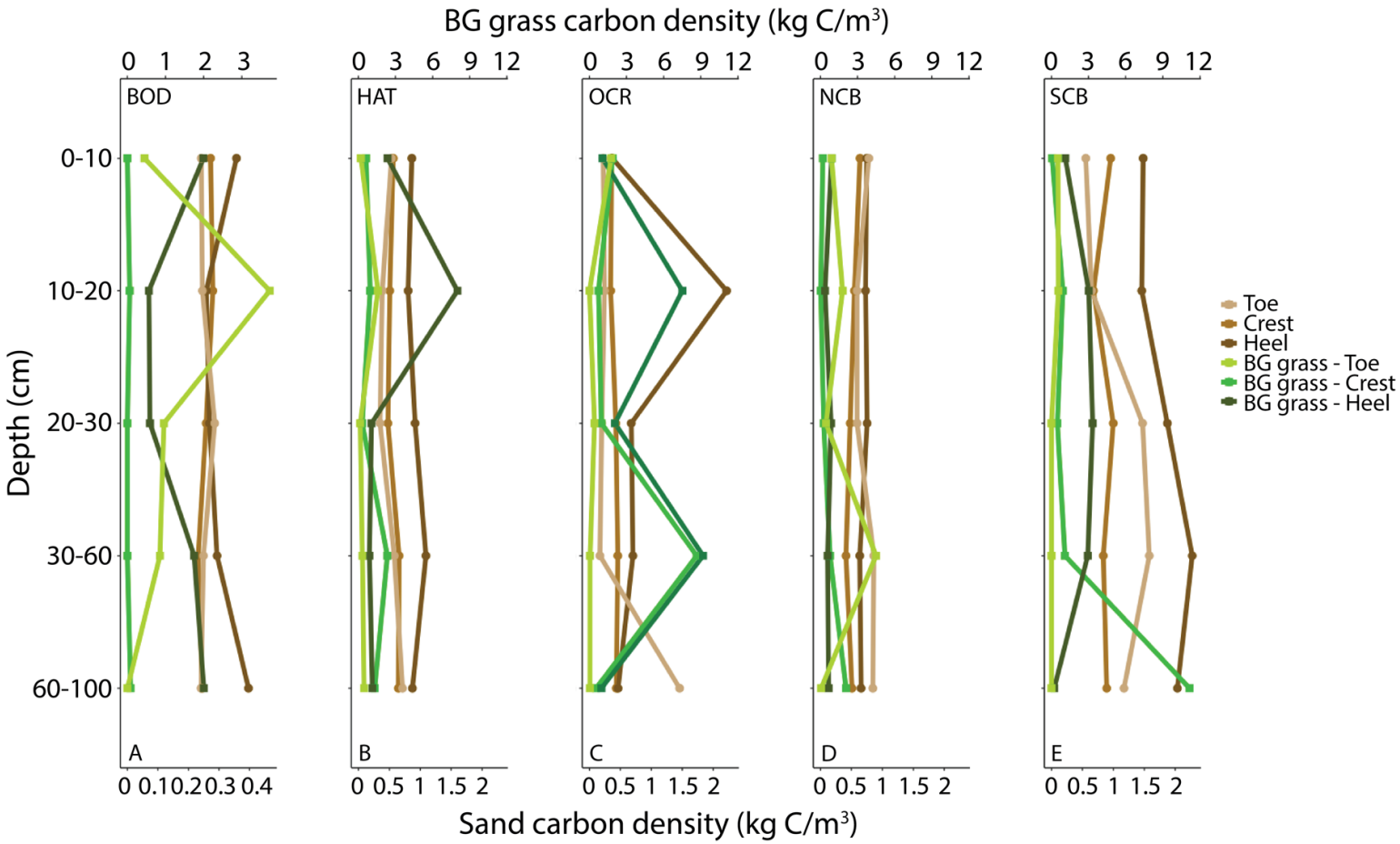

Figure 3.6. Mean carbon density (kg C/m^3) for belowground (BG; green lines) grass and sand (brown lines) at different sediment core depths and dune profile locations on the Outer Banks barrier islands, North Carolina, USA (see Figure 3.1 and Appendix C, Table C1 for island abbreviations and locations). See Appendix F, Table F3 for additional data. Note that the Bodie Island (BOD) axes in panel (A) are on a different scale than the rest of the islands because of the difference in magnitude of the values. See Table 3.5 for statistics.

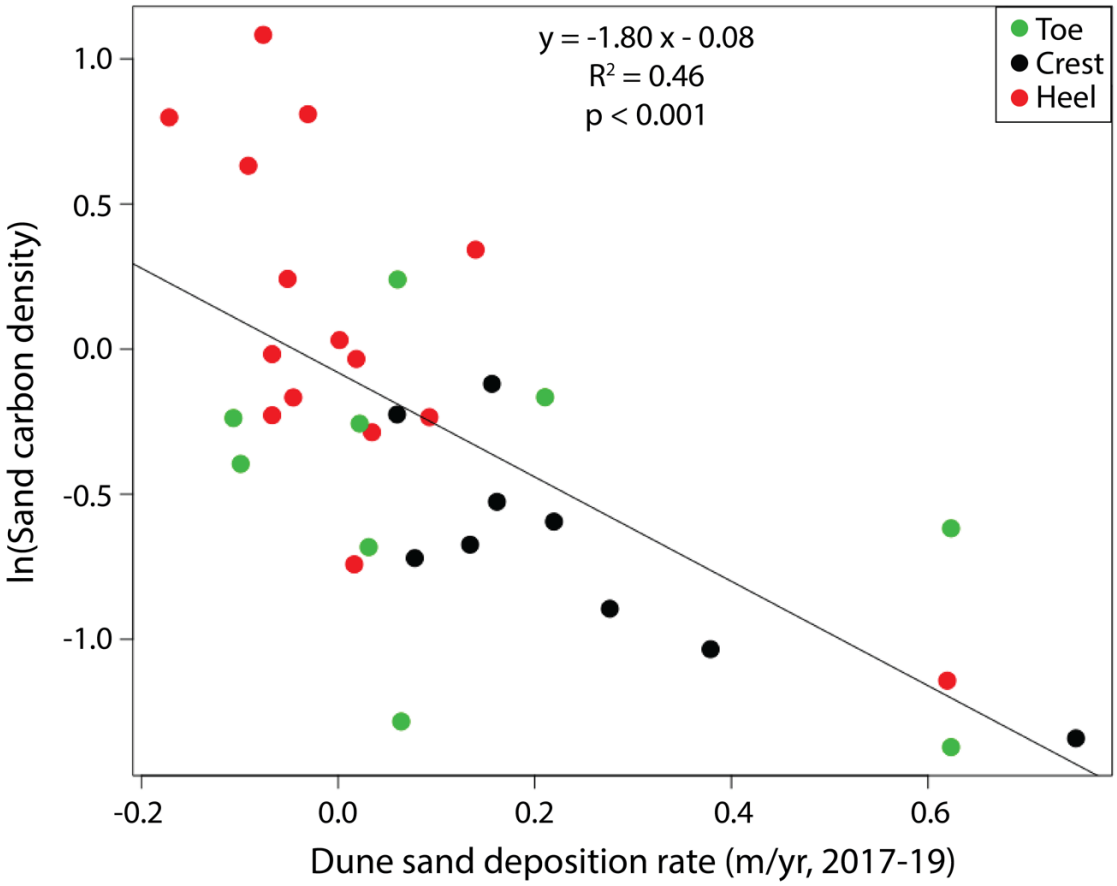

Figure 3.7. Relationship between mean sand carbon density (kg C/m^3 at the core level) and annual sand deposition (or erosion) rate to the dune from 2017-19 (m/yr). Colors indicate cores collected at the toe, crest, and heel of the dune.

3.7 References

Alongi, D. M. 2002. Present state and future of the world's mangrove forests. Environmental Conservation 29:331–349.

Atwood, T. B., R. M. Connolly, H. Almahasheer, P. E. Carnell, C. M. Duarte, C. J. Ewers Lewis, X. Irigoien, J. J. Kelleway, P. S. Lavery, P. I. Macreadie, O. Serrano, C. J. Sanders, I. Santos, A. D. L. Steven, and C. E. Lovelock. 2017. Global patterns in mangrove soil carbon stocks and losses. Nature Climate Change 7:523–528.

Bauer, B. O., and R. G. D. Davidson-Arnott. 2002. A general framework for modeling sediment supply to coastal dunes including wind angle, beach geometry, and fetch effects. Geomorphology 49:89–108.

Beaumont, N. J., L. Jones, A. Garbutt, J. D. Hansom, and M. Toberman. 2014. The value of carbon sequestration and storage in coastal habitats. Estuarine, Coastal and Shelf Science 137:32–40.

Berendse, F., E. J. Lammerts, and H. Olff. 1998. Soil organic matter accumulation and its implications for nitrogen mineralization and plant species composition during succession in coastal dune slacks. Plant Ecology 137:71–78.

Biel, R. G., S. D. Hacker, and P. Ruggiero. 2019. Elucidating coastal foredune ecomorphodynamics in the U.S. Pacific Northwest via Bayesian Networks. Journal of Geophysical Research: Earth Surface 124:1919–1938.

Bouillon, S., A. V. Borges, E. Castañeda-Moya, K. Diele, T. Dittmar, N. C. Duke, E. Kristensen, S. Y. Lee, C. Marchand, J. J. Middelburg, V. H. Rivera-Monroy, T. J. Smith, and R. R. Twilley. 2008. Mangrove production and carbon sinks: A revision of global budget estimates: Global mangrove carbon budgets. Global Biogeochemical Cycles 22:GB2013.

Bouillon, S., F. Dahdouh-Guebas, A. V.V.S., N. Koedam, and F. Dehairs. 2003. Sources of organic carbon in mangrove sediments: variability and possible ecological implications. Hydrobiologia 495:7.

Bradley, B. A., R. A. Houghton, J. F. Mustard, and S. P. Hamburg. 2006. Invasive grass reduces aboveground carbon stocks in shrublands of the Western US. Global Change Biology 12:1815–1822.

Breithaupt, J. L., J. M. Smoak, C. J. Sanders, and T. G. Troxler. 2019. Spatial variability of organic carbon, CaCO3 and nutrient burial rates spanning a mangrove productivity gradient in the coastal Everglades. Ecosystems 22:844–858.

Breithaupt, J. L., J. M. Smoak, T. J. Smith, C. J. Sanders, and A. Hoare. 2012. Organic carbon burial rates in mangrove sediments: Strengthening the global budget. Global Biogeochemical Cycles 26:GB3011.

Bridgham, S. D., J. P. Megonigal, J. K. Keller, N. B. Bliss, and C. Trettin. 2006. The carbon balance of North American wetlands. Wetlands 26:889–916.

Brown, J. K., and J. C. Zinnert. 2018. Mechanisms of surviving burial: Dune grass interspecific differences drive resource allocation after sand deposition. Ecosphere 9:e02162.

Bryant, M. A., T. J. Hesser, and R. E. Jensen. 2016. Evaluation statistics computed for the Wave Information Studies (WIS). U.S. Army Engineer Research and Development Center, Vicksburg, MS, USA.

Callaway, J. C., E. L. Borgnis, R. E. Turner, and C. S. Milan. 2012. Carbon sequestration and sediment accretion in San Francisco Bay tidal wetlands. Estuaries and Coasts 35:1163–1181.

Cao, M., and F. I. Woodward. 1998. Net primary and ecosystem production and carbon stocks of terrestrial ecosystems and their responses to climate change. Global Change Biology 4:185–198.

Charbonneau, B. R., S. M. Dohner, J. P. Wnek, D. Barber, P. Zarnetske, and B. B. Casper. 2021. Vegetation effects on coastal foredune initiation: Wind tunnel experiments and field validation for three dune-building plants. Geomorphology 378:107594.

Charbonneau, B. R., J. P. Wnek, J. A. Langley, G. Lee, and R. A. Balsamo. 2016. Above vs. belowground plant biomass along a barrier island: Implications for dune stabilization. Journal of Environmental Management 182:126–133.

Chmura, G. L., S. C. Anisfeld, D. R. Cahoon, and J. C. Lynch. 2003. Global carbon sequestration in tidal, saline wetland soils. Global Biogeochemical Cycles 17.

Cohn, N., B. Hoonhout, E. Goldstein, S. De Vries, L. Moore, O. Durán Vinent, and P. Ruggiero. 2019. Exploring marine and aeolian controls on coastal foredune growth using a coupled numerical model. Journal of Marine Science and Engineering 7:13.

Conant, R. T., K. Paustian, and E. T. Elliott. 2001. Grassland management and conversion into grassland: Effects on soil carbon. Ecological Applications 11:343–355.

Constant, V. 2019. Coastal dunes as meta-ecosystems: Connecting marine subsidies to ecosystem functions on the U.S. Pacific Northwest coast. PhD dissertation, Oregon State University.

Dean, Jr. 1974. Determination of carbonate and organic matter in calcareous sediments and sedimentary rocks by loss on ignition: Comparison with other methods. SEPM Journal of Sedimentary Research 44:242–248.

Donato, D. C., J. B. Kauffman, D. Murdiyarso, S. Kurnianto, M. Stidham, and M. Kanninen. 2011. Mangroves among the most carbon-rich forests in the tropics. Nature Geoscience 4:293–297.

Dontis, E. E., K. R. Radabaugh, A. R. Chappel, C. E. Russo, and R. P. Moyer. 2020. Carbon storage increases with site age as created salt marshes transition to mangrove forests in Tampa Bay, Florida (USA). Estuaries and Coasts 43:1470–1488.

Drius, M., M. L. Carranza, A. Stanisci, and L. Jones. 2016. The role of Italian coastal dunes as carbon sinks and diversity sources. A multi-service perspective. Applied Geography 75:127–136.

Duarte, C. M. 2017. Reviews and syntheses: Hidden forests, the role of vegetated coastal habitats in the ocean carbon budget. Biogeosciences 14:301–310.

Duarte, C. M., N. Marbà, E. Gacia, J. W. Fourqurean, J. Beggins, C. Barrón, and E. T. Apostolaki. 2010. Seagrass community metabolism: Assessing the carbon sink capacity of seagrass meadows. Global Biogeochemical Cycles 24:GB4032.

Duarte, C. M., J. J. Middelburg, and N. Caraco. 2005. Major role of marine vegetation on the oceanic carbon cycle. Biogeosciences 2:1–8.

Dugan, J. E., D. M. Hubbard, H. M. Page, and J. P. Schimel. 2011. Marine macrophyte wrack inputs and dissolved nutrients in beach sands. Estuaries and Coasts 34:839–850.

Duran, O., and L. J. Moore. 2013. Vegetation controls on the maximum size of coastal dunes. Proceedings of the National Academy of Sciences 110:17217–17222.

Millennium Ecosystem Assessment. Ecosystems and human well-being. 2005. Island Press, Washington, DC.

Enríquez, A. R., M. Marcos, A. Falqués, and D. Roelvink. 2019. Assessing beach and dune erosion and vulnerability under sea level rise: A case study in the Mediterranean Sea. Frontiers in Marine Science 6:4.

Farris, A. S., and J. H. List. 2007. Shoreline change as a proxy for subaerial beach volume change. Journal of Coastal Research 23:740–748.

Feagin, R. A., D. J. Sherman, and W. E. Grant. 2005. Coastal erosion, global sea-level rise, and the loss of sand dune plant habitats. Frontiers in Ecology and the Environment 3:359–364.

Fernández-Montblanc, T., E. Duo, and P. Ciavola. 2020. Dune reconstruction and revegetation as a potential measure to decrease coastal erosion and flooding under extreme storm conditions. Ocean & Coastal Management 188:105075.

Fox, J., M. Friendly, and G. Monette. 2018. heplots: visualizing tests in multivariate linear models. https://CRAN.R-project.org/package=heplots.

Godfrey, P. J., and M. M. Godfrey. 1973. Comparison of geological and geomorphic interactions between altered and unaltered barrier island systems in North Carolina. Pages 239–258 *in* D. R. Coates, editor. Coastal Geomorphology. State Univeristy of New York, Binghamton.

Goldstein, E. B., L. J. Moore, and O. Durán Vinent. 2017. Lateral vegetation growth rates exert control on coastal foredune hummockiness and coalescing time. Earth Surface Dynamics 5:417–427.

Goldstein, E. B., E. V. Mullins, L. J. Moore, R. G. Biel, J. K. Brown, S. D. Hacker, K. R. Jay, R. S. Mostow, P. Ruggiero, and J. C. Zinnert. 2018. Literature-based latitudinal distribution and possible range shifts of two US east coast dune grass species (*Uniola paniculata* and *Ammophila breviligulata*). PeerJ 6:e4932.

Greiner, J. T., K. J. McGlathery, J. Gunnell, and B. A. McKee. 2013. Seagrass restoration enhances “blue carbon” sequestration in coastal waters. PLOS ONE 8:e72469.

Hacker, S. D., K. R. Jay, N. Cohn, E. B. Goldstein, P. A. Hovenga, M. Itzkin, L. J. Moore, R. S. Mostow, E. V. Mullins, and P. Ruggiero. 2019. Species-specific functional morphology of four US Atlantic Coast dune grasses: Biogeographic implications for dune shape and coastal protection. Diversity 11:1–16.

Hacker, S. D., P. Zarnetske, E. Seabloom, P. Ruggiero, J. Mull, S. Gerrity, and C. Jones. 2012. Subtle differences in two non-native congeneric beach grasses significantly affect their colonization, spread, and impact. Oikos 121:138–148.

Harris, A. L., J. C. Zinnert, and D. R. Young. 2017. Differential response of barrier island dune grasses to species interactions and burial. Plant Ecology 218:609–619.

Heiri, O., A. F. Lotter, and G. Lemcke. 2001. Loss on ignition as a method for estimating organic and carbonate content in sediments: reproducibility and comparability of results 25:101–110.

Hesp, P. 2002. Foredunes and blowouts: initiation, geomorphology and dynamics. Geomorphology 48:245–268.

Hesp, P. A. 1989. A review of biological and geomorphological processes involved in the initiation and development of incipient foredunes. Proceedings of the Royal Society of Edinburgh, Section B: Biological Sciences 96:181–201.

Hesp, P. A., and I. J. Walker. 2013. Aeolian environments: coastal dunes. Pages 109–133 *in* J. Shroder, N. Lancaster, D. J. Sherman, and A. C. W. Baas, editors. Treatise on Geomorphology. Academic Press, San Diego, CA.

Hopkinson, C. S., W.-J. Cai, and X. Hu. 2012. Carbon sequestration in wetland dominated coastal systems—a global sink of rapidly diminishing magnitude. Current Opinion in Environmental Sustainability 4:186–194.

Hovenga, P. A., P. Ruggiero, N. Cohn, K. R. Jay, S. D. Hacker, M. Itzkin, and L. Moore. 2019. Drivers of dune evolution in Cape Lookout National Seashore, NC. Pages 1283–1296 Coastal Sediments 2019. World Scientific, Tampa/St. Petersburg, Florida, USA.

Hovenga, P. A., P. Ruggiero, E. B. Goldstein, S. D. Hacker, and L. J. Moore. 2021. The relative role of constructive and destructive processes in dune evolution on Cape Lookout National Seashore, North Carolina, USA. Earth Surface Processes and Landforms:esp.5210.

Howard, J., A. Sutton-Grier, D. Herr, J. Kleypas, E. Landis, E. Mcleod, E. Pidgeon, and S. Simpson. 2017. Clarifying the role of coastal and marine systems in climate mitigation. Frontiers in Ecology and the Environment 15:42–50.

van IJzendoorn, C. O., S. de Vries, C. Hallin, and P. A. Hesp. 2021. Sea level rise outpaced by vertical dune toe translation on prograding coasts. Scientific Reports 11:12792.

Intergovernmental Panel on Climate Change. 2007. Climate change 2007: the physical science basis: contribution of Working Group I to the Fourth Assessment Report of the Intergovernmental Panel on Climate Change. Page (S. Solomon, D. Qin, and M. Manning, Eds.). Cambridge University Press, Cambridge; New York.

Intergovernmental Panel on Climate Change. 2014. Climate change 2014: impacts, adaptation, and vulnerability: Working Group II contribution to the fifth assessment report of the Intergovernmental Panel on Climate Change. Page (C. B. Field and V. R. Barros, Eds.). Cambridge University Press, New York, NY.

Jackson, D. W. T., S. Costas, R. González-Villanueva, and A. Cooper. 2019. A global 'greening' of coastal dunes: An integrated consequence of climate change? Global and Planetary Change 182:103026.

Jones, M. B., and A. Donnelly. 2004. Carbon sequestration in temperate grassland ecosystems and the influence of management, climate and elevated CO_2. New Phytologist 164:423–439.

Jones, M. L. M., A. Sowerby, D. L. Williams, and R. E. Jones. 2008. Factors controlling soil development in sand dunes: evidence from a coastal dune soil chronosequence. Plant and Soil 307:219–234.

Kauffman, J. B., L. Giovanonni, J. Kelly, N. Dunstan, A. Borde, H. Diefenderfer, C. Cornu, C. Janousek, J. Apple, and L. Brophy. 2020. Total ecosystem carbon stocks at the marine-terrestrial interface: Blue carbon of the Pacific Northwest Coast, United States. Global Change Biology 26:5679–5692.

Kaviarasan, T., H. U. Dahms, M. S. Gokul, S. Henciya, K. Muthukumar, S. Shankar, and R. Arthur James. 2019. Seasonal species variation of sediment organic carbon stocks in salt marshes of Tuticorin Area, southern India. Wetlands 39:483–494.

Keijsers, J. G. S., A. V. De Groot, and M. J. P. M. Riksen. 2015. Vegetation and sedimentation on coastal foredunes. Geomorphology 228:723–734.

Keijsers, J. G. S., A. V. De Groot, and M. J. P. M. Riksen. 2016. Modeling the biogeomorphic evolution of coastal dunes in response to climate change. Journal of Geophysical Research: Earth Surface 121:1161–1181.

Kennedy, H., J. Beggins, C. M. Duarte, J. W. Fourqurean, M. Holmer, N. Marbà, and J. J. Middelburg. 2010. Seagrass sediments as a global carbon sink: Isotopic constraints. Global Biogeochemical Cycles 24:GB4026.

Kratzmann, M. G., E. A. Himmelstoss, and E. R. Thieler. 2017. National assessment of shoreline change – A GIS compilation of updated vector shorelines and associated shoreline change data for the Southeast Atlantic Coast. U.S. Geological Survey, Reston, VA, USA.

Kristensen, E., S. Bouillon, T. Dittmar, and C. Marchand. 2008. Organic carbon dynamics in mangrove ecosystems: A review. Aquatic Botany 89:201–219.

Lal, R. 2005. Forest soils and carbon sequestration. Forest Ecology and Management 220:242–258.

Lal, R., P. Smith, H. F. Jungkunst, W. J. Mitsch, J. Lehmann, P. K. R. Nair, A. B. McBratney, J. C. de Moraes Sá, J. Schneider, Y. L. Zinn, A. L. A. Skorupa, H.-L. Zhang, B. Minasny, C. Srinivasrao, and N. H. Ravindranath. 2018. The carbon sequestration potential of terrestrial ecosystems. Journal of Soil and Water Conservation 73:145A-152A.

Lazarus, E. D., and A. B. Murray. 2011. An integrated hypothesis for regional patterns of shoreline change along the Northern North Carolina Outer Banks, USA. Marine Geology 281:85–90.

Lovelock, C. E., M. F. Adame, V. Bennion, M. Hayes, J. O'Mara, R. Reef, and N. S. Santini. 2014. Contemporary rates of carbon sequestration through vertical accretion of sediments in mangrove forests and saltmarshes of south east Queensland, Australia. Estuaries and Coasts 37:763–771.

Luijendijk, A., G. Hagenaars, R. Ranasinghe, F. Baart, G. Donchyts, and S. Aarninkhof. 2018. The state of the world's beaches. Scientific Reports 8:6641.

Luyssaert, S., E.-D. Schulze, A. Börner, A. Knohl, D. Hessenmöller, B. E. Law, P. Ciais, and J. Grace. 2008. Old-growth forests as global carbon sinks. Nature 455:213–215.

Macreadie, P. I., A. Anton, J. A. Raven, N. Beaumont, R. M. Connolly, D. A. Friess, J. J. Kelleway, H. Kennedy, T. Kuwae, P. S. Lavery, C. E. Lovelock, D. A. Smale, E. T. Apostolaki, T. B. Atwood, J. Baldock, T. S. Bianchi, G. L. Chmura, B. D. Eyre, J. W. Fourqurean, J. M. Hall-Spencer, M. Huxham, I. E. Hendriks, D. Krause-Jensen, D. Laffoley, T. Luisetti, N. Marbà, P. Masque, K. J. McGlathery, J. P. Megonigal, D. Murdiyarso, B. D. Russell, R. Santos, O. Serrano, B. R. Silliman, K. Watanabe, and C. M. Duarte. 2019. The future of blue carbon science. Nature Communications 10:3998.

Mallin, M. A., J. M. Burkholder, L. B. Cahoon, and M. H. Posey. 2000. North and South Carolina coasts. Marine Pollution Bulletin 41:56–75.

Mannino, A., S. R. Signorini, M. G. Novak, J. Wilkin, M. A. M. Friedrichs, and R. G. Najjar. 2016. Dissolved organic carbon fluxes in the Middle Atlantic Bight: An integrated approach based on satellite data and ocean model products: DOC coastal fluxes and stocks. Journal of Geophysical Research: Biogeosciences 121:312–336.

Masselink, G., P. Russell, A. Rennie, S. Brooks, and T. Spencer. 2020. Impacts of climate change on coastal geomorphology and coastal erosion relevant to the coastal and marine environment around the UK. MCCIP Science Review 2020:158–189.

Mcleod, E., G. L. Chmura, S. Bouillon, R. Salm, M. Björk, C. M. Duarte, C. E. Lovelock, W. H. Schlesinger, and B. R. Silliman. 2011. A blueprint for blue carbon: toward an improved understanding of the role of vegetated coastal habitats in sequestering CO_2. Frontiers in Ecology and the Environment 9:552–560.

Middelburg, J. J., J. Nieuwenhuize, R. K. Lubberts, and O. van de Plassche. 1997. Organic carbon isotope systematics of coastal marshes. Estuarine, Coastal and Shelf Science 45:681–687.

Miller, T. L., R. A. Morton, and A. H. Sallenger. 2005. National assessment of shoreline change – A GIS compilation of vector shorelines and associated shoreline change data for the U.S. Southeast Atlantic Coast. U.S. Geological Survey, Reston, VA, USA.

Moore, L. J., O. D. Vinent, and P. Ruggiero. 2016. Vegetation control allows autocyclic formation of multiple dunes on prograding coasts. Geology 44:559–562.

Morris, J. T., P. V. Sundareshwar, C. T. Nietch, B. Kjerfve, and D. R. Cahoon. 2002. Responses of coastal wetlands to rising sea level. Ecology 83:2869–2877.

Mudd, S. M., S. M. Howell, and J. T. Morris. 2009. Impact of dynamic feedbacks between sedimentation, sea-level rise, and biomass production on near-surface marsh stratigraphy and carbon accumulation. Estuarine, Coastal and Shelf Science 82:377–389.

Mull, J., and P. Ruggiero. 2014. Estimating storm-induced dune erosion and overtopping along U.S. West Coast beaches. Journal of Coastal Research 298:1173–1187.

Mullins, E., L. J. Moore, E. B. Goldstein, T. Jass, J. Bruno, and O. D. Vinent. 2019. Investigating dune-building feedback at the plant level: Insights from a multispecies field experiment. Earth Surface Processes and Landforms 44:1734–1747.

Nellemann, C., E. Corcoran, C. M. Duarte, L. Valdés, C. De Young, L. Fonseca, and G. Grimsditch, editors. 2009. Blue carbon: the role of healthy oceans in binding carbon: a rapid response assessment. GRID-Arendal, Arendal, Norway.

Novak, A. B., M. C. Pelletier, P. Colarusso, J. Simpson, M. N. Gutierrez, A. Arias-Ortiz, M. Charpentier, P. Masque, and P. Vella. 2020. Factors influencing carbon stocks and accumulation rates in eelgrass meadows across New England, USA. Estuaries and Coasts 43:2076–2091.

Olff, H., J. Huisman, and B. F. V. Tooren. 1993. Species dynamics and nutrient accumulation during early primary succession in coastal sand dunes. The Journal of Ecology 81:693–706.

Paerl, H. W., N. S. Hall, A. G. Hounshell, R. A. Luettich, K. L. Rossignol, C. L. Osburn, and J. Bales. 2019. Recent increase in catastrophic tropical cyclone flooding in coastal North Carolina, USA: Long-term observations suggest a regime shift. Scientific Reports 9:10620.

Palm, C., H. Blanco-Canqui, F. DeClerck, L. Gatere, and P. Grace. 2014. Conservation agriculture and ecosystem services: An overview. Agriculture, Ecosystems & Environment 187:87–105.

Potter, C. 2003. Continental-scale comparisons of terrestrial carbon sinks estimated from satellite data and ecosystem modeling 1982–1998. Global and Planetary Change 39:201–213.

Psuty, N. P. 1986. A dune/beach interaction model and dune management. Thalassas 4:11–15.

R Development Core Team. 2019. R: a language and environment for statistical computing. R Foundation for Statistical Computing, Vienna, Austria. www.r-project.org.

Ranasinghe, R. 2016. Assessing climate change impacts on open sandy coasts: A review. Earth-Science Reviews 160:320–332.

Reay, D. S., F. Dentener, P. Smith, J. Grace, and R. A. Feely. 2008. Global nitrogen deposition and carbon sinks. Nature Geoscience 1:430–437.

Rossi, A. M., and M. C. Rabenhorst. 2019. Organic carbon dynamics in soils of Mid-Atlantic barrier island landscapes. Geoderma 337:1278–1290.

Ruggiero, P., G. M. Kaminsky, G. Gelfenbaum, and N. Cohn. 2016. Morphodynamics of prograding beaches: A synthesis of seasonal- to century-scale observations of the Columbia River littoral cell. Marine Geology 376:51–68.

Sallenger, A. H. 2000. Storm impact scale for barrier islands. Journal of Coastal Research 16:7.

Sallenger, A. H., K. S. Doran, and P. A. Howd. 2012. Hotspot of accelerated sea-level rise on the Atlantic coast of North America. Nature Climate Change 2:884–888.

Sarmiento, J. L., and N. Gruber. 2002. Sinks for anthropogenic carbon. Physics Today 55:30–36.

Savidge, D. K. 2004. Gulf Stream meander propagation past Cape Hatteras. Journal of Physical Oceanography 34:2073–2085.

Schaub, I., C. Baum, R. Schumann, and U. Karsten. 2019. Effects of an early successional biological soil crust from a temperate coastal sand dune (NE Germany) on soil elemental stoichiometry and phosphatase activity. Microbial Ecology 77:217–229.

Seabloom, E. W., P. Ruggiero, S. D. Hacker, J. Mull, and P. Zarnetske. 2013. Invasive grasses, climate change, and exposure to storm-wave overtopping in coastal dune ecosystems. Global Change Biology 19:824–832.

Seneca, E. D. 1969. Germination response to temperature and salinity of four dune grasses from the Outer Banks of North Carolina. Ecology 50:45–53.

Sherman, D. J., and B. O. Bauer. 1993. Dynamics of beach-dune systems. Progress in Physical Geography: Earth and Environment 17:413–447.

Short, A. D., and P. A. Hesp. 1982. Wave, beach and dune interactions in southeastern Australia. Marine Geology 48:259–284.

Stockdon, H. F., A. H. Sallenger, R. A. Holman, and P. A. Howd. 2007. A simple model for the spatially-variable coastal response to hurricanes. Marine Geology 238:1–20.

Tackett, N. W., and C. B. Craft. 2010. Ecosystem development on a coastal barrier island dune chronosequence. Journal of Coastal Research 264:736–742.

Tanentzap, A. J., and D. A. Coomes. 2012. Carbon storage in terrestrial ecosystems: do browsing and grazing herbivores matter? Biological Reviews 87:72–94.

Turner, B. L., and E. Laliberté. 2015. Soil development and nutrient availability along a 2 million-year coastal dune chronosequence under species-rich Mediterranean shrubland in southwestern Australia. Ecosystems 18:287–309.

Twilley, R. R., A. S. Rovai, and P. Riul. 2018. Coastal morphology explains global blue carbon distributions. Frontiers in Ecology and the Environment 16:503–508.

Underwood, A. J. 1997. Experiments in ecology: Their logical design and interpretation using analysis of variance. Cambridge University Press.

Van de Broek, M., S. Temmerman, R. Merckx, and G. Govers. 2016. Controls on soil organic carbon stocks in tidal marshes along an estuarine salinity gradient. Biogeosciences 13:6611–6624.

Van der Valk, A. G. 1975. The floristic composition and structure of foredune plant communities of Cape Hatteras National Seashore. Chesapeake Science 16:115–126.

Waycott, M., C. M. Duarte, T. J. B. Carruthers, R. J. Orth, W. C. Dennison, S. Olyarnik, A. Calladine, J. W. Fourqurean, K. L. Heck, A. R. Hughes, G. A. Kendrick, W. J. Kenworthy, F. T. Short, and S. L. Williams. 2009. Accelerating loss of seagrasses across the globe threatens coastal ecosystems. Proceedings of the National Academy of Sciences 106:12377–12381.

de Winter, R. C., and B. G. Ruessink. 2017. Sensitivity analysis of climate change impacts on dune erosion: case study for the Dutch Holland coast. Climatic Change 141:685–701.

Woodhouse, W. W., E. D. Seneca, and S. W. Broome. 1977. Effect of species on dune grass growth. International Journal of Biometeorology 21:256–266.

Xia, J., S. Liu, S. Liang, Y. Chen, W. Xu, and W. Yuan. 2014. Spatio-temporal patterns and climate variables controlling of biomass carbon stock of global grassland ecosystems from 1982 to 2006. Remote Sensing 6:1783–1802.

Zarnetske, P. L., S. D. Hacker, E. W. Seabloom, P. Ruggiero, J. R. Killian, T. B. Maddux, and D. Cox. 2012. Biophysical feedback mediates effects of invasive grasses on coastal dune shape. Ecology 93:1439–1450.

Zarnetske, P. L., P. Ruggiero, E. W. Seabloom, and S. D. Hacker. 2015. Coastal foredune evolution: the relative influence of vegetation and sand supply in the US Pacific Northwest. Journal of The Royal Society Interface 12:20150017.

Zhu, Z., S. Piao, R. B. Myneni, M. Huang, Z. Zeng, J. G. Canadell, P. Ciais, S. Sitch, P. Friedlingstein, A. Arneth, C. Cao, L. Cheng, E. Kato, C. Koven, Y. Li, X. Lian, Y. Liu, R. Liu, J. Mao, Y. Pan, S. Peng, J. Peñuelas, B. Poulter, T. A. M. Pugh, B. D. Stocker, N. Viovy, X. Wang, Y. Wang, Z. Xiao, H. Yang, S. Zaehle, and N. Zeng. 2016. Greening of the Earth and its drivers. Nature Climate Change 6:791–795.

Chapter 4 – The influence of marine subsidies and sand supply on dune grass production along the U.S. Central Atlantic coast

Katya R. Jay[1], Lucas Parvin[1], Judith Quintana[1], Sally D. Hacker[1]

Affiliation:

1. Department of Integrative Biology, Oregon State University, 3029 Cordley Hall, Corvallis, OR 97331, USA.

In preparation for publication

4.1 Abstract

Resource subsidies, or the flow of energy across ecosystem boundaries, can influence community structure and function and act as important nutrient sources to less productive ecosystems, particularly in marine and coastal zones. Coastal foredunes are shaped by biophysical feedbacks between vegetation and sediment and tend to have nutrient-poor growing substrates with low rates of soil formation. However, foredunes can nonetheless have very productive plant communities, suggesting that marine nutrients may subsidize sandy dune habitats. Here we considered the role of marine subsidies to dune grass production and foliar nitrogen metrics along the U.S. Outer Banks coastline and asked: 1) Do macrophyte wrack biomass and composition, sand nitrate concentration, and dune grass production vary at local and regional scales? 2) Do dune grasses utilize marine derived nitrogen (^{15}N) and, if so, how does $\delta^{15}N$ and %N vary across species, foredune profile locations, and islands? and 3) What factors, including macrophyte wrack biomass, sand nitrate, and sand supply metrics, are important to dune grass production and foliar nitrogen metrics? We found that sand nitrate concentrations increased with latitude along the Outer Banks coastline but were unrelated to macrophyte wrack biomass. In addition, dune grass production metrics varied among islands at the foredune toe but were relatively consistent across sites at the foredune crest and heel. Dune grass $\delta^{15}N$ was highest at the foredune toe and decreased at the foredune crest and heel, suggesting that grasses growing closer to the beach are using marine nutrient sources. Although dune grass %N content did not vary across the foredune profile, it did increase with latitude, as did sand nitrate concentration. We found that variability in sand nitrate

concentration was related to shoreline change rate and foredune height, while dune grass production metrics were related to foredune height and width, shoreline change rate, sand nitrate concentration, and beach slope, with the relative importance of those factors varying across the foredune profile. In addition, sites with higher dune grass foliar %N tended to have more negative shoreline change rates, taller foredunes, and higher sand nitrate concentrations, while sites with greater $\delta^{15}N$ values had more positive shoreline change rates, taller foredunes, and steeper beaches. Our results suggest that beach and foredune morphology and sand supply to the beach play an important role in mediating the delivery of marine-derived nutrients to foredunes, where dune grasses use marine nitrogen sources, especially nearest the beach. It is necessary to better understand nutrient dynamics in coastal foredunes given the potential for sea level rise, extreme storm events, nitrogen deposition, and other climate-driven changes in coastal processes to impact foredune ecosystem functions and services.

4.2 Introduction

The flow of energy, nutrients, and organic matter between ecosystems (known as ecological subsidies) connects communities across spatial boundaries (Polis et al. 1997, Loreau et al. 2003, Loreau and Holt 2004, Massol et al. 2011). These connections allow more productive donor habitats to support less productive recipient habitats, influencing important ecological functions such as food web dynamics, primary productivity, and trophic cascades (Polis and Hurd 1996, Polis et al. 1997, Leroux and Loreau 2008, Bartels et al. 2012, Menge et al. 2015, Montagano et al. 2019). Extensive research on resource subsidies in aquatic, marine, and coastal ecosystems has shown that these cross-

ecosystem exchanges are important at both local and regional scales (e.g., Polis and Hurd 1996, Menge et al. 2003, 2015, Palumbi 2003, Barrett et al. 2005, Richardson et al. 2010, Spiller et al. 2010, Hessing-Lewis and Hacker 2013, Hacker et al. 2019b, Hayduk et al. 2019).

Although this previous research has shown the importance of ecological subsidies to coastal ecosystem functions, less is known about the impact of such subsidies to coastal dunes, which provide numerous ecosystem services including coastal protection (Sallenger 2000, Ruggiero et al. 2001, 2018, Seabloom et al. 2013, Biel et al. 2017), carbon sequestration (Beaumont et al. 2014, Drius et al. 2016, Jay et al. Chapter 3), and recreation (Barbier et al. 2011). Coastal dune sands tend to be highly leached with low nutrient content, low water retention, and lack of soil formation, all factors that have the potential to contribute to limited production in dune plant communities (Willis 1963, Kachi and Hirose 1983, Ehrenfeld 1990, Day et al. 2004, Jones et al. 2004, Brown and Zinnert 2021). However, dune vegetation can be very productive (van der Valk 1974, Ripley and Pammenter 2008), suggesting that outside nutrient sources, in the form of marine subsidies, may play an important role in dune ecosystems.

Most research on marine subsidies to beaches and dunes has focused on the role of wrack in food web dynamics (Polis and Hurd 1996, Colombini and Chelazzi 2003, Dugan et al. 2003), but a few studies have used experimental and observational approaches to establish connections between dune vegetation and macroalgal wrack deposited on beaches along the Mediterranean, Dutch, and U.S. Pacific Northwest coasts (Cardona and García 2008, Del Vecchio et al. 2013, 2017, Constant 2019, van Egmond et

al. 2019). For example, research in Mediterranean dunes showed increases in vegetation cover and species richness in areas with more seagrass wrack (Del Vecchio et al. 2017) and correlations between nitrogen composition in the tissues of seagrass wrack and foredune vegetation (Cardona and García 2008). In the U.S. Pacific Northwest, Constant (2019) found that dune grass production was higher in areas with greater macrophyte wrack and sand nitrates and that grasses growing closer to the shoreline were enriched in marine nitrogen.

Macrophyte wrack deposits, which vary spatially as a function of distance to source habitat, wave climate, beach geomorphology, and tides, represent a potential source of nutrients for coastal foredune vegetation (Dugan et al. 2011, Del Vecchio et al. 2017, Reimer et al. 2018, Constant 2019). After being stranded on the beach, macrophyte wrack decomposes over time as it becomes buried by sand and colonized by invertebrates and bacteria, releasing nutrients into beach sands (Colombini and Chelazzi 2003, Gómez et al. 2018, van Egmond et al. 2019). In turn, these nutrients can adhere to sand grains and be transported landward via nearshore and aeolian processes (Oldham et al. 2014). In addition, nutrients contained in seawater may be delivered to the beach as a result of wave runup, providing a second mode of nutrient delivery from the ocean to sandy beaches and foredunes (Dugan et al. 2011, Constant 2019). Studies have shown that wrack can increase intertidal porewater nutrient levels (Dugan et al. 2011, Barreiro et al. 2013) and macrofaunal biomass, with cascading impacts on community structure and food webs (Dugan et al. 2003). In addition, Constant (2019) found increased dune grass

production in areas with greater wrack biomass, sand supply, and sand nitrate concentrations along the U.S. Pacific Northwest coast.

Coastal dunes are shaped by a combination of complex marine and terrestrial processes, some of which may also shape marine subsidies to beaches and dunes. Foredunes, or the seaward-most dune ridge, form via interactions between wind and wave climate, beach geomorphology, depositional processes, and vegetation (Short and Hesp 1982, Sherman and Bauer 1993, Hesp and Walker 2013, Duran and Moore 2013, Zarnetske et al. 2015, Keijsers et al. 2016, Ruggiero et al. 2016, Moore et al. 2016, Cohn et al. 2019a). Specifically, foredunes form via feedbacks between burial-tolerant dune grasses and aeolian sediment deposition, leading to increases in sand capture and plant growth (Hacker et al. 2012, Zarnetske et al. 2012, Keijsers et al. 2015, Brown and Zinnert 2018, Mullins et al. 2019, Biel et al. 2019, Charbonneau et al. 2021). Studies have demonstrated the importance of dune grasses to foredune morphology; for example, dune grass species, functional morphology, growth density, and belowground morphology can all play a key role in shaping foredunes (e.g., Hesp 2002, Hacker et al. 2012, 2019, Zarnetske et al. 2012, Goldstein et al. 2017, Biel et al. 2019, Jay et al. Chapter 2).

Although studies have shown the important role of dune grasses in shaping foredunes and their ecosystem functions and services via biophysical feedbacks, less is known about the environmental factors that control dune grass growth and productivity. Foredunes are thought to be stressful, nutrient limited environments (Willis 1963, Ehrenfeld 1990, Day et al. 2004, Jones et al. 2004), but dune plant productivity and biomass is often high and comparable to that of other vegetated coastal ecosystems (van

der Valk 1974, Ripley and Pammenter 2008). Previous studies in foredunes have documented aboveground biomass values that range from ~200 g/m^2 on the Virginia barrier islands (Dilustro and Day 1997), to ~ 250 g/m^2 on the Netherlands coast (Kooijman and Besse 2002), and ~ 350 g/m^2 on the North Carolina barrier islands (Jay et al. Chapter 3), which is comparable to herbaceous coastal wetlands (350 g/m^2; Jensen et al. 2019) but much lower than that of salt marshes (500-100 g/m^2; Darby and Turner 2008). The relatively high productivity in foredunes suggests that resource subsidies from adjacent marine ecosystems may provide an important source of nutrients.

Stable isotope analysis provides a mechanism to test the hypothesis that dune grasses are utilizing marine nutrient sources. Terrestrial plants are typically depleted in ^{15}N relative to atmospheric nitrogen (Högberg 1997), while marine nutrient sources are enriched in ^{15}N, the heavy isotope (Lepoint et al. 2000). Because the nitrogen composition of plant tissues should reflect that of their environment, measuring the variation in nitrogen stable isotopes in dune grasses can elucidate their nutrient sources (Högberg 1997, Craine et al. 2015). Few studies have explored the nitrogen stable isotope composition of dune grasses and its relationship with marine nutrient sources, particularly at regional scales. Evidence from the U.S. Pacific Northwest coast (Constant 2019) and the Mediterranean coast of Minorca (Cardona and García 2008) showed that plants on the foredune face were enriched in ^{15}N compared with those behind the foredune, meaning that the isotopic composition of plants growing closer to the ocean was more similar to marine wrack sources while that of plants growing farther from the ocean was more similar to atmospheric nitrogen.

Here we explore the patterns in marine subsidies and dune grass production in Outer Banks barrier island foredunes along the U.S. Central Atlantic coast. Foredunes provide critical ecosystem services on these barrier islands, which are highly vulnerable to erosion due to low elevation, extreme storm events, sea level rise, and population density (Sallenger et al. 2012, Hovenga et al. 2019, 2021, Paerl et al. 2019). Two native grasses dominate foredunes on the Central Atlantic coast: *Uniola paniculata*, a drought tolerant C_4 grass ranging from Virginia to Florida (Seneca 1969), and *Ammophila breviligulata*, a temperate C_3 grass found from North Carolina to Canada (Goldstein et al. 2018, Hacker et al. 2019a). These species overlap in the North Carolina Outer Banks, where they build dunes of differing morphologies (Woodhouse et al. 1977) and may display different stable isotopic signatures ($\delta^{15}N$) due to differences in their physiology and their abundance along the foredune profile. Two additional C_4 dune grasses found throughout this region, *Panicum amarum* and *Spartina patens*, are less abundant but have similar ranges to that of *U. paniculata*.

The coastal waters off North Carolina, a possible source of nutrients to beaches and dunes, are considered to be nitrogen limited and oligotrophic (Paerl et al. 1990, Aguilar et al. 1999). In addition, the Outer Banks are situated near an offshore boundary in ocean circulation where cold shelf/slope currents such as the Labrador Current flow south and collide with the warm, northward Gulf Stream, which turns eastward in the region offshore of Cape Hatteras (Savidge 2004, Mannino et al. 2016). These boundaries in currents impact marine nutrient delivery to the coastline, and Cape Hatteras represents a biogeophysical transition zone for macroalgae and phytoplankton in addition to dune

grasses (Mallin et al. 2000). The region north of Cape Hatteras is characterized by higher dissolved organic carbon (DOC; Mannino et al. 2016) levels as well as higher dissolved nitrate levels compared with the region south of this boundary (Balthis et al. 2019). The transition zone around Cape Hatteras provides habitat for both warm- and cold-adapted macroalgal species.

Thus, given the possible variation in marine subsidies in this region and its potential effect on dune grass production and dune building, we assessed how dune grass production and nitrogen content varied regionally as a product of marine subsidies and sand nitrate concentration. Specifically, we asked the following questions:

1) Do macrophyte wrack biomass and composition, sand nitrate concentration, and dune grass production vary at local and regional scales?
2) Do dune grasses utilize marine derived nitrogen ($\delta^{15}N$) and, if so, how does $\delta^{15}N$ and %N vary across species, foredune profile locations, and islands?
3) What factors, including macrophyte wrack biomass, sand nitrate, and sand supply metrics, are important to dune grass production and foliar nitrogen metrics?

We hypothesize that macrophyte wrack biomass and sand nitrate concentration will vary with latitude as a result of differences in marine nutrient inputs, with islands in the northern Outer Banks having greater wrack biomass and sand nitrogen content. In addition, dune grass production will vary by island and profile location, with the foredune crest and heel having greater dune grass density and biomass. We predict that dune grasses will utilize marine-derived nitrogen (high $\delta^{15}N$), and that $\delta^{15}N$ and %N in the

tissue will vary by island and dune profile location, with higher $\delta^{15}N$ occurring in the northern islands and at the foredune toe, where marine contributions are greatest. Finally, we expect that marine subsidies and beach and foredune morphometrics will influence dune grass production and foliar nitrogen metrics. In particular, increases in sand nitrate concentration and proxies for beach sand supply (i.e., multidecadal SCR and beach and dune morphometrics) will be related to higher production and %N and $\delta^{15}N$ in dune grasses.

4.3 Methods

4.3.1 Study region

We studied the sandy beaches and foredunes along seven U.S. Atlantic Coast barrier islands (the Outer Banks and Bogue Banks), from False Cape, Virginia in the north to Bogue Banks, North Carolina, USA in the south (Figure 4.1a, Appendix G, Table G1). This 350-km stretch of sandy barrier islands varies spatially in its beach geomorphology (Dolan and Lins 1985, Hovenga et al. 2019, 2021, Jay et al. Chapter 2), vegetation species and density (Figure 4.1b; Godfrey 1977, Woodhouse et al. 1977, Hacker et al. 2019, Jay et al. Chapter 2), wind and wave climate, and shoreline orientation (Figure 4.1a). The Outer Banks coastline as a whole, including our study region, is eroding at ~0.7 m yr^{-1}, with significant alongshore variability in shoreline erosion and accretion patterns (Miller et al. 2005, Hovenga et al. 2019, 2021). This region experiences a moderately energetic seasonal wind and wave climate, apart from tropical hurricanes and nor'easters that occur in the fall and winter (Bryant et al. 2016).

4.3.2 Field surveys and sample collection

We documented beach and foredune topography and vegetation communities at 112 transects across the study region in October 2016 (Bogue Banks through North Core Banks) and June 2017 (Ocracoke Island through False Cape) (Figure 4.1, Appendix G Table G1; see Hacker et al. 2019, Hovenga et al. 2019, 2021, Jay et al. Chapter 2). Transects were established perpendicular to the shoreline, extending from mean lower low water (MLLW) through the foredune toe (the seaward-most dune extent), crest (the highest point of foredune elevation), and heel (the lowest point landward of the foredune) (Appendix G, Figure G1). We established 0.25 m^2 quadrats every five meters along the foredune transect and counted the number of shoots of each grass species present within quadrats. We also used a Network Real Time Kinematic Differential Global Positioning System (R7 unit, Trimble, Sunnvyale, CA, USA) to collect elevation and position data along the entire cross-shore transect and at each vegetation quadrat on the foredune profile. To measure macrophyte wrack abundance at each transect, we estimated macrophyte wrack percent cover within 1 m^2 quadrats placed adjacent to each other for ten meters alongshore (perpendicular to the beach and foredune transect) at the wrack line, extending in both directions from the main transect.

At each transect, we collected an individual (defined as all the grass tillers attached to a single rhizome, which was extracted from the sand at ~25 cm of depth) of each grass species that was present at each foredune profile location (toe, crest, and heel). We also collected three representative macrophyte wrack patch samples from the wrack line at each transect (when present). We estimated the percent cover of each macrophyte

wrack sample prior to collection in order to later establish a relationship between wrack percent cover and biomass. Finally, we collected a sand sample at the foredune toe by using a scoop to collect sand at multiple locations at each transect.

4.3.3 Measurements of marine subsidies: macrophyte wrack and sand nitrogen

To determine macrophyte wrack biomass and composition at each site, samples were sorted by type, dried to a constant mass at 40˚C, and then weighed. We calculated the wrack composition at each transect as the proportion of the total biomass made up by each type collected. We then determined a linear relationship between the percent cover and biomass of the collected wrack samples. We established separate relationships for the two dominant types of wrack that were found at our field sites, the brown algae *Sargassum* sp. (biomass (g) = 2.81 * % cover, R^2=0.83, $p < 0.001$, see Appendix H, Figure H1) and *Zostera marina* eelgrass (biomass (g) = 0.90 * % cover, R^2=0.61, $p < 0.001$, see Appendix H, Figure H2). A few samples had trace amounts of other macrophyte species that were excluded from our processing. We then used these two equations, the proportional biomass of each wrack type, and the macrophyte wrack percent cover survey data to determine a weighted average of macrophyte wrack biomass at each transect.

To determine nitrogen content in foredune toe sand, samples were dried at 60˚C for 24 hours following field surveys. We then used the potassium chloride (KCl) extraction method described by Constant (2019), modified from Mulvaney (1996), to measure sand nitrate concentration. We analyzed samples using 2 M KCl extracts and measured the amount of nitrate obtained following cadmium reduction using a solution

buffered with ammonium chloride and sodium hydroxide (NH_4Cl + 1M NaOH). Then, to determine nitrate concentrations, we added an azo dye reagent and measured the absorbance of the solution at 540 nm wavelength using an Ocean Optics USB2000 spectrophotometer and a T300 1-cm pathlength transmission dip probe. Standards were created by dissolving sodium nitrate in a 2 M KCl solution.

4.3.4 Dune grass production measurements

Following field collection, dune grass samples were air-dried to a constant mass and then measured. We weighed each individual plant (after removing rhizomes and roots) and counted the number of shoots to obtain an average shoot weight (g/shoot) for each species. To calculate dune grass production metrics for all four grass species combined, we first summed the number of shoots of each species in each quadrat. Shoot densities were then averaged at each profile location for each transect (quadrats with no grasses present were removed from the calculations). Dune grass biomass (g/0.25 m^2) was calculated as the product of shoot density and shoot weight for each species and then summed within each quadrat. As with shoot density, biomass was averaged at each profile location for each transect.

4.3.5 Dune grass foliar nitrogen measurements

To examine marine nutrient inputs to dune grasses, we measured dune grass foliar nitrogen content (%N) and source ($\delta^{15}N$) in all four Outer Banks dune grass species at a subset of our transects (n=43; Figure 4.1a, Appendix G Table G1). Grass tissue samples were collected from the middle of the dried shoots for each plant. Tissue samples were powderized using a Spex Sigma Prep 8000D Mixer/Mill, weighed on a microbalance, and

analyzed via a continuous-flow isotope ratio mass spectrometer in the Oregon State University Staple Isotope Laboratory to obtain %N and $\delta^{15}N$ measurements.

Nitrogen stable isotope abundances were expressed using delta per mil notation (see Equation 1), indicating the deviation of the isotopic composition in each sample from the internationally accepted calibration standard (atmospheric nitrogen).

$$\delta^{15}N = \left(\left(\frac{R_{sample}}{R_{standard}}\right) - 1\right) * 1000 \qquad \text{(Equation 1)}$$

R denotes the ratio of the heavy to light isotope found in each sample ($^{15}N/^{14}N$). Thus, positive $\delta^{15}N$ values indicate that the sample is enriched in ^{15}N relative to the standard, while negative $\delta^{15}N$ values indicate that the sample is depleted in ^{15}N relative to the standard.

4.3.6 Shoreline change rate and beach and foredune morphometrics

To examine potential factors important to marine subsidies, dune grass production, and dune grass foliar nitrogen, we calculated shoreline change rate (SCR) and beach and foredune morphometrics at each of our transects. First, we calculated multidecadal SCR from 1997-2016 (the annual rate at which the shoreline position moves seaward or landward, or a measure of sediment gains and losses) as a proxy for sand supply to the beach (Farris and List 2007). Multidecadal SCR was calculated in two ways depending on the availability of airborne lidar data at different locations throughout the study region. For the southern Outer Banks transects (from Bogue Banks to North Core Banks), multidecadal SCR was calculated as the average annual change (m/yr) from 1997 to 2016 using airborne lidar data from NOAA's Digital Coast website as described in (Hovenga et al. 2019, 2021). At the northern Outer Banks transects from Ocracoke Island

to False Cape, multidecadal SCR was calculated as the average annual change (m/yr) from 1997 to 2010 using USGS shoreline position data from Kratzmann et al. (2017). For both calculations, cross-shore profiles were extracted at each transect location and shoreline positions were defined using a spatially varying MHW contour ranging from 0.33-0.46 meters (referenced to NAVD88).

Next, we extracted beach and foredune morphometrics for each transect using field topography data and following the methods of Mull and Ruggiero (2014). We extracted the approximate location of the mean high water (MHW) shoreline position using a 0.4 m contour referenced to the North American Vertical Datum 1988 (NAVD88). Beach morphometric measurements included backshore slope (the slope between MHW and the foredune toe) and beach width (the distance between MHW and the foredune toe) (Appendix G, Figure G1). Foredune morphometric measurements included the foredune toe and crest elevation (relative to MHW), foredune width (the horizontal distance between the foredune toe and crest), and foredune aspect ratio (foredune height divided by width).

4.3.7 Statistical analyses

All data were analyzed using R v.3.6.1 (R Development Core Team 2019). Residual and normal quantile plots were used to assess whether response variables conformed to the assumptions of the statistical analyses, and transformations were used when necessary.

To assess the patterns in marine subsidies, dune grass production, and dune grass foliar nitrogen metrics along Outer Banks foredunes, we used one-way and two-way

ANOVAs and Tukey HSD post-hoc tests. When significant interactions were found for the two-way ANOVAs, we used one-way ANOVAs and Tukey HSD post-hoc tests to compare between levels of each factor (Underwood 1997). First, we used one-way ANOVAs to determine whether macrophyte wrack biomass and sand nitrate concentration varied between islands. We then used two-way ANOVA to determine whether dune grass production metrics (shoot density and biomass for all four dune grass species combined) varied by island and profile location. Finally, we used one-way ANOVA to test for differences in dune grass foliar nitrogen metrics (%N and $\delta^{15}N$) by species at each foredune profile location separately (toe, crest, and heel).

To determine possible factors important to sand nitrate concentration, dune grass production, and dune grass foliar nitrogen metrics across our study system, we used multivariate regression analyses. Top models were selected using Akaike's Information Criterion (AIC) and the relative contribution of individual predictors in top models was determined using the R package 'heplots' and the function 'etasq' to calculate multivariate eta-squared (or R^2; Fox et al. 2018).

First, we explored correlations between sand nitrate concentration and a set of explanatory variables including macrophyte wrack biomass, beach and foredune morphometrics (beach width, backshore slope, foredune height, foredune width, and foredune aspect ratio), and multidecadal SCR. We then explored relationships between dune grass production and foliar nitrogen response variables (dune grass shoot density, dune grass biomass, dune grass foliar %N and $\delta^{15}N$) and explanatory variables at the transect level and at the toe, crest, and heel foredune profile locations separately. The

explanatory variables included: marine subsidies (wrack biomass and sand nitrate concentration), beach and foredune morphometrics (beach width, backshore slope, foredune height, foredune width, and foredune aspect ratio), and multidecadal SCR. For the dune grass foliar nitrogen metrics, we used an integrated measure of sand nitrate concentration that was an average of the transect and the two adjacent transects on each side.

4.4 Results

4.4.1 Spatial variability in marine subsidies

Macrophyte wrack biomass (g/m^2) varied significantly between Outer Banks islands, with no apparent latitudinal trend (Figure 4.2a, Table 4.1). North Core Banks had approximately 4-6 times greater wrack biomass than the other islands, while Shackleford Banks and False Cape had almost no macrophyte wrack (Figure 4.2a). The composition of macrophyte wrack biomass varied with latitude, reflecting a biogeographic boundary between the northern and southern Outer Banks islands (Figure 4.3). In particular, the proportion of *Zostera marina* eelgrass biomass in wrack samples decreased from north to south, while the proportion of *Sargassum* sp. biomass increased from north to south. Wrack biomass at northern (False Cape, Bodie Island) and southern (South Core Banks, Shackleford Banks, Bogue Banks) islands was comprised entirely of eelgrass or *Sargassum*, respectively (except Bogue Banks, which contained < 5% eelgrass), while the three islands in the middle (Hatteras and Ocracoke Islands, North Core Banks) had an increasing proportion of eelgrass biomass with latitude (Figure 4.3).

Sand nitrate concentration, measured at the dune toe, also varied significantly across islands (Figure 4.2b, Table 4.1). There was a latitudinal gradient where the northern Outer Banks islands generally had greater sand nitrate concentrations compared to southern Outer Banks islands, with the lowest values occurring at Shackleford Banks and Bogue Banks (Figure 4.2b).

4.4.2 Patterns in dune grass production across foredune profile locations and islands

Dune grass shoot density and biomass (for all four species combined) varied across islands and profile locations throughout the study region, with significant interactions between islands and profile locations (Figure 4.4, Table 4.3). ANOVAs and post hoc tests showed that, at most islands, dune grass density and biomass did not vary across the foredune profile, except at Hatteras Island, Ocracoke Island (grass biomass only), and North Core Banks where values were lower at the foredune toe (Table 4.3). Grass density and biomass at the foredune toe were highest at False Cape and lowest at Ocracoke Island, with little variability between remaining islands (Figure 4.4). In terms of profile location, there was little difference in dune grass density at the foredune crest, with Bogue Banks having the lowest values and no differences between the other islands. Dune grass biomass patterns at the crest showed higher combined biomass at Shackleford Banks, reflecting its high proportion of *U. paniculata* abundance (Figure 4.1b), which has much greater shoot biomass than the other species. There were no significant differences in dune grass density or biomass between islands at the foredune heel (Table 4.3).

4.4.3 Patterns in dune grass foliar nitrogen metrics by species, foredune profile location, and island

Dune grass foliar nitrogen content (%N) and source ($\delta^{15}N$) did not vary significantly between the four Outer Banks species in most cases, but results depended on the foredune profile location (Figure 4.6). *Ammophila breviligulata* had higher %N compared to *U. paniculata* at the foredune crest, but there were no differences in %N between species at the foredune toe and heel (Figure 4.6a-c). There were no significant differences in $\delta^{15}N$ between species at any of the profile locations (Figure 4.6d-f). However, $\delta^{15}N$ for *A. breviligulata* was higher than that of the other species at the foredune toe (a finding that was not significant due to high variability in these samples), which is likely related to where the species are found along the foredune profile. For example, we found that, at transects where both *A. breviligulata* and *U. paniculata* were present, the average first occurrence of *A. breviligulata* was significantly closer to the shoreline ($p < 0.05$) and at a lower elevation ($p < 0.001$) (11.4 m from the start of the dune transect and 3.4 m above MHW) compared to *U. paniculata* (16.1 m from the start of the dune transect and 4.5 m above MHW).

We found that foliar %N for *A. breviligulata* and *U. paniculata* combined varied by island but did not differ between foredune profile locations (Figure 4.6a, Table 4.3). There was a latitudinal pattern where %N was higher in plants from the northern Outer Banks islands compared to those from the southern Outer Banks islands, with no differences between islands within these regions (north and south; Figure 4.6a, Table 4.3). Foliar $\delta^{15}N$ varied by island and profile location, with significantly higher values occurring at the foredune toe compared to the foredune crest and heel (Figure 4.6, Table

4.3). Similar to %N, $\delta^{15}N$ values were highest in the northern Outer Banks and generally decreased with latitude, particularly at the foredune toe, with Bogue Banks being an exception (with values comparable to those at the northern sites; Figure 4.6b).

4.4.4 Factors important to sand nutrients and dune grass production across the Outer Banks

Our analyses showed that sand nitrate concentrations at the foredune toe were related to foredune morphology and multidecadal SCR (Table 4.4). In particular, the top model showed that higher sand nitrate concentration was associated with taller, narrower foredunes and negative multidecadal SCR values, although multidecadal SCR was not significant in the model. Foredune height explained the largest proportion of variance in sand nitrate concentration (15%), followed by foredune width (2%; Table 4.4). There was no relationship between sand nitrate concentration and macrophyte wrack biomass at our study sites (Figure 4.2).

Dune grass shoot density and biomass (for *A. breviligulata*, *U. paniculata*, *P. amarum*, and *S. patens* combined) were correlated with multidecadal SCR, beach and foredune morphometrics, and in some cases, sand nitrate concentration, with variability in the relative importance of these factors across the foredune profile (Table 4.5). At the transect level, top models showed that combined grass density and biomass were negatively correlated with multidecadal SCR and positively correlated with backshore slope and sand nitrate concentration (Table 4.5). The variance explained for each of these metrics was low (7%, 4%, and 1% for multidecadal SCR, sand nitrate concentration, and backshore slope, respectively, for grass density). At the foredune toe, combined grass density was higher in areas with wider dunes, lower macrophyte wrack biomass, and

narrower beaches, and combined grass biomass was unrelated to the explanatory variables (Table 4.5). At the foredune crest, combined grass density was highest in areas with negative multidecadal SCR values and wider dunes, and combined grass biomass was unrelated to the explanatory variables (Table 4.5). Finally, combined grass density and biomass at the foredune heel were unrelated to the explanatory variables (Table 4.5).

4.4.5 Relationships between marine subsidies, beach and dune morphometrics, and dune grass foliar nitrogen

Our analyses showed that the patterns in dune grass foliar %N and $\delta^{15}N$ response variables were correlated with multidecadal SCR, foredune morphology, and sand nitrate concentration (Table 4.6). Top models for dune grass foliar %N and $\delta^{15}N$ at the transect level showed that the two metrics were negatively and positively correlated with multidecadal SCR, respectively, and both were positively correlated with foredune height (Table 4.6). In addition, grass %N was positively correlated with sand nitrate concentration. Grasses at the foredune toe and crest had higher foliar %N in areas with taller, narrower dunes and greater sand nitrate concentration, and higher $\delta^{15}N$ in areas with more positive SCR values, taller dunes, and steeper beaches (crest only) (Table 4.6). In grasses at the foredune heel, foliar %N was negatively correlated with multidecadal SCR and positively correlated with foredune height and width, while $\delta^{15}N$ was unrelated to the explanatory variables (Table 4.6).

4.5 Discussion

In this study, we surveyed beaches and foredunes along the U.S. Outer Banks and Bogue Banks barrier islands to examine possible connections between marine nutrient sources and dune grass productivity. We used the variability in marine subsidies, dune

grass production (shoot density and biomass), and dune grass foliar nitrogen content (%N) and source ($\delta^{15}N$) to ask whether dune grasses utilize marine derived nitrogen and whether there was evidence that marine subsidies affect dune grass production. Additionally, we examined what factors might contribute to these relationships, including proxies for beach and dune sand supply (i.e., multidecadal SCR and beach and dune morphometrics).

We found that the nitrogen content and production of dune grasses was positively associated with marine nutrient subsidies, particularly sand nitrate concentration on the beach and dune interface (Figures 4.2, 4.4, 4.6, Tables 4.5, 4.6). There was a strong marine signature of nitrogen ($\delta^{15}N$) within the grasses that decreased across the foredune profile, with the highest values in grasses closest to the beach at the foredune toe (Figure 4.6). In addition, we found that sand nitrate and foliar nitrogen (both %N and $\delta^{15}N$) varied across latitudes with the highest values in foredunes on the northern islands compared to foredunes on the southern islands, suggesting a potential influence of oceanic nutrients to the beaches and foredunes in this region. Surprisingly, we found no relationship between macrophyte wrack biomass and sand nitrogen levels or grass production (Figures 4.2, 4.4). However, we did observe a strong biogeographic pattern in wrack composition, where wrack samples from sites north of Cape Hatteras were almost entirely made up of eelgrass, while those to the south had progressively larger proportions of *Sargassum* sp. (Figure 4.3).

Regression analyses also revealed that sand nitrate concentration at the foredune toe was positively associated with foredune height; in particular, sites with taller,

narrower dunes had greater sand nitrate values (Table 4.4). In turn, foliar %N and $\delta^{15}N$ metrics were positively associated with foredune height and sand nitrate levels, with greater nitrogen content and a more marine nitrogen signature found in grasses growing in areas with taller dunes and higher sand nitrate concentration (Table 4.6). We found that dune grass production was related to proxies for sand supply to the beach and dune (i.e., multidecadal SCR, foredune height, backshore slope) as well as marine subsidies, but the relative importance of these factors varied across the foredune profile (Table 4.5). Overall, our findings suggest that the interactive effects of sand supply and beach and foredune morphology mediate the delivery of marine-derived nutrients to foredunes, which varies across the foredune profile and throughout the study region.

4.5.1 Patterns in marine subsidies and dune grass production along the Outer Banks coast

Sand nitrate concentrations in our system, which ranged from 4.2-14.8 μmol/g sand depending on the island (Figure 4.2b), were low compared with those reported on the U.S. Pacific Northwest coast, where site-averaged foredune toe sand nitrate concentration ranged from ~10-105 μmol/g sand (Constant 2019). These large differences are unsurprising given that ocean productivity is much higher on the Pacific Northwest coast, where upwelling brings cold, nutrient rich water to the surface, fueling productivity of phytoplankton and macroalgae (Constant 2019). This productivity contrasts with the more oligotrophic waters off the North Carolina coast. However, sand nitrate concentrations from the Outer Banks were higher than those reported in Mediterranean coastal dunes (up to 4.1 μmol/g sand; Bonanomi et al. 2012) and Wales dune slacks (0.03 μmol/g soil; Rhymes et al. 2014)

We found clear differences in macrophyte wrack biomass and composition across the Outer Banks, providing strong evidence that wrack composition in this region varies as a result of the biogeophysical boundary in ocean currents offshore of Cape Hatteras (Figures 4.2a, 4.3). Macrophyte wrack biomass was unrelated to sand nitrate concentrations at the foredune toe (Figure 4.2), an unexpected finding given the connections between wrack deposition, sand nutrient levels, and dune grasses documented in previous studies (Cardona and García 2008, Dugan et al. 2011, Barreiro et al. 2013, Del Vecchio et al. 2013, Constant 2019). Although sand nitrate concentration was unrelated to macrophyte wrack biomass, differences in offshore marine nutrient levels are likely an important factor driving the latitudinal trends in sand nitrate and foliar nitrogen content that we observed (Figures 4.2, 4.6). Sand nitrate concentrations and dune grass foliar nitrogen values increased on the islands near Cape Hatteras and northward, where an offshore boundary in ocean circulation may impact marine nutrient delivery to beaches (Figure 4.3; Mallin et al. 2000, Savidge 2004, Mannino et al. 2016). For example, nutrient measurements in coastal waters across our study region show increases in dissolved nitrate and nitrite from 20 to 30 µg/L north of Cape Hatteras, while total nitrogen ranges from 91-158 µg/L offshore from the southern Outer Banks and 143-347 µg/L offshore from the northern Outer Banks (Balthis et al. 2019). In the U.S. Pacific Northwest, previous studies have shown that macrophyte wrack on beaches is closely linked to patterns in ocean upwelling, proximity to the nearest source habitat (i.e., estuary, rocky reef), and sand supply (Reimer et al. 2018, Constant 2019). Similarly, our findings suggest that differences in offshore nutrients and sand supply to beaches are

related to nitrate concentrations in beach sands and dune grass tissues, while biogeographic differences in macrophyte wrack composition are related to an offshore boundary in ocean circulation.

There are several possible explanations for the observed mismatch between wrack biomass and sand nitrate concentration. First, we sampled the southern Outer Banks sites 1-2 weeks after Hurricane Matthew, during which increases in total water levels may have caused a "pulse" event where additional wrack biomass was deposited on the beach, particularly at North Core Banks, which had much greater wrack biomass than other islands (Figure 4.2a). Such a pulse in wrack deposition would not be reflected in the sand samples that we collected during the same time period. Second, there are large differences in the biomass of the two types of wrack deposited on Outer Banks beaches (*Zostera marina* eelgrass north of Cape Hatteras and *Sargassum* sp. south of Cape Hatteras; Figure 4.3), where wrack patches comprised of eelgrass have much lower biomass (Appendix H, Figures H1 and H2) and sites north of Cape Hatteras had lower biomass per m^2 (Figure 4.2a). Finally, there may be seasonal patterns in macrophyte wrack deposition to beaches leading to a temporal mismatch between our samples that were collected in October (southern Outer Banks) and June (northern Outer Banks).

Dune grasses also varied in their foliar nitrogen content and source among islands in our study region. We found a similar latitudinal pattern to that observed in sand nitrate concentration (higher values in the northern Outer Banks) in %N across all profile locations and in $\delta^{15}N$ at the foredune toe (Figure 4.6), suggesting that dune grasses may be responding to differences in sand nitrate concentrations. There were a few outliers to

the pattern in $\delta^{15}N$ at the foredune toe, including higher values at Bogue Banks that were more similar to northern Outer Banks sites and very low values at Shackleford Banks, suggesting that the contribution of marine nutrient subsidies is lower at Shackleford Banks. The lower $\delta^{15}N$ values at Shackleford Banks may be related to the shoreline orientation and position of the island, which is largely protected by Cape Lookout (Figure 4.1a), and our finding that there was almost no macrophyte wrack at this site (Figure 4.2). The marine nitrogen signature was strongest at the foredune toe at all other sites and extended to the foredune crest at False Cape and Bodie Island. Our highest site-averaged $\delta^{15}N$ value at the foredune toe (4.8‰ at Bodie Island) was much lower than the maximum values (up to 8‰) reported by Constant (2019), suggesting that marine subsidies have a greater influence on dune grasses on the more productive Pacific Northwest coast. However, our $\delta^{15}N$ values at the foredune toe were very similar to those from C_3 grasses in Mediterranean foredunes (Cardona and García 2008).

Dune grass production metrics (shoot density and biomass) also varied throughout the study region (Figure 4.4, Table 4.3), likely because of gradients in shoreline change rate and sand nitrate concentration. Shoot density and biomass tended to be lower at the foredune toe, which often has higher levels physical stress and disturbance. However, False Cape was an outlier with much higher dune grass production at the toe compared to everywhere else; this finding suggests that marine nutrients may influence dune grass production, given that sand nitrate concentration, foliar %N and $\delta^{15}N$, and grass production were all high at this site (Figures 4.2, 4.4, and 4.6). There were fewer differences in dune grass production at the crest and no differences at the heel (Figure

4.4, Table 4.3), an unsurprising pattern because dune grass growth tends to be more consistent behind the crest compared with the patchier distribution of grasses on the foredune face.

4.5.2 Differences in foliar nitrogen metrics by dune grass species

We found that there was little or no difference in the nitrogen content (%N), or the source of that nitrogen ($\delta^{15}N$), among the four dune grass species in our study. The only observed differences were at the foredune crest, where *A. breviligulata* had greater %N compared to *U. paniculata*, and at the foredune toe, where *A. breviligulata* had the highest $\delta^{15}N$ value (Figure 4.5b, d). We also found that *A. breviligulata* grows significantly closer to the shoreline and at lower elevations than *U. paniculata*. Thus, higher $\delta^{15}N$ in *A. breviligulata* tissues may reflect plant zonation patterns along the foredune profile and improved access to marine nutrients for species growing closer to the beach. Our findings are similar to Constant (2019), who found that three Pacific Northwest beachgrasses did not vary significantly in their foliar %N and $\delta^{15}N$. However, the forb *Cakile edentula*, which only occurs low at the foredune toe, had greater %N and $\delta^{15}N$ in its tissues suggesting that its position on the shoreline allows it to better utilize marine derived nitrogen.

Similar to previous findings from the Pacific Northwest coast (Constant 2019), the two primary dune building grasses in our study (*A. breviligulata* and *U. paniculata*) did not vary in %N across the foredune profile, but $\delta^{15}N$ was significantly higher at the foredune toe compared to the crest and heel (Figure 4.6). The lack of variation in dune grass foliar %N across the dune profile may indicate that dune grasses can maintain

stoichiometric homeostasis, where plants maintain constant tissue nutrient composition despite variation in the nutrient composition of their growing environment (Sterner and Elser 2002, Elser et al. 2010). On the other hand, foliar nitrogen content did vary among islands (Figure 4.6), suggesting that dune grasses are responding to variability in nitrogen availability (%N) at regional scales but not at local (foredune profile) scales, while nitrogen source ($\delta^{15}N$) varied at both local and regional scales. The landward decrease in $\delta^{15}N$ across the foredune profile indicates that dune grasses at the toe likely receive nutrients from marine sources that are enriched in ^{15}N, while grasses growing behind the foredune rely on atmospheric nitrogen and fungal and microbial symbiotic associations (Högberg 1997, Lepoint et al. 2000, Cardona and García 2008). However, $\delta^{15}N$ in plants can also vary as a result of other environmental factors that could contribute to the enriched $\delta^{15}N$ signature at the toe; for example, increased nitrogen availability to plants through mechanisms including nitrogen deposition can decrease their dependence on symbionts for nitrogen fixation and lead to tissue $\delta^{15}N$ enrichment (Högberg 1997, Michelsen et al. 1998, Craine et al. 2015).

4.5.3 Importance of marine subsidies and beach and foredune morphology to dune grass production and foliar nitrogen metrics

Our finding that sites with taller foredunes and eroding beaches had greater sand nitrate concentration and dune grass production (Tables 4.4, 4.5) suggests that patterns in beach nutrients and dune grass growth are likely related to the interplay between beach and foredune sediment dynamics. The beach-dune interaction model of Psuty (1986) shows that foredune growth at the crest is greatest when SCR values are neutral or slightly negative, leading to the formation of taller foredunes, which could intercept

greater quantities of nutrient-laden sand. Thus, this suggests that the taller the foredune, the greater the sand nitrate concentration, which can in turn promote greater dune grass production.

Our results showed that dune grass production and foliar nitrogen metrics (shoot density and biomass) were related to proxies for sand supply (e.g., multidecadal SCR, backshore slope, foredune height) and sand nitrate concentration, with the relative importance of these factors varying across the foredune profile (Table 4.5). However, the explained variance in the dune grass production models was low, indicating that none of these variables were strongly related to dune grass production, which is unsurprising given that these metrics did not vary greatly across the study region at the dune crest and heel (Figure 4.4). Overall, sites with narrower and steeper beaches, taller foredunes, negative multidecadal SCR, and greater sand nitrate levels had increased dune grass production and foliar nitrogen values. Given that dunes form via biophysical feedbacks between vegetation and sand supply and foredune growth tends to be maximized in areas with slightly negative SCR (Psuty 1986), it makes sense that dune grass density and biomass would be greater in areas with taller foredunes and negative SCR. In addition, we found a positive relationship between grass density and foredune width at the toe, where *A. breviligulata* is more common and can grow densely (Hacker et al. 2019a), and previous work has shown that increases in *A. breviligulata* density are associated with increases in foredune width (Jay et al. Chapter 2). Thus, patterns in sand supply and geomorphology influence dune grass production through biophysical feedbacks and mediate the delivery of marine subsidies to the foredune toe, where dune grasses can then

utilize marine-derived nutrients. At the foredune heel, marine nutrients and beach and foredune morphometrics did not contribute to patterns in dune grass production, indicating different factors may drive patterns in dune grass production on the seaward and landward sides of the foredune.

We found that beaches with lower (or negative) multidecadal SCRs and taller foredunes had dune grasses with greater %N content at the transect level, and taller, narrower, foredunes with higher sand nitrate levels had grasses with greater %N at the foredune toe and crest (Table 4.6). In contrast, taller, wider foredunes had greater dune grass %N at the heel. Our findings suggest that marine subsidies are more important at the foredune toe and crest, and that beach and foredune morphology can alter nutrient delivery and accumulation across the foredune profile by supplying varying levels of sand to beaches and dunes, changing the area over which nutrients can accumulate, or acting as barriers to nutrient delivery. Foredune height was most important to dune grass %N at the foredune crest, followed by the toe and then the heel (explained variance in top models was 36%, 20%, and 12%, respectively), suggesting that taller dunes can capture more nutrient-laden sand at the toe and crest compared to shorter dunes, where more sand could be transported over the dune crest to the heel. Our findings are similar to those of Constant (2019), where beach and dune morphometrics were stronger predictors of grass %N and $\delta^{15}N$ than measures of marine subsidies and taller foredunes acted as barriers to marine nutrients, preventing them from reaching the heel. We know from previous studies that foredunes are much taller on the Pacific Northwest coast than in the Outer

Banks (Hacker et al. 2012, Biel et al. 2019, Jay et al. Chapter 2), meaning that they can act as more significant barriers to marine nutrient transport.

Our regression analyses also showed that multidecadal SCR, foredune height, sand nitrate concentration, and backshore slope were positively associated with dune grass $\delta^{15}N$, with significant factors varying by the foredune profile location (Table 4.6). Given that these factors are all related to sand supply, our results suggest that dune grass $\delta^{15}N$ was greatest in areas with higher sand supply to the beach and dune. Multidecadal SCR was most important at the foredune toe where dune grass $\delta^{15}N$ values were greatest, suggesting that marine nutrients delivered to the beach and foredune are ultimately being incorporated into dune grass tissues. Backshore slope and foredune height were most important at the foredune crest, suggesting that taller foredunes with steeper beaches (which also tend to be narrower beaches; Wright and Short 1984) are receiving more marine nutrients. None of the variables we tested were significant at the foredune heel, where dune grass tissues were depleted in ^{15}N, indicating that grasses at the heel likely rely on other sources of nitrogen such as atmospheric nitrogen and nitrogen-fixing symbionts.

4.5.4 Conclusions and implications

Our findings demonstrate the interactive roles of marine-derived nutrients, beach and foredune geomorphology, and shoreline change rate in shaping the productivity and nutrient sources of dune grasses along the Outer Banks coastline. These results support the hypothesis that marine nutrients provide a source of nitrogen for dune grasses, as previously shown in other studies (Cardona and García 2008, Del Vecchio et al. 2017,

Constant 2019). Further research is needed in our study system to elucidate seasonal patterns in macrophyte wrack deposition to beaches as well as possible variation in sand nutrient levels across the entire beach and foredune profile. On the U.S. Atlantic Coast, which is particularly vulnerable to coastal hazards due to accelerated rates of sea level rise, exposure to extreme storms, and high population density (Stockdon et al. 2007, Sallenger et al. 2012), foredunes play an important role in wave attenuation and hazard mitigation on low-lying barrier islands. Because dune grasses are influential in shaping dune morphology, and in turn, coastal protection services, it is necessary to understand the factors driving dune grass productivity. Climate change will likely cause shifts in ocean productivity and nitrogen deposition as well as dune grass species distributions, which may in turn affect critical dune ecosystem functions including nutrient cycling.

4.6 Acknowledgements

Funding was provided by the National Oceanic and Atmospheric Administration (NOAA) via the NOS/NCCOS/CRP Ecological Effects of Sea Level Rise Program (grant no. NA15NOS4780172) to S.D.H., grants from the Geological Society of America and OSU Integrative Biology to K.R.J., funds from the OSU STEM Leaders program to J.Q., and funds from the OSU URSA Engage program to L.P. We thank P. Hovenga, R. Mostow, M. Itzkin, E. Mullins, I. Reeves, J. Wood, N. Cohn, E. Goldstein, C. Magel, P. Ruggiero, and L. Moore for assistance with field data and sample collection and P. Hovenga for assistance with topography data processing. Thanks to J. Padilla for assistance with sample processing. We thank J. McKay for nitrogen content and stable isotope analyses. Special thanks to B. Russell and F. Chan for assistance with sand nutrient analyses and use of laboratory facilities.

Table 4.1. One-way ANOVA and Tukey HSD post-hoc test results for macrophyte wrack biomass (g/m^2) and sand nitrate concentration (µmol N/g sand) across islands (see Figure 4.1, Appendix G, Table G1 for island abbreviations)**.**

	df	SS	F	Prob > F	Tukey HSD post-hoc
Macrophyte wrack biomass (g/m^2)					
Island	7	2450	203.8	< 2E-16	NCB>BGB>OCR=BOD=HAT≥SCB>FAC>SHB
Residuals	2232	3832			
Sand nitrate concentration (µmol N/g sand)					
Island	7	17.6	5.7	1.6E-5	FAC=BOD=HAT=OCR=NCB=SCB≥SHB=BGB
Residuals	98	43.5			

Table 4.2. Two-way ANOVA and Tukey HSD post-hoc test results for grass shoot density (shoots/0.25 m^2) and grass biomass (g/0.25 m^2) for all four Outer Banks dune grass species combined [*Uniola paniculata* (UNPA), *Ammophila breviligulata* (AMBR), *Panicum amarum* (PAAM), and *Spartina patens* (SPPA)] across islands (see Figure 4.1, Appendix G, Table G1 for island abbreviations) and dune profile locations (toe, crest, and heel).

	df	SS	F	Prob > F	Tukey HSD post-hoc	
Dune grass shoot density						
Island	7	21.6	5.6	2.7E-6		
Profile location	2	4.4	4.0	0.018		
Island* Profile location	14	16.8	2.2	0.007	**FAC, BOD, OCR, SCB, SHB, BGB:** Toe = Crest = Heel **HAT, NCB:** Toe ≤ Crest = Heel	**Toe:** FAC > BOD = HAT = OCR = NCB = SCB = SHB = BGB **Crest:** BOD = HAT = OCR = SHB = FAC = SCB = NCB ≥ BGB **Heel:** BOD = HAT = OCR = SHB = NCB = SCB = FAC = BGB
Residuals	571	312.4				
Dune grass biomass						
Island	7	23.2	6.0	9.8E-7		
Profile location	2	10.7	9.6	7.6E-5		
Island* Profile location	14	16.5	2.1	0.009	**FAC, BOD, SCB, SHB, BGB:** Toe = Crest = Heel **HAT, OCR, NCB:** Toe < Crest = Heel	**Toe:** FAC = BOD = SCB = SHB ≥ HAT = OCR = NCB = BGB **Crest:** HAT = SHB ≥ FAC = BOD = OCR = NCB = SCB = BGB **Heel:** HAT = OCR = SHB = NCB = BGB = SCB = FAC = BOD
Residuals	571	316.2				

Table 4.3. Two-way ANOVA and Tukey HSD post-hoc test results for dune grass %N and ∂^{15}N for *Uniola paniculata* (UNPA) and *Ammophila breviligulata* (AMBR) combined across islands (see Figure 4.1, Appendix G, Table G1 for island abbreviations) and dune profile locations (toe, crest, and heel).

	df	SS	F	Prob > F	Tukey HSD post-hoc
Dune grass % N					
Island	7	3.3	10.7	9.6E-20	FAC=BOD=HAT=OCR≥ NCB=SCB=SHB=BGB
Profile location	2	0.2	2.3	0.11	
Island* Profile location	14	0.6	1.0	0.46	
Residuals	90	3.9			
Dune grass ∂^{15}N					
Island	7	112.7	3.8	0.001	FAC=BOD=HAT=OCR= NCB=SCB≥SHB≤BGB
Profile location	2	151.7	17.9	2.9E-7	Toe>Crest=Heel
Island* Profile location	14	38.5	0.7	0.82	
Residuals	90	382.0			

Table 4.4. Top model results (ΔAIC<2) from multiple regression analyses of the response variable sand nitrate concentration (μmol N/g sand) as a function of the explanatory variables of multidecadal shoreline change rate, beach and foredune morphometrics, and macrophyte wrack biomass. Explanatory variables included together in models were uncorrelated with Pearson correlation coefficient < |0.6|. Significance codes for explanatory variables are: ***p<0.001, **p<0.01, *p<0.05. Explanatory variables with significant p values are in bold. Response variable transformations were applied following residual investigations (residual vs. fitted plots) and Shapiro–Wilk tests for normality.

Response variable	Model	Model results
Sand nitrate concentration	[ln(Sand nitrate)] = 0.20[**Dune height**]*** – 0.01[Dune width] – 0.002[SCR] + 0.81***	AIC=230.3 ΔAIC=0 df=103 **Variance explained:** Dune height=0.15, Dune width=0.02, SCR=0.00
	[ln(Sand nitrate)] = 0.17 [**Dune height**]*** + 0.78***	AIC=231.5 ΔAIC=1.2 df=105 **Variance explained:** Dune height=0.15
	[ln(Sand nitrate)] = 0.20[**Dune height**]*** – 0.01[Dune width] + 0.79***	AIC=231.8 ΔAIC=1.5 df=105 **Variance explained:** Dune height=0.15, Dune width=0.01

Table 4.5. Top model results (ΔAIC<2) from multiple regression analyses of the response variables combined grass shoot density (shoots/0.25 m^2) and grass biomass (g/m^2) of *Ammophila breviligulata* and *Uniola paniculata* across the whole foredune profile and separately at the toe, crest, and heel, as a function of the explanatory variables of multidecadal shoreline change rate, beach and foredune morphometrics, and marine subsidies. Explanatory variables included together in models were uncorrelated with Pearson correlation coefficient < |0.6|. Significance codes for explanatory variables are: ***p<0.001, **p<0.01, *p<0.05, ^{NS}p<0.1. Explanatory variables with significant p values are in bold. Response variable transformations were applied following and residual investigations (residual vs. fitted plots) and Shapiro–Wilk tests for normality.

Response variable	Model	Model results
Grass density – Transect	[ln(Grass density+1)] = -0.04[**SCR**]** + 2.42[Backshore slope] + 0.02[**Sand nitrate**]* + 2.37***	AIC=142.25 ΔAIC=0 df=103 **Variance explained:** SCR=0.07, Sand nitrate=0.04, Backshore slope=0.01
	[ln(Grass density+1)] = -0.05[**SCR**]** + 0.05[Dune height]^{NS} + + 0.01[Sand nitrate] + 2.27***	AIC=142.74 ΔAIC=0.49 df=100 **Variance explained:** SCR=0.09, Foredune height=0.03, Sand nitrate=0.01
	[ln(Grass density+1)] = -0.04[**SCR**]*** + 0.02[Sand nitrate]^{NS} + 2.50***	AIC=143.86 ΔAIC=1.61 df=101 **Variance explained:** SCR=0.07, Sand nitrate=0.03
Grass density – TOE	[ln(Grass density+1)] = 0.02[**Dune width**]* – 0.005[**Wrack biomass**]* – [Beach width]^{NS} + 2.38***	AIC=187.08 ΔAIC=0 df=85 **Variance explained:** Foredune width=0.05, Wrack biomass=0.05, Beach width=0.04
Grass density – CREST	[ln(Grass density+1)] = -0.07[**SCR**]** + 0.08[**Dune height**]* + 2.05***	AIC=216.45 ΔAIC=0 df=106

Table 4.5 (Continued)

		Variance explained: SCR=0.08, Foredune height=0.04
Grass biomass – Transect	[ln(Grass biomass+1)] = -0.01[SCR] + 3.72[**Backshore slope**]* + 0.01[Sand nitrate] + 3.84***	AIC=96.89 ΔAIC=0 df=100 **Variance explained:** Backshore slope=0.04, Sand nitrate=0.03, SCR=0.004

Table 4.6. Top model results (ΔAIC<2) from multiple regression analyses of the response variables of grass foliar %N and ∂^{15}N for *Ammophila breviligulata* and *Uniola paniculata* combined across the across the whole foredune profile and separately at the toe, crest, and heel, as a function of the explanatory variables of multidecadal shoreline change rate, beach and foredune morphometrics, and marine subsidies. Explanatory variables included together in models were uncorrelated with Pearson correlation coefficient < |0.6|. Significance codes for explanatory variables are: ***p<0.001, **p<0.01, *p<0.05, ^{NS}p<0.1. Explanatory variables with significant p values are in bold. Response variable transformations were applied following residual investigations (residual vs. fitted plots) and Shapiro–Wilk tests for normality.

Response variable	Model	Model results
Grass % N – Transect	[ln(Grass %N)] = 0.07[**Dune height**]*** + 0.02[**Sand nitrate**]* – 0.01[SCR]^{NS} – 0.53***	AIC= -12.57 ΔAIC=0 df=110 **Variance explained:** Foredune height=0.11, Sand nitrate=0.03, SCR=0.02
	[ln(Grass %N)] = 0.06[**Dune height**]*** + 0.02[**Sand nitrate**]* – 0.52***	AIC= -11.47 ΔAIC=1.1 df=111 **Variance explained:** Foredune height=0.10, Sand nitrate=0.03
Grass % N – TOE	[ln(Grass %N)] = 0.06[**Dune height**]** – 0.35**	AIC=4.85 ΔAIC=0 df=40 **Variance explained:** Foredune height=0.20
	[ln(Grass %N)] = 0.04[Dune height]^{NS} + 0.02[Sand nitrate] – 0.38**	AIC= 5.20 ΔAIC=0.35 df=39 **Variance explained:** Foredune height=0.06, Sand nitrate=0.03
	[ln(Grass %N)] = 0.08[Dune height]** – 0.005[Dune width] – 0.38**	AIC= 5.84 ΔAIC=0.99 df=39

Table 4.6 (Continued)

		Variance explained: Foredune height=0.17, Foredune width=0.02
Grass % N – CREST	[ln(Grass %N)] = 0.10[**Dune height**]*** – 0.63***	AIC= -2.57 ΔAIC=0 df=40 **Variance explained:** Foredune height=0.36
	[ln(Grass %N)] = 0.12[**Dune height**]*** – 0.005[Dune width] – 0.62***	AIC= -1.64 ΔAIC=0.93 df=38 **Variance explained:** Foredune height=0.32, Foredune width=0.02
	[ln(Grass %N)] = 0.08[**Dune height**]** + 0.01[Sand nitrate] – 0.62***	AIC= -1.51 ΔAIC=1.06 df=38 **Variance explained:** Foredune height=0.14, Sand nitrate=0.01
Grass % N – HEEL	[Grass %N] = -0.02[**SCR**]* + 0.06[**Dune height**]* + 0.009[Dune width] – 0.59***	AIC= -10.21 ΔAIC=0 df=28 **Variance explained:** Foredune height=0.12, SCR=0.12, Foredune width=0.05
	[Grass %N] = -0.02[**SCR**]* + 0.09[**Dune height**]*** – 0.58***	AIC= -9.32 ΔAIC=0.89 df=29 **Variance explained:** Foredune height=0.33, SCR=0.12
Grass ∂^{15}N – Transect	[Grass ∂^{15}N] = 0.15[**SCR**]** + 0.26[**Dune height**]* – 0.10	AIC=523.96 ΔAIC=0 df=111 **Variance explained:** SCR=0.06, Foredune height=0.03

Table 4.6 (Continued)

	[Grass ∂^{15}N] = 0.16[**SCR**]** + 0.11[Sand nitrate]^{NS} + 0.48	AIC=525.32 ΔAIC=0 df=111 **Variance explained:** SCR=0.06, Sand nitrate=0.02
Grass ∂^{15}N – TOE	[Grass ∂^{15}N] = 0.21[**SCR**]* + 0.29[Dune height] + 1.09	AIC=184.05 ΔAIC=0 df=38 **Variance explained:** SCR=0.13, Foredune height=0.05
	[Grass ∂^{15}N] = 0.23[**SCR**]** + 2.66***	AIC=184.78 ΔAIC=0.73 df=39 **Variance explained:** SCR=0.17
Grass ∂^{15}N – CREST	[Grass ∂^{15}N] = 38.50[**Backshore slope**]** + 0.21[**SCR**]* + 0.08[**Dune height**]* – 2.00*	AIC=170.94 ΔAIC=0 df=36 **Variance explained:** Backshore slope=0.17, SCR=0.11, Foredune height=0.09

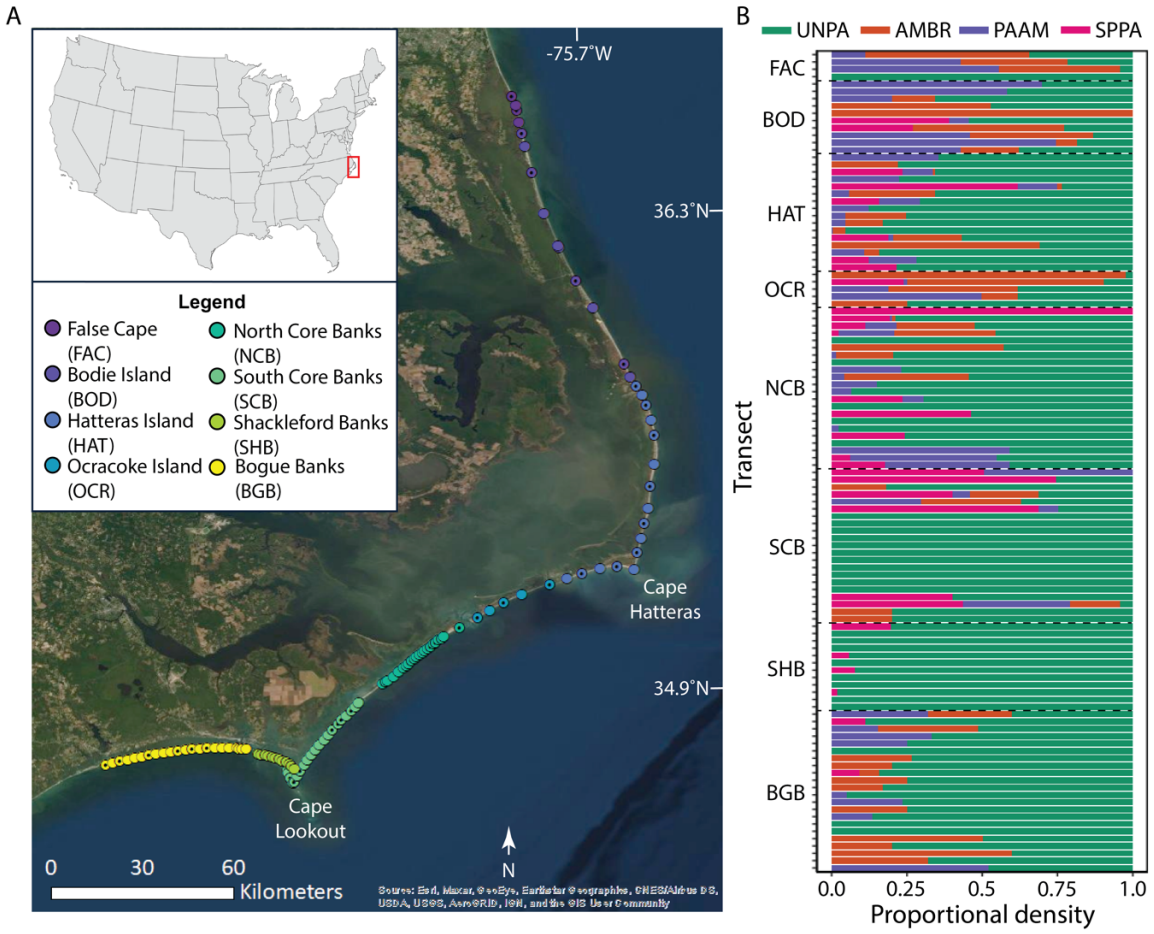

Figure 4.1. Sampling locations and dune grass proportional density across the Outer Banks barrier island foredunes, from False Cape, Virginia to Bogue Banks, North Carolina, USA (see Appendix G, Table G1 for island and transect abbreviations and locations). Note that Pea Island transects were included as part of Hatteras Island in all analyses. (A) Map of transect locations along Outer Banks and Bogue Banks foredunes. Circles with a black dot in the middle denote the 43 transects that were sampled for dune grass foliar nitrogen metrics. (B) Proportional density of the four dominant Outer Banks dune grasses [*Uniola paniculata* (UNPA), *Ammophila breviligulata* (AMBR), *Panicum amarum* (PAAM), and *Spartina patens* (SPPA)] from north to south. Dashed lines represent borders between islands.

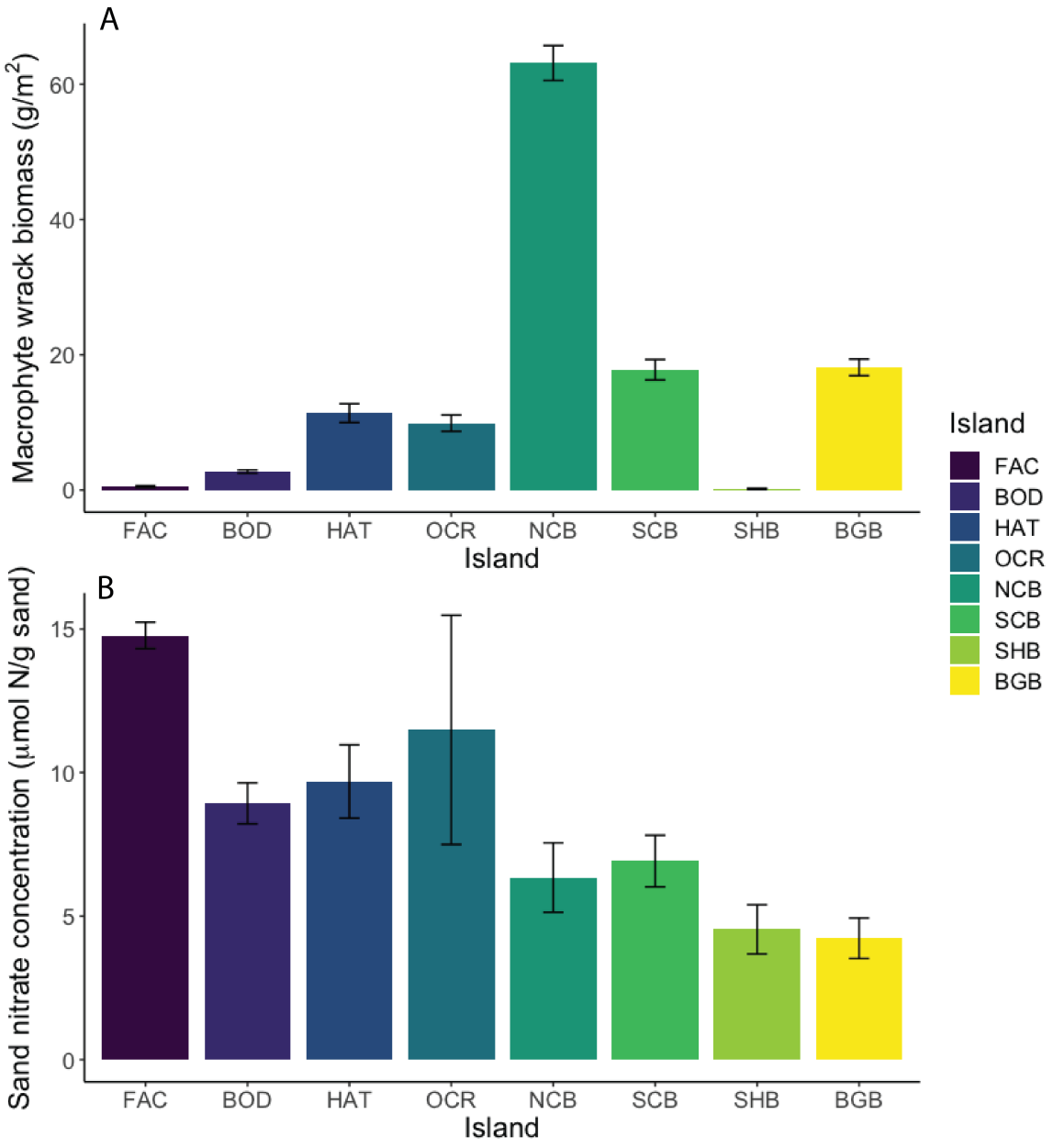

Figure 4.2. Mean (± SE) (A) macrophyte wrack biomass (g/m^2) and (B) sand nitrate concentration (µmol N/g sand) at each island on the Outer Banks barrier islands, North Carolina, USA (see Figure 4.1, Appendix G, Table G1 for island abbreviations and locations). See Table 4.1 for statistics.

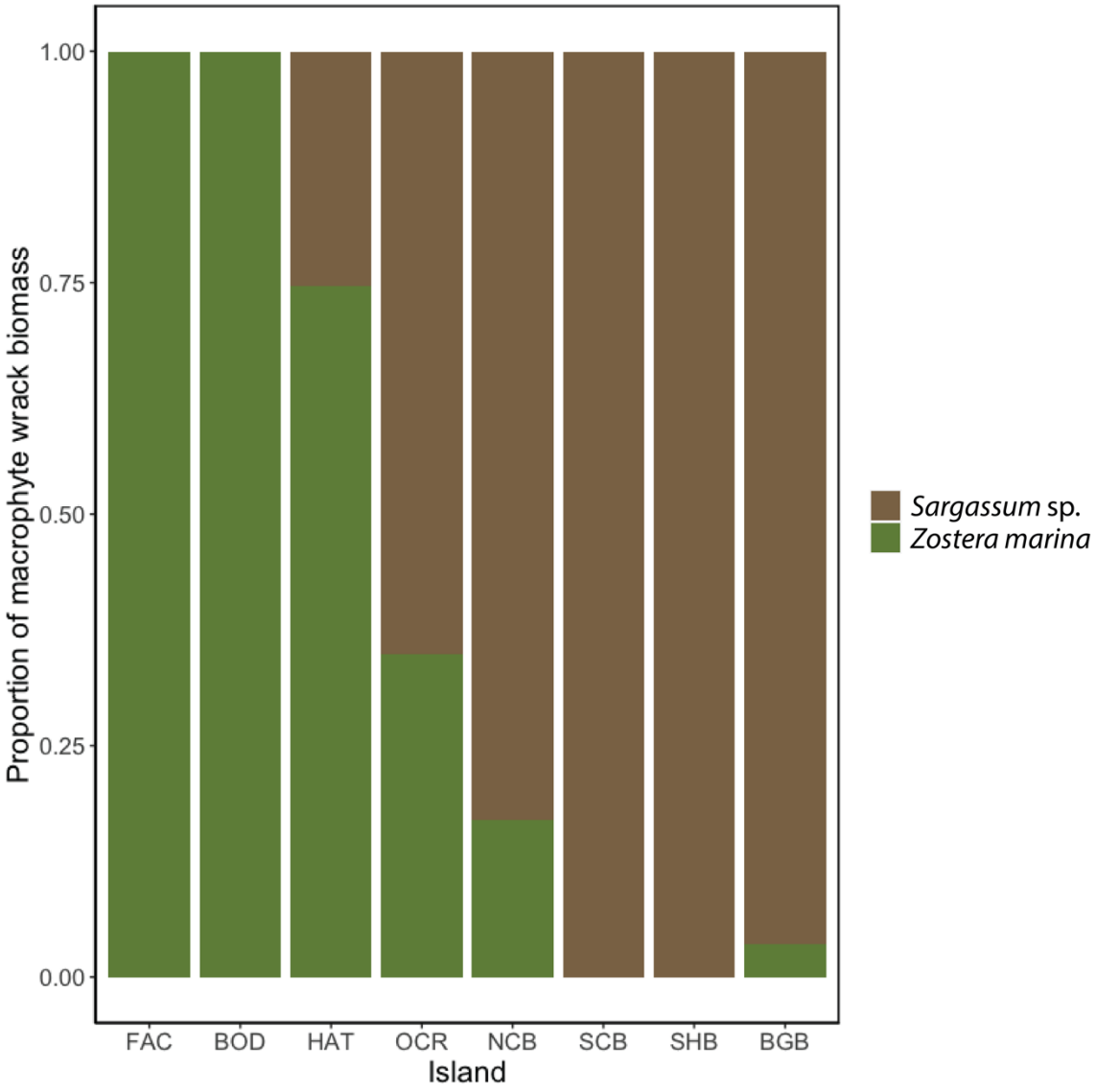

Figure 4.3. Composition of macrophyte wrack (proportional biomass of macroalgae *Sargassum* sp. and eelgrass *Zostera marina*) across Outer Banks barrier islands, USA from north to south (see Figure 4.1, Appendix G, Table G1 for island abbreviations and locations).

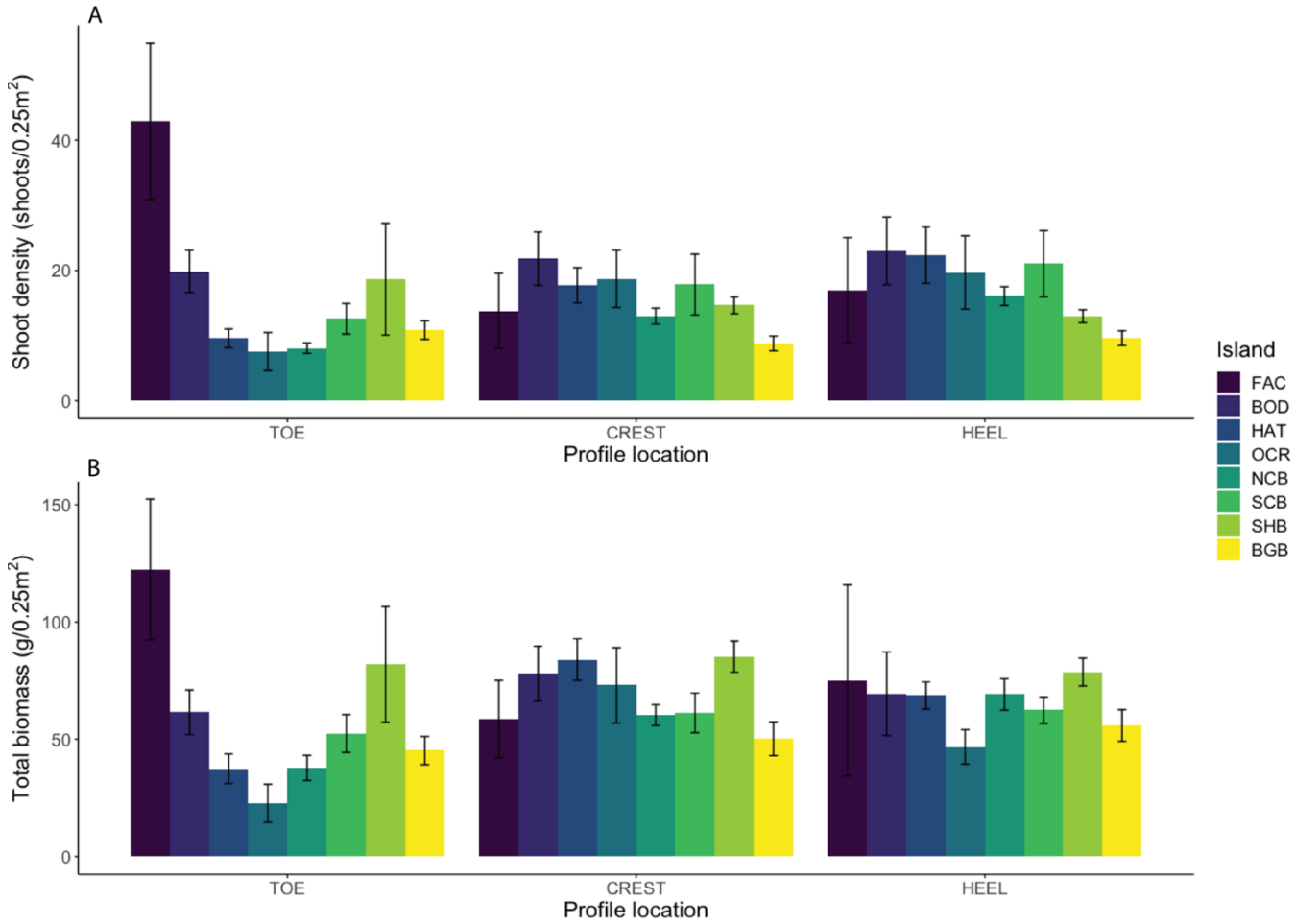

Figure 4.4. Mean (± SE) (A) shoot density (shoots/0.25 m^2) and (B) biomass (g/0.25 m^2) for the four dominant Outer Banks dune grass species [*Uniola paniculata* (UNPA), *Ammophila breviligulata* (AMBR), *Panicum amarum* (PAAM), and *Spartina patens* (SPPA)] at each foredune profile location (toe, crest, and heel) and island (listed north to south) on the Outer Banks barrier islands, USA (see Figure 4.1, Appendix G, Table G1 for island abbreviations and locations). See Table 4.2 for statistics.

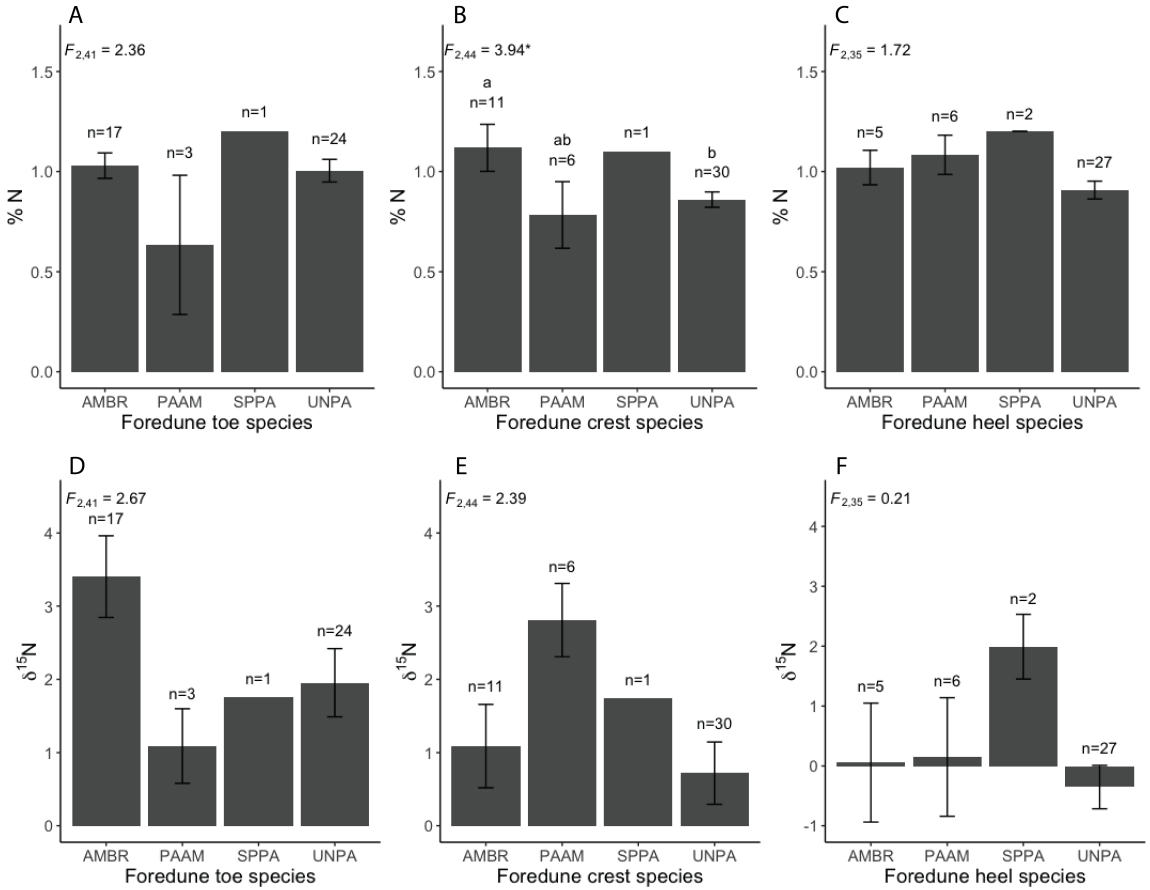

Figure 4.5. Mean (± SE) foliar nitrogen metrics (%N and ∂^{15}N) for each of the four dominant Outer Banks dune grass species [*Uniola paniculata* (UNPA), *Ammophila breviligulata* (AMBR), *Panicum amarum* (PAAM), and *Spartina patens* (SPPA)] at each foredune profile location. A) %N at the foredune toe. (B) %N at the foredune crest. (C) %N at the foredune heel. (D) ∂^{15}N at the foredune toe. (E) ∂^{15}N at the foredune crest. (F) ∂^{15}N at the foredune heel. Sample sizes and one-way ANOVA results are given in each plot, and bars that do not share letters indicate significant differences (Tukey's HSD post hoc test). * $p < 0.05$. *Spartina patens* was not included in statistical analyses due to its low sample size.

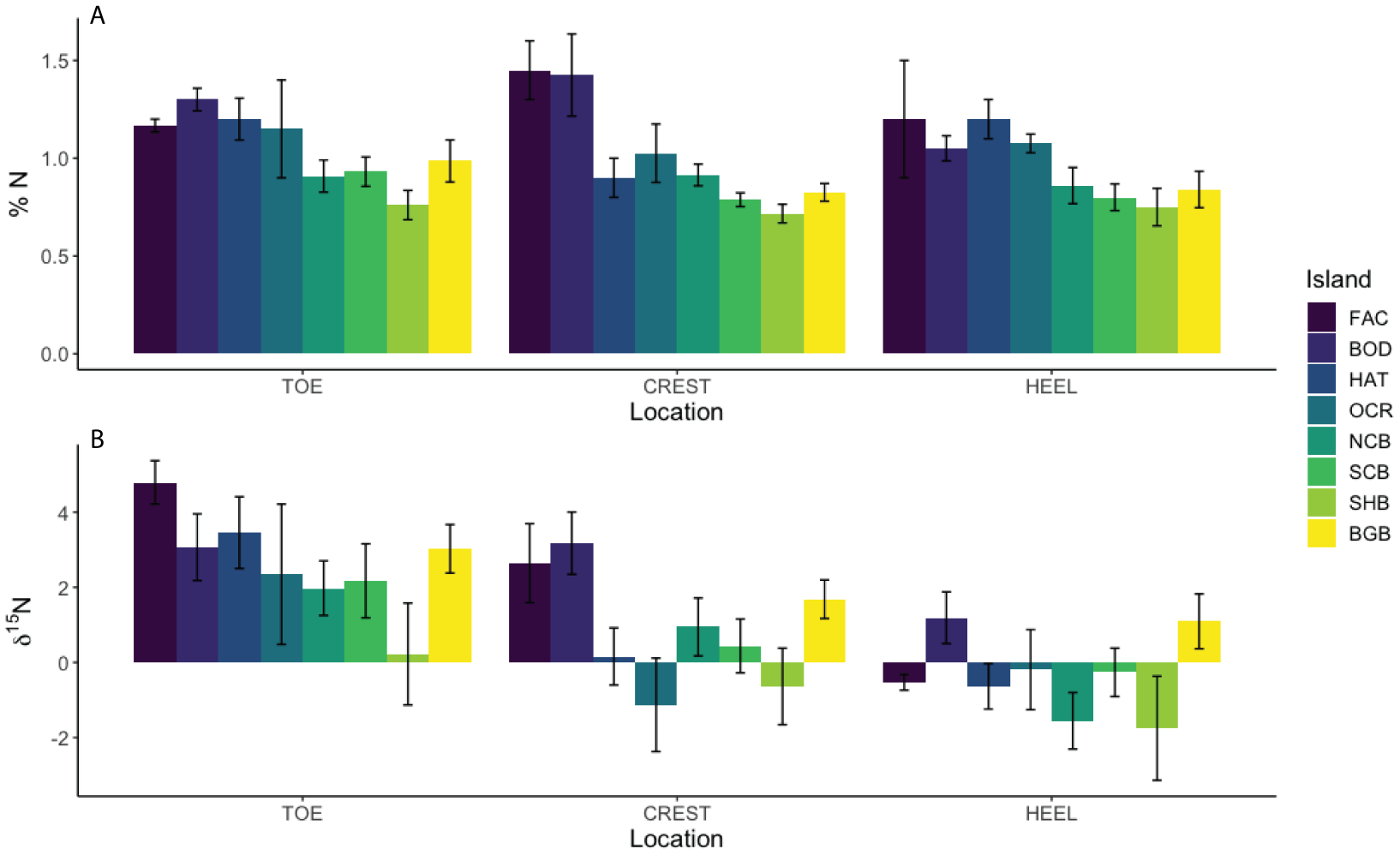

Figure 4.6. Mean (± SE) (A) %N and (B) ∂^{15}N for *Uniola paniculata* (UNPA) and *Ammophila breviligulata* (AMBR) combined at each foredune profile location (toe, crest, and heel) and island (listed north to south) on the Outer Banks barrier islands, USA (see Figure 4.1, Appendix G, Table G1 for island abbreviations and locations). See Table 4.3 for statistics.

4.7 References

Aguilar, C., M. Fogel, and H. Paerl. 1999. Dynamics of atmospheric combined inorganic nitrogen utilization in the coastal waters off North Carolina. Marine Ecology Progress Series 180:65–79.

Balthis, L., J. Hyland, C. Cooksey, M. Fulton, E. Wirth, I. Hartwell, E. Johnson, K. Kimbrough, M. Harmon, J. Hameedi, B. Gottholm, G. Lauenstein, and E. Long. 2019. National Centers for Coastal Ocean Science (NCCOS) long-term monitoring: Regional Ecological Assessments and National Benthic Inventory (NCEI Accession 0202842). NOAA National Centers for Environmental Information.

Barbier, E. B., S. D. Hacker, C. Kennedy, E. W. Koch, A. C. Stier, and B. R. Silliman. 2011. The value of estuarine and coastal ecosystem services. Ecological Monographs 81:169–193.

Barreiro, F., M. Gómez, J. López, M. Lastra, and R. de la Huz. 2013. Coupling between macroalgal inputs and nutrients outcrop in exposed sandy beaches. Hydrobiologia 700:73–84.

Barrett, K., W. B. Anderson, D. A. Wait, L. L. Grismer, G. A. Polis, and M. D. Rose. 2005. Marine subsidies alter the diet and abundance of insular and coastal lizard populations. Oikos 109:145–153.

Bartels, P., J. Cucherousset, K. Steger, P. Eklöv, L. J. Tranvik, and H. Hillebrand. 2012. Reciprocal subsidies between freshwater and terrestrial ecosystems structure consumer resource dynamics. Ecology 93:1173–1182.

Beaumont, N. J., L. Jones, A. Garbutt, J. D. Hansom, and M. Toberman. 2014. The value of carbon sequestration and storage in coastal habitats. Estuarine, Coastal and Shelf Science 137:32–40.

Biel, R. G., S. D. Hacker, and P. Ruggiero. 2019. Elucidating coastal foredune ecomorphodynamics in the U.S. Pacific Northwest via Bayesian Networks. Journal of Geophysical Research: Earth Surface 124:1919–1938.

Biel, R. G., S. D. Hacker, P. Ruggiero, N. Cohn, and E. W. Seabloom. 2017. Coastal protection and conservation on sandy beaches and dunes: context-dependent tradeoffs in ecosystem service supply. Ecosphere 8:e01791.

Bonanomi, G., A. Esposito, and S. Mazzoleni. 2012. Plant-soil feedback in herbaceous species of Mediterranean coastal dunes. Biological Letters 49:35–44.

Brown, J. K., and J. C. Zinnert. 2018. Mechanisms of surviving burial: Dune grass interspecific differences drive resource allocation after sand deposition. Ecosphere 9:e02162.

Brown, J. K., and J. C. Zinnert. 2021. Trait-based investigation reveals patterns of community response to nutrient enrichment in coastal mesic grassland. Diversity 13:19.

Bryant, M. A., T. J. Hesser, and R. E. Jensen. 2016. Evaluation statistics computed for the Wave Information Studies (WIS). U.S. Army Engineer Research and Development Center, Vicksburg, MS, USA.

Cardona, L., and M. García. 2008. Beach-cast seagrass material fertilizes the foredune vegetation of Mediterranean coastal dunes. Acta Oecologica 34:97–103.

Charbonneau, B. R., S. M. Dohner, J. P. Wnek, D. Barber, P. Zarnetske, and B. B. Casper. 2021. Vegetation effects on coastal foredune initiation: Wind tunnel experiments and field validation for three dune-building plants. Geomorphology 378:107594.

Cohn, N., B. Hoonhout, E. Goldstein, S. De Vries, L. Moore, O. Durán Vinent, and P. Ruggiero. 2019. Exploring marine and aeolian controls on coastal foredune growth using a coupled numerical model. Journal of Marine Science and Engineering 7:13.

Colombini, I., and L. Chelazzi. 2003. Influence of marine allochthonous input on sandy beach communities. Pages 115–159 *in* R. N. Gibson and R. J. A. Atkinson, editors. Oceanography and Marine Biology, An Annual Review, Volume 41. CRC Press, Boca Raton, FL.

Constant, V. 2019. Coastal dunes as meta-ecosystems: Connecting marine subsidies to ecosystem functions on the U.S. Pacific Northwest coast. PhD dissertation, Oregon State University.

Craine, J. M., E. N. J. Brookshire, M. D. Cramer, N. J. Hasselquist, K. Koba, E. Marin-Spiotta, and L. Wang. 2015. Ecological interpretations of nitrogen isotope ratios of terrestrial plants and soils. Plant and Soil 396:1–26.

Darby, F. A., and R. E. Turner. 2008. Below- and aboveground biomass of *Spartina alterniflora*: Response to nutrient addition in a Louisiana salt marsh. Estuaries and Coasts 31:326–334.

Day, F. P., C. Conn, E. Crawford, and M. Stevenson. 2004. Long-term effects of nitrogen fertilization on plant community structure on a coastal barrier island dune chronosequence. Journal of Coastal Research 20:722–730.

Del Vecchio, S., T. Jucker, M. Carboni, and A. T. R. Acosta. 2017. Linking plant communities on land and at sea: The effects of *Posidonia oceanica* wrack on the structure of dune vegetation. Estuarine, Coastal and Shelf Science 184:30–36.

Del Vecchio, S., N. Marbà, A. Acosta, C. Vignolo, and A. Traveset. 2013. Effects of *Posidonia oceanica* beach-cast on germination, growth and nutrient uptake of coastal dune plants. PLOS ONE 8:e70607.

Dilustro, J. J., and F. P. Day. 1997. Aboveground biomass and net primary production along a Virginia barrier island dune chronosequence. The American Midland Naturalist 137:27–38.

Dolan, R., and H. Lins. 1985. The Outer Banks of North Carolina. U.S. Geological Survey, Washington, DC.

Drius, M., M. L. Carranza, A. Stanisci, and L. Jones. 2016. The role of Italian coastal dunes as carbon sinks and diversity sources. A multi-service perspective. Applied Geography 75:127–136.

Dugan, J. E., D. M. Hubbard, M. D. McCrary, and M. O. Pierson. 2003. The response of macrofauna communities and shorebirds to macrophyte wrack subsidies on exposed sandy beaches of southern California. Estuarine, Coastal and Shelf Science 58:25–40.

Dugan, J. E., D. M. Hubbard, H. M. Page, and J. P. Schimel. 2011. Marine macrophyte wrack inputs and dissolved nutrients in beach sands. Estuaries and Coasts 34:839–850.

Duran, O., and L. J. Moore. 2013. Vegetation controls on the maximum size of coastal dunes. Proceedings of the National Academy of Sciences 110:17217–17222.

van Egmond, E. M., P. M. van Bodegom, J. R. van Hal, R. S. P. van Logtestijn, R. A. Broekman, M. P. Berg, and R. Aerts. 2019. Growth of pioneer beach plants is strongly driven by buried macroalgal wrack, whereas macroinvertebrates affect plant nutrient dynamics. Journal of Experimental Marine Biology and Ecology 514–515:87–94.

Ehrenfeld, J. G. 1990. Dynamics and processes of barrier island vegetation. Reviews in Aquatic Sciences 2:437–480.

Elser, J. J., W. F. Fagan, A. J. Kerkhoff, N. G. Swenson, and B. J. Enquist. 2010. Biological stoichiometry of plant production: metabolism, scaling and ecological response to global change. The New Phytologist 186:593–608.

Farris, A. S., and J. H. List. 2007. Shoreline change as a proxy for subaerial beach volume change. Journal of Coastal Research 23:740–748.

Fox, J., M. Friendly, and G. Monette. 2018. heplots: visualizing tests in multivariate linear models. https://CRAN.R-project.org/package=heplots.

Godfrey, P. J. 1977. Climate, plant response and development of dunes on barrier beaches along the U.S. East Coast. International Journal of Biometeorology 21:203–215.

Goldstein, E. B., L. J. Moore, and O. Durán Vinent. 2017. Lateral vegetation growth rates exert control on coastal foredune hummockiness and coalescing time. Earth Surface Dynamics 5:417–427.

Goldstein, E. B., E. V. Mullins, L. J. Moore, R. G. Biel, J. K. Brown, S. D. Hacker, K. R. Jay, R. S. Mostow, P. Ruggiero, and J. C. Zinnert. 2018. Literature-based latitudinal distribution and possible range shifts of two US east coast dune grass species (*Uniola paniculata* and *Ammophila breviligulata*). PeerJ 6:e4932.

Gómez, M., F. Barreiro, J. López, and M. Lastra. 2018. Effect of upper beach macrofauna on nutrient cycling of sandy beaches: metabolic rates during wrack decay. Marine Biology 165:133.

Hacker, S. D., K. R. Jay, N. Cohn, E. B. Goldstein, P. A. Hovenga, M. Itzkin, L. J. Moore, R. S. Mostow, E. V. Mullins, and P. Ruggiero. 2019a. Species-specific functional morphology of four US Atlantic Coast dune grasses: Biogeographic implications for dune shape and coastal protection. Diversity 11:1–16.

Hacker, S. D., B. A. Menge, K. J. Nielsen, F. Chan, and T. C. Gouhier. 2019b. Regional processes are stronger determinants of rocky intertidal community dynamics than local biotic interactions. Ecology 100:e02763.

Hacker, S. D., P. Zarnetske, E. Seabloom, P. Ruggiero, J. Mull, S. Gerrity, and C. Jones. 2012. Subtle differences in two non-native congeneric beach grasses significantly affect their colonization, spread, and impact. Oikos 121:138–148.

Hayduk, J. L., S. D. Hacker, J. S. Henderson, and F. Tomas. 2019. Evidence for regional-scale controls on eelgrass (Zostera marina) and mesograzer community structure in upwelling-influenced estuaries. Limnology and Oceanography 64:1120–1134.

Hesp, P. 2002. Foredunes and blowouts: initiation, geomorphology and dynamics. Geomorphology 48:245–268.

Hesp, P. A., and I. J. Walker. 2013. Aeolian environments: coastal dunes. Pages 109–133 *in* J. Shroder, N. Lancaster, D. J. Sherman, and A. C. W. Baas, editors. Treatise on Geomorphology. Academic Press, San Diego, CA.

Hessing-Lewis, M. L., and S. D. Hacker. 2013. Upwelling-influence, macroalgal blooms, and seagrass production; temporal trends from latitudinal and local scales in northeast Pacific estuaries. Limnology and Oceanography 58:1103–1112.

Högberg, P. 1997. Tansley Review No. 95 15N natural abundance in soil-plant systems. New Phytologist 137:179–203.

Hovenga, P. A., P. Ruggiero, N. Cohn, K. R. Jay, S. D. Hacker, M. Itzkin, and L. Moore. 2019. Drivers of dune evolution in Cape Lookout National Seashore, NC. Pages 1283–1296 Coastal Sediments 2019. World Scientific, Tampa/St. Petersburg, Florida, USA.

Hovenga, P. A., P. Ruggiero, E. B. Goldstein, S. D. Hacker, and L. J. Moore. 2021. The relative role of constructive and destructive processes in dune evolution on Cape Lookout National Seashore, North Carolina, USA. Earth Surface Processes and Landforms:esp.5210.

Jensen, D., K. C. Cavanaugh, M. Simard, G. S. Okin, E. Castañeda-Moya, A. McCall, and R. R. Twilley. 2019. Integrating imaging spectrometer and synthetic aperture radar data for estimating wetland vegetation aboveground biomass in coastal Louisiana. Remote Sensing 11:2533.

Jones, M. L. M., H. L. Wallace, D. Norris, S. A. Brittain, S. Haria, R. E. Jones, P. M. Rhind, B. R. Reynolds, and B. A. Emmett. 2004. Changes in Vegetation and Soil Characteristics in Coastal Sand Dunes along a Gradient of Atmospheric Nitrogen Deposition. Plant Biology 6:598–605.

Kachi, N., and T. Hirose. 1983. Limiting nutrients for plant growth in coastal sand dune soils. Journal of Ecology 71:937–944.

Keijsers, J. G. S., A. V. De Groot, and M. J. P. M. Riksen. 2015. Vegetation and sedimentation on coastal foredunes. Geomorphology 228:723–734.

Keijsers, J. G. S., A. V. De Groot, and M. J. P. M. Riksen. 2016. Modeling the biogeomorphic evolution of coastal dunes in response to climate change. Journal of Geophysical Research: Earth Surface 121:1161–1181.

Kooijman, A. M., and M. Besse. 2002. The higher availability of N and P in lime-poor than in lime-rich coastal dunes in the Netherlands. Journal of Ecology 90:394–403.

Kratzmann, M. G., E. A. Himmelstoss, and E. R. Thieler. 2017. National assessment of shoreline change – A GIS compilation of updated vector shorelines and associated shoreline change data for the Southeast Atlantic Coast. U.S. Geological Survey, Reston, VA, USA.

Lepoint, G., F. Nyssen, S. Gobert, P. Dauby, and J. Bouquegneau. 2000. Relative impact of a *Posidonia* seagrass bed and its adjacent epilithic algal community in consumer diet. Marine Biology 136:513–518.

Leroux, S. J., and M. Loreau. 2008. Subsidy hypothesis and strength of trophic cascades across ecosystems. Ecology Letters 11:1147–1156.

Loreau, M., and R. D. Holt. 2004. Spatial flows and the regulation of ecosystems. The American Naturalist 163:606–615.

Loreau, M., N. Mouquet, and R. D. Holt. 2003. Meta-ecosystems: a theoretical framework for a spatial ecosystem ecology. Ecology Letters 6:673–679.

Mallin, M. A., J. M. Burkholder, L. B. Cahoon, and M. H. Posey. 2000. North and South Carolina coasts. Marine Pollution Bulletin 41:56–75.

Mannino, A., S. R. Signorini, M. G. Novak, J. Wilkin, M. A. M. Friedrichs, and R. G. Najjar. 2016. Dissolved organic carbon fluxes in the Middle Atlantic Bight: An integrated approach based on satellite data and ocean model products: DOC coastal fluxes and stocks. Journal of Geophysical Research: Biogeosciences 121:312–336.

Massol, F., D. Gravel, N. Mouquet, M. W. Cadotte, T. Fukami, and M. A. Leibold. 2011. Linking community and ecosystem dynamics through spatial ecology. Ecology Letters 14:313–323.

Menge, B. A., T. C. Gouhier, S. D. Hacker, F. Chan, and K. J. Nielsen. 2015. Are meta-ecosystems organized hierarchically? A model and test in rocky intertidal habitats. Ecological Monographs 85:213–233.

Menge, B. A., J. Lubchenco, M. E. S. Bracken, F. Chan, M. M. Foley, T. L. Freidenburg, S. D. Gaines, G. Hudson, C. Krenz, H. Leslie, D. N. L. Menge, R. Russell, and M. S. Webster. 2003. Coastal oceanography sets the pace of rocky intertidal community dynamics. Proceedings of the National Academy of Sciences 100:12229–12234.

Michelsen, A., C. Quarmby, D. Sleep, and S. Jonasson. 1998. Vascular plant 15N natural abundance in heath and forest tundra ecosystems is closely correlated with presence and type of mycorrhizal fungi in roots. Oecologia 115:406–418.

Miller, T. L., R. A. Morton, and A. H. Sallenger. 2005. National assessment of shoreline change – A GIS compilation of vector shorelines and associated shoreline change data for the U.S. Southeast Atlantic Coast. U.S. Geological Survey, Reston, VA, USA.

Montagano, L., S. J. Leroux, M.-A. Giroux, and N. Lecomte. 2019. The strength of ecological subsidies across ecosystems: a latitudinal gradient of direct and indirect impacts on food webs. Ecology Letters 22:265–274.

Moore, L. J., O. D. Vinent, and P. Ruggiero. 2016. Vegetation control allows autocyclic formation of multiple dunes on prograding coasts. Geology 44:559–562.

Mull, J., and P. Ruggiero. 2014. Estimating storm-induced dune erosion and overtopping along U.S. West Coast beaches. Journal of Coastal Research 298:1173–1187.

Mullins, E., L. J. Moore, E. B. Goldstein, T. Jass, J. Bruno, and O. D. Vinent. 2019. Investigating dune-building feedback at the plant level: Insights from a multispecies field experiment. Earth Surface Processes and Landforms 44:1734–1747.

Mulvaney, R. L. 1996. Nitrogen-Inorganic Forms. Pages 1123–1184 *in* D. L. Sparks, A. L. Page, P. A. Helmke, R. H. Loeppert, P. N. Soltanpoor, M. A. Tabatabai, C. T. Johnston, and M. E. Sumner, editors. Methods of Soil Analysis, Part 3, Chemical Methods. Soil Science Society of America, Madison, WI.

Oldham, C., K. McMahon, E. Brown, C. Bosserelle, and P. Lavery. 2014. A preliminary exploration of the physical properties of seagrass wrack that affect its offshore transport, deposition, and retention on a beach. Limnology and Oceanography: Fluids and Environments 4:120–135.

Paerl, H. W., N. S. Hall, A. G. Hounshell, R. A. Luettich, K. L. Rossignol, C. L. Osburn, and J. Bales. 2019. Recent increase in catastrophic tropical cyclone flooding in coastal North Carolina, USA: Long-term observations suggest a regime shift. Scientific Reports 9:10620.

Paerl, H. W., J. Rudek, and M. A. Mallin. 1990. Stimulation of phytoplankton production in coastal waters by natural rainfall inputs: Nutritional and trophic implications. Marine Biology 107:247–254.

Palumbi, S. R. 2003. Ecological subsidies alter the structure of marine communities. Proceedings of the National Academy of Sciences 100:11927–11928.

Polis, G. A., W. B. Anderson, and R. D. Holt. 1997. Toward in integration of landscape and food web ecology: The dynamics of spatially subsidized food webs. Annual Review of Ecology and Systematics 28:289.

Polis, G. A., and S. D. Hurd. 1996. Linking marine and terrestrial food webs: Allochthonous input from the ocean supports high secondary productivity on small islands and coastal land communities. The American Naturalist 147:396–423.

Psuty, N. P. 1986. A dune/beach interaction model and dune management. Thalassas 4:11–15.

R Development Core Team. 2019. R: a language and environment for statistical computing. R Foundation for Statistical Computing, Vienna, Austria. www.r-project.org.

Reimer, J., S. Hacker, B. Menge, and P. Ruggiero. 2018. Macrophyte wrack on sandy beaches of the US Pacific Northwest is linked to proximity of source habitat, ocean upwelling, and beach morphology. Marine Ecology Progress Series 594:263–269.

Rhymes, J., H. Wallace, N. Fenner, and L. Jones. 2014. Evidence for sensitivity of dune wetlands to groundwater nutrients. Science of The Total Environment 490:106–113.

Richardson, J. S., Y. Zhang, and L. B. Marczak. 2010. Resource subsidies across the land–freshwater interface and responses in recipient communities. River Research and Applications 26:55–66.

Ripley, B. S., and N. W. Pammenter. 2008. Physiological characteristics of coastal dune pioneer species from the Eastern Cape, South Africa, in relation to stress and disturbance. Pages 137–154 *in* M. L. Martínez and N. P. Psuty, editors. Coastal Dunes. Springer Berlin Heidelberg, Berlin, Heidelberg.

Ruggiero, P., S. Hacker, E. Seabloom, and P. Zarnetske. 2018. The role of vegetation in determining dune morphology, exposure to sea-level rise, and storm-induced coastal hazards: A U.S. Pacific Northwest perspective. Pages 337–361 *in* L. J. Moore and A. B. Murray, editors. Barrier Dynamics and Response to Changing Climate. Springer International Publishing, Cham.

Ruggiero, P., G. M. Kaminsky, G. Gelfenbaum, and N. Cohn. 2016. Morphodynamics of prograding beaches: A synthesis of seasonal- to century-scale observations of the Columbia River littoral cell. Marine Geology 376:51–68.

Ruggiero, P., P. D. Komar, W. G. McDougal, J. J. Marra, and R. A. Beach. 2001. Wave runup, extreme water levels and the erosion of properties backing beaches. Journal of Coastal Research 17:13.

Sallenger, A. H. 2000. Storm impact scale for barrier islands. Journal of Coastal Research 16:7.

Sallenger, A. H., K. S. Doran, and P. A. Howd. 2012. Hotspot of accelerated sea-level rise on the Atlantic coast of North America. Nature Climate Change 2:884–888.

Savidge, D. K. 2004. Gulf Stream meander propagation past Cape Hatteras. Journal of Physical Oceanography 34:2073–2085.

Seabloom, E. W., P. Ruggiero, S. D. Hacker, J. Mull, and P. Zarnetske. 2013. Invasive grasses, climate change, and exposure to storm-wave overtopping in coastal dune ecosystems. Global Change Biology 19:824–832.

Seneca, E. D. 1969. Germination response to temperature and salinity of four dune grasses from the Outer Banks of North Carolina. Ecology 50:45–53.

Sherman, D. J., and B. O. Bauer. 1993. Dynamics of beach-dune systems. Progress in Physical Geography: Earth and Environment 17:413–447.

Short, A. D., and P. A. Hesp. 1982. Wave, beach and dune interactions in southeastern Australia. Marine Geology 48:259–284.

Spiller, D. A., J. Piovia-Scott, A. N. Wright, L. H. Yang, G. Takimoto, T. W. Schoener, and T. Iwata. 2010. Marine subsidies have multiple effects on coastal food webs. Ecology 91:1424–1434.

Sterner, R. W., and J. J. Elser. 2002. Ecological Stoichiometry: The Biology of Elements from Molecules to the Biosphere. Princeton University Press, Princeton, New Jersey.

Stockdon, H. F., A. H. Sallenger, R. A. Holman, and P. A. Howd. 2007. A simple model for the spatially-variable coastal response to hurricanes. Marine Geology 238:1–20.

Underwood, A. J. 1997. Experiments in ecology: Their logical design and interpretation using analysis of variance. Cambridge University Press.

van der Valk, A. G. 1974. Mineral cycling in coastal foredune plant communities in Cape Hatteras National Seashore. Ecology 55:1349–1358.

Willis, A. J. 1963. Braunton Burrows: The effects on the vegetation of the addition of mineral nutrients to the dune soils. Journal of Ecology 51:353–374.

Woodhouse, W. W., E. D. Seneca, and S. W. Broome. 1977. Effect of species on dune grass growth. International Journal of Biometeorology 21:256–266.

Wright, L. D., and A. D. Short. 1984. Morphodynamic variability of surf zones and beaches: a synthesis 56:93–118.

Zarnetske, P. L., S. D. Hacker, E. W. Seabloom, P. Ruggiero, J. R. Killian, T. B. Maddux, and D. Cox. 2012. Biophysical feedback mediates effects of invasive grasses on coastal dune shape. Ecology 93:1439–1450.

Zarnetske, P. L., P. Ruggiero, E. W. Seabloom, and S. D. Hacker. 2015. Coastal foredune evolution: the relative influence of vegetation and sand supply in the US Pacific Northwest. Journal of The Royal Society Interface 12:20150017.

Chapter 5 – Conclusion

As environmental changes compound the challenges of understanding the complex physical and ecological processes that govern coastal interface habitats, interdisciplinary approaches to these problems are particularly necessary. In this dissertation, I integrated knowledge and techniques from community ecology, coastal geomorphology, biogeochemistry, and statistics to explore how dune grasses, sand supply, and beach and dune geomorphology, and marine subsidies interact to influence foredune ecosystem functions and services across U.S. Central Atlantic Coast dune ecosystems.

In Chapter 2, I investigated the patterns in vegetation density, beach geomorphology, shoreline change rate, and foredune shape along the North Carolina Outer Banks and quantified the relative roles of physical and ecological factors in shaping foredunes in space and time. I found that proxies for sand supply to the foredune (i.e., shoreline change rate, beach width, and backshore slope) and vegetation density were associated with foredune morphology and its changes over annual time scales, but their relative importance varied depending on the timescale and the foredune morphology metric. Physical factors were most important, comprising 72-90% of the explained variance, while grass density explained a smaller proportion of the variance (10-28%). However, grass density metrics were more important when changes in foredune morphology were considered (36-50% of explained variance). I found that change in *A. breviligulata* density was the most important vegetation signal; specifically, an increase in *A. breviligulata* density was

related to an increase in foredune width. This finding corroborates the results of previous research indicating that the lateral growth form of *A. breviligulata* has important implications for foredune morphology (Hacker et al. 2012, 2019a, Zarnetske et al. 2012, 2015, Biel et al. 2019). As the first study to quantify the relative contributions of physical and ecological factors to foredune morphology on the U.S. Atlantic Coast, this research provides a foundation for investigating how future climate-driven changes in dune grass distributions, sea level, and frequency of extreme storms may impact dune ecosystem services along a vulnerable coastline.

In Chapter 3, I quantified carbon storage in aboveground and belowground vegetation and sand in Outer Banks foredunes and explored variability in these stocks in relation to sand deposition and beach geomorphology. Carbon storage varied between aboveground grass (0.1 ± 0.1 kg C/m^2), belowground grass (1.1 ± 1.6 kg C/m^3), and sand (0.9 ± 0.6 kg C/m^3) carbon stocks, with the largest proportion contained in belowground grass stocks. Sand and aboveground carbon stocks varied at regional (island) and local (foredune profile locations) scales, with values generally increasing from north to south along the Outer Banks and in the landward direction along the foredune. Regression models revealed that variability in sand carbon density was related to patterns in dune sand deposition and grass density, with the relative importance of these factors varying among islands and foredune profile locations. Islands with high sand deposition and high grass density tended to have low sand carbon density, while profile locations with lower sand deposition and higher grass density tended to have high sand carbon density, demonstrating that self-

reinforcing feedbacks between vegetation and sand determine foredune carbon storage. My findings represent the first comprehensive inventory of coastal foredune carbon storage in North America and enhance our understanding of the carbon storage ecosystem service in understudied coastal dune ecosystems.

Finally, in Chapter 4, I asked whether dune grasses utilize marine-derived nutrients and examined the role of marine nutrient subsidies, beach and foredune morphology, and sand supply in shaping dune grass production and foliar nitrogen metrics. I found that dune grasses growing closer to the beach were enriched in marine nitrogen (^{15}N) compared with those growing on the landward side of the foredune. Foliar nitrogen content (%N) and source ($\delta^{15}N$) both varied among islands but %N did not vary across the foredune profile. Moreover, proxies for sand supply and marine subsidies both influenced dune grass production and foliar nitrogen metrics. Dune grass production and foliar %N were greater in areas with higher sand nitrate concentration, taller foredunes, and eroding beaches, while foliar $\delta^{15}N$ levels increased with foredune height and sand supply. These findings add to the growing body of literature supporting the hypothesis that marine nutrients subsidize foredune vegetation (Cardona and García 2008, Del Vecchio et al. 2013, 2017, Constant 2019, van Egmond et al. 2019) and suggest that differences in sand nitrogen and sand supply on beaches mediate the amount and delivery of marine subsidies to foredunes.

Overall, my findings elucidate the processes that shape foredunes, their vegetation, and their carbon storage capacity along the U.S. Central Atlantic coastline, which is highly vulnerable to coastal erosion and sea level rise.

Understanding how dunes are modified by physical and ecological processes, as well as human-induced changes, will allow us to better predict how their accompanying services may be altered and help inform efforts to manage these critical ecosystems.

5.1 References

Biel, R. G., S. D. Hacker, and P. Ruggiero. 2019. Elucidating coastal foredune ecomorphodynamics in the U.S. Pacific Northwest via Bayesian Networks. Journal of Geophysical Research: Earth Surface 124:1919–1938.

Cardona, L., and M. García. 2008. Beach-cast seagrass material fertilizes the foredune vegetation of Mediterranean coastal dunes. Acta Oecologica 34:97–103.

Constant, V. 2019. Coastal dunes as meta-ecosystems: Connecting marine subsidies to ecosystem functions on the U.S. Pacific Northwest coast. PhD dissertation, Oregon State University.

Del Vecchio, S., T. Jucker, M. Carboni, and A. T. R. Acosta. 2017. Linking plant communities on land and at sea: The effects of *Posidonia oceanica* wrack on the structure of dune vegetation. Estuarine, Coastal and Shelf Science 184:30–36.

Del Vecchio, S., N. Marbà, A. Acosta, C. Vignolo, and A. Traveset. 2013. Effects of *Posidonia oceanica* beach-cast on germination, growth and nutrient uptake of coastal dune plants. PLOS ONE 8:e70607.

van Egmond, E. M., P. M. van Bodegom, J. R. van Hal, R. S. P. van Logtestijn, R. A. Broekman, M. P. Berg, and R. Aerts. 2019. Growth of pioneer beach plants is strongly driven by buried macroalgal wrack, whereas macroinvertebrates affect plant nutrient dynamics. Journal of Experimental Marine Biology and Ecology 514–515:87–94.

Hacker, S. D., K. R. Jay, N. Cohn, E. B. Goldstein, P. A. Hovenga, M. Itzkin, L. J. Moore, R. S. Mostow, E. V. Mullins, and P. Ruggiero. 2019. Species-specific functional morphology of four US Atlantic Coast dune grasses: Biogeographic implications for dune shape and coastal protection. Diversity 11:1–16.

Hacker, S. D., P. Zarnetske, E. Seabloom, P. Ruggiero, J. Mull, S. Gerrity, and C. Jones. 2012. Subtle differences in two non-native congeneric beach grasses significantly affect their colonization, spread, and impact. Oikos 121:138–148.

Zarnetske, P. L., S. D. Hacker, E. W. Seabloom, P. Ruggiero, J. R. Killian, T. B. Maddux, and D. Cox. 2012. Biophysical feedback mediates effects of invasive grasses on coastal dune shape. Ecology 93:1439–1450.

Zarnetske, P. L., P. Ruggiero, E. W. Seabloom, and S. D. Hacker. 2015. Coastal foredune evolution: the relative influence of vegetation and sand supply in the US Pacific Northwest. Journal of The Royal Society Interface 12:20150017.

Appendices

Appendix A Chapter 2: Supplemental Table for Transect Sampling Locations

Table A1. Latitude and longitude of transects surveyed, from False Cape, Virginia in the north to Shackleford Banks, North Carolina in the south (see Figure 2.1). Asterisks indicate transects adjacent to inlets and capes that were removed prior to statistical analysis. Island abbreviations are as described in Figure 2.1.

Island	Transect Name	Latitude	Longitude	Distance to neighboring transect (km; S or W)
False Cape	FAC_4*	36.6276652	-75.889766	3
	FAC_3	36.6017811	-75.879916	1.8
	FAC_2	36.5860808	-75.875638	3.8
	FAC_1	36.5524759	-75.868308	3.6
Bodie Island	BOD_10	36.5201078	-75.8620715	4.5
	BOD_9	36.4800983	-75.8529037	8.9
	BOD_8	36.4021958	-75.83065	13.6
	BOD_7	36.282266	-75.7938133	11.4
	BOD_6	36.1854457	-75.7521485	0.7
	BOD_5	36.1792965	-75.749355	11.6
	BOD_4	36.0828711	-75.7003949	10
	BOD_3	36.002747	-75.6486079	20.4
	BOD_2	35.8344112	-75.5582271	4.6
	BOD_1*	35.7958095	-75.540219	3.5
Pea Island	PEA_3*	35.768445	-75.5204608	3.2
	PEA_2	35.7431869	-75.5042115	3.5
	PEA_1	35.7131589	-75.4913202	5
Hatteras Island	HAT_13	35.6698157	-75.4777052	5.1
	HAT_12	35.6242763	-75.4683802	9.8
	HAT_11	35.5365675	-75.4669414	7.3

Table A1. (Continued)				
	HAT_10	35.4729693	-75.481195	7.4
	HAT_9	35.40673	-75.4858532	5
	HAT_8	35.3622823	-75.4971147	5
	HAT_7	35.3181785	-75.5080946	4.9
	HAT_6	35.2747138	-75.5174755	5.4
	HAT_5	35.226518	-75.5284563	4.5
	HAT_4	35.2346899	-75.5768313	4.8
	HAT_3	35.2277451	-75.6286256	5.1
	HAT_2	35.2123191	-75.6816534	4.4
	HAT_1*	35.1972224	-75.7268737	5
Ocracoke Island	OCR_5*	35.1816654	-75.7779723	8.3
	OCR_4	35.1510415	-75.8608008	5.6
	OCR_3	35.1267793	-75.9147228	4.5
	OCR_2	35.1049833	-75.9559919	4
	OCR_1*	35.0826812	-75.9899732	6
North Core Banks	NCB_22*	35.0530517	-76.0447896	5.2
	NCB_21	35.0270573	-76.0916687	0.9
	NCB_20	35.0216145	-76.0989634	1
	NCB_19	35.015843	-76.1066362	1.2
	NCB_18	35.0085828	-76.1167294	0.8
	NCB_17	35.0040006	-76.123335	1.1
	NCB_16	34.9969761	-76.131801	0.9
	NCB_15	34.9912825	-76.1391699	1.1
	NCB_14	34.9843826	-76.1478347	1
	NCB_13	34.9781301	-76.1559868	1
	NCB_12	34.972267	-76.163924	1

Table A1. (Continued)				
	NCB_11	34.9663064	-76.1720108	0.9
	NCB_10	34.9606305	-76.1794134	1.1
	NCB_9	34.95371	-76.1881125	1.1
	NCB_8	34.9470608	-76.1962458	0.9
	NCB_7	34.9411404	-76.2033866	1
	NCB_6	34.9346253	-76.2111514	2
	NCB_5	34.9220592	-76.2261748	2.1
	NCB_4	34.9087018	-76.2422395	2.1
	NCB_3	34.896227	-76.2588123	0.9
	NCB_2	34.8912641	-76.2658907	1
	NCB_1*	34.8857374	-76.2738852	9
South Core Banks	SCB_20*	34.8306836	-76.3454967	1.5
	SCB_19*	34.8193753	-76.3545105	1.9
	SCB_18	34.8062837	-76.3675944	2.1
	SCB_17	34.7922181	-76.3822877	2
	SCB_16	34.7785368	-76.3956676	1.6
	SCB_15	34.7665769	-76.405443	2.4
	SCB_14	34.7495076	-76.4213716	2.1
	SCB_13	34.7344208	-76.4350908	1.9
	SCB_12	34.7201798	-76.4472372	2.1
	SCB_11	34.7048951	-76.4605842	2
	SCB_10	34.6898346	-76.4734951	1.9
	SCB_9	34.6755438	-76.4850783	2
	SCB_8	34.6607904	-76.4970186	2.1
	SCB_7	34.6443710	-76.5071979	2
	SCB_6	34.6281112	-76.5170870	2.1

Table A1. (Continued)				
	SCB_5	34.6115026	-76.5274718	2
	SCB_4*	34.5945781	-76.5343936	0.4
	SCB_3	34.5927095	-76.5375693	1.8
	SCB_2	34.6065351	-76.5473031	1.9
	SCB_1	34.6222448	-76.5542065	1
	SCB_0*	34.6306684	-76.5554503	1.75
Shackleford Banks	SHB_12*	34.6340256	-76.5369748	1.1
	SHB_11*	34.6417083	-76.5437355	1
	SHB_10	34.6485386	-76.5512356	1
	SHB_9	34.6537058	-76.5604061	1.1
	SHB_8	34.658427	-76.5706677	1
	SHB_7	34.6621783	-76.5799107	1.1
	SHB_6	34.6657629	-76.5906425	1
	SHB_5	34.6688427	-76.601124	1
	SHB_4	34.6717272	-76.6115413	1
	SHB_3	34.6742112	-76.6224491	1.1
	SHB_2	34.6765883	-76.6335074	1
	SHB_1*	34.6792183	-76.643726	3.6

Appendix B Chapter 2: Supplemental Figures and Tables for Summary of Results

Table B1. Results from linear regression analyses showing top models for each response variable. Top models were chosen using ΔAIC within 4 (except see below). Explanatory variables included together in models were uncorrelated with Pearson correlation coefficient < |0.6|. Significance codes for explanatory variables are: ***p<0.001, **p<0.01, *p<0.05, .p<0.1. Response variable transformations were applied following Shapiro–Wilk tests for normality and residual investigations. Transects adjacent to inlets and capes were removed prior to analysis (n=15; see Appendix A, Table A1), with 75 transects remaining for the analysis. The two models in italics do not fit top model criteria (ΔAIC within 4) but were included due to their high R^2 values (relative to top models) and to show significant relationships between the variables.

Response variable	Linear model	Model results
Foredune height	[ln(DuneHt)] = 0.087[Multi_SCR]*** - 9.707[Backshore_slope]*** - 0.011[Beach_width]** + 0.381[Beach_width: Backshore_slope]*** + 1.962***	AIC: -5.06 ΔAIC=0 df=63 R^2=0.49
Foredune height	*[ln(DuneHt)] = 0.099[Multi_SCR]*** - 0.010[AMBR_chg]*** + 0.003[Beach_width] + 0.005[AMBR_chg:Multi SCR]* + 1.582****	*AIC: 1.58* *ΔAIC=6.64* *df=64* *R^2=0.44*
Foredune width	[ln(DuneWidth)] = 0.104[LT_SCR]** - 0.008[AMBR_chg]* + 2.094[Foreshore_slope] + 0.009[Beach_width]** + 2.083***	AIC: 82 ΔAIC=0 df=63 R^2=0.40
Foredune width	[ln(DuneWidth)] = 0.109[Multi_SCR]** + 2.681[Foreshore_slope]. + 0.009[Beach_width]* + 2.080***	AIC: 84.23 ΔAIC=2.23 df=64 R^2=0.36
Foredune width	[ln(DuneWidth)] = 0.163[Multi_SCR]*** + 2.633[Foreshore_slope]. + 2.449***	AIC: 85.42 ΔAIC=3.42 df=68 R^2= 0.28
Foredune toe elevation	[ln(DuneToeElev)] = -0.003[AMBR_chg]. + 2.314[Backshore_slope]* + 0.66***	AIC: -24.64 ΔAIC=0 df=67 R^2=0.13

Table B1.	(Continued)	
Foredune toe elevation	[ln(DuneToeElev)] = 0.025[Multi_SCR]. - 0.003[AMBR_chg]. + 2.494[Backshore_slope]* + 0.666***	AIC: -24.36 ΔAIC=0.28 df=65 R^2=0.17
Foredune height change	[ln(DuneHtChg)] = 0.003[AMBR_chg] – 2.424[Backshore_slope]* + 0.194**	AIC: -9.02 ΔAIC=0 df = 66 R^2=0.12
Foredune height change	[ln(DuneHtChg)] = – 2.851[Backshore_slope]* + 0.205**	AIC: -8.38 ΔAIC=0.64 df=67 R^2=0.08
Foredune width change	DuneWidthChg = 0.082[Annual_SCR] + 0.108[AMBR_chg]* + 0.039[Beach_width] + 2.289	AIC: 414.31 ΔAIC=0 df=64 R^2=0.14
Foredune width change	DuneWidthChg = 0.079[Annual_SCR] + 0.102[AMBR_chg]* + 12.148[Backshore_slope] + 0.212	AIC: 416.29 ΔAIC=1.98 df=64 R^2=0.11
Foredune toe elevation change	[((DuneToeElevChg + 2)^2 – 1)/2] = -0.222[Multi_SCR]** - 0.026[AMBR_chg]** + 0.019[Beach_width]** + 1.01**	AIC: 193.21 ΔAIC=0 df=67 R^2=0.22
Foredune toe elevation change	[((DuneToeElevChg + 2)^2 – 1)/2] = -0.023[AMBR_chg]** - 1.526[Backshore_slope] + 1.979	AIC: 196.89 ΔAIC=3.68 df=66 R^2=0.10
Foredune aspect ratio	[ln(DuneAspectRatio)] = 4.299[Backshore_slope]. – 0.064[Multi_SCR]* – 1.165***	AIC: 78.08 ΔAIC=0 df=66 R^2=0.12
Foredune aspect ratio	[ln(DuneAspectRatio)] = 2.554[Backshore_slope] – 0.008[Beach_width]** – 0.769***	AIC: 79.12 ΔAIC=1.04 df=66 R^2=0.15
Foredune aspect ratio	*[ln(DuneAspectRatio)] = -0.009[Beach_width]** – 0.110[ln(mean_AMBR+1)]. – 0.528****	*AIC: 85.01* *ΔAIC=6.93* *df=67* *R^2=0.17*

Table B1.	(Continued)	
Foredune aspect ratio change	[DuneAspectRatioChg] = -0.004[Annual_SCR]* – 0.003[AMBR_chg]. + 0.009	AIC: -42.12 ΔAIC=0 df=68 R^2=0.12
Foredune aspect ratio change	[DuneAspectRatioChg] = -0.004[Annual_SCR]* + 0.017	AIC: -41.24 ΔAIC=0.88 df=69 R^2=0.08

Table B2. Results of hierarchical partitioning analyses for each explanatory variable, organized by foredune morphology response variables. Values indicate the independent contribution of each explanatory variable represented as a percent of total explained variance (see Figure 2.5b). Abbreviations are as follows: Multidecadal SCR = shoreline change rate (m yr^{-1}) from 1997-2016 for the southern Outer Banks (Shackleford Banks through North Core Banks) and from 1997-2010 for the northern Outer Banks (Ocracoke Island through False Cape); Annual SCR = shoreline change rate (m yr^{-1}) from 2016-17; AMBR tiller change = change in *Ammophila breviligulata* tiller number (tillers/transect) from 2016-17; UNPA tiller change = change in *Uniola paniculata* tiller number (tillers/transect) from 2016-17; Mean comb. grass density = mean density (tillers $0.25m^{-2}$) of *Ammophila breviligulata* and *Uniola paniculata* combined at each transect.

Response variable	**Multi-decadal SCR**	**Annual SCR**	**Back-shore slope**	**Fore-shore slope**	**Beach width**	**AMBR tiller change**	**UNPA tiller change**	**Mean comb. grass density**
Foredune height	40.6	4.7	3.5	7.4	20.3	9.2	3.2	11.1
Foredune height change	1.1	0.1	46.7	6.7	9.6	31.3	0.6	3.9
Foredune width	32.2	1.9	4.2	10.1	34.7	5.6	2.9	8.5
Foredune width change	8.9	15.0	2.3	0.6	23.8	43.9	2.4	3.2
Foredune toe elevation	20.8	6.9	33.0	8.6	2.0	21.3	5.8	1.6
Foredune toe elevation change	19.3	3.4	-0.1	5.2	25.0	34.3	6.1	6.8
Foredune aspect ratio	13.7	6.7	24.6	7.9	37.4	0.7	2.2	6.8
Foredune aspect ratio change	6.1	39.8	2.9	-4.4	7.3	29.8	16.8	2.0

Appendix C Chapter 3: Supplemental Tables and Figures for Sediment Core Locations and Foredune Profiles

Table C1. Island and transect names (north to south) (see Figure 3.1) and core latitude and longitude along the foredune profile (toe, crest, and heel; see Figure C1) on the Outer Banks barrier islands, North Carolina, USA. Transects are a subset of those surveyed in Hacker et al. (2019) and Jay et al. (Chapter 2; Appendix A, Table A1). Note that latitude and longitude is missing for NCB_15 toe as no core was collected there.

Island and abbreviation	Transect name	Core profile location	Core latitude	Core longitude
Bodie Island (BOD)	BOD_1	Toe	35.7958	-75.5402
		Crest	35.7957	-75.5404
		Heel	35.7957	-75.5406
Hatteras Island (HAT)	HAT_12	Toe	35.6242	-75.4685
		Crest	35.6242	-75.4686
		Heel	35.6242	-75.4688
	HAT_7	Toe	35.3182	-75.5082
		Crest	35.3182	-75.5084
		Heel	35.3182	-75.5086
	HAT_4	Toe	35.2348	-75.5768
		Crest	35.2350	-75.5768
		Heel	35.2351	-75.5768
Ocracoke Island (OCR)	OCR_1	Toe	35.0827	-75.9901
		Crest	35.0829	-75.9901
		Heel	35.0829	-75.9902
North Core Banks (NCB)	NCB_20	Toe	35.0217	-76.0990
		Crest	35.0218	-76.0991
		Heel	35.0219	-76.0992
	NCB_16	Toe	34.9970	-76.1319
		Crest	34.9971	-76.1320
		Heel	34.9973	-76.1322
	NCB_15	Toe	–	–
		Crest	34.9914	-76.1393
		Heel	34.9915	-76.1395
South Core Banks (SCB)	SCB_9	Toe	34.6755	-76.4849
		Crest	34.6755	-76.4850
		Heel	34.6755	-76.1581
	SCB_6	Toe	34.6281	-76.5170
		Crest	34.6281	-76.5170
		Heel	34.6282	-76.5172

Table C1. (Continued)

	SCB_4	Toe	34.5945	-76.5339
		Crest	34.5945	-76.5340
		Heel	34.5945	-76.5342

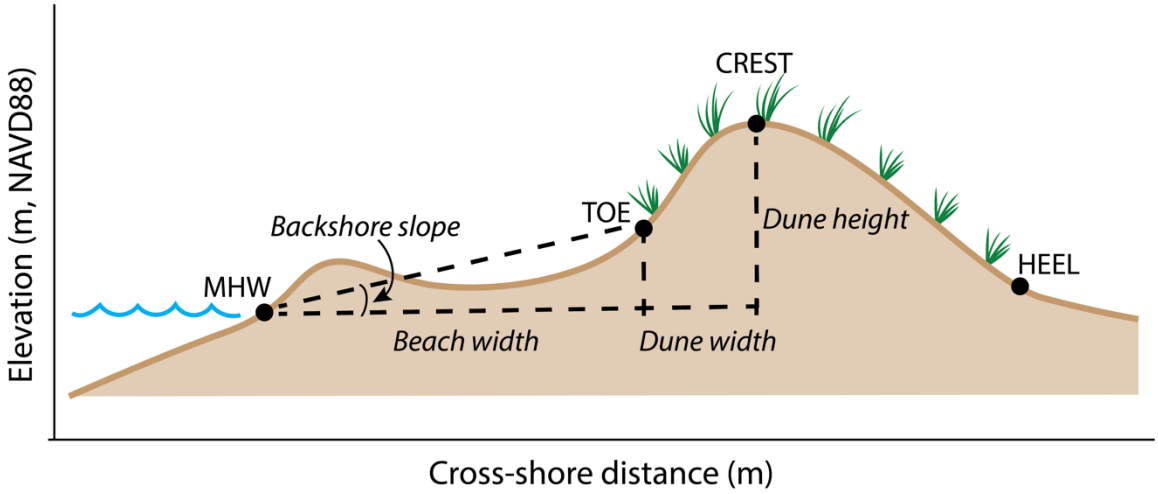

Figure C1. Beach and dune morphology parameters calculated using data from real-time kinematic GPS surveys and following the methods of Mull and Ruggiero (2014). MHW (or mean high water) was extracted using the 0.3 m MHW contour (NAVD88). Foredune morphology measurements included the position and elevation of the foredune toe (the seaward extent of the foredune), the foredune crest (the highest point on the foredune), and the foredune heel (the landward extent of the foredune, determined by an elevation minimum). Foredune height and toe elevation were calculated as the differences between MHW and foredune crest and toe elevation, respectively. Foredune width was calculated as one-half dune width (the horizontal distance between the foredune toe and crest) to capture changes in the width of the foredune face. Backshore slope was calculated as the slope between MHW and the dune toe. Beach width was calculated as the horizontal distance between MHW and the foredune toe. Figure adapted from Jay et al., Chapter 2 (see Figure 2.2).

Figure C2. Dune elevation profile plots from 2017-2019 for each transect surveyed on the Outer Banks barrier islands, North Carolina, USA, from north to south (see Figure 3.1 and Appendix C, Table C1 for profile locations and abbreviations). The colored lines denote the elevations from each year and the dots denote the locations where the cores were collected. All plots have the same y-axis scale. Note that the x-axis for HAT_4 is in northing (m) rather than easting due to the orientation of the transect.

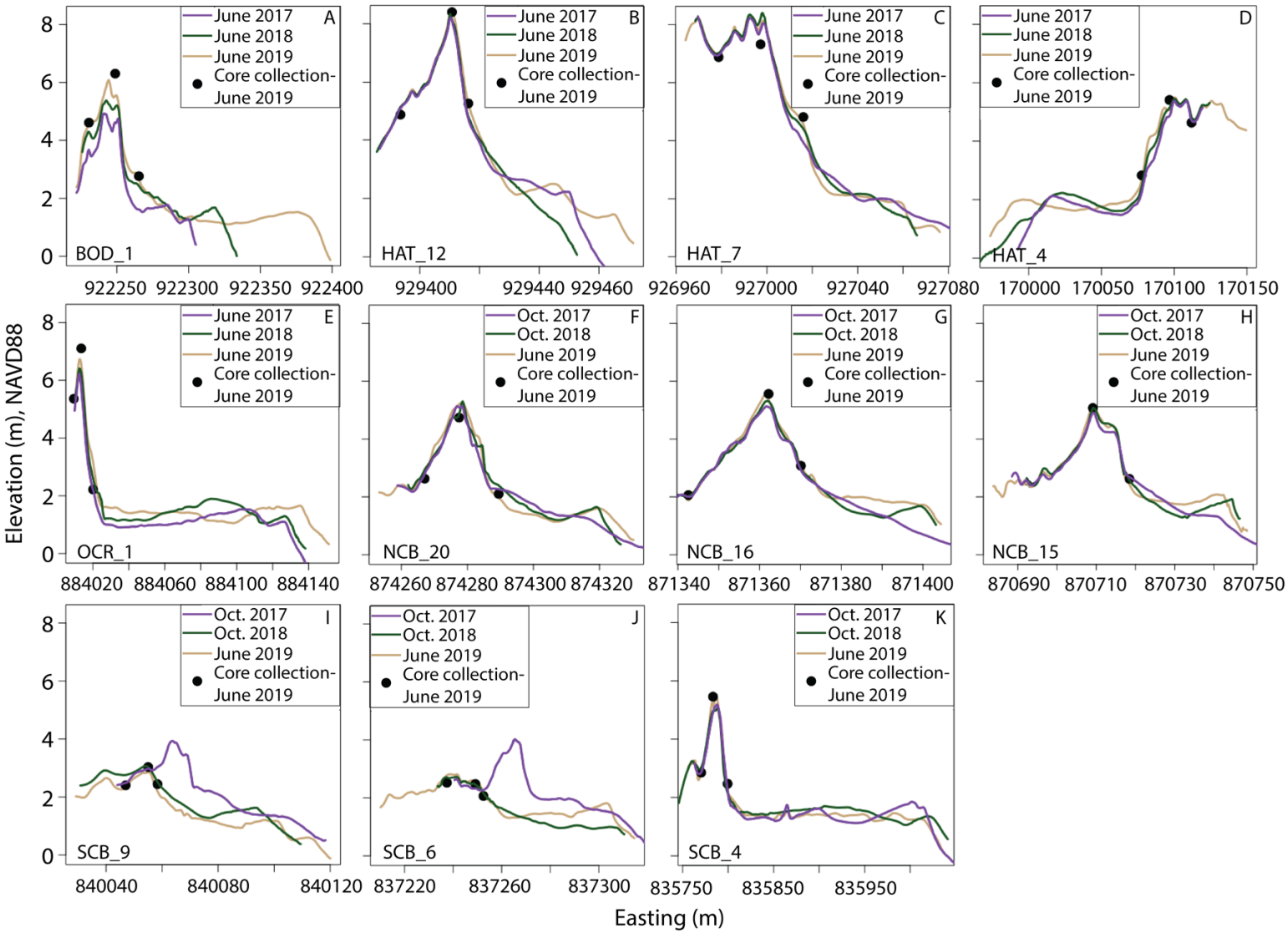
June 2017
June 2018
June 2019
Core collection-June 2019
A
BOD_1
B
HAT_12
C
HAT_7
D
HAT_4
Oct. 2017
Oct. 2018
E
OCR_1
F
NCB_20
G
NCB_16
H
NCB_15
I
SCB_9
J
SCB_6
K
SCB_4
Elevation (m), NAVD88
Easting (m)

Figure C2.

Appendix D Chapter 3: Supplemental Figures for Methods and Equipment Used for Dune Sediment Coring and Sample Extruding

Figure D1. Methods and equipment used to collect sediment cores in dunes. (A) Core tubes (10-cm diameter PVC pipe) were pounded into the toe, crest, and heel of the foredune using a sledgehammer and custom 'core head' placed over the top of the core tube to provide a surface for pounding. (B) Once the core tube was pounded into the dune, a test plug was inserted within the tube (above the sediment) to prevent sediment loss upon removal. (C) A pipe clamp and shackles were used to attach the core tube to a truck jack (attached to a plywood board) in order to remove the core from the dune. At times, the truck jack became too clogged with sand to use; in such cases, the cores were dug out of the dune using shovels. (D) A plastic end cap was placed over the end of the core tube upon removal to prevent any sediment loss. Core tubes were transported upright to avoid disturbing layers within the core.

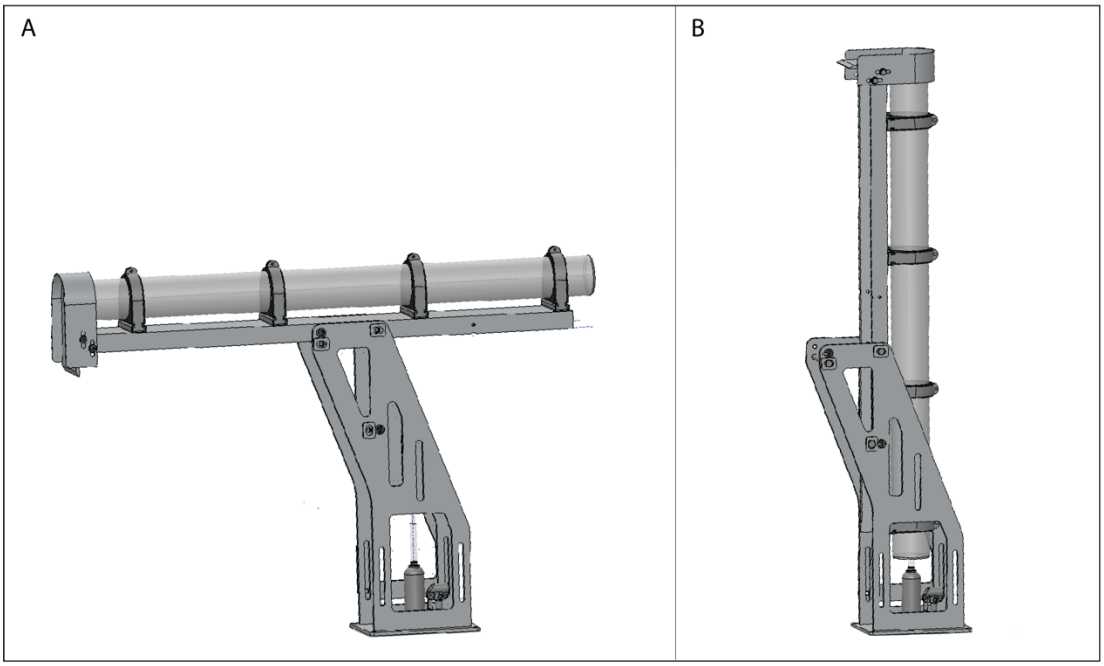

Figure D2. Custom-built extruder for dune sediment coring. (A) The extruder in the horizontal position for loading the core. (B) The extruder in the vertical position for extruding sediment. Designed by Ben Russell, Katya Jay, and John Stepanek, Oregon State University.

Figure D3. Methods and equipment for extruding sand sediment from dune cores. (A) Following core collection, the custom-built extruder (Figure D2) was attached to the truck hitch and the core tube was loaded into the extruder in the horizontal position so that the four restraining rings could be tightened around the core tube (see Figure D2a). The test plug was then removed from the top of the core (with the plastic end cap still in place) before fastening the extruder in the vertical position for use (Figure D2b). (B) During use, the extruder was stabilized from above by one person while another person used a scissor jack to insert the spacers into the core tube and slowly extrude sediment from the top. (C) and (D) A 2-cm high metal disk (10-cm diameter) was placed at the top of the core to extrude sediment in 2-cm increments for sampling. A tablespoon was used to scoop samples from within the 2-cm sample disk. The remainder of the sample was discarded, and the metal disk and sample platform were cleaned with a brush. (E) Samples were collected every other 2-cm increment and the samples in between those increments were discarded.

Appendix E Chapter 3: Supplemental Figures and Tables for Sediment Core Organic Matter and Carbon Measurements

Table E1. List of sediment core sample depths from each transect and profile location (see Figure 3.1; Appendix C, Table C1 for island abbreviations). Symbols indicate the core depths that were measured for organic matter (loss on ignition or LOI, denoted by an O) and percent organic carbon (denoted by a C). Profile locations are abbreviated as T (toe), C (crest), and H (heel). Cores varied in length and we sampled the deepest core depth for LOI measurements. Note that we did not collect a core at the toe of NCB_15.

Transect and Core		0-2	4-6	8-10	12-14	16-18	20-22	24-26	28-30	32-34	36-38	48-50	60-62	64-66	76-78	80-82	84-86	88-90	92-94	96-98	100-102	104-106	108-110	120-122
BOD_1	T	O	O	O	O	O	O	O C	O	O	O C	O	O C		O					O				O
BOD_1	C	O	O	O C	O	O	O C	O	O	O	O	O C	O		O				O				O	
BOD_1	H	O C	O	O	O	O	O	O C	O	O	O	O	O C		O C					O				
HAT_12	T	O	O	O C	O	O	O	O C	O	O	O	O	O		O C				O	O				
HAT_12	C	O C	O	O	O	O	O C		O	O	O	O	O		O C				O	O				
HAT_12	H	O	O C	O	O	O	O	O	O	O	O C	O	O		O				O C					
HAT_7	T	O	O	O C	O	O	O	O	O	O C	O	O	O		O			O			O C				
HAT_7	C	O	O	O	O	O C	O	O	O C	O	O	O	O		O				O		O C				
HAT_7	H	O	O	O C	O	O	O	O	O	O C	O	O C	O		O					O					
HAT_4	T	O	O	O	O	O	O	O C	O	O C	O C	O	O		O					O					
HAT_4	C	O	O	O	O	O C	O	O C	O	O C	O	O	O		O					O					
HAT_4	H	O	O	O C	O	O	O C	O	O	O C	O	O	O		O			O			O				

Transect and Core		0-2	4-6	8-10	12-14	16-18	20-22	24-26	28-30	32-34	36-38	48-50	60-62	64-66	76-78	80-82	84-86	88-90	92-94	96-98	100-102	104-106	108-110	120-122
OCR_1	T	O	O	O	O	O	O	O C	O	O	O	O	O C		O			O C			O			
OCR_1	C	O C	O C	O	O	O C	O	O	O	O	O	O	O		O					O				
OCR_1	H	O	O C	O	O C	O	O	O	O	O	O	O	O		O C			O						
NCB_20	T	O	O	O	O C	O C	O	O	O C	O	O	O	O		O				O					
NCB_20	C	O	O	O	O C	O C	O	O	O	O C	O	O	O		O			O						
NCB_20	H	O	O	O	O	O	O C	O	O	O C	O	O	O	O	O C				O					
NCB_16	T	O	O	O	O	O	O C	O	O	O	O	O	O		O C			O C						
NCB_16	C	O	O	O C	O	O	O	O	O	O	O	O	O C		O				O C					
NCB_16	H	O	O C	O	O	O	O	O C	O	O	O C	O	O		O		O							
NCB_15	T																							
NCB_15	C	O	O	O	O	O	O	O	O C	O	O	O C	O C		O		O	O			O			
NCB_15	H	O	O	O C	O	O	O	O	O	O C	O	O	O		O	O C		O						
SCB_9	T	O	O	O	O	O C	O C	O	O	O	O C	O	O		O					O				
SCB_9	C	O C	O	O	O	O C	O	O	O C	O	O	O	O		O				O					
SCB_9	H	O	O C	O	O	O C	O	O	O	O	O	O	O C		O					O				
SCB_6	T	O	O	O C	O	O	O	O	O	O C	O	O C	O		O			O		O				
SCB_6	C	O	O	O	O	O	O	O C	O	O	O	O	O C		O C				O					

Transect and Core		0-2	4-6	8-10	12-14	16-18	20-22	24-26	28-30	32-34	36-38	48-50	60-62	64-66	76-78	80-82	84-86	88-90	92-94	96-98	100-102	104-106	108-110	120-122
SCB_6	H	O	O	O	O	O	O C	O C	O	O	O C	O	O		O			O						
SCB_4	T	O	O C	O	O	O	O	O		O	O	O	O		O				O			O		O C
SCB_4	C	O	O	O C	O	O	O	O	O	O	O	O	O		O C				O C					
SCB_4	H	O	O	O	O	O	O	O	O	O C	O	O	O C		O C			O						

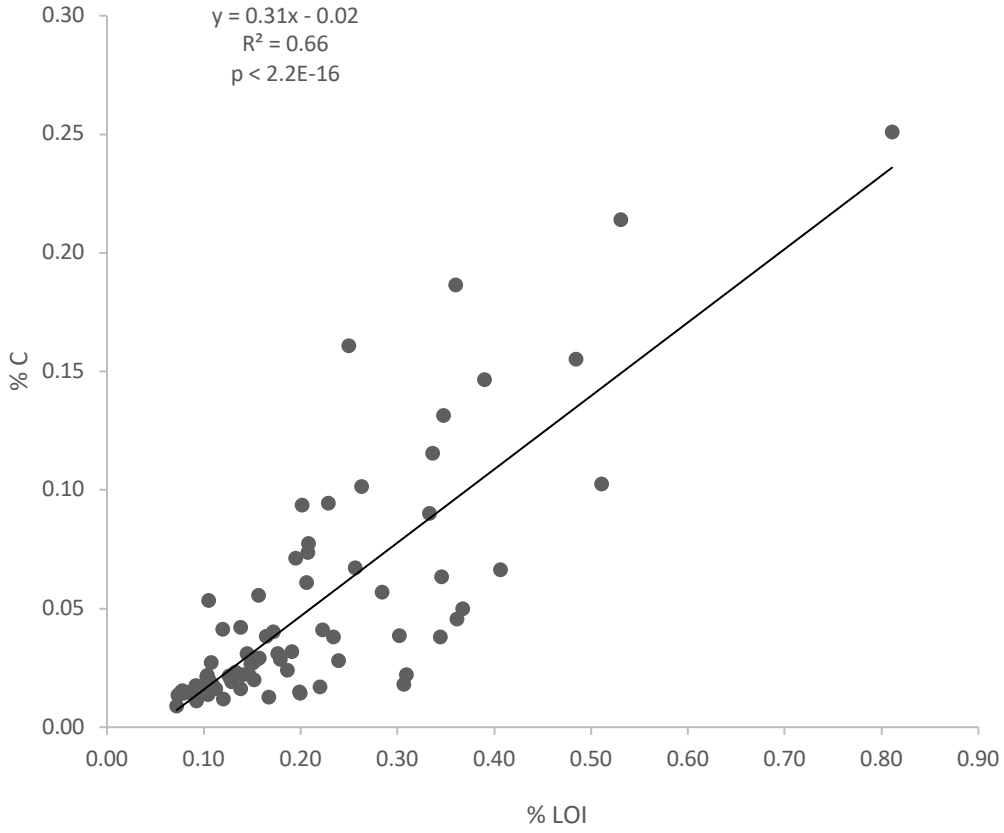

Figure E1. Linear regression relationship between percent organic matter (measured as % loss on ignition or LOI) and percent organic carbon (%C) including sediment core samples from all sites except for SCB_9.

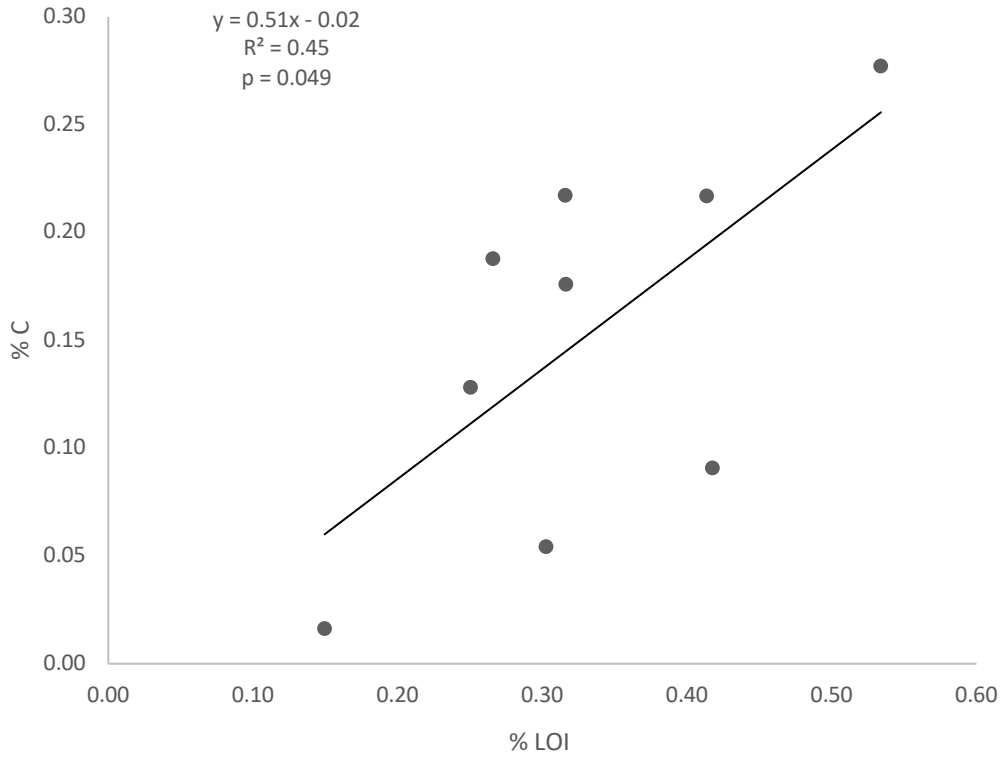

Figure E2. Linear regression relationship between percent organic matter (measured as % loss on ignition or LOI) and percent organic carbon (% C) for sediment core samples from SCB_9 only.

Appendix F Chapter 3: Supplemental Figures and Tables for Summary of Results

Table F1. Mean (± SD) aboveground (AG) dune grass stocks (kg C/m^2) and belowground (BG) dune grass and sand carbon density (kg C/m^3) across islands (see Figure 3.1; Appendix C, Table C1) and dune profile locations (toe, crest, and heel) on the Outer Banks barrier islands, North Carolina, USA. UNPA=*Uniola paniculata*, AMBR=*Ammophila breviligulata*.

Island	Profile		Sand C		BG grass C			AG grass C			UNPA AG C		AMBR AG C	
	location	n	Mean	SD	n	Mean	SD	n	Mean	SD	Mean	SD	Mean	SD
Bodie Island	Toe	15	0.254	0.054	7	0.073	0.178	7	0.004	0.004	0	0	0	0
	Crest	15	0.262	0.042	10	0.251	0.176	10	0.172	0.077	0.057	0.038	0.092	0.037
	Heel	14	0.319	0.122	10	0.769	0.632	10	0.087	0.017	0.051	0.018	0.008	0.015
Hatteras Island	Toe	43	0.529	0.409	42	0.471	1.027	42	0.036	0.027	0.009	0.013	0.023	0.013
	Crest	43	0.576	0.304	30	1.452	1.652	30	0.188	0.089	0.153	0.107	0.019	0.107
	Heel	42	0.916	0.434	27	1.560	1.256	27	0.108	0.030	0.106	0.030	0.000	0.002
Ocracoke Island	Toe	15	0.539	1.157	13	0.041	0.083	13	0.007	0.007	0	0	0.007	0.007
	Crest	14	0.409	0.108	7	6.639	3.902	7	0.118	0.049	0.118	0.049	0	0
	Heel	14	0.791	0.731	4	8.131	4.529	4	0.163	0.076	0.163	0.076	0	0
North Core Banks	Toe	42	0.745	0.256	32	0.181	0.459	32	0.019	0.026	0.016	0.028	0.003	0.009
	Crest	45	0.516	0.196	30	1.193	0.630	30	0.109	0.041	0.106	0.040	0.001	0.002
	Heel	43	0.702	0.334	33	1.074	0.562	33	0.102	0.024	0.101	0.025	0	0
South Core Banks	Toe	15	1.271	0.734	13	0.007	0.024	13	0.000	0	0.000	0	0	0
	Crest	14	0.887	0.267	10	1.616	2.170	10	0.026	0.032	0.026	0.032	0	0
	Heel	98	1.859	0.913	47	1.075	1.693	47	0.080	0.052	0.079	0.053	0	0

Table F2. Mean (± SD) for sand and belowground grass (BG) percent carbon values averaged by island and dune profile locations. Note that core samples from the toe of Hatteras Island and North Core Banks did not contain sufficient plant material at any depth to grind for analysis. Means with no SD values indicate either that there was only one sample or that no samples were ground at that site.

Island	Profile location	Sand % carbon			BG grass % carbon		
		n	Mean	SD	n	Mean	SD
Bodie Island	Toe	15	0.015	0.004	1	19.8	–
	Crest	15	0.016	0.003	1	20.0	–
	Heel	14	0.020	0.008	1	23.2	–
Hatteras Island	Toe	43	0.032	0.024	0	–	–
	Crest	43	0.037	0.020	2	44.9	4.3
	Heel	42	0.058	0.027	6	37.9	7.3
Ocracoke Island	Toe	15	0.035	0.074	1	15.4	–
	Crest	14	0.027	0.007	1	44.8	–
	Heel	14	0.054	0.051	1	39.2	–
North Core Banks	Toe	42	0.049	0.017	0	–	–
	Crest	45	0.034	0.013	3	44.4	3.2
	Heel	43	0.047	0.022	6	45.3	1.8
South Core Banks	Toe	15	0.077	0.042	0	–	–
	Crest	14	0.057	0.017	2	37.5	10.1
	Heel	98	0.117	0.057	7	40.8	3.1

Table F3. Mean (± SD) sand carbon density (kg C/m^3), sand percent carbon, and belowground (BG) grass carbon density (kg C/m^3) in core samples across islands (see Figure 3.1; Appendix C, Table C1) and core depths from the Outer Banks barrier islands, North Carolina, USA.

Island	Depth (cm)	n	Sand C density		Sand % C		BG grass C density	
			Mean	SD	Mean	SD	Mean	SD
Bodie Island	0-10	9	0.291	0.086	0.018	0.005	0.813	1.399
	10-20	6	0.261	0.037	0.016	0.002	1.450	2.294
	20-30	9	0.271	0.018	0.017	0.001	0.516	0.693
	30-60	9	0.258	0.076	0.016	0.005	0.867	1.320
	60-100	9	0.294	0.144	0.017	0.009	0.695	1.995
Hatteras Island	0-10	27	0.654	0.352	0.041	0.022	1.061	2.480
	10-20	18	0.565	0.353	0.036	0.023	3.511	8.815
	20-30	26	0.568	0.341	0.036	0.022	0.482	0.627
	30-60	26	0.784	0.534	0.050	0.034	1.213	3.224
	60-100	31	0.743	0.449	0.046	0.027	0.952	1.465
Ocracoke Island	0-10	27	0.727	0.244	0.048	0.016	1.559	1.760
	10-20	18	0.602	0.192	0.040	0.013	2.748	5.056
	20-30	27	0.612	0.314	0.040	0.020	1.143	1.420
	30-60	27	0.643	0.335	0.043	0.022	5.968	8.411
	60-100	31	0.656	0.288	0.043	0.018	0.470	0.458
North Core Banks	0-10	9	0.317	0.099	0.021	0.007	0.636	1.091
	10-20	6	0.935	1.131	0.064	0.079	0.593	1.706
	20-30	9	0.434	0.234	0.029	0.016	0.531	0.666
	30-60	9	0.443	0.329	0.030	0.022	1.629	4.498
	60-100	10	0.852	1.360	0.055	0.087	1.133	2.930
South Core	0-10	27	1.321	0.727	0.084	0.046	0.935	2.233
	10-20	18	1.283	0.777	0.082	0.050	2.508	7.424

Table F3. (Continued)

Banks	20-30	26	1.742	0.866	0.109	0.054	2.743	6.927
	30-60	27	2.039	0.932	0.130	0.061	2.403	8.943
	60-100	26	1.804	1.011	0.112	0.060	1.461	6.381

Figure F1. Mean (± SE) dune grass abundance metrics in the foredunes of the Outer Banks islands, North Carolina, USA, by transect from north to south (see Figure 3.1; Appendix C, Table C1 for island and transect abbreviations and locations). Values with no error bar indicate that there was only one quadrat at that transect and profile location. (A) Grass density in 2017 (tillers/m^2). (B) Grass density in 2018 (tillers/m^2). (C) Grass density in 2019 (tillers/m^2). (D) Grass biomass in 2017 (g/m^2). (E) Grass biomass in 2018 (g/m^2). (F) Grass biomass in 2019 (g/m^2). Note that values at SCB_6 and SCB_9 for 'toe', 'crest', and 'heel' in 2019 were all designated as heel sites in our analyses due to erosion of the toe and crest of the dune in September 2018.


A
B
C
D
E
F
BOD_1
HAT_12
HAT_7
HAT_4
OCR_1
NCB_20
NCB_16
NCB_15
SCB_9
SCB_6
SCB_4
Transect
0
100
200
Grass density (tillers/m² - 2017)
Grass density (tillers/m² - 2018)
Grass density (tillers/m² - 2019)
0
250
500
750
Grass biomass (g/m² - 2017)
Grass biomass (g/m² - 2018)
Grass biomass (g/m² - 2019)
Profile Location
Toe
Crest
Heel

Figure F1.

Figure F2. Mean sand and belowground (BG) grass carbon density (kg C/m^3) in core samples across islands (see Figure 3.1; Appendix C, Table C1), dune profile locations (toe, crest, heel) and core depths along the Outer Banks barrier islands, North Carolina, USA.

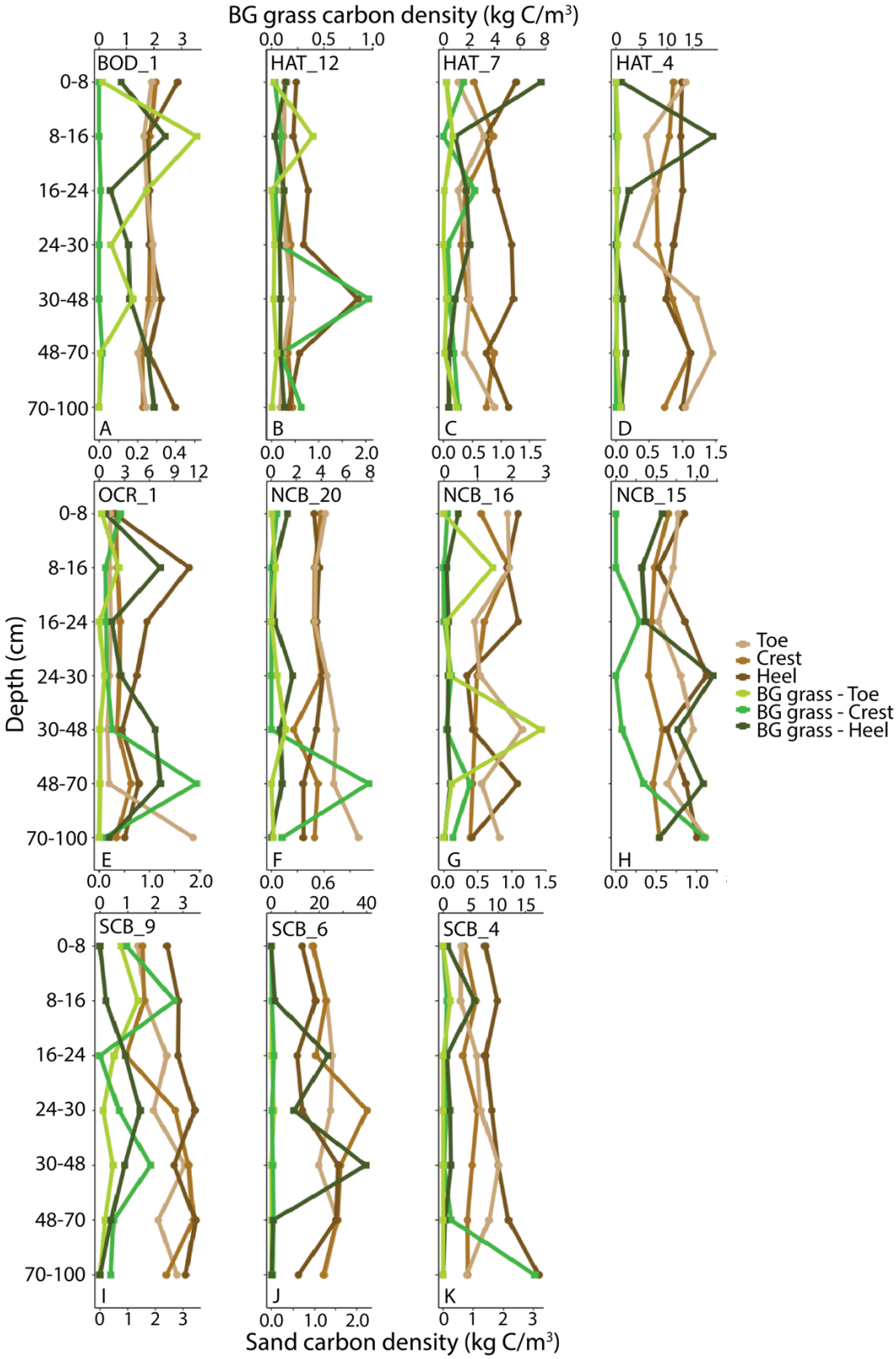
BG grass carbon density (kg C/m³)
BOD_1
HAT_12
HAT_7
HAT_4
OCR_1
NCB_20
NCB_16
NCB_15
SCB_9
SCB_6
SCB_4
A
B
C
D
E
F
G
H
I
J
K
0-8
8-16
16-24
24-30
30-48
48-70
70-100
Depth (cm)
Toe
Crest
Heel
BG grass - Toe
BG grass - Crest
BG grass - Heel
Sand carbon density (kg C/m³)

Figure F2.

Appendix G Chapter 4: Supplemental Table for Foredune Transect Locations

Table G1. Island and transect names (from north to south; see Figure 4.1) and latitude and longitude along the Outer Banks and Bogue Banks barrier islands, Virginia and North Carolina, USA. Transects are the same those surveyed in Hacker et al. (2019) and Jay et al. (Chapter 2; Appendix A, Table A1). Asterisks denote transects that were sampled for dune grass foliar $\delta^{15}N$ and %N.

Island and abbreviation	Transect name	Latitude	Longitude
False Cape (FAC)	FAC_4*	36.6277	-75.8898
	FAC_3	36.6018	-75.8799
	FAC_2*	36.5861	-75.8756
	FAC_1	36.5525	-75.8683
Bodie Island (BOD)	BOD_10*	36.5201	-75.8621
	BOD_9	36.4801	-75.8529
	BOD_8*	36.4022	-75.8307
	BOD_7	36.2823	-75.7938
	BOD_6	36.1854	-75.7521
	BOD_5	36.1793	-75.7494
	BOD_4*	36.0829	-75.7004
	BOD_3	36.0027	-75.6486
	BOD_2*	35.8344	-75.5582
	BOD_1	35.7958	-75.5402
Pea Island (PEA)	PEA_3*	35.7684	-75.5205
	PEA_2	35.7432	-75.5042
	PEA_1*	35.7132	-75.4913
Hatteras Island (HAT)	HAT_13	35.6698	-75.4777
	HAT_12*	35.6243	-75.4684
	HAT_11	35.5366	-75.4669
	HAT_10*	35.4730	-75.4812
	HAT_9	35.4067	-75.4859
	HAT_8*	35.3623	-75.4971
	HAT_7	35.3182	-75.5081
	HAT_6*	35.2747	-75.5175
	HAT_5	35.2265	-75.5285
	HAT_4*	35.2347	-75.5768
	HAT_3	35.2277	-75.6286
	HAT_2*	35.2123	-75.6817

Table G1. (Continued)

	HAT_1	35.1972	-75.7269
Ocracoke Island (OCR)	OCR_5*	35.1817	-75.7780
	OCR_4	35.1510	-75.8608
	OCR_3*	35.1268	-75.9147
	OCR_2	35.1050	-75.9560
	OCR_1*	35.0827	-75.9900
North Core Banks (NCB)	NCB_22*	35.0531	-76.0448
	NCB_21	35.0271	-76.0917
	NCB_20*	35.0216	-76.0990
	NCB_19	35.0158	-76.1066
	NCB_18*	35.0086	-76.1167
	NCB_17	35.0040	-76.1233
	NCB_16*	34.9970	-76.1318
	NCB_15	34.9913	-76.1392
	NCB_14	34.9844	-76.1478
	NCB_13	34.9781	-76.1560
	NCB_12	34.9723	-76.1639
	NCB_11	34.9663	-76.1720
	NCB_10	34.9606	-76.1794
	NCB_9*	34.9537	-76.1881
	NCB_8	34.9471	-76.1962
	NCB_7	34.9411	-76.2034
	NCB_6	34.9346	-76.2112
	NCB_5	34.9221	-76.2262
	NCB_4	34.9087	-76.2422
	NCB_3	34.8962	-76.2588
	NCB_2*	34.8913	-76.2659
	NCB_1	34.8857	-76.2739
South Core Banks (SCB)	SCB_20	34.8307	-76.3455
	SCB_19	34.8194	-76.3545
	SCB_18*	34.8063	-76.3676
	SCB_17	34.7922	-76.3823
	SCB_16*	34.7785	-76.3957
	SCB_15	34.7666	-76.4054
	SCB_14*	34.7495	-76.4214
	SCB_13	34.7344	-76.4351
	SCB_12	34.7202	-76.4472

Table G1. (Continued)

	SCB_11	34.7049	-76.4606
	SCB_10	34.6898	-76.4735
	SCB_9	34.6755	-76.4851
	SCB_8	34.6608	-76.4970
	SCB_7	34.6444	-76.5072
	SCB_6*	34.6281	-76.5171
	SCB_5	34.6115	-76.5275
	SCB_4*	34.5946	-76.5344
	SCB_3	34.5927	-76.5376
	SCB_2*	34.6065	-76.5473
	SCB_1	34.6222	-76.5542
	SCB_0*	34.6307	-76.5555
Shackleford Banks (SHB)	SHB_12	34.6340	-76.5370
	SHB_11*	34.6417	-76.5437
	SHB_10	34.6485	-76.5512
	SHB_9*	34.6537	-76.5604
	SHB_8	34.6584	-76.5707
	SHB_7*	34.6622	-76.5799
	SHB_6	34.6658	-76.5906
	SHB_5*	34.6688	-76.6011
	SHB_4	34.6717	-76.6115
	SHB_3*	34.6742	-76.6224
	SHB_2	34.6766	-76.6335
	SHB_1*	34.6792	-76.6437
Bogue Banks (BGB)	BGB_22	34.6938	-76.6791
	BGB_21	34.6937	-76.6894
	BGB_20	34.6944	-76.7003
	BGB_19	34.6951	-76.7064
	BGB_18	34.6970	-76.7286
	BGB_17	34.6975	-76.7497
	BGB_16	34.6971	-76.7715
	BGB_15*	34.6959	-76.7934
	BGB_14	34.6943	-76.8148
	BGB_13*	34.6920	-76.8376
	BGB_12	34.6896	-76.8577
	BGB_11*	34.6865	-76.8820
	BGB_10	34.6837	-76.9021

Table G1. (Continued)

	BGB_9	34.6807	-76.9219
	BGB_8	34.6771	-76.9458
	BGB_7*	34.6740	-76.9654
	BGB_6	34.6700	-76.9879
	BGB_5	34.6661	-77.0087
	BGB_4	34.6615	-77.0294
	BGB_3*	34.6562	-77.0520
	BGB_2	34.6505	-77.0935
	BGB_1*	34.6443	-77.0936

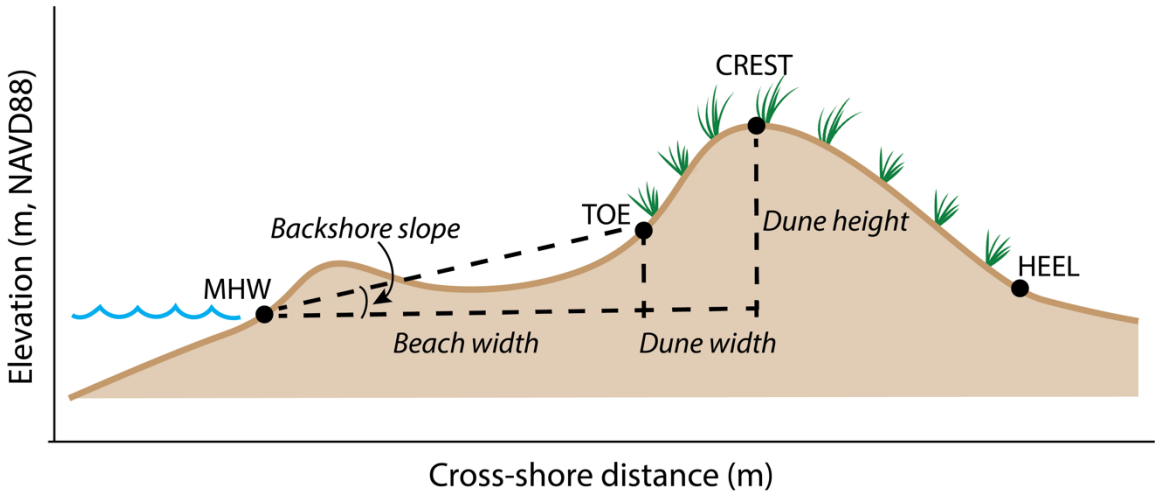

Figure G1. Beach and foredune morphology parameters calculated using data from real-time kinematic GPS surveys and following the methods of Mull and Ruggiero (2014). MHW (or mean high water) was extracted using the 0.3 m MHW contour (NAVD88). Foredune morphology measurements included the position and elevation of the foredune toe (the seaward extent of the foredune), the foredune crest (the highest point on the foredune), and the foredune heel (the landward extent of the foredune, determined by an elevation minimum). Foredune height and toe elevation were calculated as the differences between MHW and foredune crest and toe elevation, respectively. Foredune width was calculated as one-half dune width (the horizontal distance between the foredune toe and crest) to capture changes in the width of the foredune face. Backshore slope was calculated as the slope between MHW and the dune toe. Beach width was calculated as the horizontal distance between MHW and the foredune toe. Figure from Jay et al., Chapter 3 (see Appendix C, Figure C1).

Appendix H Chapter 4: Supplemental Figures and Tables for Macrophyte Wrack Percent Cover and Biomass Measurements

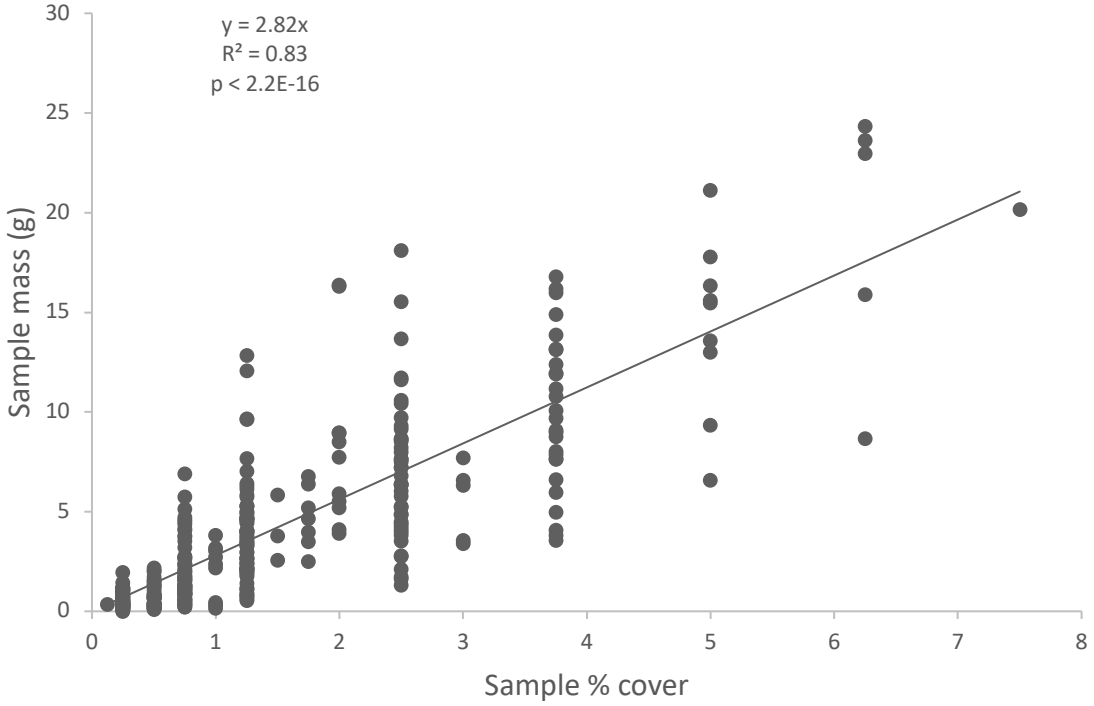

Figure H1. Linear regression relationship between macrophyte wrack percent cover (in a 1 m^2 quadrat) and macrophyte wrack biomass (g) for brown algae *Sargassum* sp. samples.

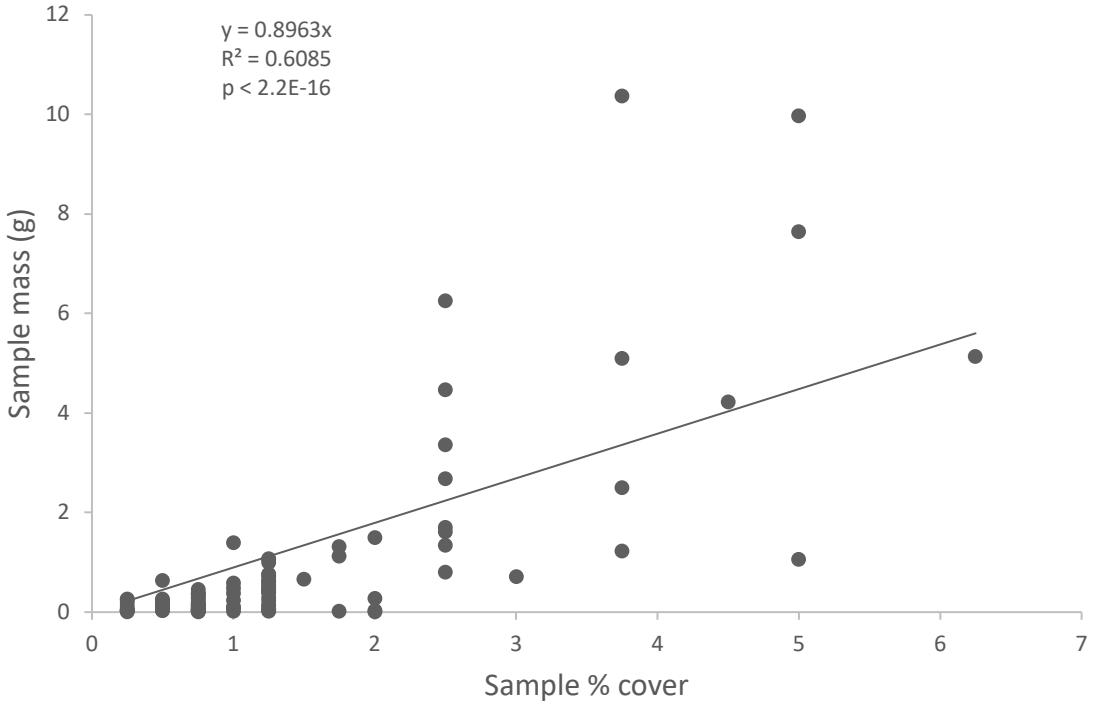

Figure H2. Linear regression relationship between macrophyte wrack percent cover (in a 1 m^2 quadrat) and macrophyte wrack biomass (g) for eelgrass *Zostera marina* samples.